

**On the numerical solution of Fisher's and
FitzHugh-Nagumo equations using some finite
difference methods**

by

Koffi Messan Agbavon

Submitted in partial fulfillment of the requirements for the degree

Philosophiae Doctor

In the Department of Mathematics and Applied Mathematics

In the Faculty of Natural and Agricultural Sciences

University of Pretoria


Pretoria

February 3, 2020

Declaration

I, Koffi Messan Agbavon declare that the thesis which I hereby submit for the degree Philosophiae Doctor at the University of Pretoria, is my own work and has not previously been submitted by me for a degree at this or any other tertiary institution.

SIGNATURE:



DATE:

04/02/2020

This thesis is dedicated to my late father, Kossi Agbavon and mother Houngnewo Gbongli.

Acknowledgement

Grateful heart to almighty God for the life and inspiration, wisdom throughout these years. It is my pleasure to express my innermost gratitude to my wonderful supervisor

Prof A. R. Appadu, for his immeasurable expertise, encouragement, care and guidance.

My acknowledgement goes also to the South African DST/NRF SARCHe on Mathematical Models and Methods in Bioengineering and Biosciences ($M^3 B^2$) grant 82770 and special thanks to Prof J. Banasiak for financial support and with who I had useful discussion on Functional Analysis (travelling wave) in the first and second year of my thesis.

I am grateful to University of Pretoria especially the Department of Mathematics and Applied Mathematics for providing me with the necessary facility. I am grateful also to all the staff especially the previous Dean of Faculty of Natural and Agricultural Science(Prof Jean Lubuma), Prof Roumen Anguelov, Prof Rachid Ouifki and Prof Michael Chapwanya who helps me to improve the introduction of my thesis and allows me to attend some of his lectures on Numerical Analysis (WTW 733). I am thankful also to Lorelle September, Ronel Oosthuizen and Rachel Combrink for positive support and willingness to help when I am in need.

I feel privileged to acknowledge and appreciate all my friends who contributed in one way or the other namely; Dr Tesfalem, Dr Abey, Dr Bahru, Dr Valaire Yatat, Mr Richard, Mr Gediyon, Mr Usman, Godfred, Emmanuel, Ambrose, Chigo and Americo to the successful completion of this PhD work, reason being that there is a saying which goes thus “a good appreciation of what is done makes the mind dispose to doing it well again”. I am also grateful to

Prof Barry Green and Prof Jeff Sanders from AIMS South Africa. I also thank some staff and friends from University of Lome’ namely; Prof Amah D’Almeida, Prof Yaogan Messah, Komi Afassinou, David Kudawoo and Michel Badatcho.

I am thankful to my mother HOUNGNEWO GBONGLI and late father KOSI FIAGAN AGBAVON. Thanks to all your endless prayers for me. Thanks to my siblings Remi and his family, Alex and his family, Anani, Akuete, and Akuelevi for their love, support and prayers. I am grateful to my lovely friend Marguerite and her mother and brothers to let me visit them. I am finally thankful to all my Catholic friends from KwaZulu Natal and to CRC (Christian Revival Church) members for endless prayers. I end up my acknowledgement to these motivational quote of Christopher McDougall “*Every morning in Africa, a gazelle wakes up. It knows it must run faster than the fastest lion or it will be killed. Every morning a lion wakes up. It knows it must outrun the slowest gazelle or it will starve to death. It doesn’t matter whether you are a lion or a gazelle: when the sun comes up, you’d better be running*” and of Woodrow Wilson “*You are not here merely to make a living. You are*

here in order to enable the world to live more amply, with greater vision, with a finer spirit of hope and achievement. You are here to enrich the world, and you impoverish yourself if you forget the errand.”

Title: On the numerical solution of Fisher's and FitzHugh-Nagumo equations using some finite difference methods.

Name of the Candidate : Koffi Messan Agbavon

Supervisor ¹ : Prof. A. R. Appadu

Co-supervisor ² : Prof. J. Banasiak

Department : ¹ Mathematics and Applied Mathematics, Nelson Mandela University, ² Mathematics and Applied Mathematics, University of Pretoria.

Degree : Philosophiae Doctor

Abstract

In this thesis, we make use of numerical schemes in order to solve Fisher's and FitzHugh-Nagumo equations with specified initial conditions. The thesis is made up of six chapters.

Chapter 1 gives some literatures on partial differential equations and chapter 2 provides some concepts on finite difference methods, nonstandard finite difference methods and their properties, reaction-diffusion equations and singularly perturbed equations.

In chapter 3, we obtain the numerical solution of Fisher's equation when the coefficient of diffusion term is much smaller than the coefficient of reaction (Li et al., 1998). Li et al. (1998) used the Moving Mesh Partial Differential Equation (MMPDE) method to solve a scaled Fisher's equation with coefficient of reaction being 10^4 and coefficient of diffusion equal to one and the initial condition consisted of an exponential function. The problem considered is quite challenging and the results obtained by Li et al. (1998) are not accurate due to the fact that MMPDE is based on familiar arc-length or curvature monitor function. Qiu and Sloan (1998) constructed a suitable monitor function called modified monitor function and used it with the Moving Mesh Differential Algebraic Equation (MMDAE) method in order to solve the same problem as Li et al. (1998) and better result were obtained. However, each problem has its own choice of monitor function which makes the choice of the monitor function an open question. We use the Forward in Time Central Space (FTCS) scheme and the Nonstandard Finite Difference (NSFD) to solve the scaled Fisher's equation and we find that the temporal step size must be very small in order to obtain accurate results and comparable to Qiu and Sloan (1998). This causes the computational time to be long if the domain is large. We use two techniques to modify these two

schemes either by introducing artificial viscosity or using the approach of [Ruxun et al. \(1999\)](#). These techniques are efficient and give accurate results with a larger temporal step size. We prove that these four methods are consistent with the partial differential equation and we also obtain the region of stability.

Chapter 4 is an improvement and extension of the work from [Namjoo and Zibaei \(2018\)](#) whereby the standard FitzHugh-Nagumo equation with specified initial and boundary conditions is solved. [Namjoo and Zibaei \(2018\)](#) constructed two versions of nonstandard finite difference (NSFD1, NSFD2) and also derived two schemes (one explicit and the other implicit) constructed from the exact solution. However, they presented results using the nonstandard finite difference schemes only. We showed that one of the nonstandard finite difference schemes (NSFD1) has convergence issues and we obtain an improvement for NSFD1 which we call NSFD3. We perform a stability analysis of the schemes constructed from the exact solution and found that the explicit scheme is not stable for this problem. We study some properties of the five methods (NSFD1, NSFD2, NSFD3, two schemes obtained using the exact solution) such as stability, positivity and boundedness. The performance of the five methods is compared by computing L_1 , L_∞ errors and the rate of convergence for two values of the threshold of Affect effect, γ namely; 0.001 and 0.5 for small and large spatial domains at time, $T = 1.0$. Tests on rate of convergence are important here as we are dealing with nonlinear partial differential equations and therefore the Lax-Equivalence theorem cannot be used.

In chapter 5, we consider FitzHugh-Nagumo equation with the parameter β referred to as intrinsic growth rate. We chose a numerical experiment which is quite challenging for simulation due to shock-like profiles. We construct four versions of nonstandard finite difference schemes and compared the performance by computing L_1 , L_∞ errors, rate of convergence with respect to time and CPU time at given time, $T = 0.5$ using three values of the intrinsic growth rate, β namely; $\beta = 0.5, 1.0, 2.0$.

Chapter 6 highlights the salient features of this work.

Contents

Declaration	i
Dedication	ii
Acknowledgement	iii
Abstract	v
List of Publications	xvi
Conferences and Seminars	xvii
1 Introduction	1
1.1 Why study of Fisher’s and FitzHugh-Nagumo equations?	2
1.2 Contributions of the thesis to the scientific literature	3
2 Mathematical preliminaries	5
2.1 Finite difference methods	5
2.1.1 General formulation	5
2.1.2 Nonstandard-finite difference scheme	23
2.1.3 Reaction diffusion equation	31
2.1.4 Singularly perturbed reaction diffusion equation problems	32
3 On the Numerical Solution of Fisher’s equation with coefficient of diffusion term much smaller than coefficient of reaction term	34
3.1 Introduction	34
3.1.1 Background of Fisher’s equation	35
3.2 Organisation of chapter	37
3.3 Moving Mesh method	37

3.3.1	Modified Monitor Function	40
3.4	Numerical experiments	41
3.5	Forward in Time Central Space (FTCS)	42
3.5.1	Stability	43
3.5.2	Numerical results using FTCS	44
3.6	FTCS- ϵ scheme	49
3.7	Nonstandard Finite Difference Schemes (NSFD)	55
3.7.1	Positivity and Boundedness: Relation between time and space step-sizes	56
3.8	NSFD- ϵ schemes	62
3.9	Artificial viscosity	69
3.9.1	FTCS with artificial viscosity	70
3.9.2	Nonstandard Finite Difference method with artificial viscosity	74
3.10	The stability of computed solution and the sensitivity of the solution to the boundary condition ahead of the wave in term of local pertubation	77
3.11	Conclusion	80
4	Comparative study of some Numerical methods for the standard FitzHugh- Nagumo equation	81
4.1	Introduction	81
4.2	Organisation of the chapter	83
4.3	Numerical experiment	83
4.4	Construction of numerical scheme from exact solution	84
4.5	Scheme of Namjoo and Zibaei	84
4.5.1	Explicit scheme	87
4.5.2	Implicit scheme	92
4.6	Nonstandard Finite Difference Scheme (NSFD)	97
4.6.1	NSFD1 scheme	97
4.6.2	NSFD2 scheme	101
4.6.3	NSFD3 scheme	106
4.7	Conclusion	109
5	Construction and analysis of some nonstandard finite difference methods for the FitzHugh-Nagumo equation	111
5.1	Introduction	111

5.1.1	Biological description of the parameter γ and β	112
5.2	Organisation of the chapter	113
5.3	Numerical experiment	113
5.4	Basic dynamical behaviour and a priori bound of Eq. (5.1)	114
5.5	Nonstandard Finite Difference Scheme (NSFD)	114
5.6	NSFD1 Scheme	115
5.7	NSFD2 scheme	120
5.8	NSFD3 scheme	124
5.9	NSFD4 Scheme	128
5.10	Errors estimate for NSFD3	132
5.11	Relationship between physical behaviour and numerical solution and discussion over the obtained results from NSFD1, NSFD2, NSFD3, NSFD4	134
5.12	Implicit nonstandard finite difference for Fitzhugh-Nagumo equation	137
5.13	Conclusion	137
6	Conclusion and future work	139
6.1	Conclusion	139
6.2	Some limitations of nonstandard finite difference	141
6.3	Future work	142
	Bibliography	144

List of Figures

2.1	One dimensional finite difference discretization	6
3.1	Plot of u against x for Problem 1 using FTCS scheme at time 2.5×10^{-3} at some different values of k and $h = 0.01$, $T_{max} = 2.5 \times 10^{-3}$	48
3.2	Plot of u against x for Problem1 using FTCS- ϵ scheme at time 2.5×10^{-3} and some different values of k and $h = 0.01$, $\epsilon = 0.01$, $T_{max} = 2.5 \times 10^{-3}$	53
3.3	Plot of u against x for Problem 1 using NSFD scheme at time 2.5×10^{-3} at some different values of k and $h = 0.01$	61
3.4	Plot of u against x for Problem 1 using NSFD- ϵ scheme at time 2.5×10^{-3} at some different values of k and $h = 0.01$, $\epsilon = 0.01$	68
3.5	Plot of u against x for Problem 1 using FTCS with artificial viscosity at time 2.5×10^{-3} at some different values of k and $h = 0.01$, $\sigma = 2.0$, $T_{max} = 2.5 \times 10^{-3}$	73
3.6	Plot of u against x for Problem 1 using NSFD with artificial viscosity at time 2.5×10^{-3} , at some different values of k and $h = 0.01$, $\sigma = 2.0$, $T_{max} = 2.5 \times 10^{-3}$	76
4.1	Plot of $ \xi $ against w using explicit scheme described by Eq. (4.34) from Namjoo and Zibaei (2018).	89
4.2	Plot of u against x using explicit scheme described by Eq. (4.34) from Namjoo and Zibaei (2018) at Time, $T = 1.0$ where $x \in [0, 1]$ for 4.2a, 4.2c and $x \in [0, 10]$ for 4.2b and 4.2d.	92
4.3	Plot of $ \xi $ against w using implicit scheme described by Eq. (4.51) from Namjoo and Zibaei (2018).	94
4.4	Plot of u against x using implicit scheme described by (4.51) from Namjoo and Zibaei (2018) at time, $T = 1.0$ where $x \in [0, 1]$ for 4.4a, 4.4c and $x \in [0, 10]$ for 4.4b and 4.4d.	97
4.5	Plot of u against x using NSFD1 scheme at time $T = 1.0$, where $x \in [0, 1]$, for 4.5a, 4.5c and $x \in [0, 10]$ for 4.5b and 4.5d.	101

4.6	Plot of u against x using NSFD2 scheme at time $T = 1.0$, where $x \in [0, 1]$ for 4.6a, 4.6c and $x \in [0, 10]$ for 4.6b, 4.6d.	105
4.7	Plot of u against x using NSFD3 scheme at time $T = 1.0$, where $x \in [0, 1]$ for 4.7a, 4.7c and $x \in [0, 10]$ for 4.7b and 4.7d.	109
5.1	Plot of u vs x using NSFD1 scheme at time $T = 0.5$, where $x \in [-10, 10]$ for different values of β namely; 0.5, 1.0, 2.0.	118
5.2	Plot of error vs x using NSFD1 scheme at time $T = 0.5$, where $x \in [-10, 10]$ for different values of β respectively 0.5, 1.0, 2.0.	119
5.3	Plot of u against x using NSFD2 scheme at time $T = 0.5$, where $x \in [-10, 10]$ for different values of β namely; 0.5, 1.0, 2.0.	122
5.4	Plot of error against x using NSFD2 scheme at time $T = 0.5$, where $x \in [-10, 10]$ for different values of β respectively 0.5, 1.0, 2.0.	123
5.5	Plot of u against x using NSFD3 scheme at time $T = 0.5$, where $x \in [-10, 10]$ for different values of β namely; 0.5, 1.0, 2.0.	126
5.6	Plot of error against x using NSFD3 scheme at time $T = 0.5$, where $x \in [-10, 10]$ for different values of β respectively 0.5, 1.0, 2.0.	127
5.7	Plot of u against x using NSFD4 scheme at time $T = 0.5$, where $x \in [-10, 10]$ for different values of β namely; 0.5, 1.0, 2.0.	130
5.8	Plot of error against x using NSFD4 scheme at time $T = 0.5$, where $x \in [-10, 10]$ for different values of β respectively 0.5, 1.0, 2.0.	131
5.9	Plot of numerical solution, u vs $x \in [-10, 10]$ and vs $t \in [0, 20]$ using NSFD3. . .	136
5.10	Plot of numerical solution, u vs $x \in [-10, 10]$ vs γ using NSFD3 for different values of γ namely; 0.1, 0.2, 0.3, 0.4, 0.5, 0.6, 0.7, 0.8, 0.9.	136

List of Tables

3.1	Computation of L_1 and L_∞ errors using MMPDE and MMDAE methods with $\rho = 10^4$, $\alpha = 1.5$, $\beta = 0.1$, $a = 1.015$, $\tau = 10^{-7}$, $N = 50$, at time, $t = 2.5 \times 10^{-3}$.	41
3.2	L_1 and L_∞ errors and CPU time at some different values of time-step size, k for Problem 1 with $\rho = 10^4$ at time 2.5×10^{-3} with spatial mesh size, $h = 0.01$ using FTCS scheme, where $T_{max} = 2.5 \times 10^{-3}$.	45
3.3	Rate of convergence with k and spatial mesh size, $h = 0.01$, $\epsilon = 0.01$, of Problem 1 using FTCS.	45
3.4	L_1 and L_∞ errors and CPU time at some different values of time-step size, k for Problem 2 with $\rho = 10^4$ at time 2.5×10^{-3} with spatial mesh size, $h = 0.01$ using FTCS scheme, where $T_{max} = 2.5 \times 10^{-3}$.	46
3.5	L_1 and L_∞ errors and CPU time at some different values of time-step size, k for Problem 1 and spatial mesh size, $h = 0.01$, $\epsilon = 0.01$ using FTCS- ϵ , where $T_{max} = 2.5 \times 10^{-3}$.	54
3.6	Rate of convergence with k and spatial mesh size, $h = 0.01$, $\epsilon = 0.01$, of Problem 1 using FTCS- ϵ .	54
3.7	L_1 and L_∞ errors and CPU time at some different values of time-step size, k and spatial mesh size, $h = 0.01$, $\epsilon = 0.01$, of Problem 2 using FTCS- ϵ , where $T_{max} = 2.5 \times 10^{-3}$.	55
3.8	Rate of convergence with k and spatial mesh size, $h = 0.01$, $\epsilon = 0.01$, of Problem 1 using NSFD.	58
3.9	L_1 and L_∞ errors and CPU time at some different values of time-step size, k for Problem 1 at time 2.5×10^{-3} with spatial mesh size, $h = 0.01$ using NSFD scheme, where $T_{max} = 2.5 \times 10^{-3}$.	59
3.10	L_1 and L_∞ errors and CPU time at some different values of time-step size, k for Problem 2 at time 2.5×10^{-3} with spatial mesh size, $h = 0.01$ using NSFD scheme, where $T_{max} = 2.5 \times 10^{-3}$.	60

3.11	L_1 and L_∞ errors and CPU time at some different values of time-step size, k for Problem 1 at time 2.5×10^{-3} with spatial mesh size, $h = 0.01$, $\epsilon = 0.01$ using NSFD- ϵ scheme, $T_{max} = 2.5 \times 10^{-3}$	66
3.12	Rate of convergence with k and spatial mesh size, $h = 0.01$, $\epsilon = 0.01$, of Problem 1 using NSFD- ϵ , Optimal $k \cong 2.5 \times 10^{-3}/334$	66
3.13	L_1 and L_∞ errors and CPU time at some different values of time-step size, k for Problem 2 at time 2.5×10^{-3} with spatial mesh size, $h = 0.01$, $\epsilon = 0.01$ using NSFD- ϵ scheme, $T_{max} = 2.5 \times 10^{-3}$	67
3.14	Rate of convergence with k and spatial mesh size, $h = 0.01$, $\epsilon = 0.01$, of Problem 1 using FTCS with artificial viscosity, optimal $k = 2.5 \times 10^{-3}/880$	71
3.15	L_1 and L_∞ errors CPU time at some different values of time-step size, k for Problem 1 with $\rho = 10^4$ at time 2.5×10^{-3} with spatial mesh size, $\sigma = 2.0$, $h=0.01$ using FTCS with artificial viscosity.	72
3.16	Rate of convergence with k and spatial mesh size, $h = 0.01$, $\epsilon = 0.01$, of Problem 1 using NSFD with artificial viscosity Optimal $k = 2.5 \times 10^{-3}/1000$	75
3.17	L_1 and L_∞ errors and CPU time at some different values of time step size, k for Problem 1 at time 2.5×10^{-3} with spatial mesh size, $h = 0.01$, $\sigma = 2.0$ using NSFD with artificial viscosity method.	77
4.1	Computation of L_1 and L_∞ errors and CPU time using explicit scheme described by Eq. (4.34) from Namjoo and Zibaei (2018) with $\gamma = 0.001$, $h = 0.1$, $0 \leq x \leq 1$ at time, $T = 1.0$	88
4.2	Computation of L_1 and L_∞ errors and CPU time using explicit scheme described by Eq. (4.34) from Namjoo and Zibaei (2018) with $\gamma = 0.001$, $h = 0.1$, $0 \leq x \leq 10$ at time, $T = 1.0$	89
4.3	Computation of L_1 and L_∞ errors and CPU time using explicit scheme described by Eq. (4.34) from Namjoo and Zibaei (2018) with $\gamma = 0.5$, $h = 0.1$, $0 \leq x \leq 1$ at time, $T = 1.0$	90
4.4	Computation of L_1 and L_∞ errors and CPU time using explicit scheme described by Eq. (4.34) from Namjoo and Zibaei (2018) with $\gamma = 0.5$, $h = 0.1$, $0 \leq x \leq 10$ at time, $T = 1.0$	90
4.5	Computation of L_1 and L_∞ errors using implicit scheme described Eq. (4.51) from Namjoo and Zibaei (2018) with $\gamma = 0.001$, $h = 0.1$, $0 \leq x \leq 1$ at time, $T = 1.0$	95

4.6	Computation of L_1 and L_∞ errors using implicit scheme described Eq. (4.51) from Namjoo and Zibaei (2018) with $\gamma = 0.001$, $h = 0.1$, $0 \leq x \leq 10$ at time, $T = 1.0$	95
4.7	Computation of L_1 and L_∞ errors using implicit scheme described Eq. (4.51) from Namjoo and Zibaei (2018) with $\gamma = 0.5$, $h = 0.1$, $0 \leq x \leq 1$ at time, $T = 1.0$	96
4.8	Computation of L_1 and L_∞ errors using implicit scheme from Namjoo and Zibaei (2018) with $\gamma = 0.5$, $h = 0.1$, $0 \leq x \leq 10$ at time, $T = 1.0$	96
4.9	Computation of L_1 and L_∞ errors, CPU time and rate of convergence in time using NSFD1 with $\gamma = 0.001$, $h = 0.1$, $0 \leq x \leq 1$ at time, $T = 1.0$	99
4.10	Computation of L_1 and L_∞ errors, CPU time and rate of convergence in time using NSFD1 with $\gamma = 0.001$, $h = 0.1$, $0 \leq x \leq 10$ at time, $T = 1.0$	99
4.11	Computation of L_1 and L_∞ errors CPU time and rate of convergence in time using NSFD1 with $\gamma = 0.5$, $h = 0.1$, $0 \leq x \leq 1$ at time, $T = 1.0$	100
4.12	Computation of L_1 and L_∞ errors, CPU time and rate of convergence using NSFD1 with $\gamma = 0.5$, $h = 0.1$, $0 \leq x \leq 10$ at time, $T = 1.0$	100
4.13	Computation of L_1 and L_∞ errors, CPU time and rate of convergence using NSFD2 with $\gamma = 0.001$, $h = 0.1$, $0 \leq x \leq 1$, $T = 1.0$	103
4.14	Computation of L_1 and L_∞ errors, CPU time and rate of convergence using NSFD2 with $\gamma = 0.001$, $h = 0.1$, $0 \leq x \leq 10$, $T = 1.0$	104
4.15	Computation of L_1 and L_∞ errors, CPU time and rate of convergence using NSFD2 with $\gamma = 0.5$, $h = 0.1$, $0 \leq x \leq 1$, $T = 1.0$	104
4.16	Computation of L_1 and L_∞ errors, CPU time and rate of convergence using NSFD2 with $\gamma = 0.5$, $h = 0.1$, $0 \leq x \leq 10$, $T = 1.0$	104
4.17	Computation of L_1 and L_∞ errors, CPU time and rate of convergence in time using NSFD3 with $\gamma = 0.001$, $h = 0.1$, $0 \leq x \leq 1$, $T = 1.0$	107
4.18	Computation of L_1 and L_∞ errors, CPU time and rate of convergence in time using NSFD3 with $\gamma = 0.001$, $h = 0.1$, $0 \leq x \leq 10$, $T = 1.0$	107
4.19	Computation of L_1 and L_∞ errors, CPU time and rate of convergence in time using NSFD3 with $\gamma = 0.5$, $h = 0.1$, $0 \leq x \leq 1$, $T = 1.0$	108
4.20	Computation of L_1 and L_∞ errors, CPU time and rate of convergence using NSFD3 with $\gamma = 0.5$, $h = 0.1$, $0 \leq x \leq 10$, $T = 1.0$	108
5.1	Computation of L_1 , L_∞ errors, rate of convergence and CPU time using NSFD1 for $-10 \leq x \leq 10$, $\gamma = 0.2$, $h = 0.1$, $\beta = 0.5$, $T = 0.5$	116

5.2	Computation of L_1, L_∞ errors, rate of convergence and CPU time using NSFD1 for $-10 \leq x \leq 10, \gamma = 0.2, h = 0.1, \beta = 1, T = 0.5$	117
5.3	Computation of L_1, L_∞ errors, rate of convergence and CPU time using NSFD1 for $-10 \leq x \leq 10, \gamma = 0.2, h = 0.1, \beta = 2, T = 0.5$	117
5.4	Computation of L_1, L_∞ errors, rate of convergence and CPU time using NSFD2 for $-10 \leq x \leq 10, \gamma = 0.2, h = 0.1, \beta = 0.5, T = 0.5$	121
5.5	Computation of L_1, L_∞ errors, rate of convergence and CPU time using NSFD2 for $-10 \leq x \leq 10, \gamma = 0.2, h = 0.1, \beta = 1, T = 0.5$	121
5.6	Computation of L_1, L_∞ errors, rate of convergence and CPU time using NSFD2 for $-10 \leq x \leq 10, \gamma = 0.2, h = 0.1, \beta = 2.0, T = 0.5$	121
5.7	Computation of L_1 and L_∞ errors, rate of convergence and CPU time using NSFD3 for $-10 \leq x \leq 10, \gamma = 0.2, h = 0.1, \beta = 0.5, T = 0.5$	125
5.8	Computation of L_1 and L_∞ errors, rate of convergence and CPU time using NSFD3 for $-10 \leq x \leq 10, \gamma = 0.2, h = 0.1, \beta = 1, T = 0.5$	125
5.9	Computation of L_1 and L_∞ errors, rate of convergence and CPU time using NSFD3 for $-10 \leq x \leq 10, \gamma = 0.2, h = 0.1, \beta = 2, T = 0.5$	125
5.10	Computation of L_1, L_∞ errors, rate of convergence and CPU time using NSFD4 for $-10 \leq x \leq 10, \gamma = 0.2, h = 0.1, \beta = 0.5, T = 0.5$	129
5.11	Computation of L_1, L_∞ errors, rate of convergence and CPU time using NSFD4 for $-10 \leq x \leq 10, \gamma = 0.2, h = 0.1, \beta = 1, T = 0.5$	129
5.12	Computation of L_1, L_∞ errors, rate convergence and CPU time using NSFD4 for $-10 \leq x \leq 10, \gamma = 0.2, h = 0.1, \beta = 2, T = 0.5$	129

List of Publications

1. Journal

- a) K.M. Agbavon, A.R. Appadu and M. Khumalo, On the numerical solution of Fisher's equation with coefficient of diffusion term much smaller than coefficient of reaction term, *Advances in Difference Equations*, 2019 (2019), 146.
- b) K.M. Agbavon, A.R. Appadu, Construction and analysis of some nonstandard finite difference methods for the FitzHugh-Nagumo equation. *Numerical Methods for Partial Differential Equations* (Under review).

2. Book chapter

K.M. Agbavon, A.R. Appadu and B. Inan, Comparative study of some Numerical methods for the standard FitzHugh-Nagumo equation. Accepted for publication in the book titled: *Communications in Mathematical Computations and Applications*, Springer.

3. Proceedings

A.R. Appadu and K.M. Agbavon, Comparative study of some numerical methods for FitzHugh-Nagumo equation, *Proceedings of the International Conference of Numerical Analysis and Applied Mathematics (ICNAAM 2018)*, Rhodes, 2116, 1, 030036 (2019).

Conferences and Seminars

1. Conferences

- a) 27-29 March 2019: South African Numerical and Applied Mathematics (SANUM) international conference on Data science and mathematical biology, University of Pretoria, Hatfield, Pretoria. Title of the talk: Construction and analysis of some nonstandard finite difference methods for the FitzHugh-Nagumo equation.
- b) 24-29 June 2018: Biomath international conference on Mathematical Methods Models in Bioscience and a School of Young Scientists (SYS) at the Institute of Mechanics of the Bulgarian Academy of Sciences in Sofia, Bulgaria. Title of the talk: Comparison of some numerical methods for the FitzHugh-Nagumo equation.
- c) 25-30 June 2017: Biomath international conference on Mathematical Methods Models in Bioscience and a School of Young Scientists (SYS) at Skukuza Camp in Kruger Park, South Africa. Title of talk: On the Numerical Solution of Fisher's equation and Gray-Scott's equation.

2. Seminars

2016-2019, Tuesday, 3 pm-4 pm: Biomath Coffee seminar.

28- 30 May, 2017-2019: Postgraduate seminar.

Titles of talk:

- a) On the Numerical Solution of Fisher's equation with coefficient of diffusion term much smaller than coefficient of reaction term.
- b) Comparative study of some Numerical methods for the standard FitzHugh-Nagumo equation.
- c) Construction and analysis of some nonstandard finite difference methods for the FitzHugh-Nagumo equation.

Chapter 1

Introduction

The study of nonlinear partial differential equations of phenomena (dispersion, dissipation, diffusion, convection) arising in inhomogeneous system is of huge concern from mathematical, physical and biological points of view. The theoretical design based on nonlinear partial differential equations with varying or non-varying coefficients can precisely portray, for instance, the wave dynamics of pulses circulating in inhomogeneous systems (Triki and Wazwaz, 2013). Remarkably, nonlinear partial differential equations with variable coefficients describe well in diverse physical or material circumstances than their constant coefficients counterparts. The importance is to find closed form solutions for nonlinear partial differential equations of physical or practical suitability. This could be a difficult task and sometimes impossible due to the fact that in many practical problems, the resulting nonlinear partial differential equations of interest are non-integrable. The integrability part of nonlinear partial differential equations is an important concept due to its link with the understanding of the physical and dynamical phenomena in nonlinear systems (Ma, 2005). For instance, the Kuramoto-Sivashinsky equation, the Ginzburg–Landau equation, the Korteweg-de Vries-Burgers equation, the Fisher’s equation, the Burgers-Huxley equation and the FitzHugh-Nagumo equation, just to mention few, are practically well-known equations of this sort (Öziş and Köroğlu, 2009). An exception takes place when a non-integrable nonlinear partial differential equations becomes integrable for some given values of the parameters involved into the equation. In this instance, the exact solutions can be written explicitly. There are various results on local and global solutions of nonlinear partial differential equations that present existence, uniqueness, smoothness and stability of solutions. However none of these results give the standard formulae that solve these nonlinear partial differential equations. Therefore, looking for some exact meaningful solutions is a hot topic because of the wide applications of nonlinear partial differential equations in physics,

chemistry, fluid dynamics, plasma, optical fibers, flame propagation, logistic growth, neurophysiology, brownian motion process, autocatalytic, nuclear reactor theory and biology as well as other areas of engineering (Johnson et al., 2012, Wang et al., 2014). That is why it is necessary to consider the numerical approximation. Meanwhile, many numerical techniques have been developed for solving PDEs. For instance, we can mention the finite difference methods (Strikwerda, 2004), finite element methods (Zienkiewicz et al., 1977), finite volume methods (LeVeque et al., 2002). We can further mention, spectral methods (Chatelin, 1983), meshfree methods (Liu and Gu, 2005). We can also include domain decomposition methods (Toselli and Widlund, 2006), multigrid methods (Rüde, 1993) and many more which are commonly used. Throughout this thesis, some standard finite difference and nonstandard finite difference methods are used to discretize some reaction diffusion equations especially Fisher's equations and FitzHugh-Nagumo equations.

1.1 Why study of Fisher's and FitzHugh-Nagumo equations?

As stated above, the Fisher's equation is one example of partial differential equation model and used to describe a lot of phenomena. The equation incorporates diffusion term and logistic nonlinearity. It was first used by Fisher's to describe the propagation of a mutant gene. The propagation is in form of wave. The wave appears as a result of a balance between weak nonlinearity and dispersion. This wave is characterized by two properties (Hariharan et al., 2009)

- (1) A localized wave propagates without change of its properties like shape, velocity, etc.
- (2) Localized wave are stable against mutual collisions and retain their identities.

It is worthy to notice that the interaction between nonlinear convection with genuine nonlinear dispersion generates waves with compact support called 'compactons' with width independent of the amplitude (contrary to wave that narrows as the amplitude increases). However, when diffusion takes part instead of dispersion, energy release by nonlinearity balances energy consumption by diffusion (Hariharan et al., 2009). More details on the background and how it was solved will be our study in chapter 3.

The pioneering work of Hodgkin and Huxley (1952) in the early 1950's have given the base of good mathematical models for the conduction of nerve impulses along an axon (Keener and Sneyd, 1998). These models take the form of a system of ordinary differential equations, coupled

to a diffusion equation and are hard to analyse. A decade later, [FitzHugh \(1961\)](#) and [Nagumo et al. \(1962\)](#) tackle the same problem (propagation of the nerve impulses along an axon) and their model was simpler and describe the qualitative behaviour. There are two basic problems in the modelling of propagation of the nerve impulses, namely; the threshold problem and the travelling wave problem. The first problem is to prove that small solutions decay to zero as time goes to infinity. This agrees with the biological fact that a minimum stimulus is needed to 'trigger' a nerve; smaller stimuli lead to no signal transmitted down the axon. The second problem falls into two parts. The signals transported by the axon have a characteristic shape and speed. This leads one to investigate whether there are solutions ([Rauch and Smoller, 1978](#)). More investigation is done in chapters 4 and 5.

These two equations are encountered in chemical kinetics and population dynamics, which embody problems such as nonlinear evolution of a population, neutron population in a nuclear reaction, in logistic population growth models, flame propagation, neurophysiology, autocatalytic chemical reactions, and branching Brownian motion processes ([Hariharan et al., 2009](#)). Reasons being, this drew attention to many researchers.

1.2 Contributions of the thesis to the scientific literature

As we stated earlier, our study is based on two major equations, namely; Fisher's equation and FitzHugh-Nagumo equation.

In chapter 3 of our study, we obtain the numerical solution of Fisher's equation when the coefficient of diffusion term is much smaller than the coefficient of reaction ([Li et al., 1998](#)). This problem was solved by [Li et al. \(1998\)](#) based on a method called Moving Mesh Partial Differential Equation (MMPDE) with coefficient of reaction being 10^4 and coefficient of diffusion equal to one and the initial condition consisted of an exponential function. The results obtained by [Li et al. \(1998\)](#) are not efficient because MMPDE is based on familiar arc-length or curvature monitor function. Further investigation was done by [Qiu and Sloan \(1998\)](#) where they constructed a suitable monitor function called modified monitor function. They utilised it with the Moving Mesh Differential Algebraic Equation (MMDAE) method in order to solve the same problem as [Li et al. \(1998\)](#). They obtained better results. However, each problem has its own choice of monitor function. Reason being, the choice of the monitor function is an open question. In our study, we constructed four new numerical methods based on Forward in Time Central Space (FTCS) and the Nonstandard Finite Difference (NSFD) in order to solve the scaled Fisher's

equation. We also use two techniques namely; by introducing artificial viscosity or using the approach of [Ruxun et al. \(1999\)](#). We find that the temporal step size must be very small in order to obtain accurate results and comparable to [Qiu and Sloan \(1998\)](#). This causes the computational time to be long if the domain is large. Our four proposed techniques give efficient and accurate results with a larger temporal step size. We prove that these four methods are consistent with the original partial differential equation.

In chapter 4 of our study, we give an improvement and extension of the work from [Namjoo and Zibaei \(2018\)](#) whereby the standard FitzHugh-Nagumo equation with specified initial and boundary conditions is solved. In their study, [Namjoo and Zibaei \(2018\)](#) constructed two versions of nonstandard finite difference namely; NSFD1, NSFD2. They also constructed two schemes (one explicit and the other implicit) from the exact solution. However, they gave results using the nonstandard finite difference schemes only. In our study, we show that NSFD1 has convergence issues and we give an improvement for NSFD1 called NSFD3. We carry out a stability analysis of the schemes constructed from the exact solution and found that the explicit scheme has stability issue. We investigate the stability, positivity and boundedness the five methods namely; NSFD1, NSFD2, NSFD3, two schemes obtained using the exact solution. We further study the performance of the five methods by computing L_1 , L_∞ errors and the rate of convergence for two values of the threshold of Affect effect, γ namely; 0.001 and 0.5 for small and large spatial domains at time, $T = 1.0$. The study of rate of convergence is justificatory due to the fact that we are dealing with nonlinear partial differential equations and therefore the Lax-Equivalence theorem cannot be used.

In chapter 5, we consider more general consideration of FitzHugh-Nagumo equation with the parameter β referred to as intrinsic growth rate. We chose a numerical experiment which is quite challenging for simulation due to shock-like profiles. In this part of our study, we construct four versions of nonstandard finite difference schemes. We investigate the performance of the four constructed method by computing L_1 , L_∞ errors, rate of convergence with respect to time and CPU time at given time, $T = 0.5$. We use three different values of intrinsic growth rate, β namely; $\beta = 0.5, 1.0, 2.0$.

Chapter 6 is a conclusion of the thesis with future research directions.

Chapter 2

Mathematical preliminaries

In this chapter, we give some concepts on standard finite difference, nonstandard finite difference, reaction diffusion equation and singularly perturbed equations.

2.1 Finite difference methods

Some of the main references used for this chapter are from [Strikwerda \(2004\)](#), [Ames \(2014\)](#) and [Frey \(2019\)](#). Finite Difference Method (FDM) is one of the methods used to solve differential equations that are difficult or impossible to solve analytically. The concept of FDM is focused on approximating differentials. The most commonly used are central finite difference schemes, forward finite difference schemes, backward finite difference schemes.

2.1.1 General formulation

The formulation of finite difference methods is almost the same as the numerical schemes used to solve ordinary differential equations. It entails approximating the differential operator by substituting the derivatives in the differential equation using finite difference quotients. The domain is divided in space and in time and approximations are evaluated in space or in time. The error between the numerical solution and the exact solution is defined by the error that is introduced by going from a differential operator to a difference operator. This type of error is called discretization error or truncation error. For instance for 1D partial differential equation on the interval (α, β) , $\alpha < \beta$, the points, $x_m = \alpha + m h$, $t_n = n k$, $m = 0, 1, \dots, N$, $n = 0, 1, \dots$, are called grid points where $h = \frac{\beta - \alpha}{N}$ and k is time step size. The finite difference solution, denoted by u_m^n , is the approximation of the solution at the grid point (x_m, t_n) as shown in Figure 2.1. For the sake of clarity and simplicity, we shall treat the one-dimensional case only.

For any finite difference scheme, the major insight behind is in regard of the definition of a smooth function u , at a point $x \in \mathbb{R}$:

$$u'(x) = \lim_{h \rightarrow 0} \frac{u(x+h) - u(x)}{h}, \quad (2.1)$$

and to the fact that h tends to 0 without vanishing and also h should be sufficiently small to get a good approximation (the error computed in this approximation goes to zero when h tends towards zero). For the adequately smooth function u in the neighbourhood of x , this error is quantified by using a Taylor expansion.

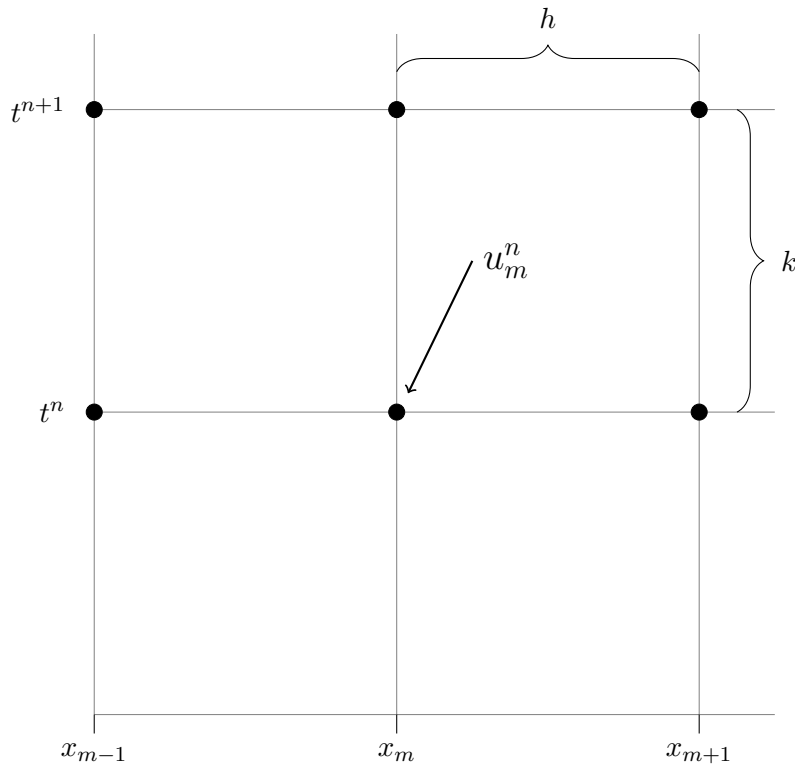


Figure 2.1: One dimensional finite difference discretization

Taylor series

Definition 2.1. A continuous function u is of class C^n if the first up to n th derivative of the function u exist and are continuous.

Consider a continuous function u of class C^2 in the neighbourhood of x . For any $h > 0$ and sufficiently small, we have

$$\left| \frac{u(x+h) - u(x)}{h} - u'(x) \right| \leq Ch, \quad C = \sup_{y \in [x, x+h_0]} \frac{|u''(y)|}{2}, \quad (2.2)$$

for $h \leq h_0$ ($h_0 > 0$ given). This approximation is called forward difference. We can also define the backward difference in the same way by taking the point $x - h$. More generally, we define an approximation of order p of the derivative.

Definition 2.2 (Frey (2019)). *The approximation of the derivative u' at point x is of order p ($p > 0$) if there exists a constant $C > 0$, independent of h , such that the error between the derivative and its approximation is bounded by Ch^p which is $O(h^p)$.*

Evidently, other approximations can be taken into consideration. In order to boost the accuracy of the approximation, we make clear an approximation, called the central difference approximation, by taking the points $x - h$ and $x + h$ into account.

For $\forall h \in (0, h_0)$, we have

$$\left| \frac{u(x+h) - u(x-h)}{2h} - u'(x) \right| \leq Ch^2, \quad C = \sup_{y \in [x-h_0, x+h_0]} \frac{|u^{(3)}(y)|}{6}, \quad (2.3)$$

which defines the second order approximation of u' .

Lemma 2.1 (Frey (2019)). *Suppose u is continuous function of class C^4 on an interval $[x - h_0, x + h_0]$, $h_0 > 0$. Then, there exists a constant $C > 0$ such that for every $\forall h \in (0, h_0)$ we have*

$$\left| \frac{u(x+h) - 2u(x) + u(x-h)}{h^2} - u''(x) \right| \leq Ch^2, \quad C = \sup_{y \in [x-h_0, x+h_0]} \frac{|u^{(4)}(y)|}{12}. \quad (2.4)$$

The differential quotient $\frac{u(x+h) - 2u(x) + u(x-h)}{h^2}$ is a consistent second-order approximation of the second derivative u'' of u at point x .

Remark 2.1. *The order estimate depends on the regularity of the function u . For instance if a continuous u is of class C^2 or C^3 , then the error is respectively of order one or h only.*

Finite difference formulation for a one-dimensional problem

We consider a bounded domain $\Omega = (0, 1) \subset \mathbb{R}$ and $u : \bar{\Omega} \rightarrow \mathbb{R}$ solving the non-homogeneous Dirichlet problem:

$$\begin{cases} -u''(x) + c(x)u(x) = f(x), & x \in (0, 1), \\ u(0) = \alpha, \quad u(1) = \beta, \end{cases} \quad (2.5)$$

where c and f are two given functions, defined on $\bar{\Omega}$, $c \geq 0$.

Variational theory and approximation

We know that if $c \in \mathcal{L}^\infty(\Omega)$ and $f \in \mathcal{L}^2(\Omega)$, then the solution u of the problem (2.5) exists. Moreover, if $c = 0$, the explicit formularization of u is

$$u(x) = \int_{\Omega} K(x, y) f(y) dy + \alpha + x(\beta - \alpha), \quad K(x, y) = \begin{cases} x(1 - y) & \text{if } y \geq x, \\ y(1 - x) & \text{if } y < x. \end{cases} \quad (2.6)$$

Still, when $c \neq 0$, then there is no explicit expression for the solution u . Hence the necessity for numerical approximation of the solution u . The equidistributed grid points are introduced $(x_m)_{0 \leq m \leq N+1}$ and are determined by $x_m = mh$, where N is an integer and the spacing h , is $h = \frac{1}{N+1}$. The points x_0 and x_{N+1} , are such that $x_0 = 0$ and $x_{N+1} = 1$ at the boundary of Ω . Furthermore, at each point, the numerical value of the solution, $u_m = u(x_m)$ is the principal objective to find. In that way, $u(x_0)$ and $u(x_{N+1})$ are set to be $u(x_0) = \alpha$ and $u(x_{N+1}) = \beta$.

Remark 2.2. *The fundamental idea of the finite difference estimation is the numerical solution is not specified on the full domain Ω but at a finite number of points in Ω only.*

Finite difference scheme

Assuming the function c and f are at least such that $c, f \in C^0(\bar{\Omega})$ and the vector $u_h \in \mathbb{R}^N$ (components $u_m, m \in \{1, 2, \dots, N\}$), where u is the solution of problem (2.5).

$$\begin{cases} -\frac{u_{m+1} - 2u_m + u_{m-1}}{h^2} + c(x_m)u_m = f(x_m), & m \in \{1, \dots, N\}, \\ u_0 = \alpha, \quad u_{N+1} = \beta, \end{cases} \quad (2.7)$$

which can be rewritten

$$A_h u_h = b_h, \quad (2.8)$$

where A_h is the tridiagonal matrix defined as

$$A_h = A_h^{(0)} + \begin{pmatrix} c(x_1) & 0 & \cdots & 0 \\ 0 & c(x_2) & \cdots & \vdots \\ \vdots & \vdots & c(x_{N-1}) & \vdots \\ 0 & 0 & \cdots & c(x_N) \end{pmatrix} \quad (2.9)$$

with

$$A_h^{(0)} = \frac{1}{h^2} \begin{pmatrix} 2 & -1 & 0 & \cdots & 0 \\ -1 & 2 & -1 & \ddots & \vdots \\ \vdots & \ddots & \ddots & \ddots & \vdots \\ \vdots & \ddots & -1 & 2 & -1 \\ 0 & \cdots & 0 & -1 & 2 \end{pmatrix} \text{ and } b_h = \begin{pmatrix} f(x_1) + \frac{\alpha}{h^2} \\ f(x_2) \\ \vdots \\ f(x_{N-1}) \\ f(x_N) + \frac{\beta}{h^2} \end{pmatrix}. \quad (2.10)$$

The issue raised by the consideration of Eq. (2.8) is associated to the existence of a solution. In other words, we have to find if the matrix A_h is invertible or not. The following proposition is the answer to the issue.

Proposition 2.1 (Frey (2019)). *Suppose $c \geq 0$. Then, the matrix A_h is symmetric positive definite.*

Proof. By observation, A_h is symmetric. Consider a vector $v = (v)_{1 \leq m \leq N} \in \mathbb{R}^N$. Since $c \geq 0$, we have

$$v^t A_h v = v^t A_h^0 v + \sum_{m=1}^N c(x_m) v_m^2 \geq v^t A_h^0 v.$$

We just need to show that A_h^0 is positive definite. It follows that

$$h^2 v^t A_h v = x_1^2 + (x_2 - x_1)^2 + \cdots + (x_N - x_{N-1})^2 + x_N^2.$$

Hence $v^t A_h v \geq 0$.

Furthermore, if $v^t A_h v = 0$ then all term, $x_1^2 + (x_2 - x_1)^2 x_{m-1} - x_m = x_1 = x_N = 0$. We conclude that all $x_m = 0$. Hence the result. \square

Remark 2.3. *We note $u(x)$ is the exact solution of the problem (2.5). $u_m = u(x_m)$, is the numerical solution at x_m of (2.5). At $x = x_m$, $u(x_m)$ is the exact solution. We note, $U_m = U(x_m)$ the numerical solution that approximates $u_m = u(x_m)$ at $x = x_m$.*

Remark 2.4. *Summary for the notation of finite differences for the problem (2.5):*

Theory (continuous)	Finite differences (discrete)
domain $\Omega = [0, 1]$	$I_N = \{0, \frac{1}{N+1}, \dots, 1\}$
Unknown $u : [0, 1] \rightarrow \mathbb{R}$, $u \in C^2(\Omega)$	$U_h = (U_1, \dots, U_N) \in \mathbb{R}^N$
Conditions $u(0) = \alpha$, $u(1) = \beta$	$U_0 = \alpha$, $U_{N+1} = \beta$
equation $-u'' + cu = f$	$-\frac{U_{m+1} - 2U_m + U_{m-1}}{h^2} + c(x_m)U_m = f(x_m)$

Consistent scheme

The concept of consistency and accuracy enables to understand how well a numerical scheme approximates an equation. A formal definition of the consistency is introduced and can be utilized for any partial differential equation defined on a domain Ω such that

$$(Lu)(x) = f(x), \quad \forall x \in \Omega,$$

where L is assumed to be differential operator and Lu states that the equation relies on u and on its derivatives at any point x . For every index m , a numerical approximation can be recorded as

$$(L_h u)(x_m) = f(x_m), \quad \forall m \in \{1, \dots, N\}.$$

L_h is the differential operator. For instance the problem (2.5) can be written in the form

$$\begin{aligned} (Lu)(x) &= -u''(x) + c(x)u(x) \text{ and} \\ (L_h u)(x_m) &= -\frac{u(x_{m+1}) - 2u(x_m) + u(x_{m-1}))}{h^2} + c(x_m)u(x_m), \quad \forall m \in \{1, \dots, N\}. \end{aligned} \quad (2.11)$$

Definition 2.3. A finite difference scheme is said to be consistent with the partial differential equation it represents, if for any sufficiently smooth solution u of this equation, the truncation error of the scheme, corresponding to the vector $\epsilon_h \in \mathbb{R}^N$ whose components are defined as:

$$(\epsilon_h)_m = (L_h u)(x_m) - f(x_m), \quad \forall m \in \{1, \dots, N\}, \quad (2.12)$$

goes uniformly towards zero with respect to x , when h tends to zero, i.e. if

$$\lim_{h \rightarrow 0} \|\epsilon_h\| = 0.$$

Furthermore, if there exists a constant $C > 0$, independent of u and its derivatives, such that, for all $h \in (0, h_0)$ ($h_0 > 0$ given) we have:

$$\|\epsilon_h\| \leq Ch^p,$$

with $p > 0$, then the scheme is said to be accurate of order p for the norm $\|\cdot\|$.

For example, the numerical scheme (2.7) is consistent and second order accurate in space for the norm $\|\cdot\|_\infty$. Indeed assume $u \in C^4(\Omega)$ and $-u'' + cu = f$. It follows

$$\begin{aligned} (\epsilon_h)(x_m) &= -\frac{u(x_{m+1}) - 2u(x_m) + u(x_{m-1}))}{h^2} + c(x_m)u(x_m) - f(x_m) \\ &= -u''(x_m) + \frac{h^2}{12}u^{(4)}(\zeta_m) + c(x_m)u(x_m) - f(x_m) \\ &= \frac{h^2}{12}u^{(4)}(\zeta_m) \end{aligned} \quad (2.13)$$

where $\zeta_m \in (x_{m-1}, x_{m+1})$. Thus

$$\|\epsilon_h\|_\infty \leq \frac{h^2}{12} \sup_{y \in \Omega} |u^{(4)}(y)|. \quad (2.14)$$

Finite difference scheme for time-dependent problems

We start defining the grid points in the (t, x) plane in the analysis of finite difference schemes. Let h and k be positive numbers; thus the grid will be the points $(t_n, x_m) = (nk, mh)$ for integers n and m arbitrarily chosen. For any function v such that on the grid (nk, mh) , we write v_m^n to denote v at the grid point (t_n, x_m) . The notation u_m^n for $u(t_n, x_m)$ is also used when u is defined for continuously varying (t, x) . The interest is in grids with small values of h and k . In many cases, the quantities that called h and k , are denoted by Δx and Δt respectively. The fundamental idea of finite difference schemes is to substitute derivatives by finite differences. Here are two examples of approximations:

$$\begin{aligned} \frac{\partial u}{\partial t} &\simeq \frac{u(t_n + k, x_m) - u(t_n, x_m)}{k} \quad \text{or} \\ &\simeq \frac{u(t_n + k, x_m) - u(t_n - k, x_m)}{2k}, \end{aligned} \quad (2.15)$$

$$\begin{aligned} \frac{\partial u}{\partial t} &\simeq \frac{u(t + k, x) - u(t, x)}{k} \quad \text{or} \\ &\simeq \frac{u(t + k, x) - u(t - k, x)}{2k}. \end{aligned} \quad (2.16)$$

Example 2.1. We give some useful schemes for the approximation of the advection equation

$$u_t + a u_x = 0, \quad (2.17)$$

where a stands for the wave speed, t represents time, and x represents the spatial variable:

Numerical scheme	Name of the scheme
$\frac{u_m^{n+1} - u_m^n}{k} + a \frac{u_{m+1}^n - u_m^n}{h} = 0$	Forward-time forward-space scheme
$\frac{u_m^{n+1} - u_m^n}{k} + a \frac{u_m^n - u_{m-1}^n}{h} = 0$	Forward-time backward-space scheme
$\frac{u_m^{n+1} - u_m^n}{k} + a \frac{u_{m+1}^n - u_{m-1}^n}{2h} = 0$	Forward-time central-space scheme
$\frac{u_m^{n+1} - u_{m-1}^n}{2k} + a \frac{u_{m+1}^n - u_{m-1}^n}{2h} = 0$	Leapfrog scheme
$\frac{u_m^{n+1} - (u_{m+1}^n - u_{m-1}^n)}{k} + a \frac{u_{m+1}^n - u_{m-1}^n}{2h} = 0$	Lax-Friedrichs scheme

Example 2.2 (Recktenwald (2004)). We consider one dimensional transient heat conduction equation in slab of material with thickness L . defined by

$$u_t = \alpha u_{xx}, \quad 0 \leq x \leq L, \quad t \geq 0,$$

where $u = u(t, x)$ is an unknown variable, and α is a constant coefficient. The domain of the solution is a semi-infinite strip of width L that continues indefinitely in time. The material property α is the thermal diffusivity. In practice, the solution is obtained only for a finite time. The solution to the heat equation demands specification of boundary conditions at $x = 0$ and $x = L$, and initial conditions at $t = 0$. Simple boundary and initial conditions are $u(t, 0) = u_0$, $u(t, L) = u_L$, $u(0, x) = f_0(x)$ (Neumann or mixed boundary conditions can be specified).

Numerical scheme	Name of the scheme
$\frac{u_m^{n+1} - u_m^n}{k} + \alpha \frac{u_{m+1}^n - 2u_m^n + u_{m-1}^n}{h^2} = 0$	Forward-time, Centered Space approximation
$\frac{u_m^n - u_{m-1}^n}{k} + \alpha \frac{u_{m-1}^n - 2u_m^n + u_{m+1}^n}{h^2} = 0$	Backward-time, Centered Space approximation
$-\frac{\alpha}{2h^2}u_{m-1}^n + \left(\frac{1}{k} + \frac{\alpha}{h^2}\right)u_m^n - \frac{\alpha}{2h^2}u_{m+1}^n$ $=$ $\frac{\alpha}{2h^2}u_{m-1}^{n-1} + \left(\frac{1}{k} - \frac{\alpha}{h^2}\right)u_{m-1}^n + \frac{\alpha}{2h^2}u_{m+1}^{n-1}$	Crank-Nicolson approximation

Convergence and Consistency

The most fundamental property that a scheme must have so as to be convergent is that its solutions approximate the solution of the given partial differential equation and that the approximation enhances as the grid spacings, h and k , go towards zero. Before any discussion, we consider linear partial differential equations of the form

$$P(\partial_t, \partial_x) = f(t, x). \quad (2.18)$$

Definition 2.4 (Strikwerda (2004)). A one-step finite difference scheme approximating a partial differential equation is a convergent scheme if for any solution to the partial differential equation, $u(t, x)$, and solutions to the finite difference scheme, v_m^n , such that v_m^0 converges to $u_0(x)$ as mh converges to x , then v_m^n converges to $u(t, x)$ as (nk, mh) converges to (t, x) as h, k converge to 0.

Showing that any given scheme is convergent is not straightforward in general. Nevertheless, there are two concepts which are easy to check: consistency and stability. First, we define consistency.

Definition 2.5. Assume $Pw = f$, is a partial differential equation and $P_{k,h}$, a finite difference scheme. We say that the finite difference scheme is consistent with the partial differential equation if for any smooth function w at (t, x) ,

$$Pw - P_{k,h}w \rightarrow 0, \text{ as } k, h \rightarrow 0.$$

Example 2.3 (Forward-time forward-space scheme).

$$Pw = w_t + w_x, \text{ where the operator } P, \text{ is } P = \partial_t + \partial_x.$$

We also have

$$P_{k,h}w = \frac{w_m^{n+1} - w_m^n}{k} + a \frac{w_{m+1}^n - w_m^n}{h}, \text{ where } w_m^n, \text{ is } w_m^n = w(nk, mh).$$

Taylor series of the function ϕ in t and x about (t_n, x_m) gives

$$\begin{aligned} w_m^{n+1} &= w_m^n + k w_t + \frac{1}{2} k^2 w_{tt} + O(k^3), \\ w_{m+1}^n &= w_m^n + h w_x + \frac{1}{2} h^2 w_{xx} + O(h^3), \end{aligned} \tag{2.19}$$

and it follows that

$$P_{k,h}w = w_t + a w_x + \frac{1}{2} k w_{tt} + \frac{1}{2} a h w_{xx} + O(k^2) + O(h^2).$$

Thus

$$Pw - P_{k,h}w \rightarrow 0 \text{ as } k \rightarrow 0 \text{ and } h \rightarrow 0.$$

Hence, the consistency.

Remark 2.5 (Strikwerda (2004)). Consistency signifies that the smooth solution of the partial differential equation is an approximate solution of the finite difference scheme. Likewise, convergence implies that a solution of the finite difference scheme is an approximate solution of the partial differential equation. Consistency is not sufficient condition for a scheme to be convergent but it is certainly necessary.

Stability

A scheme must verify other conditions apart from consistency for it to be convergent. The definition which follows for stability is for the homogeneous initial value problem.

Definition 2.6 (Strikwerda (2004)). *A finite difference scheme $P_{k,h}v_m^n = 0$ for a first-order equation is stable in a stability region Λ if there is an integer J such that for any positive time T , there is a constant C_T such that*

$$h \sum_{m=-\infty}^{+\infty} |v_m^n|^2 \leq C_T h \sum_{j=0}^J \sum_{m=-\infty}^{+\infty} |v_m^j|^2, \quad 0 \leq nT \leq T, \quad \text{with } (k, h) \in \Lambda, \quad (2.20)$$

which is equivalent to

$$\|v^n\|_h \leq \left(C_T \sum_{j=0}^J \|v^j\|_h^2 \right)^{\frac{1}{2}}, \quad \|w\|_h = \left(h \sum_{m=-\infty}^{+\infty} |w_m|^2 \right)^{\frac{1}{2}}, \quad \text{for any grid function } w. \quad (2.21)$$

Example 2.4 (Sufficient condition for stability for forward-time forward-space scheme). *Consider the scheme of the form*

$$w_m^{n+1} = \alpha w_m^n + \beta w_{m+1}^n.$$

The scheme is stable under the condition $|\alpha| + |\beta| \leq 1$. Indeed, using the Definition 2.6, we have

$$\begin{aligned} \sum_{m=-\infty}^{+\infty} |w_m^{n+1}|^2 &= \sum_{m=-\infty}^{+\infty} |\alpha w_m^n + \beta w_{m+1}^n|^2 \\ &\leq \sum_{m=-\infty}^{+\infty} (|\alpha|^2 |w_m^n|^2 + |\alpha||\beta|(|w_m^n|^2 + |w_{m+1}^n|^2) + |\beta|^2 |w_{m+1}^n|^2), \end{aligned} \quad (2.22)$$

where $2|\alpha||\beta||w_m^n||w_{m+1}^n| \leq |\alpha||\beta|(|w_m^n|^2 + |w_{m+1}^n|^2)$. The sum can be divided over the terms with indices m and $m+1$ and the index can be displaced so that all terms have the index m :

$$\begin{aligned} \sum_{m=-\infty}^{+\infty} (|\alpha|^2 |w_m^n|^2 + |\alpha||\beta|(|w_m^n|^2 + |w_{m+1}^n|^2) + |\beta|^2 |w_{m+1}^n|^2) &= \sum_{m=-\infty}^{+\infty} (|\alpha|^2 |w_m^n|^2 + |\alpha||\beta||w_m^n|^2) \\ &\quad + \sum_{m=-\infty}^{+\infty} (|\alpha||\beta||w_{m+1}^n|^2 + |\beta|^2 |w_{m+1}^n|^2), \\ &= \sum_{m=-\infty}^{+\infty} (|\alpha|^2 + 2|\alpha||\beta| + |\beta|^2) |w_m^n|^2, \\ &= \sum_{m=-\infty}^{+\infty} (|\alpha| + |\beta|)^2 |w_m^n|^2. \end{aligned} \quad (2.23)$$

Hence

$$\sum_{m=-\infty}^{+\infty} |w_m^{n+1}|^2 \leq (|\alpha| + |\beta|)^{2n} \sum_{m=-\infty}^{+\infty} |w_m^n|^2, \quad \forall n. \quad (2.24)$$

It follows

$$\sum_{m=-\infty}^{+\infty} |w_m^n|^2 \leq (|\alpha| + |\beta|)^{2n} \sum_{m=-\infty}^{+\infty} |w_m^0|^2, \quad (2.25)$$

The quantity $|\alpha| + |\beta|$ is at most 1 in magnitude. Thus scheme is stable.

Remark 2.6 (Strikwerda (2004)). The notion of stability for finite difference schemes is thoroughly on familiar terms to the notion of well-posedness for initial value problems for partial differential equations ($Pu = f$).

Definition 2.7 (Strikwerda (2004)). The initial value problem for the first-order partial differential equation $Pu = 0$ is well-posed if for any time $T > 0$, there is a constant C_T such that any solution $u(t, x)$ satisfies

$$\int_{-\infty}^{+\infty} |u(t, x)|^2 dx \leq C_T \int_{-\infty}^{+\infty} |u(0, x)|^2 dx, \quad 0 \leq t \leq T. \quad (2.26)$$

Theorem 2.1 (The Lax equivalence theorem, Strikwerda (2004)). A consistent finite difference scheme for a linear partial differential equation for which the initial value problem is well-posed is convergent if and only if it is stable.

Remark 2.7 (Strikwerda (2004)). The Lax equivalence theorem is an example of the top-dog kind of mathematical theorem. It brings back a substantial notion that is arduous to define straightforward with other notions that are comparatively simple to check. The utility of the Lax theorem emerges both from the fluency of checking consistency and stability and the relationship between these notions and the notion of convergence.

Theorem 2.2 (The Courant-Friedrichs-Lewy Condition, Strikwerda (2004)). For an explicit scheme for an hyperbolic equation (2.17) of the form $w_m^{n+1} = \alpha w_{m-1}^n + \beta w_m^n + \gamma w_{m+1}^n$ with $\frac{k}{h} = \lambda$ held constant, a necessary condition for stability is the Courant-Friedrichs-Lewy (CFL) condition

$$|a \lambda| \leq 1.$$

For systems of equations for which p is a vector and α , β and γ are matrices, we must have $|a_i \lambda| \leq 1$ for all eigenvalues a_i of the matrix A .

Theorem 2.3. There are no explicit, unconditionally stable, consistent finite difference schemes for hyperbolic systems of partial differential equations.

Fourier Analysis

In this section, we introduce and bring to knowledge the fundamental properties of Fourier analysis, which is a substantial tool for studying finite difference schemes and their solutions. The Fourier transform, $\hat{u}(x)$ for a function, $u(x)$ defined on the real line \mathbb{R} , is

$$\hat{u}(y) = \frac{1}{\sqrt{2\pi}} \int_{-\infty}^{+\infty} e^{-iyx} u(x) dx, \quad (2.27)$$

and the Fourier inversion formula, is stated by

$$u(x) = \frac{1}{\sqrt{2\pi}} \int_{-\infty}^{+\infty} e^{iw x} \hat{u}(y) dy. \quad (2.28)$$

Example 2.5 (Example of the Fourier transform). *Consider the function*

$$u(x) = \begin{cases} e^{-x} & \text{if } x \geq 0, \\ 0 & \text{if } x < 0. \end{cases} \quad (2.29)$$

We have

$$\hat{u}(y) = \frac{1}{\sqrt{2\pi}} \int_0^{+\infty} e^{-iyx} e^{-x} dx = \frac{1}{\sqrt{2\pi}} \frac{1}{1+iy}. \quad (2.30)$$

We define the grid of integers, $h\mathbb{Z}$ by $h\mathbb{Z} = \{hm : m \in \mathbb{Z}\}$. If the spacing between the grid points is h , a change on variables can be made and the Fourier transform is

$$\hat{u}(x) = \frac{1}{\sqrt{2\pi}} \sum_{m=-\infty}^{+\infty} e^{-imhw} h u_m, \quad w \in [-\pi/h, \pi/h], \quad (2.31)$$

and the inversion formula is

$$u_m = \frac{1}{\sqrt{2\pi}} \int_{-\pi/h}^{\pi/h} e^{imh\xi} \hat{u}(w) dw, \quad w \in [-\pi/h, \pi/h]. \quad (2.32)$$

Remark 2.8 (Strikwerda (2004)). *Fourier transform is unique.*

Remark 2.9 (Strikwerda (2004)). *A substantial end result of the preceding definitions is that the L_2 norm of u which is*

$$\|u\|_2 = \left(\int_{-\infty}^{+\infty} |u(x)|^2 dx \right)^{1/2} \quad (2.33)$$

is the same L_2 norm of \hat{u} ie

$$\|\hat{u}\|_h^2 = \int_{-\pi/h}^{\pi/h} |u(w)|^2 dw = \|u\|_2^2.$$

Indeed using the Parseval's relation for functions in $L_2(h\mathbb{Z})$, we have

$$\begin{aligned}
\|\hat{u}\|_h^2 &= \int_{-\pi/h}^{\pi/h} |\hat{u}(w)|^2 dw = \int_{-\pi/h}^{\pi/h} \frac{\hat{u}(w)}{\sqrt{2\pi}} \frac{1}{\sqrt{2\pi}} \sum_{m=-\infty}^{+\infty} e^{-imhw} dw u_m h \\
&= \frac{1}{\sqrt{2\pi}} \sum_{m=-\infty}^{+\infty} \int_{-\pi/h}^{\pi/h} e^{-imhw} \overline{\hat{u}(w)} dw u_m h \\
&= \sum_{m=-\infty}^{+\infty} \frac{1}{\sqrt{2\pi}} \int_{-\pi/h}^{\pi/h} e^{-imhw} \hat{u}(w) dw u_m h = \sum_{m=-\infty}^{+\infty} \overline{u_m} u_m h \\
&= \|u\|_h^2.
\end{aligned} \tag{2.34}$$

Von Neumann Analysis

A substantial application of Fourier analysis is the Von Neumann analysis of stability of finite difference schemes. With the usage of Fourier analysis, the necessary and sufficient conditions can be given for the stability of finite difference schemes.

Remark 2.10 (Strikwerda (2004)). *The Von Neumann method is simpler to use and is more popular than other methods used for stability. By means of the Fourier transform, the determination of the stability of a scheme is shortened to comparatively easy algebraic considerations.*

Before further discussion, we consider forward-time backward-space scheme

$$u_m^{n+1} = (1 - a\lambda) u_m^n + a\lambda u_{m-1}^n, \quad \lambda = \frac{k}{h}, \tag{2.35}$$

From inversion formula of Fourier transform (2.32), we have used $u_j = \frac{1}{\sqrt{2\pi}} \int_{-\pi/h}^{\pi/h} e^{ijhw} \hat{u}(w) dw$, with $j = m - 1, m$ and substituting in (2.36)

$$u_m^{n+1} = \frac{1}{\sqrt{2\pi}} \int_{-\pi/h}^{\pi/h} e^{imhw} [1 - a\lambda + a\lambda e^{-ihw}] \hat{u}^n(w) dw, \tag{2.36}$$

and comparing it to inversion formula

$$u_m^{n+1} = \frac{1}{\sqrt{2\pi}} \int_{-\pi/h}^{\pi/h} e^{imhw} \hat{u}^{n+1}(w) dw. \tag{2.37}$$

Since from (5.9), the Fourier transform is unique, we deduce

$$\begin{aligned}
\hat{u}_m^{n+1}(w) &= [1 - a\lambda + a\lambda e^{-ihw}] \hat{u}^n(w) \\
&= \xi(hw) \hat{u}^n(w), \quad \text{with } g(hw) = 1 - a\lambda + a\lambda e^{-ihw}.
\end{aligned} \tag{2.38}$$

Since the statement (2.38) is true for all n , we have

$$\hat{u}_m^n(w) = [\xi(hw)]^n \hat{u}^0(w). \tag{2.39}$$

Remark 2.11 (Strikwerda (2004)). *The function w is called amplification factor due to the fact that its magnitude is the measure that the amplitude of each rate or frequency in the solution, given by $\hat{u}^n(w)$, is intensified in advancing the solution one time step. Furthermore, for the wide variety of schemes the information about them are contained in their amplification factor in particular the stability and accuracy.*

For studying the well-posedness of the equation (2.39), we use the definition 2.20 and Parseval's relation,

$$\begin{aligned} h \sum_{m=-\infty}^{+\infty} |u_m^n|^2 &= \int_{-\pi/h}^{\pi/h} |\hat{u}^n(w)|^2 dw \\ &= \int_{-\pi/h}^{\pi/h} |\xi(hw)|^{2n} |\hat{u}^0(w)|^2 dw. \end{aligned} \quad (2.40)$$

Therefore we notice that the stability inequality (2.20) will satisfy, with $J = 0$, if $|\xi(hw)|^{2n}$ is suitably bounded. We just need to evaluate $|\xi(\theta)| = |\xi(hw)| = |1 - a\lambda + a\lambda e^{-i\theta}|$ with $\theta = hw$ and $e^{-i\theta} = \cos(\theta) - i \sin(\theta)$.

$$|\xi(\theta)|^2 = (1 - a\lambda + a\lambda \cos(\theta))^2 + a^2 \lambda^2 \sin^2(\theta) \quad (2.41)$$

$$= 1 - 4a\lambda(1 - a\lambda) \sin^2\left(\frac{\theta}{2}\right) \quad (2.42)$$

We have the boundedness of $|\xi(\theta)|$ if only $0 \leq a\lambda \leq 1$. Therefore

$$h \sum_{m=-\infty}^{+\infty} |u_m^n|^2 \leq \int_{-\pi/h}^{\pi/h} |\hat{u}^0(w)|^2 dw \quad (2.43)$$

$$= h \sum_{m=-\infty}^{+\infty} |u_m^0|^2. \quad (2.44)$$

Hence the definition 2.6.

Remark 2.12 (Strikwerda (2004)). *If $a\lambda$ does not belong to the interval $[0, 1]$ and λ is fixed as h and k goes toward zero, then $|\xi(\theta)|$ is greater than one for some values of θ , and the scheme is unstable.*

The Stability Condition

The following theorem gives the exact condition for stability of constant coefficient one-step schemes. Despite the fact that in the example we evaluated, the amplification factor ξ was a function only of $\theta = hw$, mostly ξ will also depend on h and k . Generally, to permit for more

equations to satisfy inequality (2.20) in the Definition 2.6, we have to permit the magnitude of the amplification factor to exceed one by a small amount.

Theorem 2.4 (Strikwerda (2004)). *A one-step finite difference scheme (with constant coefficients) is stable in a stability region Λ if and only if there is a constant K (independent of θ , k , and h) such that*

$$|\xi(\theta, k, h)| \leq 1 + K k, \quad (2.45)$$

with $(k, h) \in \Lambda$. If $\xi(\theta, k, h)$ is independent of h and k , the stability condition (2.45) can be replaced with the restricted stability condition

$$|\xi(\theta)| \leq 1. \quad (2.46)$$

Corollary 2.1 (Strikwerda (2004)). *If a scheme as in Theorem 2.4 is modified so that the modifications result only in the addition to the amplification factor of terms that are $O(k)$ uniformly in w , then the modified scheme is stable if and only if the original scheme is stable.*

Proof of Theorem 2.4. Let $|\xi(\theta, k, h)| \leq 1 + K k$ with $(k, h) \in \Lambda$. By Parseval's relation and the definition of ξ , we have that

$$\|u^n\|_h^2 = \int_{-\pi/h}^{\pi/h} |\xi(hw, k, h)|^{2n} |\hat{u}^0(w)|^2 dw,$$

and it follows that

$$\|u^n\|_h^2 \leq \int_{-\pi/h}^{\pi/h} (1 + K k)^{2n} |\hat{u}^0(w)|^2 dw = (1 + K k)^{2n} \|u^0\|_h^2.$$

For $n \leq T/k$ in the inequality (2.20) of the Definition 2.6, we have

$$(1 + K k)^n \leq (1 + K k)^{T/k} \leq e^{K k}.$$

Hence $\|u^n\|_h \leq e^{K k} \|u^0\|_h$ and the Definition 2.20 is satisfied. Thus the scheme is stable.

Assume there is a positive constant C such that $|\xi(\theta, k, h)| > 1 + C k$ with $(k, h) \in \Lambda$. There is an interval of θ such that $\theta \in [\theta_1, \theta_2]$ and then we construct a function u_m^0 , as

$$\hat{u}^0(w) = \begin{cases} 0 & \text{if } hw \notin [\theta_1, \theta_2], \\ \sqrt{h(\theta_2 - \theta_1)^{-1}} & \text{if } hw \in [\theta_1, \theta_2]. \end{cases}$$

$$\begin{aligned} \|u^n\|_h^2 &= \int_{-\pi/h}^{\pi/h} |\xi(hw, k, h)|^{2n} |\hat{u}^0(w)|^2 dw = \int_{-\theta_1/h}^{\theta_2/h} |\xi(hw, k, h)|^{2n} \frac{h}{\theta_2 - \theta_1} dw \\ &\geq (1 + C k)^{2n} \geq \frac{1}{2} e^{2CT} \|u^0\|_h^2, \text{ for } n \text{ near } T/k. \end{aligned}$$

Which proves that the scheme is unstable if C can be arbitrarily large. Hence the scheme is unstable if there is no domain in which $\xi(\theta, k, h)$ can be bounded.

For the inequality (2.46), we use the Taylor series of $\xi(\theta, k, h)$ in k and h , we have

$$\xi(\theta, k, h) = \xi(\theta, 0, 0) + O(h) + O(k).$$

If $h = \lambda^{-1} k$, then the term that $O(h)$ are also $O(k)$. Moreover, since θ is restricted to the compact set $[-\pi, \pi]$, the $O(k)$ terms are uniformly bounded. Therefore by the Corollary 2.4 the stability condition is

$$|\xi(\theta, 0, 0)| \leq 1 + K k,$$

But the left-hand side of the above relation is independent of k , and the inequality must fulfil for all small positive values of k . We have, thus, that the preceding valuation holds if and only if

$$|\xi(\theta, 0, 0)| \leq 1.$$

Hence the stability condition (2.46) in the Theorem 2.4.

□

Remark 2.13 (Strikwerda (2004)). *We remark:*

1. *This theorem shows that to find the stability of a finite difference scheme we need to consider only the amplification factor $\xi(\omega h)$.*
2. *If we consider the forward-time forward-space scheme for which the amplification factor is $\xi(\omega h) = 1 + a \lambda + a \lambda e^{i\theta}$, $\theta = \omega h$ and $|\xi(\theta)|^2 = 1 + 4 a \lambda (1 + a \lambda) \sin^2(\frac{\theta}{2})$ where a is positive and λ is constant. Since λ is constant, we use the restricted stability condition (2.46), and we see that $|\xi|$ is greater than 1 for θ not equal to 0, and therefore this scheme is unstable. If a is negative, then the forward-time forward-space scheme is stable for $-1 \leq a \lambda \leq 0$.*

Remark 2.14 (Stability Conditions for Variable Coefficients). *The stability analysis as studied in the previous section does not apply straightforward to problems with variable coefficients. Nevertheless, the stability conditions obtained for constant coefficient schemes can be applied to present stability conditions for the same scheme applied to equations with variable coefficients. For instance, the Lax-Friedrichs scheme applied to $u_t + a(t, x) u_x = 0$ is*

$$u_m^{n+1} = \frac{1}{2} (u_{m+1}^n - u_{m-1}^n) - \frac{1}{2} a(t_n, x_m) \lambda (u_{m+1}^n - u_{m-1}^n).$$

The condition for stability for this scheme shows that $|a(t_n, x_m) \lambda| \leq 1$ be satisfied for all values of (t_n, x_m) in the domain of computation. The general methodology is that one takes into consideration each of the frozen coefficient problems emerging from the scheme. The frozen coefficient problems are the constant coefficient problems obtained by applying the coefficients at their values affected at each point in the domain of the computation. The variable coefficient problem is likewise stable as long as each frozen coefficient problem is stable (The proof of this result can be found in (Kreiss, 1962, Lax and Nirenberg, 1966)). If the stability condition as found from the frozen coefficient problems is contravened in a small region, the instability phenomena that emerge will generate in that area and will not improve outside that area.

Remark 2.15 (Numerical Stability and Dynamic Stability, Strikwerda (2004)). The term stability is used in a number of situations in applied mathematics and engineering, and it is important to make the nuance of the applications of this term. The stability in the Definition 2.6 can be named the numerical stability of finite difference schemes. In applied mathematics, it is frequent to consider dynamic stability, which assigns to the property of a system in which small variations from a reference state will disintegrate, or at least not increase, with time. Dynamic stability assigns to the behavior of solutions as time progresses, while the numerical stability of a scheme always gives reference to the behavior of solutions over a finite interval of time as the grid is refined.

Order of Accuracy for time-dependent problems

In this section we present the order of accuracy of a scheme for time-dependent problems, which can be seen as an expansion of the definition of consistency. In previous sections, we categorized schemes as acceptable or not acceptable only based if or not they are convergent by means of the Lax equivalence theorem (stability and consistency). Nonetheless, various convergent schemes may differ significantly in how well their solutions give approximation to the solution of the differential equation.

Definition 2.8 (Strikwerda (2004)). A scheme $P_{k,h}u = R_{k,h}f$ that is consistent with the differential equation

$Pu = f$ is accurate of order p in time and order q in space if for any smooth function $w(t, x)$

$$P_{k,h}w - R_{k,h}Pw = O(k^p) + O(h^q). \quad (2.47)$$

We say a scheme is accurate of order (p, q) .

Remark 2.16 (Strikwerda (2004)). The quantity $P_{k,h}w - R_{k,h}Pw$ is called truncation error of the scheme. We see that the consistency demands only $P_{k,h}w - R_{k,h}Pw$ to be $O(1)$ while the accuracy takes into account the more precise information on the convergence.

Example 2.6 (Strikwerda (2004)). Lax-Wendroff scheme for the one-way wave equation

$u_t + a u_x = f$ is

$$u_m^{n+1} = u_m^n - \frac{a\lambda}{2} (u_{m+1}^n - u_{m-1}^n) + \frac{a^2\lambda^2}{2} (u_{m+1}^n - 2u_m^n + u_{m-1}^n) + \frac{k}{2} (f_m^{n+1} + f_m^n) - \frac{ak\lambda}{2} (f_{m+1}^n - f_{m-1}^n). \quad (2.48)$$

Taylor series evaluated on (2.48) at (t_n, x_m) gives

$$P_{k,h}w = w_t + \frac{k}{2} w_{tt} + a w_x - \frac{a^2k}{2} w_{xx} + O(k^2) + O(h^2)$$

$$R_{k,h}f = R_{k,h}Pw = w_t + a w_x + \frac{k}{2} w_{tt} - \frac{a^2k}{2} w_{xx} + O(k^2) + O(h^2) \text{ with } f = w_t + a w_x = Pw. \quad (2.49)$$

Hence the Lax-Wendroff scheme is accurate of order $(2, 2)$. With $R_{k,h}f_m^n = f_m^n$, Lax-Wendroff scheme is accurate with order $(1, 2)$.

Remark 2.17 (Strikwerda (2004)). The above Definition 2.8 is not completely in order. For instance, it cannot be used to the Lax-Friedrichs scheme, which contains the term $k^{-1}h^2 w_{xx}$ in the Taylor series expansion of $P_{k,h}w$. We hence give the following definition, which is mostly applicable. We suppose that the time step is chosen as a function of the space step, $k = \Lambda(h)$, where Λ is a smooth function of h and $\Lambda(0) = 0$.

Definition 2.9 (Strikwerda (2004)). A scheme $P_{k,h}u = R_{k,h}f$ with $k = \Lambda(h)$ that is consistent with the differential equation $Pu = f$ is accurate of order p in time and order q in space if for any smooth function $w(t, x)$

$$P_{k,h}w - R_{k,h}Pw = O(h^r). \quad (2.50)$$

Remark 2.18. If $\Lambda(h) = \lambda h$, then the Lax-Friedrichs scheme is consistent with the one-way wave equation.

Rate of convergence for time-dependent problems

In this section, we study the rate of convergence for time-dependent problems. It measures how fast a sequence converges. We consider the ordinary differential equation

$$u_t = f(u, t), \quad u(0) = u_0, \quad 0 \leq t \leq T.$$

The rate of convergence is known as the global order of accuracy and describes the decrease in error $\max_{n \in \{0, 1, \dots, \frac{T}{k}\}} |v^n - u^n|$ one can expect for a given decrease in time step k in the limit $k \rightarrow 0$.

Definition 2.10. Assume that the forcing function $f(u, t)$ is sufficiently smooth (In particular, we need $f(u, t)$ to have p continuous derivatives). A numerical method has a global order of accuracy p if

$$\max_{n \in \{0, 1, \dots, \frac{T}{k}\}} |v^n - u^n| \leq c k^p, \quad k \rightarrow 0.$$

For practical suitability, we consider the following definitions

Definition 2.11 (Miyata and Sakai (2012)). For a vector $\bar{x} \in \mathbb{R}^N$, L_1 and L_∞ norms are defined by $\|\bar{x}\|_1 = \sum_{i=1}^N |\bar{x}^i|$ and $\|\bar{x}\|_\infty = \max\{|\bar{x}^i|, i = 1, \dots, N\}$.

Definition 2.12 (Sutton (2018)). Suppose $\{t^n\}_0^N$ forms a partition of $[0, T]$, with $t_n = nk$ for $n = 0, \dots, N$, where $k = T/N$. Suppose a vector $\bar{x} \in \mathbb{R}^N$, defined by

$$\|\bar{x}\|_{L^p(0, t^n)} = \begin{cases} \left(\|\bar{x}\|_{L^p(0, t^{n-1})} + \tau(\bar{x}^n)^p \right)^{\frac{1}{p}} & \text{for } p \in [0, \infty), \\ \max\{\|\bar{x}\|_{L^p(0, t^{n-1})}, \bar{x}^n\} & \text{for } p = \infty. \end{cases} \quad (2.51)$$

The rate of convergence with respect to time is defined by

$$\text{rate}_i(t) = \frac{\log(\bar{x}^i(t)) - \log(\bar{x}^{i-1}(t))}{\log(k^i) - \log(k^{i-1})}.$$

2.1.2 Nonstandard-finite difference scheme

The finite difference methods have been broadly utilized for the numerical solution of ordinary and partial differential equations (Forsythe and Wasow, 1960, Strikwerda, 2004). They are based often on two conditions which are the consistency of the discrete scheme with the original differential equation and the stability (zero-stability in the jargon of Lambert (1991)) of the discrete method. These conditions are substantial and are indubitable, due to the fact that they give an assurance of convergence with, in several cases, optimal rates of convergence (rate in term of accuracy and efficiency) of the discrete solution to the exact one (Anguelov and Lubuma, 2001). One weakness of these traditional conditions is that key qualitative properties of the exact solution are not conveyed to the numerical solution. In application, the limit 0 of the step size h , with which zero-stability is affected, is not attained. Therefore, the agreed disadvantage might be disastrous. One way of eluding this is to consider further notions of stability, which are based on what Lambert (1991) names syntax of a stability definition with the following definition (Stuart and Humphries (1998) also show the conditions for numerical

methods for differential equations to produce dynamical systems, which are almost identical to those generated by the differential equations):

Definition 2.13. *We impose certain conditions C_p on the differential equation, which force the solution to display a stability property. We apply a discrete method to the differential equation. We ask what conditions C_m must be imposed on the discrete scheme in order that the numerical solution displays a stability property analogous to that displayed by the exact solution.*

Nonstandard finite difference methods were established empirically by pioneer Mickens in (Mickens, 1994, 2000) for solving practical problems in applied sciences and engineering. The derivations are generally based on the notion of dynamical consistency (Mickens, 2005). The concept of dynamical consistency performs an important role in the construction of discrete models which provide a significant difficulty in the computation of numerical solutions. This difficulty is numerical instabilities. Indeed numerical instabilities are solutions to discrete equations that do not link to any solutions of the original differential equations (Mickens, 1994). The dynamical consistency is defined with respect to peculiar properties of a physical system which vary mostly from one system to another. These properties must preserve positivity, boundedness, monotonicity of the solutions, correct number and stability of fixed-points and other special solutions. Furthermore, the dynamical consistency is a general standard property to limit the possible construction of NSFD scheme (Mickens, 2005). The utility and strength of NSFD procedures are that they don't need any a priori knowledge of the exact solutions to the differential equation (Mickens, 2005). They come from the enforcement of certain physical system necessities on the discrete model equations as found by dynamical consistency. In conclusion, the lack of dynamical consistency leads to numerical instability. This practically appears for some values of the parameters or step-sizes (Mickens, 2005). Despite the fact that nonstandard methods give satisfactory results to their users, these methods have not been controlled to strict mathematical analysis. We recall some of following theory formulated by Anguelov and Lubuma (2001).

Remark 2.19. *The idea behind saying that "The utility and strength of NSFD procedures are that they don't need any a priori knowledge of the exact solutions to the differential equation" is justified by Mickens (2005) by stating that "the power and usefulness of NSFD derive from the imposition of certain physical system requirements on the discrete model equations as determined by the principle of dynamical consistency.*

General overview

We consider the initial-value problem for an autonomous first-order system of ordinary differential equations

$$Dw := \frac{dw}{dt} = g(w); \quad w(t_0) = w_0, \quad w \in \mathbb{R}^n, \quad (2.52)$$

where w is the vector of unknown functions, w_0 and $g \in \mathbb{R}^n$ are given. The time, $t \in [t_0, T]$, $t_0 \geq 0$ is finite and the limit time T might be ∞ as for dynamical systems. We assume that the function g verifies the Lipschitz condition (Gear, 1971) which guarantees the uniqueness of the solution. We discretize the time by $\{t_n := t_0 + n h\}_{n \geq 0}$, n an integer (t_n time at n) and $h > 0$ is the step-size. We signify by w_n an approximate solution of $w(t_n)$ at the point t_n . The solution to the discrete finite difference equation

$$D_h w_n = G_h(w_n), \quad (2.53)$$

is, w_n and defined by

$$w_n \approx w(t_n). \quad (2.54)$$

We also define

$$\sum_{j=0}^p \alpha_j w_{n+j} = h \sum_{j=0}^p \beta_j g_{n+j}, \quad g_{n+j} = g(w_{n+j}), \quad \alpha_p = 1, \quad |\alpha_0| + |\beta_0| > 0. \quad (2.55)$$

Definition 2.14. *The scheme (2.53) is (zero-) stable, if there exist constants $K > 0$ and h_0 such that, there holds, $\forall h \in (0, h_0]$, the relation $\|z_n - \tilde{z}_n\| \leq K \epsilon$ whenever $\|\delta_n - \tilde{\delta}_n\| \leq \epsilon$ for a given accuracy $\epsilon > 0$ and for any two perturbations δ_n and $\tilde{\delta}_n$ of the data in Eq. (2.53) with corresponding perturbed solutions z_n and \tilde{z}_n .*

Definition 2.15. *Assume that the solution of problem (2.52) satisfies some property P . The difference Eq. (2.53) or (2.55) is called (qualitatively) stable with respect to property P (or P -stable) if, for every $h > 0$, the set of discrete solutions satisfies property P .*

Definition 2.16. *The method Eq. (2.53) or (2.55) is called an exact difference scheme of (2.52), if the relation Eq. (2.54) between the discrete solution w_n and the exact solution $w(t_n)$ holds for any $h > 0$ with, however, the equality symbol " $=$ " in lieu of " \approx ".*

Theorem 2.5 (Mickens (1994)). *Let $t \rightarrow H.(t, t_0; \cdot)$ be the solution operator that associates the data (w_0, g) with the unique solution $w(t)$ of the system (2.52) at the time t :*

$$w(t) = H_g(t, t_0; w_0). \quad (2.56)$$

Then Eq. (2.52) has the exact difference scheme

$$w_{n+1} = H_g(t_{n+1}, t_n; w_n). \quad (2.57)$$

Remark 2.20. We notice that there is no sufficient information from the Theorem 2.5 to how an exact difference scheme could genuinely be constructed. At least, important positive efforts have been made for several class of problems (Mickens, 1994).

Example 2.7. Application of Theorem 2.5 (Anguelov and Lubuma, 2001). We consider one dimension differential equation (2.52) with $g(w) = \lambda w^m$, where $m \in \mathbb{N}$, and $\lambda \neq 0$ is a constant. The solution operator in Eq. (2.56) is

$$H_g(t, t_0; w_0) = \begin{cases} w_0 e^{\lambda(t-t_0)} & \text{if } m = 1, \\ w_0 [1 + (1 - m) \lambda (t - t_0) w_0^{m-1}]^{-(m-1)} & \text{if } m \geq 2. \end{cases} \quad (2.58)$$

and Eq. (2.57) may be rewritten as

$$\begin{cases} \frac{w_{n+1} - w_n}{(e^{\lambda h} - 1)/\lambda} = \lambda w_n & \text{if } m = 1, \\ \frac{w_{n+1} - w_n}{h} = \lambda \frac{(m-1)[w_{n+1}^m - w_n^m]}{w_{n+1}^{m-1} - w_n^{m-1}} & \text{if } m \geq 2. \end{cases} \quad (2.59)$$

Remark 2.21. The selection of the denominator functions of the discrete derivative for time derivatives has no general rule. Nevertheless particular forms for precise equation can be easily found. The common functions usually used in Mickens (1994) are

$$\phi(k) = \frac{1 - e^{-\lambda k}}{\lambda}, \quad (2.60)$$

where λ is some parameter emerging in the differential equation.

From the example above we can formulate the following of Nonstandard finite difference scheme

Definition 2.17 (Mickens (1994)). The method (2.53) is called a nonstandard finite difference method, if at least one of the following conditions is met:

1. In the first-order discrete derivative $D_h w_n$, the traditional denominator h is replaced by a nonnegative function $\phi(h)$ such that

$$\phi(h) = h + O(h^2) \text{ as } h \rightarrow 0; \quad (2.61)$$

2. Nonlinear terms in $g(w)$ are approximated in a nonlocal way, i.e by a suitable function of several points of the mesh (In example 2.58, $w^2(t^*) \approx w_{n+1}w_n$ and $w^3(t^*) \approx 2w_{n+1}^2w_n^2/(w_{n+1} + w_n)$, where t^* is fixed point such that $t_n = t^*$ with $n \rightarrow \infty$, $h \rightarrow 0$).

Remark 2.22. Definition 2.17 is effectual for derivatives of higher-order m on condition that the right hand-side of E. (2.17) is replaced by $h^m + O(h^{m+1})$.

Theorem 2.6 (Anguelov and Lubuma (2001)). If Eq. (2.53) represents a standard finite difference scheme that is consistent and zero-stable, then any corresponding nonstandard finite difference scheme in Definition 2.17 is necessarily consistent. Furthermore, if the nonstandard scheme is constructed according to the first bullet in Definition 2.17, then this scheme is zero-stable provided that the operator G_h satisfies, for some $M > 0$ independent of h and for any bounded sequences (w_n) and (\tilde{w}_n) in \mathbb{R} , the Lipschitz condition

$$\sup_n \|G_h(w_n) - G_h(\tilde{w}_n)\| \leq M \sup_n \|w_n - \tilde{w}_n\|.$$

Proof. Consider the standard and nonstandard finite difference scheme respectively

$$\frac{N w_n}{h} = G_h(w_n) \text{ and } \frac{N w_n}{\phi(h)} = \tilde{G}_h(w_n) \quad (2.62)$$

with N is relevant difference operator and $G_h(\tilde{w}_n)$ is an approximate of $g(w(t^*))$. We have, taking w as an exact solution of Eq. (2.52)

$$\frac{N w(t^*)}{\phi(h)} - \tilde{G}_h(w(t^*)) = \frac{h}{\phi(h)} \left[\frac{N w(t^*)}{h} - G_h(w(t^*)) \right] + \frac{h}{\phi(h)} G_h(w(t^*)) - \tilde{G}_h(w(t^*)) \rightarrow 0 \quad (2.63)$$

as $h \rightarrow 0$ and due to the fact that $\lim_{h \rightarrow 0} \frac{h}{\phi(h)} = 1$. Hence the consistency of (2.63).

Consider two perturbations δ_n and $\tilde{\delta}_n$ such that $\|\delta_n - \tilde{\delta}_n\| \leq \epsilon$ and with its disturbed solutions z_n and \tilde{z}_n . Also consider the following perturbations

$$\gamma_n = \left[\frac{\phi(h)}{h} - 1 \right] G_h(z_n) + \frac{\phi(h)}{h} \delta_n, \text{ and } \tilde{\gamma}_n = \left[\frac{\phi(h)}{h} - 1 \right] G_h(\tilde{z}_n) + \frac{\phi(h)}{h} \tilde{\delta}_n$$

for the standard scheme (2.62) with the same disturbed solutions z_n and \tilde{z}_n . Since G_h is Lipschitz and $\lim_{h \rightarrow 0} \frac{h}{\phi(h)} = 1$ we have, for $h \ll 0$ (relatively small) which does not depend on ϵ

$$\|\gamma_n - \tilde{\gamma}_n\| \leq 2\epsilon + M \left| \frac{\phi(h)}{h} - 1 \right| \sup_j \|z_j - \tilde{z}_j\| \leq 2\epsilon + \frac{1}{2K} \sup_j \|z_j - \tilde{z}_j\|,$$

where K which is constant comes from the zero stable Definition (2.14) of the standard. It follows from the Definition (2.14) that

$$\|z_n - \tilde{z}_n\| \leq 2K\epsilon + (1/2) \sup_j \|z_j - \tilde{z}_j\| \leq 4K\epsilon.$$

□

We are going to show the importance of renormalizing the denominator function ϕ in the discrete derivative in nonstandard finite difference schemes. We start with the following definition

Definition 2.18 (Fixed-point definition). *A constant solution vector \tilde{w} is called fixed-point or critical point of the differential equation (2.52) if it verifies*

$$g(\tilde{w}) = 0. \quad (2.64)$$

Assume \tilde{w} is given fixed point of the differential equation with disturbed (perturbed) trajectory and equation

$$w(t) = \tilde{w} + \epsilon(t) \quad \text{and} \quad \frac{d\epsilon}{dt} = J\epsilon + \|\epsilon\|\alpha(\epsilon), \quad (2.65)$$

with J Jacobian, $J \equiv Jf(\tilde{w}) = (\partial^i g(\tilde{w})/\partial^j w)_{1 \leq i, j \leq n}$ and all its eigenvalues (λ_i) with nonzero real parts

$$\forall i, i \in [1, n], \operatorname{Re} \lambda_i \neq 0 \quad (2.66)$$

and $\alpha(\epsilon) \rightarrow 0$ as $\|\epsilon\| \rightarrow 0$. For simplicity, the interest will be on small values of $\|\epsilon\|$ and hence

$$\frac{d\epsilon}{dt} = J\epsilon. \quad (2.67)$$

Definition 2.19. *Suppose that A is a square matrix of size n , $x \neq 0$ is a vector in \mathbb{C}^n and λ is a scalar in \mathbb{C} . Then we say that x is an eigenvector of A associated with an eigenvalue λ if*

$$Ax = \lambda x.$$

Definition 2.20. *Suppose that A is a square matrix of size n , and λ an eigenvalue of A . Then the eigenspace of A for λ denoted by $\varepsilon_A(\lambda)$, is the set of all the eigenvectors of A for λ together with the inclusion of the zero vector.*

Definition 2.21. *A fixed-point \tilde{w} of the differential equation (2.52) is called linearly stable provided that the solution ϵ of Eq. (2.67) corresponding to a small enough initial data $\epsilon(0) \equiv \epsilon_0$, $\|\epsilon_0\| \ll 1$ say, satisfies $\lim_{t \rightarrow \infty} \|\epsilon(t)\| = 0$. Otherwise, the fixed-point is called linearly unstable.*

Remark 2.23. *A fixed-point \tilde{w} of Eq. (2.52) is linearly stable if only if $\operatorname{Re} \lambda_j < 0$ for all j , and unstable if only if $\operatorname{Re} \lambda_j > 0$ for at least one j .*

We consider the following discrete case of Eq. (2.65) perturbed solution which states

$$w_n = \tilde{w} + \epsilon_n \quad \text{and} \quad D_h \epsilon_k = J_h \epsilon_n. \quad (2.68)$$

Definition 2.22. Assume that a fixed-point \tilde{w} of (2.52) that satisfies (2.66) is a solution of the discrete method (2.53). We say that the constant solution \tilde{w} is linearly stable or unstable depending on whether $\|\epsilon_n\|$ tends to 0 or not, for $n \rightarrow \infty$, where ϵ_n is a solution of Eq. (2.68) for a given $\|\epsilon_0\| \ll 1$.

Definition 2.23. The finite difference method (2.53) is called elementary stable if for any value of the step size h , its only fixed-points \tilde{w} are those of the differential system (2.52), the linear stability properties of each Eq. (2.52) being the same for both the differential system and the discrete method.

Theorem 2.7 (Lambert (1991)). Assume that the linear multi-step method (2.55) is consistent and zero-stable. If fixed-points of the equation (2.52) are all linearly unstable and are the only fixed-points of Eq. (2.55), then the method (2.55) is elementary stable. If, however, Eq. (2.52) has at least one linearly stable fixed-point and if the order or step p of the method (2.55) is greater than 1, then this scheme is elementary unstable when the method (2.68) has a bounded region of absolute stability.

Remark 2.24. Theorem 2.7 gives a justification of the rules formulated by Mickens (1994) regarding the to order of the difference equation. Its full proof can be seen in Anguelov and Lubuma (2001).

The focus of the following part is on the importance of nonlocal approximation of nonlinear terms. We start by studying the general conservative oscillator differential equation

$$\frac{d^2 w}{dt^2} + a^2 w g(w^2) = 0, \quad (2.69)$$

where for an initial t_0 , $w : (t_0, T) \mapsto \mathbb{R}$ and a is a given real constant, and the function g is such that its indefinite integral K

$$K(z) = \int_0^z g(s) ds < \infty, \quad g : \mathbb{R} \mapsto \mathbb{R}. \quad (2.70)$$

The equation (2.69) can be rewritten in terms of first integral which is the conservation law of energy $V(w; t)$ along the trajectory w as follows

$$V(w; t) := \frac{1}{2} \left[\left(\frac{dw}{dt} \right)^2 + a^2 K(w^2) \right] = \text{Constant}. \quad (2.71)$$

Our goal is to derive a discrete scheme that is stable in regard to the conservation of energy. With $g(w^2) \equiv 1$, the nonstandard finite difference method is:

$$\frac{w_{n+1} - 2w_n + w_{n-1}}{\left(\frac{4}{a^2}\right) \sin^2\left(\frac{ha}{2}\right)} + a^2 w_n = 0, \quad (2.72)$$

which is exact finite difference scheme of Eq. (2.69) (Mickens, 1994). We introduce the discrete energy along the trajectory $\{w_s\}$ at the time t_n such that

$$V_h(w_n) := \frac{1}{2} \left[\left(\frac{w_{n+1} - w_n}{\phi(h)} \right)^2 + a^2 L_h(w_n) \right]. \quad (2.73)$$

with $L_h(w_n)$ is an approximate of the potential energy $K(w^2)$. With discrete conservation law of energy,

$$V_h(w_n) = V_h(w_{n-1}), \quad \forall n \geq 1. \quad (2.74)$$

It follows

$$\frac{w_{n+1} - 2w_n + w_{n-1}}{\phi^2(h)} + a^2 w_n \frac{L_h(w_n) - L_h(w_{n-1})}{w_n w_{n+1} - w_{n-1} w_n} = 0. \quad (2.75)$$

The discrete scheme obtained in Eq. (2.75) is consistent with original equation (2.69) due to the fact that

$$\lim_{h \rightarrow 0} \frac{w(t_{n+1}) - 2w(t_n) + w(t_{n-1}))}{\phi^2(h)} = \frac{d^2 w}{dt^2}(t^*).$$

and w being a solution of Eq. (2.69). Let chose L_h such that

$$\lim_{h \rightarrow 0} \frac{L_h(w(t_n)) - L_h(w(t_{n-1}))}{w(t_n) w(t_{n+1}) - w(t_{n-1}) w(t_n)} = g(w^2(t^*)) \quad (2.76)$$

It follows that with mean theorem and using Eq. (2.70) we have,

$$\frac{L_h(w_n) - L_h(w_{n-1})}{w_n w_{n+1} - w_{n-1} w_n} = \frac{K(w_n w_{n+1}) - K(w_{n-1} w_n)}{w_n w_{n+1} - w_{n-1} w_n} \iff L_h(w_{n-1}) = K(w_{n-1} w_n), \quad n \geq 1. \quad (2.77)$$

We end with the following theorem:

Theorem 2.8. (Anguelov and Lubuma, 2001) *With any function, ϕ satisfying $\phi(h) = h + O(h^2)$ with $h \rightarrow 0$ and keeping (2.70) in mind, the nonstandard finite difference scheme*

$$\frac{w_{n+1} - 2w_n + w_{n-1}}{\phi^2(h)} + a^2 w_n \frac{K(w_n w_{n+1}) - K(w_{n-1} w_n)}{w_n w_{n+1} - w_{n-1} w_n} = 0. \quad (2.78)$$

for approximating Eq. (2.69) is stable with respect to the property of conservation of energy (2.74). In the particular case when $g(w^2) \equiv 1$ and $\phi^2(h)$ coincide with the denominator of the fraction in Eq. (2.72), the method (2.78) reduces to the exact scheme of the harmonic oscillator.

If we set

$$\gamma(w_{n-1}, w_n, w_{n+1}) = \frac{K(w_n w_{n+1}) - K(w_{n-1} w_n)}{w_n w_{n+1} - w_{n-1} w_n}$$

Then this satisfies the symmetry property

$$\gamma(w_{n-1}, w_n, w_{n+1}) = \gamma(w_{n+1}, w_n, w_{n-1}).$$

2.1.3 Reaction diffusion equation

Reaction-diffusion partial differential equations give useful mathematical models for a wide range of phenomena in the life and engineering sciences (Edelstein-Keshet, 1988, Smoller, 2012). For various such systems, the dependent variables show physical variables that can not be negative (population or concentration densities). Mathematically, reaction–diffusion systems have the form of semi-linear parabolic partial differential equations. They are in the general form

$$\frac{\partial u}{\partial t} = \underline{D} \frac{\partial^2 u}{\partial x^2} + R(u), \quad (2.79)$$

where $u(x, t)$ accounts the unknown vector function, \underline{D} is a diagonal matrix of diffusion coefficients, and R represents for all local reactions. The solutions of reaction-diffusion equations show a broad range of behaviours, incorporating the formation of travelling waves and wave-like phenomena as well as other self-organized patterns like stripes, hexagons or more intricate structure like dissipative solitons (Camassa et al., 1998, Yildirim, 2009).

Example 2.8 (One-component reaction-diffusion equations). *The simplest reaction-diffusion equation is in one spatial dimension in plane geometry (Kolmogorov–Petrovsky–Piskunov equation) and when*

$$\frac{\partial u}{\partial t} = \underline{D} \frac{\partial^2 u}{\partial x^2} + R(u),$$

we have

$R(u)$	Name of the equation
$u(1 - u)$	Fisher's equation
$u(1 - u^2)$	Rayleigh–Bénard convection equation
$u(1 - u)(u - \alpha), 0 < \alpha < 1$	FitzHugh-Nagumo equation
$u^2 - u^3$	Zeldovich equation

Example 2.9. *Consider the following reaction-diffusion equation*

$$\frac{\partial u_i}{\partial t} = D_i \frac{\partial^2 u_i}{\partial x^2} + f_i(u_1, u_2, \dots, u_n) u_i, \quad i = 1, 2, 3, \dots, N, \quad (2.80)$$

where D_i are nonnegative diffusion coefficients and the f_i are polynomial functions of (u_1, u_2, \dots, u_N) . We restrain the argument to systems modeled by Eq. (2.80) for which the $u_i(x, t)$ exhibit density variables; as a result

$$u_i(x, 0) \geq 0 \implies u_i(x, t) \geq 0,$$

which is a "positivity condition" on the dependent variables. A nonstandard discretisation of Eq. (2.80) from *Mickens (1999)* is

$$\frac{[u_i]_m^{n+1} - [u_i]_m^n}{k} = D_i \frac{[u_i]_{m+1}^n - 2[u_i]_m^n + [u_i]_{m-1}^n}{h^2} + g^i(u)[u_i]_m^n - h^i(u)[u_i]_m^{n+1}, \quad (2.81)$$

where $g^i(u) = g^i([u_1]_m^n, [u_2]_m^n, \dots, [u_n]_m^n)$ and $h^i(u) = h^i([u_1]_m^n, [u_2]_m^n, \dots, [u_n]_m^n)$ (we also have the important property $g^i(u) \geq 0$, $h^i(u) \geq 0$, if $[u_j]_m^n \geq 0$, $j = 1, 2, \dots, N$) are respectively the collection of functions obtained from the positive and negative coefficient terms in $f_i(u)$ such that

$$f_i(u_1, u_2, \dots, u_N)u_i = \begin{cases} \sum_p \beta_p^i \prod_{l=1}^N ([u_l]_m^n)^{p_l^i} [u_i]_m^n & \text{if } \beta_p^i \geq 0, \\ \sum_p -|\beta_p^i| \prod_{l=1}^N ([u_l]_m^n)^{p_l^i} [u_i]_m^{n+1} & \text{if } \beta_p^i \leq 0. \end{cases} \quad (2.82)$$

where p_l^i are nonnegative integers, $P \equiv (p_1^i, p_2^i, \dots, p_N^i)$ is a vector quantity, β_p^i are constants. Also the first-order time derivative and second-order space derivative are replaced respectively by usual forward Euler and Central difference representation (*Strikwerda, 2004*)

$$\begin{aligned} \frac{\partial u_i}{\partial t} &\rightarrow \frac{[u_i]_m^{n+1} - [u_i]_m^n}{k}, \\ \frac{\partial^2 u_i}{\partial x^2} &\rightarrow \frac{[u_i]_{m+1}^n - 2[u_i]_m^n + [u_i]_{m-1}^n}{h^2}. \end{aligned} \quad (2.83)$$

2.1.4 Singularly perturbed reaction diffusion equation problems

Singularly perturbed problems concern a disturbance parameter which multiplies the highest derivative term in the model-equation of the problem. The solution to this kind of problems is typified by layer regions which are small parts of the domain beyond which the solution incurs stiff changes. It is widely known that classical methods (for instance the classical backward Euler or Crank–Nicolson scheme) are not suitable when the perturbation parameter becomes narrow unless very fine meshes are utilized for spatial discretization. That is to say, this approach has two side effects: it increases the round-off error and the computational cost. Singularly perturbed problems can be represented as

$$u_t + L_{x,\epsilon}u = f(x, t), \quad (-\infty, \infty), \quad t > 0, \quad (2.84)$$

where, $L_{x,\epsilon}u$ is spatial differential operator and defined as follows

$$L_{x,\epsilon}u \equiv -\epsilon u_{xx} + b(x, t)u, \quad \epsilon > 0, \quad b \geq 0. \quad (2.85)$$

Eq. (2.85) into Eq. (2.84) give

$$u_t = \epsilon u_{xx} + F(u(x, t)), \quad \text{where, } F(u(x, t)) = b(x, t)u + f(x, t), \quad (-\infty, \infty), \quad t > 0. \quad (2.86)$$

For specific initial condition and boundary condition, Eq. (2.86) can be regarded as Fisher's equation, which is one example of singularly perturbed problems.

Several authors have treated stationary singularly perturbed and time-dependent singularly perturbed problems. For mentioning few, [Lubuma and Patidar \(2006\)](#), [Patidar \(2005, 2007\)](#) used the class of fitted mesh methods and the class of fitted operator methods (based on finite difference) to solve stationary singularly perturbed problems and [Clavero et al. \(2003\)](#), [Munyakazi and Patidar \(2013\)](#) utilized respectively fitted operator finite methods and uniformly convergent scheme to solve time-dependent singularly perturbed problems. For Eq. (2.84) defined such that

$$\forall (x, t) \in Q = \Omega \times (0, T] \equiv (0, 1) \times (0, T), \quad (2.87)$$

subject to boundary conditions

$$u(x, 0) = 0, \quad x \in \bar{\Omega}, \quad u(0, t) = u(1, t) = 0, \quad t \in (0, T]. \quad (2.88)$$

We have the time semidiscretization on \bar{w}^K , as in [Munyakazi and Patidar \(2013\)](#) by backward Euler method such that

$$\bar{w}^K = \{t_n = n\tau, \quad 0 \leq n \leq K, \quad \tau = T/K\} \quad (2.89)$$

and

$$\begin{aligned} \frac{z(x, t_n) - z(x, t_{n-1})}{\tau} + L_{x,\epsilon}(z(x, t_n)) &= f(x, t_n), \quad 1 \leq n \leq K, \\ z(x, 0) = 0, \quad \forall x \in (0, 1), \quad z(0, t_n) &= z(1, t_n) = 0. \end{aligned} \quad (2.90)$$

When we consider the following partition of the interval $[0, 1]$

$$x_0 = 0, \quad x_m = x_0 + mh, \quad m = 1, \dots, N, \quad h = x_m - x_{m-1}, \quad x_N = 1, \quad N \geq 0,$$

then the fully discrete method for Eq. (2.84) as in [Munyakazi and Patidar \(2013\)](#) using properties of [Mickens \(1994\)](#) is

$$L_\epsilon^{N,K} U_m^n \equiv \frac{U_m^n - U_m^{n-1}}{\tau} + L_{x,\epsilon}^N U_m^n = f_m^n, \quad L_{x,\epsilon}^N U_m^n \equiv -\epsilon \left[\frac{U_{m+1}^n - 2U_m^n + U_{m-1}^n}{\phi_m^2} \right] + b_m^n U_m^n, \quad (2.91)$$

where the discrete initial and boundary conditions

$$\begin{aligned} U_m^0 &= 0, \quad m = 0, \dots, N, \quad U_0^n = U_N^n = 0, \quad 1 \leq n \leq K, \\ \phi_m &= \frac{2}{\rho_m} \sinh\left(\frac{\rho_m h}{2}\right), \quad \rho_m = \sqrt{\left(\frac{1}{\tau} + b_m^n\right) \epsilon^{-1}}. \end{aligned} \quad (2.92)$$

Chapter 3

On the Numerical Solution of Fisher's equation with coefficient of diffusion term much smaller than coefficient of reaction term

*A version of this chapter has been published in *Advances in Difference Equations* as [Agbavon et al. \(2019a\)](#).*

3.1 Introduction

Real life problems are mainly modelled by partial differential equations (PDEs) and the applications can be in engineering, physics, chemistry, ecology, biology and other related fields of science. PDEs are in different forms and can be linear or nonlinear, homogeneous or nonhomogeneous, elliptic, hyperbolic, parabolic.

PDEs have some specifications which give the information how smooth the solution is, how rapid information propagates and the impact of initial and boundary conditions (which help to find if a particular approach is suitable to the problem being portrayed by the PDEs).

For some example of modelling of real life, we can mention for instance, the wave propagation in compressible two-phase flow ([Zeidan et al., 2007](#)), the pattern-forming dynamical systems ([Müller and Timmer, 2004](#)), the stochastic failures and repairs of the components, changes in the interconnections of subsystems, sudden environment changes ([Sakthivel and Luo, 2009](#)), the

two-phase gas-magma mixture problem (Zeidan, 2016), the inverse problems (oil reservoir simulations, the conductivity differences between bone and muscle tissue) in Colton et al. (1990), the unsteady cavitation in liquid hydrogen flows (Da Silva and Zeidan, 2017), the interaction of shocks for isentropic drift-flux Zeidan et al. (2018).

Our study will be based on reaction diffusion equations which is one form of PDEs and are mostly used in modelling of transport of air, adsorption of pollutants in soil, diffusion of neutrons, food processing, modelling of biological and ecological systems, modelling of semiconductors, oil reservoir flow transport among others (Chen and Kojouharov, 1999). Some tangible applications are modelling of amazing patterns and phenomena such as tree-grass interactions in fire-prone savannas (Yatat et al., 2018), pulse splitting and shedding (Gray-Scott equation)(Doelman et al., 1997). Gray-Scott equation has some applications namely: reaction and competition in excitable systems, autocatalysis, reaction between two chemical species which have different diffusivities (Houdek et al., 1999), modelling of Labyrinthine patterns (Hagberg and Meron, 1994) which are formed in models of catalytic reactions. There are only few cases for which the analytical solution to such reaction-diffusion equations exists, therefore the necessity of constructing numerical methods which are accurate and efficient.

In this work, our interest is on Fisher's equation (Fisher, 1937) which describes spontaneous growth and spread of a dominant gene. Fisher considers a population which is distributed linearly in a habitat (shore line) with uniform density. If the mutation happens at any point of the habitat, the mutant gene is expected to increase at the risk of the allelomorphs previously occupying the same position. This occurrence will be first terminated in the neighbourhood of the mutation and later in the adjacent portion of its range. Assuming the range to be long enough likened with the distance separating the locations of offspring from those of their parents, there will be, from the origin a wave of increase in the gene frequency.

3.1.1 Background of Fisher's equation

We consider Fisher (1937)'s equation which is given by

$$u_t = u_{xx} + u(1 - u), \quad (3.1)$$

where $x \in (-\infty, +\infty)$, $t > 0$ and the boundary and initial conditions are

$$\lim_{x \rightarrow -\infty} u(x, t) = 1, \quad \lim_{x \rightarrow +\infty} u(x, t) = 0, \quad (3.2)$$

$$u(x, 0) = u_0(x). \quad (3.3)$$

The above problem (Fisher, 1937) was solved by Kolmogorov (1937) by introducing the concepts of travelling waves and the existence of wave speed c . Moreover they showed that the speed of propagation c of the waves is greater than two ($c \geq 2$) if the initial condition $u_0(x)$ is in the interval $[0, 1]$ and the type of solution is $u(x, t) = v(\xi)$ where $\xi = x - ct$ satisfying $u \in [0, 1]$ for all ξ . They also proved that such solutions do not exist for $c \in [0, 1)$. The studies in Hagstrom and Keller (1986) showed that if for a positive function as initial condition which verifies the boundary conditions given by (3.2) on \mathbb{R} and if

$$u_0(x) \sim e^{-\beta} \text{ as } x \rightarrow \infty, \quad (3.4)$$

then the solution, u contains a travelling wave speed which is a function of β , where

$$c(\beta) = \begin{cases} \beta + \frac{1}{\beta}, & \beta \leq 1, \\ 2, & \beta \geq 1. \end{cases} \quad (3.5)$$

Furthermore, they proved that if the initial amplitude drops sufficiently quickly as x goes to infinity, then the propagation speed of the wave (which determines the behaviour of initial condition) has the minimum value, $c = 2$.

The numerical implementation of Eq. (3.1) with boundary and initial conditions given respectively by (3.2) and (3.3) involving the travelling wave solution is challenging due to the dependence of sensitive solution of the initial data behaviour at infinity. For instance, the problem (3.1) with initial condition (3.3) (called Cauchy problem) is replaced by an initial and boundary value problem on the finite spatial domain $[x_l, x_r]$. Moreover, Gazdag and Canosa (1974) resolved this issue by imposing an asymptotic representation of the boundary condition (3.2) at $x = x_l$, $x = x_r$. They found that the solution moves close to a travelling wave of the minimum speed, $c = 2$. They concluded that the demanding time to change to the minimum wave speed profile is linked to the right-hand cut off point $x = x_r$. The same approach was adopted by Hagstrom and Keller (1986) with the wave speed greater than the minimum wave speed $c = 2$. They showed that the travelling wave solutions can be interpreted in finite domain by constructing accurately the asymptotic boundary conditions at $x = x_l$ and $x = x_r$. They obtained good results with $u(x_l, t) = 1$ and $u(x_r, t) = 0$ for $t \geq 0$.

Many authors like Canosa (1973) and Hagstrom and Keller (1986) have worked on the issue of stability and sensitivity of the solution to the boundary of travelling wave. For instance the equilibrium solutions $u = 0$ and $u = 1$ of Eq. (3.1) are respectively unstable and stable to small perturbations. Moreover they demonstrated that all travelling waves are stable to small

perturbations of compact support but unstable of infinite support.

Anguelov et al. (2005) solved the same problem (3.1) by using a periodic initial condition with θ -non standard method. They concluded that their method is elementary stable in limit case of space independent variable, stable with respect to the boundedness and positivity property and finally stable with respect to the conservation of energy in the stationary case.

3.2 Organisation of chapter

The chapter is organised as follows. In section 3.3, we describe in details how the moving mesh method with monitor function is implemented. In section 3.4, we describe numerical experiments considered as in Li et al. (1998), Qiu and Sloan (1998). In sections 3.5 and 3.6, the Forward in Time Central in Space (FTCS) and FTCS- ϵ difference scheme are studied and numerical results are displayed. Sections 3.7 and 3.8 are devoted to derivation and properties of NSFD and NSFD- ϵ scheme and results are presented. In section 3.9, we add artificial viscosity to both FTCS and NSFD and study properties of new schemes and present some results. The stability of computed solution and the sensitivity of the solution to the boundary condition ahead of the wave in term of local perturbation are done in section 3.10. In section 3.11, we highlight the salient features of this chapter. All simulations are performed using matlab R2014a software on an intel core2 as CPU.

3.3 Moving Mesh method

Li et al. (1998) have considered a scaled Fisher's equation in the form

$$u_t = u_{xx} + \rho u(1 - u), \quad (3.6)$$

where $x \in (-\infty, +\infty)$, $t > 0$ and ρ is a positive large constant. The boundary and initial conditions are given by Eqs. (3.2) and (3.3) respectively. The exact solution to this problem is

$$u(x, t) = \left[1 + \exp \left(\sqrt{\frac{\rho}{6}} x - \frac{5\rho}{6} t \right) \right]^{-2}, \quad (3.7)$$

with wave speed, $c = 5\sqrt{\rho/6}$ and the minimum wave speed, $c = 2\sqrt{\rho}$. Li et al. (1998) used the method called Moving Mesh Partial Differential Equation (MMPDE). They got poor results when ρ is chosen 10^4 . They concluded that the Moving Mesh Partial Differential Equation (MMPDE) is not suitable for reaction-diffusion equation (Fisher's equation in particular) when the reaction term is much greater than the diffusion term with initial condition consisting of

an exponential function. This is due to the fact that MMPDE is based on familiar arc-length or curvature monitor function and does not produce accurate results (Mulholland et al., 1997). Qiu and Sloan (1998) improved the results of Li et al. (1998) by constructing a specific monitor function and used the method of Moving Mesh Differential Algebraic Equation (MMDAE). The technique of Moving Mesh method (MMPDE) has been utilized broadly over the last few years to find a solution to time-dependent partial differential equations (PDEs). The method consists of moving the mesh points as time change with motion designed to minimise some measurement in computational error (Qiu and Sloan, 1998).

We consider the variables ζ and t with ζ defined by one-to-one coordinate transformation of the form

$$x = x(\zeta, t), \quad \zeta_m = -1 + \frac{2m}{N}, \quad m = 0, \dots, N, \quad (3.8)$$

where ζ_m are spaced nodes in the interval $[-1, 1]$ to the nodes $\{x_m\}_{m=0}^N$ in the interval $[x_l, x_r]$, with

$$x_l = x_0(t) < x_1(t) < \dots < x_N(t) = x_r, \quad \forall t \geq 0.$$

Remark 3.1. The set of $\{\zeta_m\}_{m=0}^N$ forms a partition $(\{0, 1\}^{\mathbb{N}}$, where \mathbb{N} , set of natural number) of $[-1, 1]$. There is bijection between the set $\{0, 1\}^{\mathbb{N}}$ and the set of real number $\mathbb{R} = (-\infty, \infty)$.

Remark 3.2. $x_m(t)$ is time dependent due of the definition of moving mesh (moving the mesh points as time change) method.

We can rewrite (3.6) in semi-discrete form such that

$$\dot{u}_m - \dot{x}_m \frac{u_{m+1} - u_{m-1}}{x_{m+1} - x_{m-1}} = \frac{2}{x_{m+1} - x_{m-1}} \left(\frac{u_{m+1} - u_m}{x_{m+1} - x_m} - \frac{u_m - u_{m-1}}{x_m - x_{m-1}} \right) + \rho u_m (1 - u_m), \quad (3.9)$$

for $m = 1, 2, \dots, N - 1$ by using the Lagrangian form (Mulholland et al., 1997)

$$\dot{u} - \dot{x} \partial_x u = \partial_x u_x + \rho u (1 - u). \quad (3.10)$$

Moreover \dot{u} , \dot{x} are the derivatives with respect to t , independent of ζ and $\{x_m\}_{m=0}^N$ and $\{u_m\}_{m=0}^N$ are the time-dependent vectors for approximations. In order to adjust the mesh to the solution as presented in Huang et al. (1994), they introduced the equidistribution principle which is

$$\int_{x_l}^{x(\zeta, t)} M(s, t) ds = \zeta \int_{x_l}^{x(x_r)} M(s, t) ds, \quad (3.11)$$

where $M > 0$ indicates the monitor function that has to be equally distributed between the nodes x_l , x_r . Differentiation of Eq. (3.11) with respect to ζ gives

$$\partial_\zeta [M(x(\zeta, t)) \partial_\zeta x(\zeta, t)] = 0. \quad (3.12)$$

Furthermore, the equation (3.12) has been used in Huang et al. (1994) to derive a collection of moving mesh and the most accurate of this collection is

$$\partial_{\zeta\zeta}\dot{x} = -\frac{1}{\tau}\partial_{\zeta}(M\partial_{\zeta}x), \quad (3.13)$$

denoted by MMPDE6 with τ , small positive parameter ($\tau \ll 1$). Under the condition that the discretization has been done on the grid ζ_i and using the second order central differences leads to semi-discrete form of moving mesh equation

$$\dot{x}_{m-1} - 2\dot{x}_m + \dot{x}_{m+1} = -\frac{1}{\tau} \left[M'_{m+1/2}(x_{m+1} - x_m) - M'_{m+1/2}(x_m - x_{m-1}) \right], \quad (3.14)$$

for $m = 1, 2, \dots, N - 1$ with $M'_{m+\frac{1}{2}}$ being smoothed monitor function as established in Mulholland et al. (1997) and Huang et al. (1994) by

$$M'_{m+\frac{1}{2}} = \frac{\sum_{k=m-p}^{m+p} M_{k+1/2}^2 \left(\frac{q}{q+1}\right)^{|k-m|}}{\sum_{k=m-p}^{m+p} \left(\frac{q}{q+1}\right)^{|k-m|}}, \quad (3.15)$$

where q is positive real number and p is non-negative integer. Furthermore, setting

$$M'_{m+1/2}(x_{m+1} - x_m) - M'_{m+1/2}(x_m - x_{m-1}) = 0, \quad (3.16)$$

in Eq. (3.14) leads to Moving Mesh Differential-Algebraic Equation (MMDAE) developed by Mulholland et al. (1997). This method combines the systems (3.9) and (3.16). The difference between MMPDE6 and MMDAE is that MMPDE6 accommodates a parameter τ that shows the time used to attain equidistribution from some initial state while MMDAE enforces the approximate equidistribution condition (3.16) at each moment of time in the time discretisation. Each problem has its own choice of monitor function. This makes the choice of monitor function an open question. Following Qiu and Sloan (1998), Mulholland et al. (1997) and Huang et al. (1994), the monitor function (arc-length) is defined by

$$M(x, t) = \sqrt{1 + \alpha^2(\partial_x u)^2}, \quad (3.17)$$

with its discrete approximation $M_{m+\frac{1}{2}}$ being

$$M_{m+\frac{1}{2}} = \sqrt{1 + \alpha^2 \left(\frac{u_{m+1} - u_m}{x_{m+1} - x_m} \right)^2}, \quad (3.18)$$

where the parameter α measures the amplitude to which the solution slope has control over the mesh location.

It has been shown in Qiu and Sloan (1998) that moving mesh based on the arc-length and

curvature monitor function are not convenient for the computational solution of Eq. (3.6). Indeed, firstly the computed solution at $t = 2.5 \times 10^{-3}$ is susceptible to the choice of τ (at values 10^{-3} , 10^{-5} , 10^{-7} with α fixed at 2 and $x_l = -0.2$, $x_r = 0.8$) in Eq. (3.13) in the moving mesh using the arc-length monitor function. Secondly, the common monitor function utilized is one in which the first derivative in (3.17) is substituted by the second derivative and we have

$$M(x, t) = (1 + \alpha^2(\partial_{xx}u)^2)^{1/4}, \quad (3.19)$$

with its discrete approximation being

$$M_{m+\frac{1}{2}}^4 = 1 + \alpha^2 \left[\frac{1}{x_{m+1} - x_m} \left(\frac{u_{m+2} - u_m}{x_{m+2} - x_m} - \frac{u_{m+1} - u_{m-1}}{x_{m+1} - x_{m-1}} \right) \right]^2. \quad (3.20)$$

The results show the same sensitivity as in the case of arc-length monitor function. There is oscillation of the solution at the front of wave. In the quest for obtaining the accurate result, Qiu and Sloan (1998) introduced the Modified Monitor function.

3.3.1 Modified Monitor Function

The modified monitor function is one constructed to give a great nodal density and hence a better accuracy at the wave front. It has been shown by Hagstrom and Keller (1986) and by Gazdag and Canosa (1974) that the difficulties which occur in simulating numerically the travelling waves for Fisher's equation come from the front of the wave. This is why significant care should be taken in formulation of boundary conditions at $x = x_r$. Furthermore the results in Gazdag and Canosa (1974) showed that the numerical solution of all travelling wave are stable to small disturbances with compact support and unstable with infinite extent especially to truncation errors inserted at the wave front. It is, consequently, what is an origin of inaccuracy of truncations errors than similar truncations errors introduced at the back of the wave. In this regard, the modified monitor function is

$$M(x, t) = [1 + \alpha^2(1 - u)^2 + \beta^2(a - u)^2(u_{xx})^2]^{1/2}, \quad (3.21)$$

where α , β and a are real specific parameters carefully chosen. The expressions $(1 - u)^2$, $(a - u)^2$ are designed to give more influence of the curvature region at the front of the wave than the corresponding curvature region at the back of the wave.

Remark 3.3. α , β and a are real specific parameters and carefully chosen due to the fact finding the accurate monitor function is an open problem. The monitor function is based on an accurate choice α , β and a so that one can expect accurate and efficient results. Each problem has its

choice of monitor function. That is why a care should be taken regarding to these parameters so that the monitor function can suit well to the problem.

With $\alpha = 1.5$, $\beta = 0.1$, $a = 1.015$, $t = 2.5 \times 10^{-3}$ in the computations of MMDAE and the modified monitor function given by Eq. (3.21), the maximum pointwise error, 9.25×10^{-3} is much smaller than the corresponding error $O(1)$ using the arc-length monitor function. With the method of MMPDE6, the situation is less improved than the method of MMDAE which is also far better than the method of arc-length monitor function. Indeed with the parameter $\tau = 10^{-7}$ and time, $t = 2.5 \times 10^{-3}$, L_∞ error is 4.29×10^{-2} . For the values greater than $N = 50$ with $\tau = 10^{-7}$ and time, $t = 2.5 \times 10^{-3}$, the error is not diminished. Whenever the reduction is applied in the value of τ , we have the reduction in the value of L_∞ error.

Methods	L_1 error	L_∞ error	CPU
MMPDE	4.29×10^{-2}	$O(1)$	ext
MMDAE	9.25×10^{-3}	$k \times 10^{-2}$	0.86ext

Table 3.1: Computation of L_1 and L_∞ errors using MMPDE and MMDAE methods with $\rho = 10^4$, $\alpha = 1.5$, $\beta = 0.1$, $a = 1.015$, $\tau = 10^{-7}$, $N = 50$, at time, $t = 2.5 \times 10^{-3}$.

Remark 3.4. "ext" in Table 3.1 is a value of computational time of MMPDE compares to computational time value "0.86ext" of MMDAE as it is in Qiu and Sloan (1998).

Remark 3.5. L_1 and L_∞ errors are chosen as like in (Li et al., 1998) and (Qiu and Sloan, 1998). Moreover, L_1 and L_∞ errors are computed to see how far the numerical solution is from the exact solution for a given problem in term of L_1 and L_∞ norms (please to the Definition 2.11 of L_1 and L_∞ norms).

3.4 Numerical experiments

We consider two problems. Firstly, we consider the same problem as in Qiu and Sloan (1998) which involves solving:

Problem 1

$$u_t = u_{xx} + 10^4 u(1 - u),$$

for $x \in [-0.2, 0.8]$, with boundary conditions $\lim_{x \rightarrow -\infty} u(x, t) = 1$ and $\lim_{x \rightarrow +\infty} u(x, t) = 0$ and time is 2.5×10^{-3} .

The initial condition is

$$u(x, 0) = \left[1 + \exp \left(\sqrt{\frac{\rho}{6}} x \right) \right]^{-2}. \quad (3.22)$$

Secondly, we consider a slight modification of Problem 1. We use a larger domain with the same boundary and initial conditions and the same propagation time.

Problem 2

$$u_t = u_{xx} + 10^4 u(1 - u),$$

for $x \in [-10, 90]$, with boundary conditions $\lim_{x \rightarrow -\infty} u(x, t) = 1$ and $\lim_{x \rightarrow +\infty} u(x, t) = 0$ and time is 2.5×10^{-3} .

The initial condition is

$$u(x, 0) = \left[1 + \exp \left(\sqrt{\frac{\rho}{6}} x \right) \right]^{-2}. \quad (3.23)$$

In next sections, we present the numerical methods used and study the properties.

Remark 3.6. *As we stated in the introduction, [Hagstrom and Keller \(1986\)](#) have proved that travelling wave solutions with speeds greater than $c \geq 2$ can be accurately represented on a finite domain. Their success is based on the choice of boundary conditions at the isolated points. They imposed on these isolated points an asymptotic representation of the boundary condition which take into account of the initial data in the discarded region. They presented, nonetheless, that the solution is accurate using*

$$\lim_{x \rightarrow -\infty} u(x, t) = 1, \text{ and } \lim_{x \rightarrow +\infty} u(x, t) = 0, \text{ for } t \geq 0.$$

For the numerical experiment, we use $x \in [-0.2, 0.8]$ and the boundary condition is

$$u(-0.2, t) = \left[1 + \exp \left(-0.2 \sqrt{\frac{\rho}{6}} - \frac{5\rho}{6} t \right) \right]^{-2}, \quad u(0.8, t) = \left[1 + \exp \left(0.8 \sqrt{\frac{\rho}{6}} - \frac{5\rho}{6} t \right) \right]^{-2}.$$

Also we use $x \in [-10, 90]$, the boundary condition is

$$u(-10, t) = \left[1 + \exp \left(10 \sqrt{\frac{\rho}{6}} - \frac{5\rho}{6} t \right) \right]^{-2}, \quad u(90, t) = \left[1 + \exp \left(90 \sqrt{\frac{\rho}{6}} - \frac{5\rho}{6} t \right) \right]^{-2}.$$

3.5 Forward in Time Central Space (FTCS)

The Forward in Time Central Space (FTCS) scheme when used to discretise Eq. (3.6) gives ([Chen-Charpentier and Kojouharov, 2013](#))

$$\frac{u_m^{n+1} - u_m^n}{k} = \frac{u_{m+1}^n - 2u_m^n + u_{m-1}^n}{h^2} + \rho u_m^n (1 - u_m^n). \quad (3.24)$$

A single expression for the FTCS scheme is

$$u_m^{n+1} = (1 - 2R)u_m^n + k\rho u_m^n(1 - u_m^n) + R(u_{m+1}^n + u_{m-1}^n), \quad (3.25)$$

where $R = \frac{k}{h^2}$. The time-step size and spatial mesh are denoted by k and h respectively.

3.5.1 Stability

Eq. (3.6) is nonlinear and hence Fourier series stability analysis cannot be applied directly. We need to freeze the coefficients before applying Von Neumann Stability Analysis (Durrant, 2010). Taha and Ablowitz (1984) obtained the stability of a method proposed by Zabuský and Kruskal (1965) for Korteweg de Vries (KdV) equation using the method of freezing coefficients and Von Neumann Stability Analysis. The scheme derived by Zabuský and Kuskal for the KdV equation, $u_t + 6uu_x + u_{xxx} = 0$ is

$$\begin{aligned} \frac{u_m^{n+1} - u_m^{n-1}}{2k} + 6 \left(\frac{u_{m+1}^n + u_m^n + u_{m-1}^n}{3} \right) \left(\frac{u_{m+1}^n - u_{m-1}^n}{2h} \right) \\ + \frac{1}{2h^3} (u_{m+2}^n - 2u_{m+1}^n + 2u_{m-1}^n - u_{m-2}^n) = 0. \end{aligned} \quad (3.26)$$

To obtain stability, Taha and Ablowitz (1984) expressed uu_x as $u_{max}u_x$ and used the ansatz $u_m^n = \xi^n e^{Imw}$ where w is the phase angle. They obtained the following equation

$$\frac{\xi - \xi^{-1}}{2k} + \frac{6|u_{max}|}{h} \text{I} \sin(w) + \frac{1}{2h^3} (e^{2Iw} - 2e^{Iw} + 2e^{-Iw} - e^{-2Iw}) = 0,$$

which can be written as

$$\xi = \xi^{-1} - \frac{12k|u_{max}|}{h} \text{I} \sin(w) - \frac{k}{h^3} (e^{2Iw} - 2e^{Iw} + 2e^{-Iw} - e^{-2Iw}).$$

The linear stability requirement is

$$\frac{k}{h} \left| \frac{1}{h^2} - 2|u_{max}| \right| \leq \frac{2}{3\sqrt{3}}. \quad (3.27)$$

Appadu et al. (2017) used the method of freezing coefficient and Von Neumann stability analysis to obtain region of stability of some schemes for Eq. (3.6). We use the same idea in order to obtain stability region of FTCS scheme. We rewrite Eq. (3.25) as

$$u_m^{n+1} = \left(1 - \frac{2k}{h^2} \right) u_m^n + \frac{k}{h^2} (u_{m+1}^n + u_{m-1}^n) + k\rho u_m^n - (k\rho u_m^n) |u_{max}|, \quad (3.28)$$

where u_{max} is the frozen coefficient. It follows by using Fourier series analysis on Eq. (3.28) that the amplification factor is given by

$$\xi = 1 + \frac{2k}{h^2} (\cos(w) - 1) + k\rho(1 - |u_{max}|). \quad (3.29)$$

In our numerical experiment, $u_{max} = 1$ and $\rho = 10^4$. Hence we obtain

$$\xi = 1 - \frac{4k}{h^2} \sin^2\left(\frac{w}{2}\right). \quad (3.30)$$

For stability, we must have $|\xi| \leq 1$ for $w \in [-\pi, \pi]$ and therefore

$$-1 \leq 1 - \frac{4k}{h^2} \sin^2\left(\frac{w}{2}\right) \leq 1, \quad (3.31)$$

and this leads to

$$k \leq \frac{h^2}{2}. \quad (3.32)$$

For $h = 0.01$, we obtain $k \leq 5 \times 10^{-5}$. The time of the experiment is $T_{max} = 2.5 \times 10^{-3}$ and for the stability, the temporal step size is less than or equal to 5×10^{-5} or $T_{max}/50$. For order of accuracy of FTCS, we use Taylor series expansion about point (n, m) of (3.25) and it gives

$$\begin{aligned} u + ku_t + \frac{k^2}{2}u_{tt} + \frac{k^3}{6}u_{ttt} + O(k^4) &= \left(1 - \frac{2k}{h^2} + k\rho\right)u - k\rho u^2 \\ &+ \frac{k}{h^2} \left(u + hu_x + \frac{h^2}{2}u_{xx} + \frac{h^3}{6}u_{xxx} + \frac{h^4}{24}u_{xxxx} + O(h^5)\right) \\ &+ \frac{k}{h^2} \left(u - hu_x + \frac{h^2}{2}u_{xx} - \frac{h^3}{6}u_{xxx} + \frac{h^4}{24}u_{xxxx} + O(h^5)\right), \end{aligned} \quad (3.33)$$

which to gives

$$u_t - u_{xx} - \rho u(1 - u) = -\frac{k}{2}u_{tt} - \frac{k^2}{6}u_{ttt} + \frac{h^2}{12}u_{xxxx} + O(k^4) + O(h^5). \quad (3.34)$$

FTCS scheme is first order accurate in time and second order accurate in space.

3.5.2 Numerical results using FTCS

We tabulate some errors namely L_1 and L_∞ errors and display CPU times when Problem 1 and 2 are solved using FTCS at some different values of time-step size with spatial step size $h = 0.01$. The errors are displayed in Tables (3.2) and (3.4).

Time step (k)	L_1 error	L_∞ error	CPU (s)
$T_{max}/52$	2.8968×10^{-1}	1.5200	0.648
$T_{max}/100$	6.5144×10^{-2}	6.9877×10^{-1}	0.719
$T_{max}/200$	3.2980×10^{-2}	3.9927×10^{-1}	0.672
$T_{max}/300$	2.0727×10^{-2}	2.5613×10^{-1}	0.693
$T_{max}/400$	1.4262×10^{-2}	1.7830×10^{-1}	0.708
$T_{max}/500$	1.0268×10^{-2}	1.2943×10^{-1}	0.730
$T_{max}/600$	7.5557×10^{-3}	9.5605×10^{-2}	0.770
$T_{max}/700$	5.5929×10^{-3}	7.1038×10^{-2}	0.791
$T_{max}/800$	4.1068×10^{-3}	5.2473×10^{-2}	0.816
$T_{max}/900$	2.9425×10^{-3}	3.7988×10^{-2}	0.866
$T_{max}/1000$	2.0059×10^{-3}	2.6389×10^{-2}	0.904
$T_{max}/1100$	1.2404×10^{-3}	1.6901×10^{-2}	0.932
$T_{max}/1200$	6.2983×10^{-4}	9.0013×10^{-3}	1.233
$T_{max}/1300$	1.9347×10^{-4}	2.3240×10^{-3}	1.055
$T_{max}/1400$	4.2509×10^{-4}	4.3458×10^{-3}	1.141
$T_{max}/1500$	8.3336×10^{-4}	8.7691×10^{-3}	1.245
$T_{max}/1600$	1.1913×10^{-3}	1.3138×10^{-2}	1.366

Table 3.2: L_1 and L_∞ errors and CPU time at some different values of time-step size, k for Problem 1 with $\rho = 10^4$ at time 2.5×10^{-3} with spatial mesh size, $h = 0.01$ using FTCS scheme, where $T_{max} = 2.5 \times 10^{-3}$.

Time step (k)	L_1 error	Rate of convergence
$T_{max}/100$	6.5144×10^{-2}	
$T_{max}/200$	3.2980×10^{-2}	0.982
$T_{max}/400$	1.4262×10^{-2}	1.209

Table 3.3: Rate of convergence with k and spatial mesh size, $h = 0.01$, $\epsilon = 0.01$, of Problem 1 using FTCS.

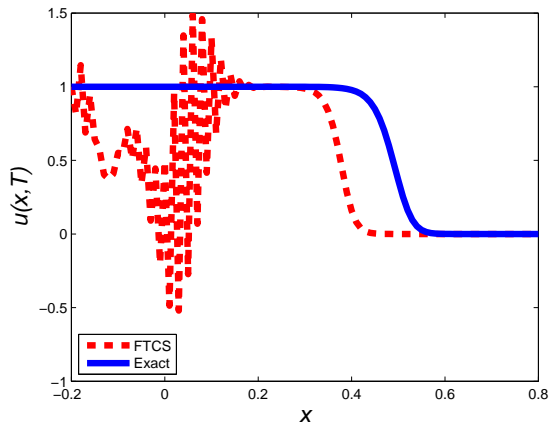
Remark 3.7. We recall that FTCS scheme is first order accurate in time and second order accurate in space. The computed rate of convergence is with respect to time.

Time step (k)	L_1 error	L_∞ error	CPU (s)
$T_{max}/52$	2.8667×10^{-1}	1.5040	1.368
$T_{max}/100$	6.5144×10^{-2}	6.9877×10^{-1}	2.183
$T_{max}/200$	3.2980×10^{-2}	3.9927×10^{-1}	4.532
$T_{max}/300$	2.0727×10^{-2}	2.5613×10^{-1}	7.689
$T_{max}/400$	1.4262×10^{-2}	1.7830×10^{-1}	11.509
$T_{max}/500$	1.0268×10^{-2}	1.2943×10^{-1}	16.099
$T_{max}/600$	7.5557×10^{-3}	9.5605×10^{-2}	22.270
$T_{max}/700$	5.5929×10^{-3}	7.1038×10^{-2}	28.343
$T_{max}/800$	4.1068×10^{-3}	5.2473×10^{-2}	35.383
$T_{max}/900$	2.9425×10^{-3}	3.7988×10^{-2}	43.181
$T_{max}/1000$	2.0059×10^{-3}	2.6389×10^{-2}	51.644
$T_{max}/1100$	1.2404×10^{-3}	1.6901×10^{-2}	61.532
$T_{max}/1200$	6.2983×10^{-4}	9.0013×10^{-3}	71.195
$T_{max}/1300$	1.9347×10^{-4}	2.3240×10^{-3}	82.456
$T_{max}/1400$	4.2509×10^{-4}	4.3458×10^{-3}	94.146
$T_{max}/1500$	8.3336×10^{-4}	8.7691×10^{-3}	107.725
$T_{max}/1600$	1.1913×10^{-3}	1.3138×10^{-2}	118.352

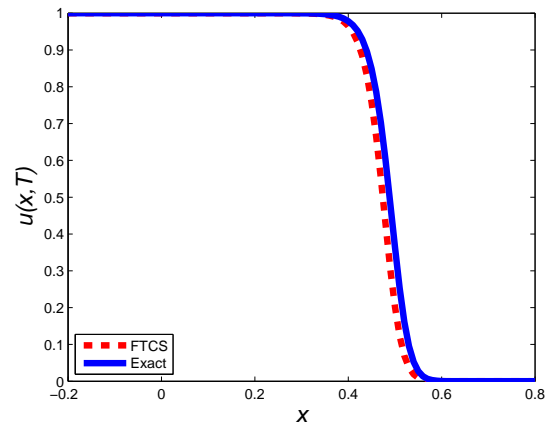
Table 3.4: L_1 and L_∞ errors and CPU time at some different values of time-step size, k for Problem 2 with $\rho = 10^4$ at time 2.5×10^{-3} with spatial mesh size, $h=0.01$ using FTCS scheme, where $T_{max} = 2.5 \times 10^{-3}$.

We observe from Tables (3.2) and (3.4) that L_1 and L_∞ errors are almost the same with different computational times which to be expected due to the fact as we increase the length of the domain, the computational time increases. As we decrease the time-step size, L_1 and L_∞ errors initially decrease and reach minimum when $k \simeq T_{max}/1300$ and then the errors increase again. For k close to $T_{max}/50$, the dispersion error is quite large. Comparing Tables (3.2) and (3.4) to Table (3.1), we notice that L_1 and L_∞ errors from FTCS method at an optimal temporal step size are quite smaller than L_1 and L_∞ errors from MMPDE and MMDAE methods. Some plots of u against x are depicted in Fig. (3.1) using $h = 0.01$ and some different values of k .

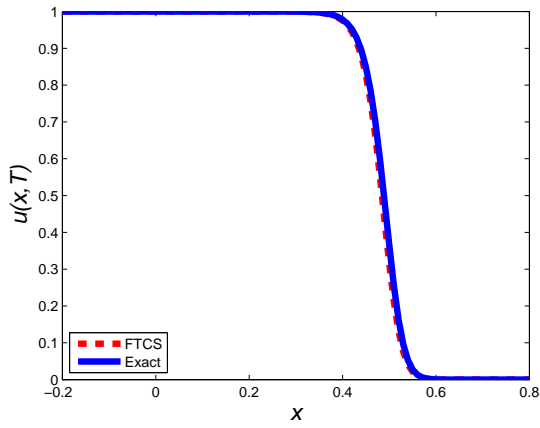
Remark 3.8. *In the Table 3.2, the CPU time is not monotonically increasing with the decreasing time step size it might be due to the fact that the partial differential equation considered is very stiff (problem Eq. 3.6 the boundary and initial conditions given by Eqs. (3.2) and (3.3) respectively) with $\rho = 10^4$. Initially, we have considerable phase lag at $k = \frac{T_{max}}{52}$. As we decrease the time step size, there is less phase lag. At time $k = \frac{T_{max}}{1300}$, we have optimal results. If we decrease k further, then we start to have phase lead.*



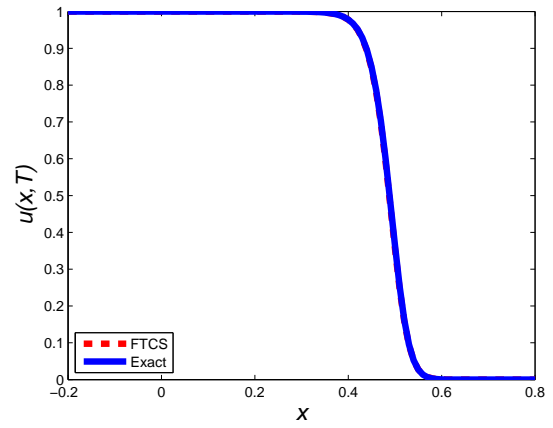
(a) $k = T_{max}/52$



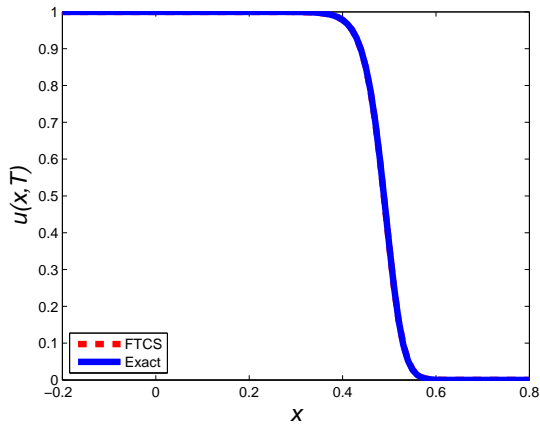
(b) $k = T_{max}/400$



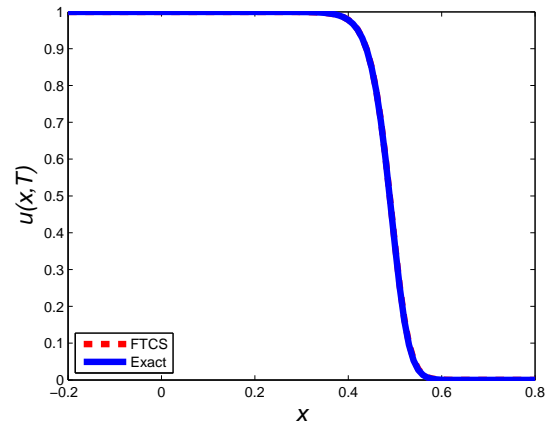
(c) $k = T_{max}/800$



(d) $k = T_{max}/1200$



(e) $k = T_{max}/1300$



(f) $k = T_{max}/1400$

Figure 3.1: Plot of u against x for Problem 1 using FTCS scheme at time 2.5×10^{-3} at some different values of k and $h = 0.01$, $T_{max} = 2.5 \times 10^{-3}$.

3.6 FTCS- ϵ scheme

In this section, we modify the FTCS scheme in order to obtain FTCS- ϵ . Ruxun et al. (1999) have designed a new scheme by modifying Lax-Wendroff (LW) scheme when used to discretise the linear advection equation given by

$$u_t + c u_x = 0, \quad c > 0. \quad (3.35)$$

We describe briefly their approach. To solve Eq. (3.35), a simple explicit consistent scheme can be constructed and the scheme is of the form

$$u_m^{n+1} = a_1 u_{m+1}^n + a_0 u_m^n + a_{-1} u_{m-1}^n. \quad (3.36)$$

Taylor series expansion of (3.36) gives

$$(1 + k D_t + \frac{k^2}{2!} D_t^2 + \dots) u_m^n = \left[(a_1 + a_0 + a_{-1}) + h(a_1 - a_{-1}) D_x + \frac{h^2}{2!} (a_1 + a_{-1}) D_x^2 + \frac{h^3}{3!} (a_1 - a_{-1}) D_x^3 + \dots \right] u_m^n, \quad (3.37)$$

where $D_t = \frac{\partial}{\partial t}$, $D_x = \frac{\partial}{\partial x}$. Ruxun et al. (1999) arrive at the following theorem:

Theorem 3.1. *Assume that the solution $u(x, t)$ of Eq. (3.35) be smooth enough and the scheme given by (3.36) be consistent with the original partial differential Eq. (3.35) and the spatial mesh size, h small enough then*

$$\begin{aligned} a_1 + a_0 + a_{-1} &= 1, \\ a_1 - a_{-1} &= c \frac{k}{h}. \end{aligned} \quad (3.38)$$

Proof. Rewriting the equation (3.37)

$$\left[1 - (a_1 + a_0 + a_{-1}) + k D_t - h(a_1 - a_{-1}) D_x + \frac{k^2}{2!} D_t^2 - \frac{h^2}{2!} (a_1 + a_{-1}) D_x^2 - \frac{h^3}{3!} (a_1 - a_{-1}) D_x^3 + \dots \right] u_m^n = 0. \quad (3.39)$$

It follows that $a_1 + a_0 + a_{-1} = 1$ and $a_1 - a_{-1} = c \frac{k}{h}$.

□

The Lax-Wendroff (LW) scheme discretising Eq. (3.35) is given by

$$u_m^{n+1} = \frac{1}{2}(r^2 - r)u_{m+1}^n + (1 - r^2)u_m^n + \frac{1}{2}(r^2 + r)u_{m-1}^n, \quad (3.40)$$

where $r = c\frac{k}{h}$. From the CFL condition, the scheme is stable if $0 < r \leq 1$.

Clearly, LW is not a monotone and positive scheme. A simple approach to construct a monotonic scheme is to reform the LW scheme. [Ruxun et al. \(1999\)](#) constructed the LW- ϵ scheme which is given by

$$u_m^{n+1} = \left(\frac{r^2 - r}{2} + \epsilon_1 \right) u_{m+1}^n + (1 - r + \epsilon_2) u_m^n + \left(\frac{r^2 + r}{2} + \epsilon_3 \right) u_{m-1}^n. \quad (3.41)$$

For consistency, we set $\epsilon_1 + \epsilon_2 + \epsilon_3 = 0$ and $\epsilon_1 - \epsilon_3 = 0$. Hence $\epsilon_2 = -2\epsilon_1$. We let $\epsilon_2 = -\epsilon$. LW- ϵ scheme is therefore

$$u_m^{n+1} = \left(\frac{r^2 - r}{2} + \frac{\epsilon}{2} \right) u_{m+1}^n + (1 - r - \epsilon) u_m^n + \left(\frac{r^2 + r}{2} + \frac{\epsilon}{2} \right) u_{m-1}^n, \quad (3.42)$$

with $0 \leq \epsilon \ll 1$. By working with dissipation and dispersion remainders, they found that $\epsilon = 1/4$ gives rise to a positive, monotonic scheme which is still second-order accurate.

We attempt to derive FTCS- ϵ scheme by adding numerical dissipation to the scheme to reduce numerical dispersion in the profile. We propose the following scheme

$$u_m^{n+1} = \left(1 - \frac{2k}{h^2} + k\rho \right) u_m^n + \frac{k}{h^2} u_{m+1}^n + \frac{k}{h^2} u_{m-1}^n - k\rho (u_m^n)^2 + \epsilon_1 u_{m-1}^n + \epsilon_2 u_m^n + \epsilon_3 u_{m+1}^n. \quad (3.43)$$

Theorem 3.2. *FTCS- ϵ scheme (3.43) is consistent with the original scaled equation (3.6) and is first order accurate both in time and in space if and only if $\epsilon_1 + \epsilon_2 + \epsilon_3 = 0$ and $\epsilon_3 - \epsilon_1 = 0$.*

Proof. 1) Taylor series expansion about point (n, m) gives

$$\begin{aligned} u + ku_t + \frac{k^2}{2} u_{tt} + \frac{k^3}{6} u_{ttt} + O(k^4) &= \left(1 - \frac{2k}{h^2} + k\rho \right) u - k\rho u^2 \\ &+ \frac{k}{h^2} \left(u + hu_x + \frac{h^2}{2} u_{xx} + \frac{h^3}{6} u_{xxx} + O(h^4) \right) \\ &+ \frac{k}{h^2} \left(u - hu_x + \frac{h^2}{2} u_{xx} - \frac{h^3}{6} u_{xxx} + O(h^4) \right) \\ &+ \epsilon_1 \left(u - hu_x + \frac{h^2}{2} u_{xx} - \frac{h^3}{6} u_{xxx} + O(h^4) \right) \\ &+ \epsilon_3 \left(u + hu_x + \frac{h^2}{2} u_{xx} + \frac{h^3}{6} u_{xxx} + O(h^4) \right) \\ &+ \epsilon_2 u, \end{aligned} \quad (3.44)$$

which simplifies as

$$\begin{aligned} u + ku_t + \frac{k^2}{2} u_{tt} + \frac{k^3}{6} u_{ttt} + O(k^4) &= (1 + k\rho + \epsilon_1 + \epsilon_2 + \epsilon_3) u + (-\epsilon_1 + \epsilon_3) hu_x - k\rho u^2 + \\ &\left(k + \frac{\epsilon_1}{2} h^2 + \frac{\epsilon_3}{2} h^2 \right) u_{xx} + \left(-\frac{\epsilon_1}{6} + \frac{\epsilon_3}{6} \right) h^3 u_{xxx} + O(h^4). \end{aligned} \quad (3.45)$$

On rearranging, we get

$$\begin{aligned} u - (1 + \epsilon_1 + \epsilon_2 + \epsilon_3) u + ku_t - h(\epsilon_3 - \epsilon_1) u_x - ku_{xx} - k\rho u + k\rho u^2 \\ = -\frac{k^2}{2} u_{tt} - \frac{k^3}{6} u_{ttt} + \frac{h^3}{6} (\epsilon_3 - \epsilon_1) u_{xxx} + \frac{h^2}{2} (\epsilon_1 + \epsilon_3) u_{xx} + O(h^4) + O(k^4). \end{aligned} \quad (3.46)$$

We recall that we are solving Eq. (3.6). Therefore for consistency, we must have $\epsilon_1 + \epsilon_2 + \epsilon_3 = 0$ and $\epsilon_3 - \epsilon_1 = 0$. We thus have $\epsilon_3 = \epsilon_1 = \epsilon$ and $\epsilon_2 = -2\epsilon_1 = -2\epsilon$. Hence the FTCS- ϵ scheme is given by

$$u_m^{n+1} = u_m^n + \frac{k}{h^2} (u_{m+1}^n - 2u_m^n + u_{m-1}^n) + k\rho u_m^n - k\rho(u_m^n)^2 + \epsilon(u_{m+1}^n - 2u_m^n + u_{m-1}^n), \quad (3.47)$$

and the scheme is consistent.

- 2) For order of accuracy, we consider Eq. (3.46) and we replace $\epsilon_3 = \epsilon_1 = \epsilon$ and $\epsilon_2 = -2\epsilon_1 = -2\epsilon$ and we have

$$ku_t - ku_{xx} - k\rho u + k\rho u^2 = -\frac{k^2}{2}u_{tt} - \frac{k^3}{6}u_{ttt} + h^2\epsilon u_{xx} + O(h^4) + O(k^4). \quad (3.48)$$

Dividing by k , gives

$$u_t - u_{xx} - \rho u + \rho u^2 = -\frac{k}{2}u_{tt} - \frac{k^2}{6}u_{ttt} + \frac{h^2}{k}\epsilon u_{xx} + \frac{h^2}{12}u_{xxx} + O\left(\frac{h^4}{k}\right) + O(k^3). \quad (3.49)$$

FTCS- ϵ scheme is first order accurate both in time and in space. □

Theorem 3.3. *FTCS- ϵ scheme (3.43) is stable under the condition*

$$\frac{k}{h^2} \leq \frac{1}{2} - \epsilon$$

for the time step, k and the spatial size, h .

Proof. For stability analysis, we apply Fourier series analysis and we obtain the amplification factor ξ , as

$$\xi = 1 - \frac{2k}{h^2} + \frac{2k}{h^2} \cos(w) + k\rho - k\rho u_{max} + \epsilon(2\cos(w) - 2), \quad (3.50)$$

We choose $u_{max} = 1$, $\rho = 10^4$ and therefore,

$$\xi = 1 - 4\sin^2\left(\frac{w}{2}\right) \left(\epsilon + \frac{k}{h^2}\right). \quad (3.51)$$

For stability, $|\xi| \leq 1$ and this gives

$$2\left(\epsilon + \frac{k}{h^2}\right) \sin^2\left(\frac{w}{2}\right) \leq 1, \quad (3.52)$$

which finally yields

$$\frac{k}{h^2} \leq \frac{1}{2} - \epsilon. \quad (3.53)$$

□

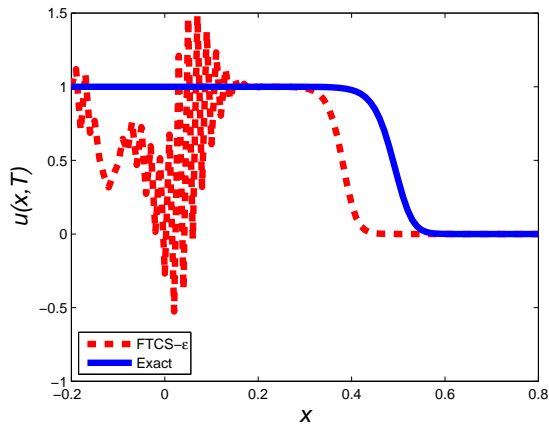
For $h = 0.01$, $\epsilon = 0.01$, we have the stability region given by $k \leq 4.90 \times 10^{-5}$.

We tabulate some errors namely L_1 and L_∞ errors and display CPU times for Problem 1 and 2 using FTCS- ϵ at some different values of time-step size with spatial step size, $h = 0.01$, and $\epsilon = 0.01$. The

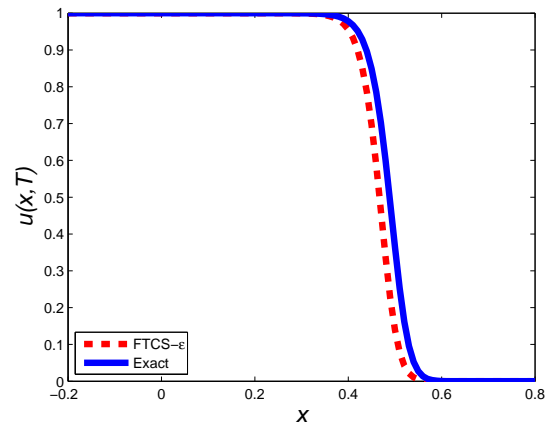
errors are displayed in Tables (3.5) and (3.7). The time is $T_{max} = 2.5 \times 10^{-3}$ and the timestep size is less than or equal 4.90×10^{-5} .

We observe from Tables (3.5) and (3.7) that the L_1 and L_∞ errors are the same and the CPU time is different. As we increase the length of the domain, it is obvious that CPU time must increase. As we decrease the time-step size, L_1 and L_∞ errors initially decrease and reach minimum when $k \approx T_{max}/315$ and then the errors increase again. For k close to $T_{max}/100$, the dispersion error is quite large.

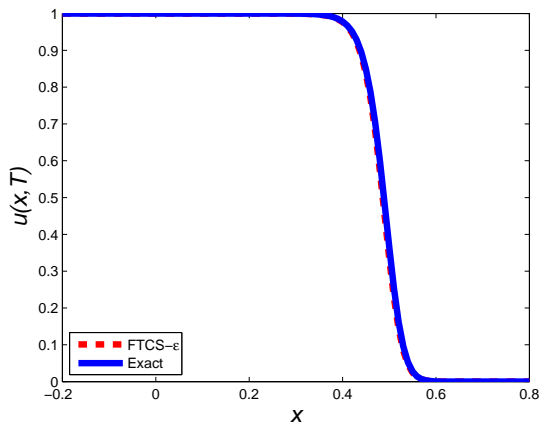
Comparing Tables (3.2) and (3.4) to Table (3.1), we notice that L_1 and L_∞ errors from FTCS- ϵ method at an optimal step size are quite smaller than those obtained using MMPDE and MMDAE methods.



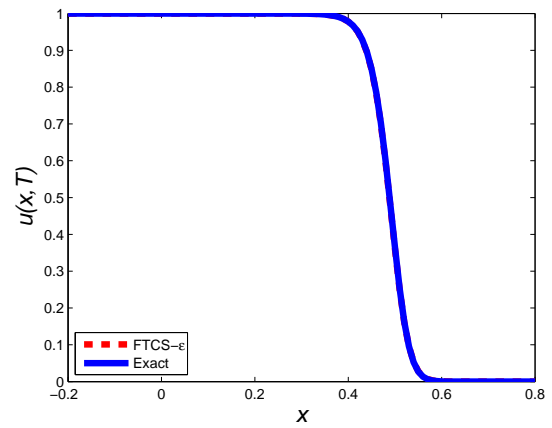
(a) $k = T_{max}/53$



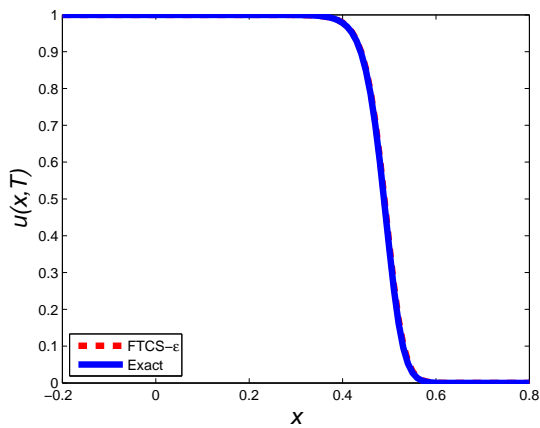
(b) $k = T_{max}/200$



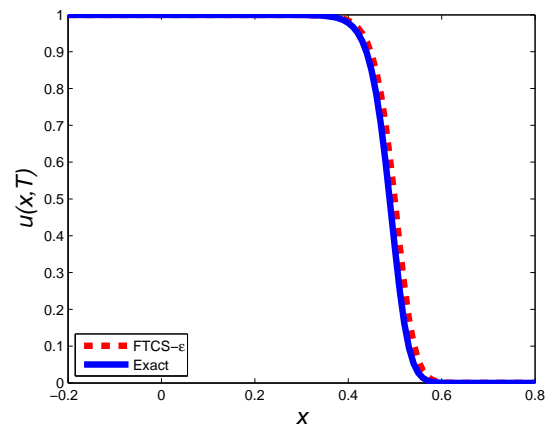
(c) $k = T_{max}/300$



(d) $k = T_{max}/315$



(e) $k = T_{max}/325$



(f) $k = T_{max}/400$

Figure 3.2: Plot of u against x for Problem1 using FTCS- ϵ scheme at time 2.5×10^{-3} and some different values of k and $h = 0.01$, $\epsilon = 0.01$, $T_{max} = 2.5 \times 10^{-3}$.

Time step (k)	L_1 error	L_∞ error	CPU(s)
$T_{max}/53$	2.8025×10^{-1}	1.5265	0.764
$T_{max}/100$	5.9959×10^{-2}	6.6244×10^{-1}	0.783
$T_{max}/200$	2.1273×10^{-2}	2.6296×10^{-1}	0.796
$T_{max}/300$	2.4401×10^{-3}	3.1737×10^{-2}	0.928
$T_{max}/310$	9.7448×10^{-4}	1.3521×10^{-2}	0.850
$T_{max}/315$	3.2771×10^{-4}	4.7040×10^{-3}	0.799
$T_{max}/320$	4.6757×10^{-4}	4.6218×10^{-3}	0.814
$T_{max}/325$	1.1657×10^{-3}	1.2769×10^{-2}	0.902
$T_{max}/350$	4.5061×10^{-3}	5.3608×10^{-2}	0.821
$T_{max}/375$	7.6305×10^{-3}	9.1590×10^{-2}	0.927
$T_{max}/400$	1.0576×10^{-2}	1.2682×10^{-1}	0.927
$T_{max}/500$	2.1076×10^{-2}	2.4515×10^{-1}	0.925
$T_{max}/600$	3.0241×10^{-2}	3.4502×10^{-1}	0.868

Table 3.5: L_1 and L_∞ errors and CPU time at some different values of time-step size, k for Problem 1 and spatial mesh size, $h = 0.01$, $\epsilon = 0.01$ using FTCS- ϵ , where $T_{max} = 2.5 \times 10^{-3}$.

Time step (k)	L_1 error	Rate of convergence
$T_{max}/100$	5.9959×10^{-2}	
$T_{max}/200$	2.1273×10^{-2}	1.495

Table 3.6: Rate of convergence with k and spatial mesh size, $h = 0.01$, $\epsilon = 0.01$, of Problem 1 using FTCS- ϵ .

Remark 3.9. The optimal k is approximately $\frac{T_{max}}{315}$. That why we use $\frac{T_{max}}{100}$ and $\frac{T_{max}}{200}$. Reason being, we don't need adding further rows to compute the convergence rate.

Time step (k)	L_1 error	L_∞ error	CPU(s)
$T_{max}/53$	2.8025×10^{-1}	1.5265	1.488
$T_{max}/100$	5.9959×10^{-2}	6.6244×10^{-1}	2.265
$T_{max}/200$	2.1273×10^{-2}	2.6296×10^{-1}	4.704
$T_{max}/300$	2.4401×10^{-3}	3.1737×10^{-2}	7.819
$T_{max}/310$	9.7448×10^{-4}	1.3521×10^{-2}	8.154
$T_{max}/315$	3.2771×10^{-4}	4.7040×10^{-3}	8.429
$T_{max}/320$	4.6757×10^{-4}	4.6218×10^{-3}	8.537
$T_{max}/325$	1.1657×10^{-3}	1.2769×10^{-2}	8.732
$T_{max}/350$	4.5061×10^{-3}	5.3608×10^{-2}	9.779
$T_{max}/375$	7.6305×10^{-3}	9.1590×10^{-2}	10.678
$T_{max}/400$	1.0576×10^{-2}	1.2682×10^{-1}	11.692
$T_{max}/500$	2.1076×10^{-2}	2.4515×10^{-1}	16.319
$T_{max}/600$	3.0241×10^{-2}	3.4502×10^{-1}	21.644

Table 3.7: L_1 and L_∞ errors and CPU time at some different values of time-step size, k and spatial mesh size, $h = 0.01$, $\epsilon = 0.01$, of Problem 2 using FTCS- ϵ , where $T_{max} = 2.5 \times 10^{-3}$.

3.7 Nonstandard Finite Difference Schemes (NSFD)

Diverse explicit NSFD schemes have been suggested for Fisher's equation with respect to their performances (Anguelov et al., 2005, Mickens, 1994, 1997). These performances are stability of fixed points, positivity, boundedness of solutions etc. More notions on NSFD with definition and properties is in chapter 2, section 2.1.2.

Following Mickens (2002), a non-standard finite difference scheme for Eq. (3.6) is

$$\frac{u_m^{n+1} - u_m^n}{\phi(k)} - \frac{u_{m+1}^n - 2u_m^n + u_{m-1}^n}{[\psi(h)]^2} = \rho u_m^n - \rho \left(\frac{u_{m+1}^n + u_m^n + u_{m-1}^n}{3} \right) u_m^{n+1}, \quad (3.54)$$

where the simple choice was made for the two denominator functions

$$\phi(k) = k; \quad \psi(h) = h^2, \quad (3.55)$$

and where non-local representation was used for the u^2 terms;

$$u^2 \rightarrow \left(\frac{u_{m+1}^n + u_m^n + u_{m-1}^n}{3} \right) u_m^{n+1}. \quad (3.56)$$

A single expression of the scheme is

$$u_m^{n+1} = \frac{\left(1 + k\rho - \frac{2k}{h^2}\right) u_m^n + \frac{k}{h^2} (u_{m+1}^n + u_{m-1}^n)}{1 + k\rho \left(\frac{u_{m+1}^n + u_m^n + u_{m-1}^n}{3}\right)}. \quad (3.57)$$

3.7.1 Positivity and Boundedness: Relation between time and space step-sizes

In this subsection, we study the positivity and boundedness properties of NSFD.

From the initial data, if $u(x, 0) = f(x)$, such that $0 \leq f(x) \leq 1$, we have $0 \leq u(x, t) \leq 1$ (Mickens, 1997).

Theorem 3.4. *The scheme (3.57) is positive and definite if there is a constant Γ , $0 \leq \Gamma < 1$ such that the inequality*

$$k \leq \frac{h^2}{2} \left[\frac{1 - \Gamma}{1 - \frac{\rho h^2}{2}} \right]$$

holds for the time step, k and spatial size, h .

Proof. If the quantity u_m^{n+1} from Eq. (3.57) is required to satisfy positivity condition ($u_m^{n+1} \geq 0$) if $u_m^n \geq 0$, then we must have

$$\Gamma = 1 + k\rho - 2R \geq 0, \quad R = \frac{k}{h^2}. \quad (3.58)$$

It follows that

$$1 - \Gamma = 2R - k\rho. \quad (3.59)$$

We have

$$0 \leq 2R - k\rho \leq 1, \quad (3.60)$$

which gives

$$0 \leq k \left[\frac{2}{h^2} - \rho \right] \leq 1. \quad (3.61)$$

It follows that

$$k \leq \frac{h^2}{2} \left[\frac{1 - \Gamma}{1 - \frac{\rho h^2}{2}} \right] \quad \text{and} \quad 0 \leq \Gamma < 1, \quad (3.62)$$

which is the condition required for positivity (Mickens, 1997). \square

Remark 3.10. *The same result can be obtained by using the Von Neumann stability analysis.*

Indeed, for stability, the amplification factor, ξ is given by

$$\xi = \frac{1 + k\rho - \frac{2k}{h^2}(1 - \cos(w))}{1 + k\rho u_{max}} = \frac{1 + k\rho - \frac{4k}{h^2} \sin^2\left(\frac{w}{2}\right)}{1 + k\rho u_{max}}. \quad (3.63)$$

We requires $|\xi| \leq 1$. Since $u_{max} = 1$, we have

$$\frac{2k}{h^2} \sin^2\left(\frac{w}{2}\right) \leq 1 + k\rho. \quad (3.64)$$

For $w \in [-\pi, \pi]$, we have

$$\frac{2k}{h^2} \leq 1 + k\rho \Rightarrow k \leq \frac{h^2}{2} \left[\frac{2R - k\rho}{1 - \frac{\rho h^2}{2}} \right], \quad (3.65)$$

which yield using Eq. (3.59)

$$k \leq \frac{h^2}{2} \left[\frac{1 - \Gamma}{1 - \frac{\rho h^2}{2}} \right] \quad \text{and} \quad 0 \leq \Gamma < 1. \quad (3.66)$$

We note that we get the same inequality between k and h for stability and positive definiteness to be satisfied. For $h = 0.01$, $\rho = 10^4$, we have $k \leq 10^{-4}$ or $k \leq \frac{T_{max}}{25}$.

Theorem 3.5. *If $0 \leq u_m^n \leq 1$ and the condition*

$$k = \frac{h^2}{3} \left[\frac{1}{1 - \frac{\rho h^2}{3}} \right]$$

holds for the time step, k and space step, h then the scheme (3.57) is bounded.

Proof. We assume that $0 \leq u_m^n \leq 1$. We rewrite Eq. (3.57) as

$$u_m^{n+1} = \frac{\Gamma u_m^n + R(u_{m+1}^n + u_{m-1}^n)}{1 + \left(\frac{\rho k}{3}\right)(u_{m+1}^n + u_m^n + u_{m-1}^n)}. \quad (3.67)$$

From (Mickens, 1997), Eq. (3.67) takes the symmetric form if $\Gamma = R$. It follows that

$$k = \frac{h^2}{3} \left[\frac{1}{1 - \frac{\rho h^2}{3}} \right]. \quad (3.68)$$

Hence

$$R = \frac{k}{h^2} = \left(\frac{1}{3}\right) \left[\frac{1}{1 - \frac{\rho h^2}{3}} \right]. \quad (3.69)$$

Taking into account the symmetric condition (3.69), Eq. (3.67) can be rewritten as

$$u_m^{n+1} = \frac{R(u_m^n + u_{m+1}^n + u_{m-1}^n)}{1 + \left(\frac{k\rho}{3}\right)(u_{m+1}^n + u_m^n + u_{m-1}^n)}. \quad (3.70)$$

We know that $0 \leq u_m^n \leq 1$. It follows that

$$0 \leq \frac{u_m^n + u_{m+1}^n + u_{m-1}^n}{3} \leq 1. \quad (3.71)$$

By multiplying Eq. (3.71) by $1 - \frac{\rho h^2}{3}$ and dividing by $1 - \frac{\rho h^2}{3}$, we have

$$\left[1 - \frac{\rho h^2}{3}\right] \frac{u_m^n + u_{m+1}^n + u_{m-1}^n}{3 \left[1 - \frac{\rho h^2}{3}\right]} \leq 1, \quad (3.72)$$

which can be rewritten

$$\frac{u_m^n + u_{m+1}^n + u_{m-1}^n}{3 \left[1 - \frac{\rho h^2}{3}\right]} - \left[\frac{\rho h^2}{3}\right] \frac{u_m^n + u_{m+1}^n + u_{m-1}^n}{3 \left[1 - \frac{\rho h^2}{3}\right]} \leq 1. \quad (3.73)$$

It follows that

$$\frac{u_m^n + u_{m+1}^n + u_{m-1}^n}{3 \left[1 - \frac{\rho h^2}{3}\right]} \leq 1 + \frac{h^2}{3} \left[\frac{1}{1 - \frac{\rho h^2}{3}} \right] \left(\frac{\rho}{3}\right) (u_m^n + u_{m+1}^n + u_{m-1}^n). \quad (3.74)$$

Using Eqs. (3.69) and (3.68), we have

$$R(u_m^n + u_{m+1}^n + u_{m-1}^n) \leq 1 + \frac{k\rho}{3} (u_m^n + u_{m+1}^n + u_{m-1}^n), \quad (3.75)$$

which gives

$$0 \leq u_m^{n+1} = \frac{R(u_m^n + u_{m+1}^n + u_{m-1}^n)}{1 + \left(\frac{k\rho}{3}\right)(u_{m+1}^n + u_m^n + u_{m-1}^n)} \leq 1. \quad (3.76)$$

Hence the boundedness of u_m^{n+1} . □

We tabulate L_1 and L_∞ errors and CPU time when Problem 1 and 2 are solved using NSFD scheme at some different values of time-step size k , with spatial step size, $h = 0.01$. The errors are displayed in Tables (3.9) and (3.10). As the time-step size is reduced, the errors initially decrease and optimal k is approximately equal to $T_{max}/1500$. On further decreasing k , the errors start to increase.

Time step (k)	L_1 error	Rate of convergence
$T_{max}/50$	1.2304×10^{-1}	
$T_{max}/100$	7.0554×10^{-2}	0.8023
$T_{max}/200$	3.6165×10^{-2}	0.9641
$T_{max}/400$	1.6095×10^{-2}	1.1680

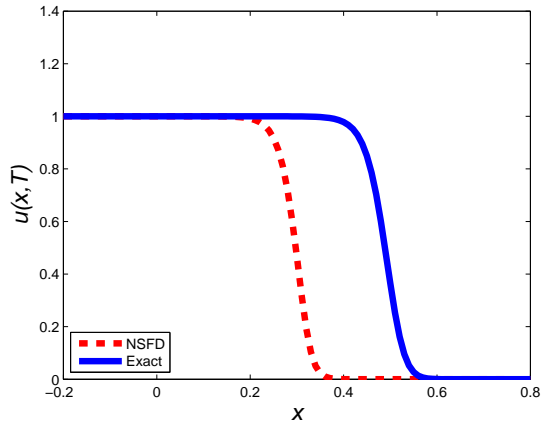
Table 3.8: Rate of convergence with k and spatial mesh size, $h = 0.01$, $\epsilon = 0.01$, of Problem 1 using NSFD.

Time step (k)	L_1 error	L_∞ error	CPU
$T_{max}/25$	1.9125×10^{-1}	9.8876×10^{-1}	0.683
$T_{max}/50$	1.2304×10^{-1}	9.2384×10^{-1}	0.743
$T_{max}/100$	7.0554×10^{-2}	7.0761×10^{-1}	0.689
$T_{max}/200$	3.6165×10^{-2}	4.1770×10^{-1}	0.724
$T_{max}/300$	2.3031×10^{-2}	2.7850×10^{-1}	0.738
$T_{max}/400$	1.6095×10^{-2}	1.9599×10^{-1}	0.758
$T_{max}/500$	1.1808×10^{-2}	1.4689×10^{-1}	0.831
$T_{max}/600$	8.8945×10^{-3}	1.1268×10^{-1}	0.814
$T_{max}/700$	6.7864×10^{-3}	8.7538×10^{-2}	0.854
$T_{max}/800$	5.1909×10^{-3}	6.8368×10^{-2}	0.900
$T_{max}/900$	3.9428×10^{-3}	5.3310×10^{-2}	0.960
$T_{max}/1000$	2.9430×10^{-3}	4.1187×10^{-2}	0.972
$T_{max}/1100$	2.1324×10^{-3}	3.1229×10^{-2}	0.939
$T_{max}/1200$	1.4815×10^{-3}	2.2908×10^{-2}	0.995
$T_{max}/1300$	9.7728×10^{-4}	1.5854×10^{-2}	1.034
$T_{max}/1400$	6.3200×10^{-4}	9.8018×10^{-3}	1.077
$T_{max}/1500$	4.5216×10^{-4}	4.5522×10^{-3}	1.175
$T_{max}/1600$	5.0673×10^{-4}	5.3751×10^{-3}	1.210
$T_{max}/1700$	8.4460×10^{-4}	7.6933×10^{-3}	1.263
$T_{max}/1800$	1.1475×10^{-3}	1.0160×10^{-2}	1.298

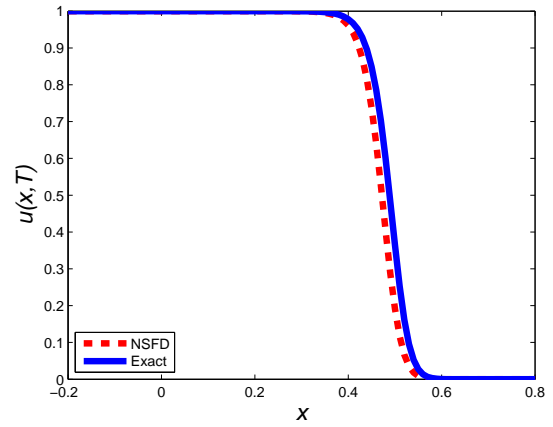
Table 3.9: L_1 and L_∞ errors and CPU time at some different values of time-step size, k for Problem 1 at time 2.5×10^{-3} with spatial mesh size, $h = 0.01$ using NSFD scheme, where $T_{max} = 2.5 \times 10^{-3}$.

Time step (k)	L_1 error	L_∞ error	CPU(s)
$T_{max}/25$	1.9125×10^{-1}	9.8876×10^{-1}	1.130
$T_{max}/50$	1.2304×10^{-1}	9.2384×10^{-1}	1.470
$T_{max}/100$	7.0554×10^{-2}	7.0761×10^{-1}	2.280
$T_{max}/200$	3.6165×10^{-2}	4.1770×10^{-1}	4.844
$T_{max}/300$	2.3031×10^{-2}	2.7850×10^{-1}	7.950
$T_{max}/400$	1.6095×10^{-2}	1.9599×10^{-1}	12.219
$T_{max}/500$	1.1808×10^{-2}	1.4689×10^{-1}	17.052
$T_{max}/600$	8.8945×10^{-3}	1.1268×10^{-1}	22.408
$T_{max}/700$	6.7864×10^{-3}	8.7538×10^{-2}	28.688
$T_{max}/800$	5.1909×10^{-3}	6.8368×10^{-2}	35.804
$T_{max}/900$	3.9428×10^{-3}	5.3310×10^{-2}	44.176
$T_{max}/1000$	2.9430×10^{-3}	4.1187×10^{-2}	52.029
$T_{max}/1100$	2.1324×10^{-3}	3.1229×10^{-2}	61.695
$T_{max}/1200$	1.4815×10^{-3}	2.2908×10^{-2}	77.506
$T_{max}/1300$	9.7728×10^{-4}	1.5854×10^{-2}	97.953
$T_{max}/1400$	6.3200×10^{-4}	9.8018×10^{-3}	98.065
$T_{max}/1500$	4.5216×10^{-4}	4.5522×10^{-3}	110.000
$T_{max}/1600$	5.0673×10^{-4}	5.3751×10^{-3}	110.565
$T_{max}/1700$	8.4460×10^{-4}	7.6933×10^{-3}	115.565
$T_{max}/1800$	1.1475×10^{-3}	1.0160×10^{-2}	118.565

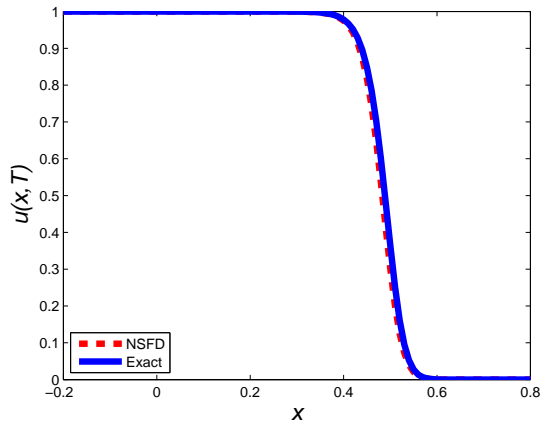
Table 3.10: L_1 and L_∞ errors and CPU time at some different values of time-step size, k for Problem 2 at time 2.5×10^{-3} with spatial mesh size, $h = 0.01$ using NSFD scheme, where $T_{max} = 2.5 \times 10^{-3}$.



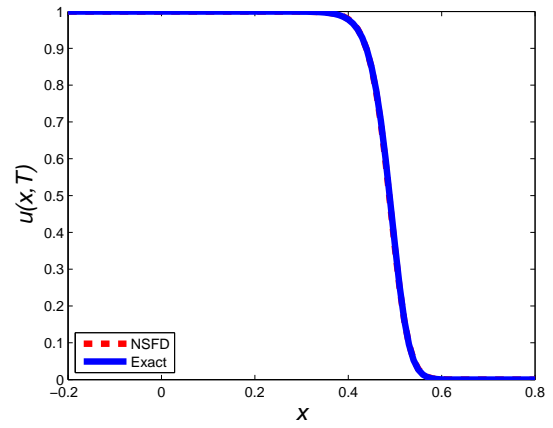
(a) $k = T_{max}/25$



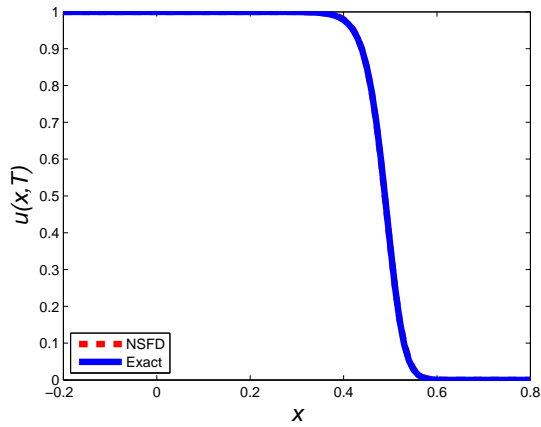
(b) $k = T_{max}/400$



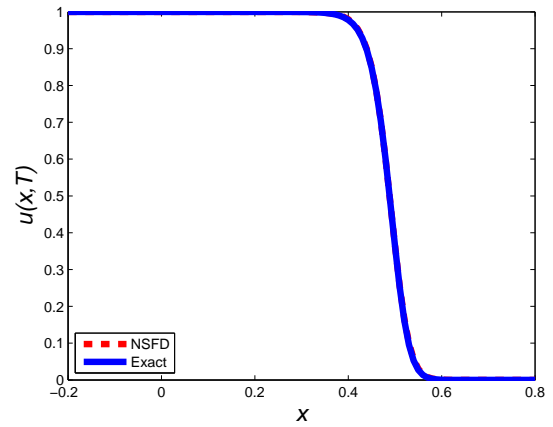
(c) $k = T_{max}/800$



(d) $k = T_{max}/1400$



(e) $k = T_{max}/1500$



(f) $k = T_{max}/1600$

Figure 3.3: Plot of u against x for Problem 1 using NSFD scheme at time 2.5×10^{-3} at some different values of k and $h = 0.01$.

3.8 NSFD- ϵ schemes

We construct the NSFD- ϵ by adding the expression $\epsilon_1 u_{m+1}^n + \epsilon_2 u_m^n + \epsilon_3 u_{m-1}^n$ to u_m^{n+1} to Eq. (3.57).

We thus have

$$u_m^{n+1} = \frac{(1 + k\rho - \frac{2k}{h^2})u_m^n + \frac{k}{h^2}(u_{m+1}^n + u_{m-1}^n)}{1 + k\rho \left(\frac{u_{m+1}^n + u_m^n + u_{m-1}^n}{3} \right)} + \epsilon_1 u_{m+1}^n + \epsilon_2 u_m^n + \epsilon_3 u_{m-1}^n. \quad (3.77)$$

Theorem 3.6. *The NSFD- ϵ scheme (3.77) is consistent with the original scaled equation (3.6) and is first order accurate in time and first order accurate in space if only $\epsilon_1 + \epsilon_2 + \epsilon_3 = 0$ and $\epsilon_3 - \epsilon_1 = 0$.*

Proof. 1) Using Taylor series expansion about (n, m) , we have

$$\begin{aligned} u + ku_t + \frac{k^2}{2}u_{tt} + \frac{k^3}{6}u_{ttt} + O(k^4) &= \frac{ku_{xx} + (1 + k\rho)u}{1 + k\rho u + \frac{k\rho h^2}{3}u_{xx}} + (\epsilon_1 + \epsilon_2 + \epsilon_3)u \\ &+ h(\epsilon_3 - \epsilon_1)u_x + \frac{h^2}{2}(\epsilon_1 + \epsilon_2)u_{xx} + \frac{h^3}{6}(\epsilon_3 - \epsilon_1)u_{xxx} + O(h^4), \end{aligned} \quad (3.78)$$

which can be written as

$$\begin{aligned} \left(1 + k\rho u + \frac{k\rho h^2}{3}u_{xx}\right)u_t + \left(\frac{k}{2} + \frac{k}{2}\rho u + \frac{k^2}{6}\rho h^2 u_{xx}\right)u_{tt} + \left(\frac{k^2}{6} + \frac{k^3}{6}\rho u + \frac{k^3}{18}\rho h^2 u_{xx}\right)u_{ttt} \\ + \rho u^2 + \frac{\rho h^2}{3}uu_{xx} = u_{xx} + \rho u + (\epsilon_1 + \epsilon_2 + \epsilon_3)u \left(\frac{1}{k} + \frac{\rho h^2}{3}u_{xx}\right) \\ + (\epsilon_3 - \epsilon_1)u_x \left(\frac{h}{k} + h\rho u \frac{\rho h^3}{3}u_{xx}\right) + (\epsilon_1 + \epsilon_2)u_{xx} \left(\frac{h^2}{k} + h^2\rho u + \frac{\rho h^4}{3}u_{xx}\right) \\ + (\epsilon_3 - \epsilon_1)u_{xxx} \left(\frac{h^3}{k} + h^3\rho u \frac{\rho h^5}{3}u_{xx}\right) + O(k^4) + O(h^4). \end{aligned} \quad (3.79)$$

When $k, h \rightarrow 0$, we recover

$$u_t = u_{xx} + \rho u(1 - u), \quad (3.80)$$

if $\epsilon_1 + \epsilon_2 + \epsilon_3 = 0$ and $\epsilon_1 - \epsilon_3 = 0$. It thus follows that $\epsilon_1 = \epsilon_3 = \epsilon$ and $\epsilon_2 = -2\epsilon$.

2) For accuracy, we next consider Eq. (3.79) with $\epsilon_1 = \epsilon_3 = \epsilon$ and $\epsilon_2 = -2\epsilon$. It follows that

$$\begin{aligned} \left(1 + k\rho u + \frac{k\rho h^2}{3}u_{xx}\right)u_t + \left(\frac{k}{2} + \frac{k}{2}\rho u + \frac{k^2}{6}\rho h^2 u_{xx}\right)u_{tt} + \left(\frac{k^2}{6} + \frac{k^3}{6}\rho u + \frac{k^3}{18}\rho h^2 u_{xx}\right)u_{ttt} \\ + \rho u^2 + \frac{\rho h^2}{3}uu_{xx} = u_{xx} + \rho u - \epsilon u_{xx} \left(\frac{h^2}{k} + h^2\rho u + \frac{\rho h^4}{3}u_{xx}\right) + O(k^4) + O(h^4). \end{aligned} \quad (3.81)$$

We rewrite Eq. (3.81) in the form

$$\begin{aligned} u_t - u_{xx} - \rho u + \rho u^2 &= -\left(k\rho u + \frac{k\rho h^2}{3}u_{xx}\right)u_t - \left(\frac{k}{2} + \frac{k}{2}\rho u + \frac{k^2}{6}\rho h^2 u_{xx}\right)u_{tt} \\ &- \epsilon \left(\frac{\rho h^2}{3}u + \frac{h^2}{k} + h^2\rho u + \frac{\rho h^4}{3}u_{xx}\right)u_{xx} - \left(\frac{k^2}{6} + \frac{k^3}{6}\rho u + \frac{k^3}{18}\rho h^2 u_{xx}\right)u_{ttt} \\ &+ O(k^4) + O(h^4). \end{aligned} \quad (3.82)$$

We conclude that NSFD- ϵ is first order accurate in time and first order accurate in space. \square

Positivity and Boundedness

Here we study the dynamical consistency of the NSFD- ϵ scheme

Theorem 3.7. *The scheme NSFD- ϵ (3.77) is positive definite if there is Γ such that $0 \leq \Gamma < 1 - 2\epsilon$, and the condition*

$$k \leq \frac{h^2}{2} \left[\frac{1 - 2\epsilon - \Gamma}{1 - \frac{\rho h^2}{2} (1 - 2\epsilon)} \right]$$

holds. Furthermore if $0 \leq u_m^n \leq 1$, $\forall m$ and the condition

$$k = \frac{h^2}{3} \left[\frac{1 - 3\epsilon}{1 - \frac{\rho h^2}{3} (1 - 3\epsilon)} \right]$$

holds for the time step, k and the space step, h then the scheme NSFD- ϵ (3.77) is bounded.

Proof. 1) We study the positivity of the method. We rewrite Eq. (3.77) as

$$u_m^{n+1} = \frac{\Gamma u_m^n + R(u_{m+1}^n + u_{m-1}^n)}{1 + k\rho \left(\frac{u_{m+1}^n + u_m^n + u_{m-1}^n}{3} \right)}. \quad (3.83)$$

where

$$\begin{aligned} \Gamma &= 1 + k\rho - \frac{2k}{h^2} - 2\epsilon \left[1 + k\rho \left(\frac{u_{m+1}^n + u_m^n + u_{m-1}^n}{3} \right) \right] \text{ and} \\ R &= \frac{k}{h^2} + \epsilon \left[1 + k\rho \left(\frac{u_{m+1}^n + u_m^n + u_{m-1}^n}{3} \right) \right]. \end{aligned} \quad (3.84)$$

We assume that $0 \leq u_m^n \leq 1$. Then u_m^{n+1} is positive if

$$\Gamma = 1 + k\rho - \frac{2k}{h^2} - 2\epsilon \left[1 + k\rho \left(\frac{u_{m+1}^n + u_m^n + u_{m-1}^n}{3} \right) \right] \geq 0. \quad (3.85)$$

By taking the maximum of u_j^n , $j = m - 1, m, m + 1$, we have

$$\Gamma = 1 + k\rho - \frac{2k}{h^2} - 2\epsilon \left(1 + k\rho \frac{3|u_{max}|}{3} \right) \geq 0, \quad (3.86)$$

which gives

$$\Gamma = 1 + k\rho - \frac{2k}{h^2} - 2\epsilon(1 + k\rho) \geq 0, \quad (3.87)$$

since $u_{max} = 1$. It follows from Eq. (3.87) that

$$1 - 2\epsilon - \Gamma = k \left[\frac{2}{h^2} - \rho(1 - 2\epsilon) \right] \leq 1 - 2\epsilon. \quad (3.88)$$

Hence u_m^{n+1} is positive if

$$k \leq \frac{h^2}{2} \left[\frac{1 - 2\epsilon - \Gamma}{1 - \frac{\rho h^2}{2} (1 - 2\epsilon)} \right] \text{ and } 0 \leq \Gamma < 1 - 2\epsilon. \quad (3.89)$$

Remark 3.11. *We can obtain the same result of positivity condition by using the amplification factor*

Indeed, for stability analysis we apply Fourier series analysis to Eq. (3.83) to obtain the amplification factor ξ . Thus

$$\xi = \frac{1 + k\rho - \frac{2k}{h^2}}{1 + k\rho|u_{max}|} - 2\epsilon + 2 \left[\frac{\frac{k}{h^2}}{1 + k\rho|u_{max}|} + \epsilon \right] \cos(w). \quad (3.90)$$

For the stability, we have $|\xi| \leq 1$. Since $u_{max} = 1$, we solve

$$-2 \leq -2 \left[2\epsilon + \frac{\frac{2k}{h^2}}{1 + k\rho} \right] \sin^2 \left(\frac{w}{2} \right) \leq 0, \quad (3.91)$$

and obtain, for $w \in [-\pi, \pi]$

$$k \leq \frac{h^2}{2} \left[\frac{1 - 2\epsilon}{1 - \frac{\rho h^2}{2} (1 - 2\epsilon)} \right]. \quad (3.92)$$

Hence

$$k \leq \frac{h^2}{2} \left[\frac{1 - 2\epsilon - \Gamma}{1 - \frac{\rho h^2}{2} (1 - 2\epsilon)} \right]. \quad (3.93)$$

2) For the boundedness of NSFD- ϵ , we use the symmetric condition by taking $R = \Gamma$ from Eq. (3.83).

It follows that

$$1 + k\rho - \frac{2k}{h^2} - \frac{k}{h^2} = 3\epsilon \left(1 + k\rho \frac{3|u_{max}|}{3} \right). \quad (3.94)$$

With $u_{max} = 1$, we have

$$k = \frac{h^2}{3} \left[\frac{1 - 3\epsilon}{1 - \frac{\rho h^2}{3} (1 - 3\epsilon)} \right] \quad (3.95)$$

and

$$\frac{k}{(1 - 3\epsilon)h^2} = \frac{1}{3} \left[\frac{1}{1 - \frac{\rho h^2}{3} (1 - 3\epsilon)} \right], \quad (3.96)$$

which is the symmetric condition. Using Eq. (3.96), Eq. (3.83) becomes

$$u_m^{n+1} = \frac{\Gamma (u_{m+1}^n + u_m^n + u_{m-1}^n)}{1 + k\rho \left(\frac{u_{m+1}^n + u_m^n + u_{m-1}^n}{3} \right)}. \quad (3.97)$$

We know that $0 \leq u_j^n \leq 1$, $j = m - 1, m, m + 1$. It follows that

$$\frac{u_{m+1}^n + u_m^n + u_{m-1}^n}{3} \leq 1. \quad (3.98)$$

By multiplying and dividing Eq. (3.98) by $\left(1 - \frac{\rho h^2}{3} (1 - 3\epsilon) \right)$, we have

$$\left[1 - \frac{\rho h^2}{3} (1 - 3\epsilon) \right] \frac{u_{m+1}^n + u_m^n + u_{m-1}^n}{3 \left[1 - \frac{\rho h^2}{3} (1 - 3\epsilon) \right]} \leq 1. \quad (3.99)$$

It follows that

$$\frac{u_{m+1}^n + u_m^n + u_{m-1}^n}{3 \left[1 - \frac{\rho h^2}{3} (1 - 3\epsilon) \right]} \leq 1 + \frac{\rho}{3} \left(\frac{h^2}{3} \right) \left[\frac{1 - 3\epsilon}{1 - \frac{\rho h^2}{3} (1 - 3\epsilon)} \right] (u_{m+1}^n + u_m^n + u_{m-1}^n). \quad (3.100)$$

From Eq. (3.95) and the symmetric condition (3.96), we have

$$\Gamma (u_{m+1}^n + u_m^n + u_{m-1}^n) \leq 1 + \frac{k\rho}{3} (u_{m+1}^n + u_m^n + u_{m-1}^n). \quad (3.101)$$

It follows that

$$0 \leq u_m^{n+1} = \frac{\Gamma(u_{m+1}^n + u_m^n + u_{m-1}^n)}{1 + \frac{k\rho}{3}(u_{m+1}^n + u_m^n + u_{m-1}^n)} \leq 1. \quad (3.102)$$

Hence the boundedness of NSFD- ϵ method.

Remark 3.12. *We can obtain different result without symmetric condition (3.96).*

Indeed, generally without symmetric condition (3.96), we consider the boundedness of u_m^{n+1} in case of NSFD and we find the boundedness of NSFD- ϵ by stating from Eq. (3.77) that

$$0 \leq u_m^{n+1} \leq 1 + \epsilon(u_{m-1}^n - 2u_m^n + u_{m+1}^n). \quad (3.103)$$

We rewrite $\epsilon(u_{m+1}^n - 2u_m^n + u_{m-1}^n)$ as

$$\epsilon(u_{m-1}^n - 2u_m^n + u_{m+1}^n) = \epsilon(u_{m-1}^n + u_{m+1}^n) - 2\epsilon u_m^n. \quad (3.104)$$

Since u_j^n , $j = m-1, m, m+1$, are bounded ($0 \leq u_j^n \leq 1$), hence from Eq. (3.104), we have

$$\epsilon(u_{m-1}^n + u_{m+1}^n) - 2\epsilon u_m^n \leq 2\epsilon - 2\epsilon u_m^n, \quad (3.105)$$

due to the fact $\epsilon(u_{m-1}^n + u_{m+1}^n) \leq 2\epsilon$. It follows that

$$\epsilon(u_{m-1}^n + u_{m+1}^n) - 2\epsilon u_m^n \leq 2\epsilon - 2\epsilon u_m^n = 2\epsilon(1 - u_m^n). \quad (3.106)$$

The quantity $1 - u_m^n$ in Eq. (3.106) is bounded by

$$0 \leq (1 - u_m^n) \leq 1. \quad (3.107)$$

It follows from Eqs. (3.106) and Eq(3.107) that

$$\epsilon(u_{m-1}^n - 2u_m^n + u_{m+1}^n) = \epsilon(u_{m-1}^n + u_{m+1}^n) - 2\epsilon u_m^n \leq 2\epsilon. \quad (3.108)$$

Hence the boundedness of u_m^{n+1} for NSFD- ϵ method from Eq. (3.103) is such that

$$0 \leq u_m^{n+1} \leq 1 + 2\epsilon. \quad (3.109)$$

□

Since $\epsilon = 0.01$, $h = 0.01$, we have from (3.89), $k \leq 9.6078 \times 10^{-5}$ or $k \leq T_{max}/26$ for positivity or stability. We tabulate L_1 and L_∞ errors and CPU time when Problem 1 and 2 are solved using NSFD- ϵ scheme at some different values of time-step size, k with spatial step size, $h = 0.01$. The errors are displayed in Tables (3.11) and (3.13).

Time step (k)	L_1 error	L_∞ error	CPU (s)
$T_{max}/26$	1.8636×10^{-1}	9.8705×10^{-1}	0.653
$T_{max}/50$	1.2102×10^{-1}	9.1868×10^{-1}	0.662
$T_{max}/100$	6.5470×10^{-2}	6.7456×10^{-1}	0.670
$T_{max}/200$	2.4582×10^{-2}	2.9094×10^{-1}	0.682
$T_{max}/300$	4.8806×10^{-3}	5.9139×10^{-2}	0.699
$T_{max}/333$	1.0091×10^{-3}	9.5627×10^{-3}	0.715
$T_{max}/334$	9.9448×10^{-4}	1.0714×10^{-2}	0.707
$T_{max}/335$	1.0119×10^{-3}	1.1866×10^{-2}	0.787
$T_{max}/400$	8.5987×10^{-3}	1.0311×10^{-1}	0.722
$T_{max}/500$	1.9385×10^{-2}	2.2445×10^{-1}	0.780

Table 3.11: L_1 and L_∞ errors and CPU time at some different values of time-step size, k for Problem 1 at time 2.5×10^{-3} with spatial mesh size, $h = 0.01$, $\epsilon = 0.01$ using NSFD- ϵ scheme, $T_{max} = 2.5 \times 10^{-3}$.

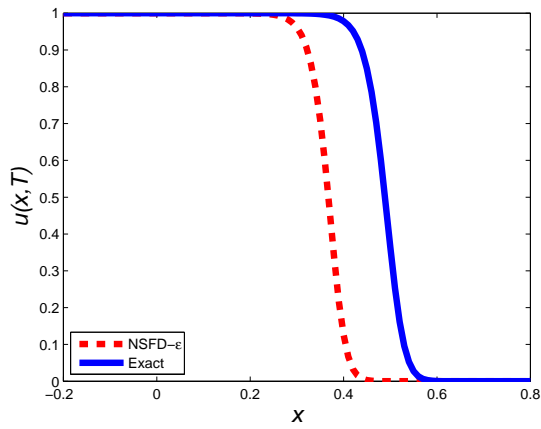
Time step (k)	L_1 error	Rate of convergence
$T_{max}/50$	1.2102×10^{-1}	
$T_{max}/100$	6.5470×10^{-2}	0.886
$T_{max}/200$	2.4582×10^{-2}	1.413

Table 3.12: Rate of convergence with k and spatial mesh size, $h = 0.01$, $\epsilon = 0.01$, of Problem 1 using NSFD- ϵ , Optimal $k \cong 2.5 \times 10^{-3}/334$.

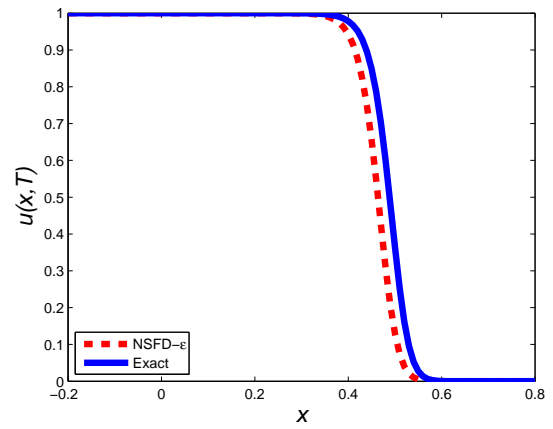
Remark 3.13. The optimal k is approximately $\frac{T_{max}}{334}$. That why we use $\frac{T_{max}}{50}$, $\frac{T_{max}}{100}$, $\frac{T_{max}}{200}$. Reason being, we don't need adding further rows to compute the convergence rate.

Time step (k)	L_1 error	L_∞ error	CPU (s)
$T_{max}/26$	1.8636×10^{-1}	9.8705×10^{-1}	1.137
$T_{max}/50$	1.2102×10^{-1}	9.1868×10^{-1}	1.485
$T_{max}/100$	6.5470×10^{-2}	6.7456×10^{-1}	2.391
$T_{max}/200$	2.4582×10^{-2}	2.9094×10^{-1}	4.880
$T_{max}/300$	4.8806×10^{-3}	5.9139×10^{-2}	8.207
$T_{max}/333$	1.0091×10^{-3}	9.5627×10^{-3}	9.437
$T_{max}/334$	9.9448×10^{-4}	1.0714×10^{-2}	9.534
$T_{max}/335$	1.0119×10^{-3}	1.1866×10^{-2}	9.540
$T_{max}/400$	8.5987×10^{-3}	1.0311×10^{-1}	12.181
$T_{max}/500$	1.9385×10^{-2}	2.2445×10^{-1}	17.074

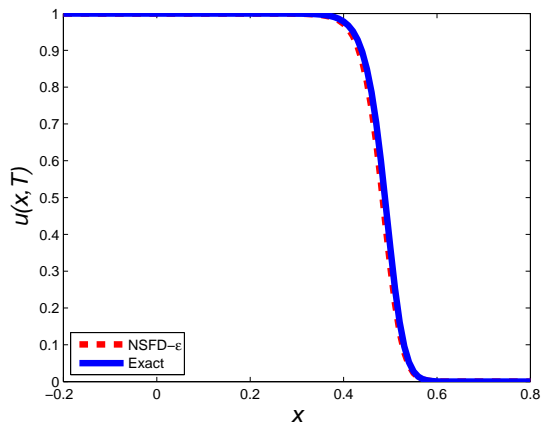
Table 3.13: L_1 and L_∞ errors and CPU time at some different values of time-step size, k for Problem 2 at time 2.5×10^{-3} with spatial mesh size, $h = 0.01$, $\epsilon = 0.01$ using NSFD- ϵ scheme, $T_{max} = 2.5 \times 10^{-3}$.



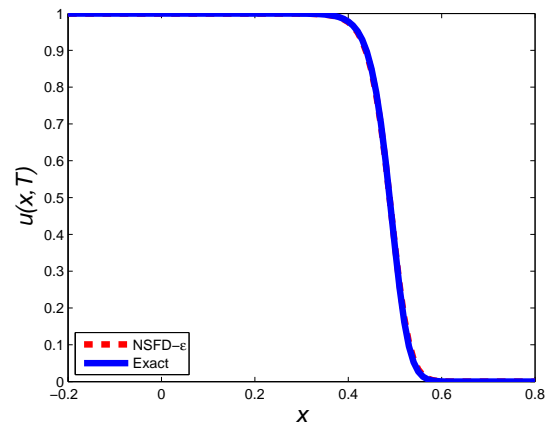
(a) $k = T_{max}/50$



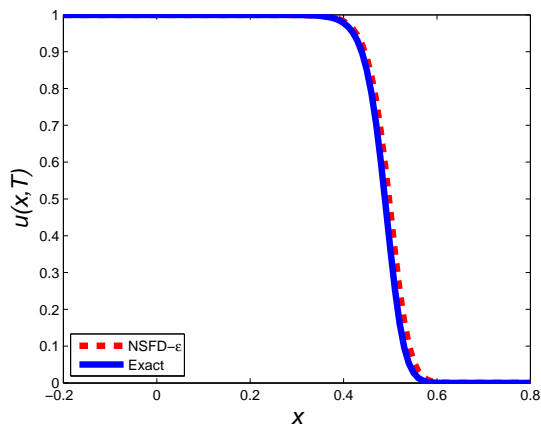
(b) $k = T_{max}/200$



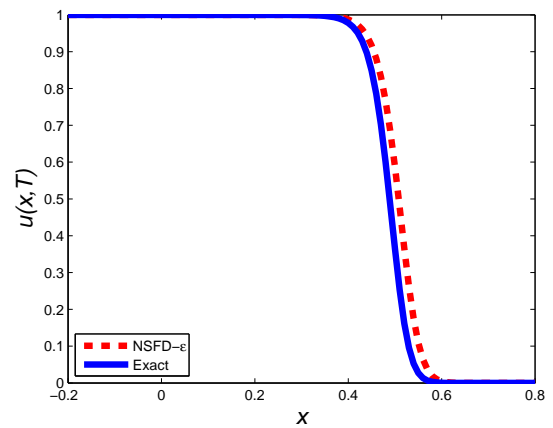
(c) $k = T_{max}/300$



(d) $k = T_{max}/334$



(e) $k = T_{max}/400$



(f) $k = T_{max}/500$

Figure 3.4: Plot of u against x for Problem 1 using NSFD- ϵ scheme at time 2.5×10^{-3} at some different values of k and $h = 0.01$, $\epsilon = 0.01$.

3.9 Artificial viscosity

We observe from the numerical results of FTCS and NSFD that the schemes are plagued by dispersion at time step size quite close to the stability limit of the temporal step size at $h = 0.01$. We propose to make use of artificial viscosity approach. The method of artificial viscosity was first introduced by [VonNeumann and Richtmyer \(1950\)](#), who explicitly added a viscosity term to the inviscid gas dynamics equations in order to permit the computation of shock waves. Their approach was to change the momentum and energy equations by adding dissipation in form of viscosity term to the pressure that would give shock waves thickness and also to space out the computational mesh. The artificial viscosity was purposely made proportional to the second derivative (u_{xx} which is positive in compression and negative in expansion) to ensure the mathematical consistency. It should satisfy some constraints like the modified equation must possess solutions without any discontinuities, the Rankine-Hugoniot conditions must hold (for conservations equations) and the dissipative term be negligible outside of the shock waves ([Campbell and Shashkov, 2001](#)).

It is also known that artificial viscosity can be expressed implicitly following the work of [Noh and Protter \(1963\)](#) who first presented an analysis of the implicit artificial viscosity of the upwind method applied to linear advection equation. It has been proved that for a given unstable numerical method, in general for first order linear equations it can be stabilized by adding a sufficient large viscosity term. Other forms of artificial viscosity can be found in [Landshoff \(1955\)](#) and [Wilkins \(1980\)](#) who attribute it to [Kurapatenko \(1967\)](#).

Finally, it was specified by [Caramana et al. \(1998\)](#) that an artificial viscosity should have the following properties:

1. Dissipativity: The artificial viscosity must only act to decrease kinetic energy.
2. Galilean invariance: The viscosity should vanish smoothly as the velocity field becomes constant.
3. Self-similar motion invariance: The viscosity should vanish for uniform contraction and rigid rotation.
4. Wave-front invariance: The viscosity should have no effect along a wave front of constant phase, on a grid aligned with shocks.
5. Viscous force continuity: The viscous force should go to zero continuously as compression vanishes and remain zero for expansion.

We start with a simple linear advection equation, $u_t + u_x = 0$ (Eq. (3.35) with $c = 1$). We add the artificial viscosity $\sigma h u_{xx}$ to obtain

$$u_t + u_x = \sigma h u_{xx}. \quad (3.110)$$

When $h \rightarrow 0$, we recover the initial linear advection equation $u_t + u_x = 0$ and σ is a real parameter. The numerical discretisation for Eq. (3.110) is

$$\frac{u_m^{n+1} - u_m^n}{k} + D_0 u_m^n = \sigma h D_+ D_- u_m^n, \quad (3.111)$$

where $D_+u_m^n = \frac{u_{m+1}^n - u_m^n}{h}$, $D_-u_m^n = \frac{u_m^n - u_{m-1}^n}{h}$, $D_0u_m^n = \frac{u_{m+1}^n - u_{m-1}^n}{2h}$ are respectively forward, backward and centred differencing operators. By rewriting Eq. (3.111), we have

$$u_m^{n+1} = u_m^n - k D_0u_m^n + \sigma k h D_+D_-u_m^n. \quad (3.112)$$

As $h \rightarrow 0$, the scheme given by Eq. (3.112) is a consistent approximation of Eq. (3.35) with $c = 1$.

3.9.1 FTCS with artificial viscosity

We need to solve

$$u_t = u_{xx} + \rho u(1 - u). \quad (3.113)$$

We add $\sigma h u_{xx}$ and obtain a new equation,

$$u_t = u_{xx} + \rho u(1 - u) + \sigma h u_{xx}, \quad h \rightarrow 0. \quad (3.114)$$

The numerical scheme used to discretise Eq. (3.114) is

$$\frac{u_m^{n+1} - u_m^n}{k} = \frac{u_{m+1}^n - 2u_m^n + u_{m-1}^n}{h^2} + \rho u_m^n(1 - u_m^n) + \sigma h \left(\frac{u_{m+1}^n - 2u_m^n + u_{m-1}^n}{h^2} \right) \quad (3.115)$$

which can be rewritten as

$$u_m^{n+1} = \left[1 - \frac{2k}{h^2}(1 + \sigma h) \right] u_m^n + k\rho u_m^n(1 - u_m^n) + \frac{k}{h^2}(1 + \sigma h)(u_{m+1}^n + u_{m-1}^n). \quad (3.116)$$

Theorem 3.8. *The FTCS with artificial viscosity (3.116) is first order accurate in time and space.*

Proof. For the order of accuracy, Taylor series expansion about the point (n, m) of (3.116) gives

$$\begin{aligned} u + ku_t + \frac{k^2}{2}u_{tt} + \frac{k^3}{6}u_{ttt} &= \left(1 - \frac{2k}{h^2}(1 + \sigma h) \right) u + k\rho u(1 - u) \\ &\quad + \frac{k}{h^2}(1 + \sigma h)(2u + h^2u_{xx}) + O(k^4) + O(h^4), \end{aligned} \quad (3.117)$$

which gives

$$u_t - u_{xx} - \rho u(1 - u) = -\frac{k}{2}u_{tt} - \frac{k^2}{6}u_{ttt} + \sigma h u_{xx} + O(k^3) + O\left(\frac{h^4}{k}\right). \quad (3.118)$$

We conclude that FTCS with artificial viscosity is first order accurate in time and first order accurate in space.

If $\sigma = 0$, we recover the FTCS scheme. □

Theorem 3.9. *The FTCS with artificial viscosity given by Eq. (3.116) is stable under the condition*

$$k \leq \frac{h^2}{2} \left[\frac{1}{1 + \sigma h} \right],$$

for the time step k , and the spatial size, h .

Proof. The amplification factor, ξ of FTCS scheme with artificial viscosity is

$$\xi = 1 + \frac{2k}{h^2}(1 + \sigma h)(\cos(w) - 1) + k\rho(1 - |u_{max}|). \quad (3.119)$$

We chose $u_{max} = 1$ based on numerical experiment chosen and have

$$\xi = 1 - \frac{4k}{h^2}(1 + \sigma h)\sin^2\left(\frac{w}{2}\right). \quad (3.120)$$

The stability region is

$$k < \frac{h^2}{2} \left[\frac{1}{1 + \sigma h} \right]. \quad (3.121)$$

□

We choose $\sigma = 2.0$, $h = 0.01$ and obtain $k < 4.9020 \times 10^{-5}$ or $T_{max}/51$.

We tabulate L_1 and L_∞ errors and CPU time when Problem 1 is solved using FTCS with artificial viscosity at some different values of time-step size, k with spatial step size, $h = 0.01$, $\sigma = 2.0$. The errors are displayed in Table 3.15.

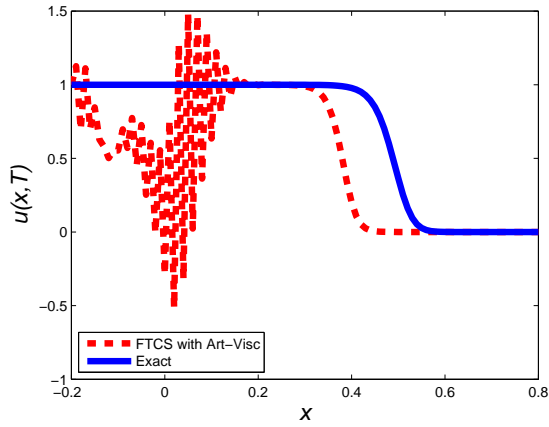
Time step (k)	L_1 error	Rate of convergence
$T_{max}/100$	6.2546×10^{-2}	
$T_{max}/200$	3.0034×10^{-2}	1.058
$T_{max}/400$	1.1108×10^{-2}	1.435

Table 3.14: Rate of convergence with k and spatial mesh size, $h = 0.01$, $\epsilon = 0.01$, of Problem 1 using FTCS with artificial viscosity, optimal $k = 2.5 \times 10^{-3}/880$.

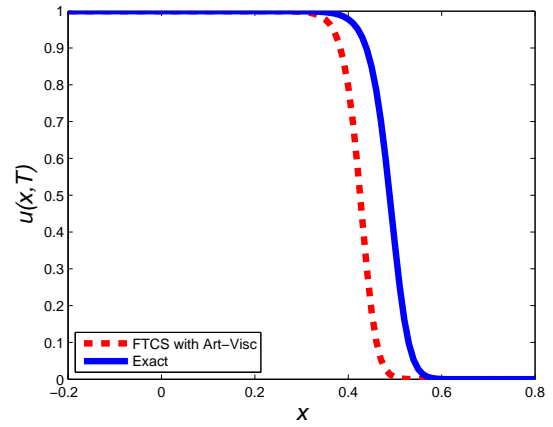
Time step (k)	L_1 error	L_∞ error	CPU(s)
$T_{max}/53$	2.6947×10^{-1}	1.5155	0.737
$T_{max}/100$	6.2546×10^{-2}	6.8175×10^{-1}	0.737
$T_{max}/200$	3.0034×10^{-2}	3.6771×10^{-1}	0.742
$T_{max}/300$	1.7645×10^{-2}	2.1809×10^{-1}	0.758
$T_{max}/400$	1.1108×10^{-2}	1.3983×10^{-1}	0.782
$T_{max}/500$	7.0695×10^{-3}	8.9529×10^{-2}	0.800
$T_{max}/600$	4.3263×10^{-3}	5.5222×10^{-2}	0.847
$T_{max}/700$	2.3414×10^{-3}	3.0552×10^{-2}	0.856
$T_{max}/800$	8.5592×10^{-4}	1.2040×10^{-2}	0.907
$T_{max}/850$	3.1048×10^{-4}	4.4291×10^{-3}	0.913
$T_{max}/860$	2.2700×10^{-4}	3.0141×10^{-3}	0.918
$T_{max}/870$	1.6308×10^{-4}	1.8608×10^{-3}	0.923
$T_{max}/880$	1.3833×10^{-4}	2.3032×10^{-3}	0.926
$T_{max}/890$	2.3267×10^{-4}	2.9465×10^{-3}	0.930
$T_{max}/900$	3.3881×10^{-4}	3.6042×10^{-3}	0.951
$T_{max}/1000$	1.2861×10^{-3}	1.4273×10^{-2}	0.967
$T_{max}/1100$	2.0648×10^{-3}	2.3789×10^{-2}	1.001
$T_{max}/1200$	2.7162×10^{-3}	3.1756×10^{-2}	1.042
$T_{max}/1300$	3.2692×10^{-3}	3.8522×10^{-2}	1.071
$T_{max}/1400$	3.7445×10^{-3}	4.4336×10^{-2}	1.124
$T_{max}/1500$	4.1573×10^{-3}	4.9385×10^{-3}	1.142

Table 3.15: L_1 and L_∞ errors CPU time at some different values of time-step size, k for Problem 1 with $\rho = 10^4$ at time 2.5×10^{-3} with spatial mesh size, $\sigma = 2.0$, $h=0.01$ using FTCS with artificial viscosity.

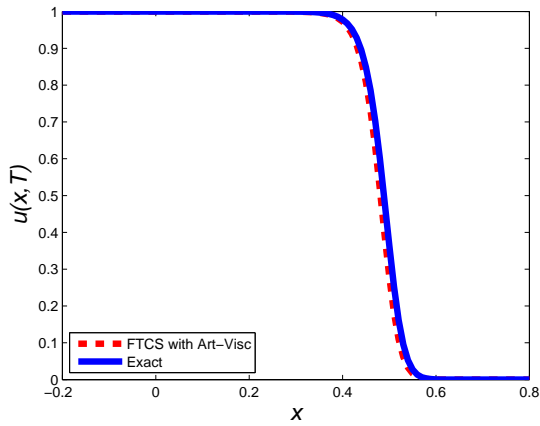
From the Table 3.15 we deduce that FTCS with artificial viscosity can give accurate results at a smaller CPU as compared to FTCS provided σ is correctly chosen.



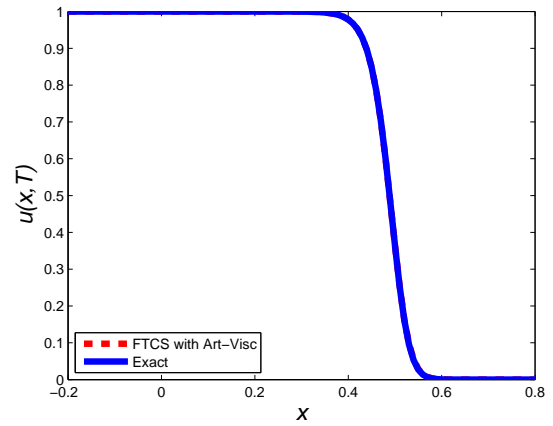
(a) $k = T_{max}/53$



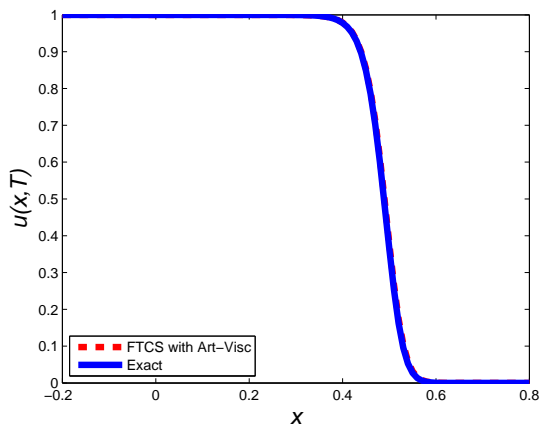
(b) $k = T_{max}/100$



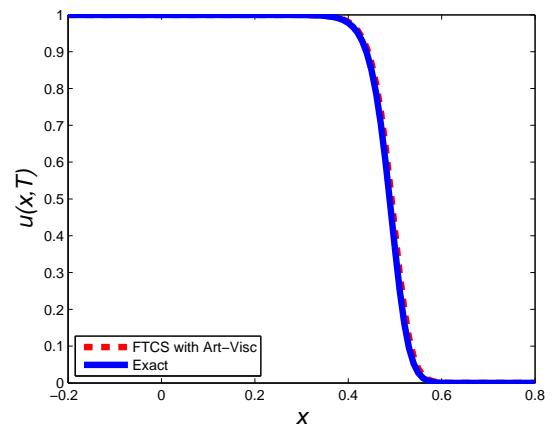
(c) $k = T_{max}/500$



(d) $k = T_{max}/880$



(e) $k = T_{max}/1000$



(f) $k = T_{max}/1500$

Figure 3.5: Plot of u against x for Problem 1 using FTCS with artificial viscosity at time 2.5×10^{-3} at some different values of k and $h = 0.01$, $\sigma = 2.0$, $T_{max} = 2.5 \times 10^{-3}$.

3.9.2 Nonstandard Finite Difference method with artificial viscosity

Nonstandard Finite Difference (Mickens, 2002) scheme with artificial viscosity to discretise Eq. (3.114) is

$$\begin{aligned} \frac{u_m^{n+1} - u_m^n}{k} = & \frac{u_{m+1}^n - 2u_m^n + u_{m-1}^n}{h^2} + \rho u_m^n - \rho \left(\frac{u_{m+1}^n + u_m^n + u_{m-1}^n}{3} \right) u_m^{n+1} \\ & + \sigma h \left(\frac{u_{m+1}^n - 2u_m^n + u_{m-1}^n}{h^2} \right). \end{aligned} \quad (3.122)$$

A single expression for the scheme is

$$u_m^{n+1} = \frac{(1 + k\rho - 2\beta) u_m^n + \beta(u_{m+1}^n + u_{m-1}^n)}{1 + k\rho \left(\frac{u_{m+1}^n + u_m^n + u_{m-1}^n}{3} \right)} \quad \text{where } \beta = \frac{k}{h^2}(1 + \sigma h). \quad (3.123)$$

Theorem 3.10. *NSFD with artificial viscosity (3.123) is first order accurate in time and space.*

Proof. Taylor series expansion of the above scheme about (m, n) gives

$$\left(u + ku_t + \frac{k^2}{2}u_{tt} + \frac{k^3}{6}u_{ttt} \right) \left(1 + k\rho u + k\rho \frac{h^2}{3}u_{xx} \right) = (1 + k\rho)u + ku_{xx} + O(k^4) + O(h^4), \quad (3.124)$$

which can be written as

$$\begin{aligned} u_t - u_{xx} - \rho u + \rho u^2 - \sigma h u_{xx} = & - \left(\rho u \frac{h^2}{3} - \sigma h \right) u_{xx} - k \left(\frac{\rho u}{3} + \frac{\rho h^2}{3}u_{xx} \right) u_t \\ & - \left(\frac{k}{3} + \frac{k^2}{2} \left(\frac{\rho u}{3} + \frac{\rho h^2}{3}u_{xx} \right) \right) u_{tt} \\ & - \left(\frac{k^2}{6} + \frac{k^3}{6} \left(\frac{\rho u}{3} + \frac{\rho h^2}{3}u_{xx} \right) \right) u_{ttt} \\ & + O(k^4) + O(h^4). \end{aligned} \quad (3.125)$$

We conclude that NSFD with artificial viscosity is first order accurate in time and first order accurate in space. \square

Positivity and Boundedness

Theorem 3.11. *The NSFD with artificial viscosity (3.123) is positive definite if and only if the condition*

$$k \leq \frac{h^2}{2} \left[\frac{1 - \Gamma}{1 + \sigma h - \frac{\rho h^2}{2}} \right] \quad \text{and } 0 \leq \Gamma < 1, \quad (3.126)$$

holds for the time step, k and space step, h .

Proof. The scheme given by Eq. (3.123) is positive if $\Gamma = 1 + k\rho - \frac{2k}{h^2}(1 + \sigma h) \geq 0$. Hence the positive definite condition. \square

For $h = 0.01$, $\sigma = 2.0$, we have from Eq. (3.126) $k \leq 9.6154 \times 10^{-5}$.

Theorem 3.12. *The NSFD with artificial viscosity (3.123) is bounded if the condition*

$$\frac{k}{h^2} = \left(\frac{1}{3}\right) \left[\frac{1}{1 + \frac{\rho\sigma}{3} - \frac{\rho h^2}{3}} \right]$$

holds for the time step, k and space step, h and $0 \leq u_m^n \leq 1$, for all m .

Proof. For boundedness, we start by assuming that $0 \leq u_m^n \leq 1$. We apply the same steps as in case of NSFD without artificial viscosity by letting

$$\Gamma = 1 + k\rho - 2R, \quad R = \beta = \frac{k}{h^2}(1 + \sigma h). \quad (3.127)$$

and we use the symmetric condition

$$R = \frac{k}{h^2} = \left(\frac{1}{3}\right) \left[\frac{1}{1 + \frac{\rho\sigma}{3} - \frac{\rho h^2}{3}} \right]. \quad (3.128)$$

Thus gives

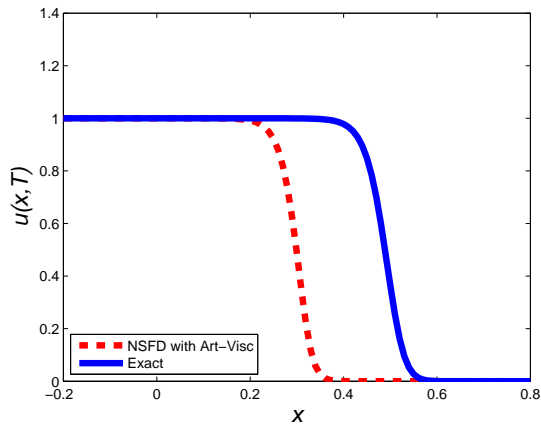
$$0 \leq u_m^{n+1} \leq 1. \quad (3.129)$$

Hence the boundedness of u_m^{n+1} . □

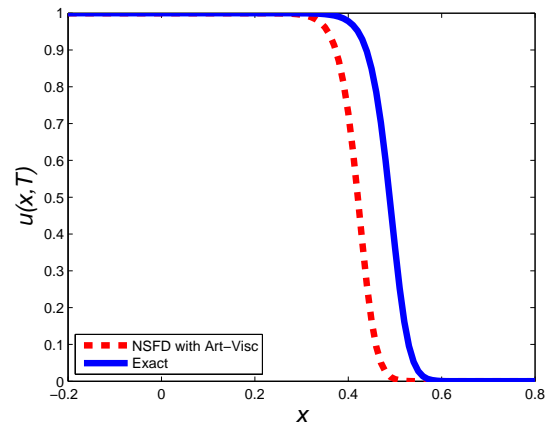
We tabulate L_1 and L_∞ errors, CPU time when Problem 1 are solved using NSFD with artificial viscosity scheme at some different values of time-step size, k with spatial step size, $h = 0.01$, $\sigma = 2.0$. The errors are displayed respectively in Table 3.17.

Time step (k)	L_1 error	Rate of convergence
$T_{max}/50$	1.2102×10^{-1}	
$T_{max}/100$	6.8010×10^{-2}	0.8314
$T_{max}/200$	3.3252×10^{-2}	1.0320
$T_{max}/400$	1.2961×10^{-2}	1.3590

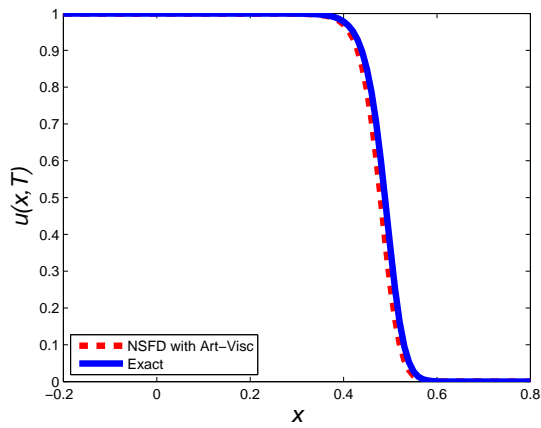
Table 3.16: Rate of convergence with k and spatial mesh size, $h = 0.01$, $\epsilon = 0.01$, of Problem 1 using NSFD with artificial viscosity Optimal $k = 2.5 \times 10^{-3}/1000$.



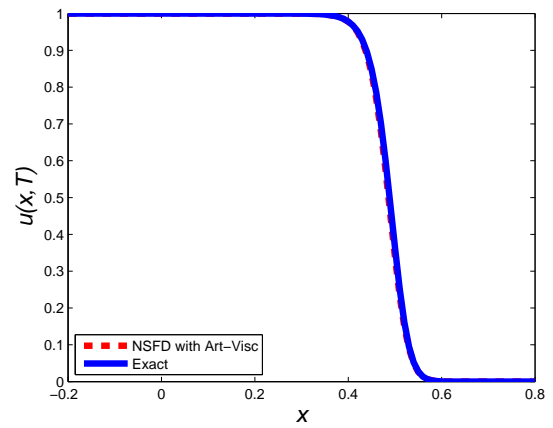
(a) $k = T_{max}/25$



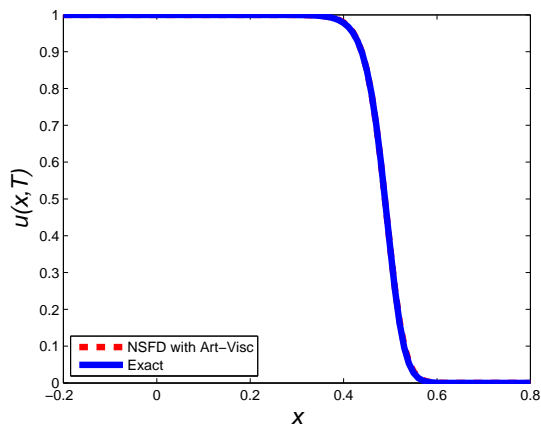
(b) $k = T_{max}/100$



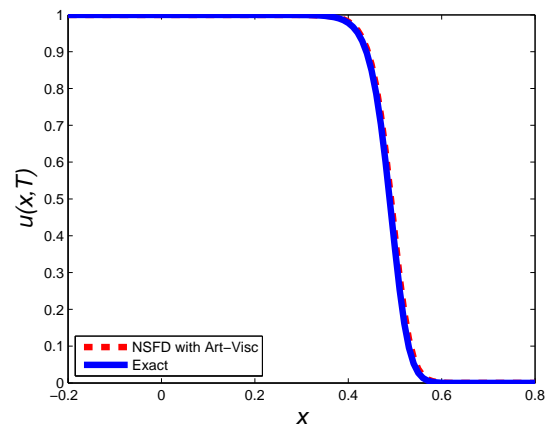
(c) $k = T_{max}/500$



(d) $k = T_{max}/800$



(e) $k = T_{max}/1000$



(f) $k = T_{max}/1500$

Figure 3.6: Plot of u against x for Problem 1 using NSFD with artificial viscosity at time 2.5×10^{-3} , at some different values of k and $h = 0.01$, $\sigma = 2.0$, $T_{max} = 2.5 \times 10^{-3}$.

Time step (k)	L_1 error	L_∞ error	CPU(s)
$T_{max}/25$	1.8982×10^{-1}	9.8811×10^{-1}	0.891
$T_{max}/50$	1.2102×10^{-1}	9.1869×10^{-1}	0.893
$T_{max}/100$	6.8010×10^{-2}	6.9128×10^{-1}	0.897
$T_{max}/200$	3.3252×10^{-2}	3.8653×10^{-1}	0.928
$T_{max}/300$	1.9973×10^{-2}	2.4143×10^{-1}	0.998
$T_{max}/400$	1.2961×10^{-2}	1.5892×10^{-1}	0.999
$T_{max}/500$	8.6255×10^{-3}	1.0838×10^{-1}	1.019
$T_{max}/600$	5.6799×10^{-3}	7.3290×10^{-2}	1.041
$T_{max}/700$	3.5494×10^{-3}	4.7746×10^{-2}	1.089
$T_{max}/800$	1.9544×10^{-3}	2.8406×10^{-2}	1.355
$T_{max}/900$	8.4110×10^{-4}	1.3294×10^{-2}	1.355
$T_{max}/950$	5.2648×10^{-4}	7.1035×10^{-3}	1.564
$T_{max}/1000$	4.4308×10^{-4}	5.5908×10^{-3}	1.664
$T_{max}/1050$	7.8758×10^{-4}	8.5810×10^{-3}	1.683
$T_{max}/1100$	1.1865×10^{-3}	1.1836×10^{-2}	1.684
$T_{max}/1200$	1.8866×10^{-3}	1.9106×10^{-2}	1.687
$T_{max}/1300$	2.4809×10^{-3}	2.5706×10^{-2}	1.688
$T_{max}/1400$	2.9918×10^{-3}	3.1732×10^{-2}	1.690
$T_{max}/1500$	3.4356×10^{-3}	3.6977×10^{-2}	1.745

Table 3.17: L_1 and L_∞ errors and CPU time at some different values of time step size, k for Problem 1 at time 2.5×10^{-3} with spatial mesh size, $h = 0.01$, $\sigma = 2.0$ using NSFD with artificial viscosity method.

3.10 The stability of computed solution and the sensitivity of the solution to the boundary condition ahead of the wave in term of local pertubation

In this section, we recall some of results of [Qiu and Sloan \(1998\)](#). Consider, c the speed of travelling waves solution. It can be written in the form $u(x, t) = v(x - ct)$, for some function v of the scalar variable

$\xi = x - ct$. v is solution of the boundary value problem by considering Eq. (3.6)

$$\begin{aligned} \frac{d^2 v}{d\xi^2} + c \frac{dv}{d\xi} + \rho v(1-v) &= 0, \\ \lim_{\xi \rightarrow -\infty} v(\xi) &= 1, \quad \lim_{\xi \rightarrow +\infty} v(\xi) = 0. \end{aligned} \quad (3.130)$$

Let $u(x, t) = z(\xi, t)$. It follows that z , verifies the following boundary value problem

$$\begin{aligned} \frac{\partial z}{\partial t} = \frac{\partial^2 z}{\partial \xi^2} + c \frac{\partial z}{\partial \xi} + \rho z(1-z) &= 0, \\ \lim_{\xi \rightarrow -\infty} z(\xi) &= 1, \quad \lim_{\xi \rightarrow +\infty} z(\xi) = 0. \end{aligned} \quad (3.131)$$

Comparing the two equations Eq. (3.130) and Eq. (3.131), we deduce that the travelling wave is a steady-state solution of Eq. (3.131).

To carry out a linear stability analysis we denote

$$z(\xi, t) = v(\xi) + \theta(\xi, t) \quad (3.132)$$

where squares of θ are adequately small to be neglected. The linearisation about v shows that θ verifies

$$\frac{\partial \theta}{\partial t} = \frac{\partial^2 \theta}{\partial \xi^2} + c \frac{\partial \theta}{\partial \xi} + \rho(1-2v)\theta. \quad (3.133)$$

Our interest is on local perturbations. We impose therefore the boundary condition

$$\theta(\pm L, t) = 0 \quad (3.134)$$

where L is such that $L = x_r = -x_l$ and $[x_l, x_r] \subset (-\infty, +\infty)$ for convenience. By the use of self-adjoint form and by means of the transformation $\theta(\xi, t) = [e^{-c\xi/2}] \times g$ from Canosa (1973), Eq. (3.133) g is solution of

$$\frac{\partial g}{\partial t} = \frac{\partial^2 g}{\partial \xi^2} + \left(-\frac{c^2}{4} + \rho - 2v \right) g \quad (3.135)$$

verifying the boundary conditions Eq. (3.134). We note that as $\xi \rightarrow \infty$, θ must decay to zero at least as $O(e^{-c\xi})$ so $g = [e^{c\xi/2}] \theta(\xi, t)$ will decay exponentially $|\xi| \rightarrow \infty$. Hagan (1982) showed that (3.130) there is a unique travelling wave solution for each value c such that $c \geq 2\sqrt{\rho}$. Furthermore, the wave profile is given by the solution on the trajectory that connects the fixed points at $v \in \{0, 1\}$. Under the condition $c \geq 2\sqrt{\rho}$, we rewrite Eq. (3.135) as

$$\frac{\partial g}{\partial t} = \frac{\partial^2 g}{\partial \xi^2} + \rho(1-r^2-2v)g, \quad (3.136)$$

where $r = \frac{c^2}{4\rho} \geq 1$. To perform stability analysis of the computed solution, we consider an even grid points $\{\xi_m\}_{m=0}^{N+1}$ with $\xi = -L + mh$ and $h = 2L/(N+1)$.

For the simplicity of the analysis, we use FTCS- ϵ scheme in term of semi-discretisation. The analysis for other methods (NSFD- ϵ , FTCS with artificial viscosity, NSFD with artificial viscosity) are almost the same.

We denote $g_m = g_m(t)$ the approximation at the point (ξ, t) , the set of semi-discrete equations of Eq. (3.136) is

$$\begin{aligned} \dot{g}_m &= \left(\epsilon + \frac{1}{h^2}\right) g_{m-1} - \left[2 \left(\epsilon + \frac{1}{h^2}\right) - \rho h^2 (1 - r^2 - 2v_m)\right] g_m + \left(\epsilon + \frac{1}{h^2}\right) g_{m+1}, \quad m = 1, 2, \dots, N, \\ g_0 &= g_{N+1} = 0. \end{aligned} \quad (3.137)$$

For the simplicity of the analysis, v_m is given by the exact solution

$$v_m = \left[1 + e(\sqrt{\frac{\rho}{6}}\xi_m)\right]^{-2}, \quad (3.138)$$

The system Eq. (3.137) can be rewritten in matrix form as

$$\dot{G} = MG \quad (3.139)$$

where $G = [g_1, g_2, \dots, g_N]^t$ and

$$M = \frac{1}{h^2} \text{tridiag} \left\{ \epsilon + \frac{1}{h^2}, -\left(2 \left(\epsilon + \frac{1}{h^2}\right) + a_m\right), \epsilon + \frac{1}{h^2} \right\} \quad (3.140)$$

with

$$a_m = \rho h^2 (r^2 + 2v_m - 1). \quad (3.141)$$

Theorem 3.13 (Bell (1965)). *Let $A = [a_{ij}]$ be an $n \times n$ complex matrix, and let R_i be the sum of the moduli the off-diagonal elements in the i -th row. Then each eigenvalue of A lies in the union of circles*

$$|z - a_{ii}| \leq R_i, \quad i = 1, 2, \dots, n.$$

The analogue result holds if the columns of A are considered.

Since $v \in \{0, 1\}$ and $r \geq 1$, it follows from Gerschgorin's Theorem 3.13 that the eigenvalues of the symmetric matrix M are all real and negative. Hence $\|G\|$ decays exponentially with time and the system is linearly stable to local disturbances. Hence the rate of decay of a perturbation on nodal values at the back of the wave is greater than that for a perturbation on nodal values at the front of the wave (Qiu and Sloan, 1998).

It is worthy to notify how the stability on the finite domain differs from that on the infinite domain. We note, initially, $\frac{dv}{d\xi} = v_\xi$ is a solution of $\mathcal{L} v_\xi = 0$ where \mathcal{L} denotes the linear differential operator given by

$$\mathcal{L} = \frac{\partial^2}{\partial \xi^2} + c \frac{\partial}{\partial \xi} + \rho(1 - 2v). \quad (3.142)$$

Furthermore, v_ξ decays exponentially to zero as $|\xi| \rightarrow \infty$ and it follows that \mathcal{L} has a zero eigenvalue.

A perturbation, μv_ξ that is a multiple of v_ξ will hence remain to exist with no decay or growth, and since

$$v(\xi + \mu) = v(\xi) + \mu v_\xi(\xi) + O(\mu^2). \quad (3.143)$$

It results that small perturbations of this type may only ensue in a phase shift of the original travelling wave. The finite domain problem does not show this property since $v_\xi \neq 0$ at $\xi = \pm L$, but numerical approximations over a large finite domain may be expected to have a tendency to suffer phase errors that arise from perturbations.

To prop up this conjecture, one should note that if \mathcal{L}_h denotes the second-order central difference approximation to \mathcal{L} and if $(v_\xi)_h$ denotes the vector $\{dv/d\xi(\xi_m)\}_{m=0}^{N+1}$, then the residual $\mathcal{L}_h(v_\xi)_h$ is $O(h^2)$ as $h \rightarrow 0$ for a fixed value of L . For adequately small h , and adequately large L , $(v_\xi)_h$ is a close approximation to an eigenvector of \mathcal{L}_h corresponding to the nearly zero eigenvalue. The tendency of $\mathcal{L}_h(v_\xi)_h$ to zero as $h \rightarrow 0$ is easily verified numerically.

3.11 Conclusion

In this chapter, we have initially used FTCS and NSFD scheme to solve Fisher's equation when the coefficient of diffusion is much less than coefficient of reaction term and the initial condition consists of an exponential function. The time-step size must be relatively small in order to obtain accurate results and the CPU time becomes large if the domain is large.

We propose four schemes namely FTCS- ϵ , NSFD- ϵ , FTCS with Artificial Viscosity, NSFD with artificial viscosity and they give quite accurate results at larger time-step size and consequently smaller CPU time as compared to FTCS and NSFD methods. Also the L_1 and L_∞ errors at optimal time step size and $h = 0.01$ are smaller than when using MMPDE and MMDAE methods.

Chapter 4

Comparative study of some Numerical methods for the standard FitzHugh-Nagumo equation

*A version of this chapter was accepted as [Agbavon et al. \(2019b\)](#) in the book entitled: *Communications in Mathematical Computations*, Springer.*

4.1 Introduction

Partial differential equations are widely used to describe or model the complex phenomena in real life and applications are in fluid mechanics, solid-state physics, plasma wave and chemical physics ([Johnson et al., 2012](#), [Wang et al., 2014](#)). The standard FitzHugh-Nagumo equation is an important application of nonlinear partial differential equation and used to model the transmission of nerve impulses ([FitzHugh, 1961](#), [Nagumo et al., 1962](#)). It is also used in circuit theory, biology and population genetics ([Aronson and Weinberger, 1978](#)) as mathematical models. It is given by

$$u_t - u_{xx} = u(1 - u)(u - \gamma), \quad (4.1)$$

where γ controls the global dynamics of the equation and is in the interval $(0, 1)$ ([Xu et al., 2014](#)) and $u(x, t)$ is the unknown function which depends on the temporal variable, t and the spatial variable, x .

Background

The first fruitful mathematical representation of electrophysiology was the main model established by Hodgkin and Huxley in the early 1950's. Hodgkin and Huxley carried out voltage clamp experiments on a squid giant axon and changed their studies of transmembrane potential, currents, and conductance, into a circuit-like model. The result was a system of four ordinary differential equations (ODEs) that

precisely portrayed noticeable propagation alongside an axon. Although the complex Hodgkin-Huxley equations showed to be a good model to describe a signal propagation along a nerve, they are hard to be analysed. [FitzHugh \(1961\)](#) and [Nagumo et al. \(1962\)](#) tackled this problem a decade later when they restrained the original system of four variables down to a simpler model of only two variables. Their simple model is much easier to be analysed and it still describes the main phenomena of the dynamics: (1) a sufficiently large stimulus will start off a significant response, and (2) after such a stimulus and response, the medium needs a period of recuperation time before it can be impuled again. These two properties are characterised as excitable ($\gamma < 0$: the nerve is in excitable mode) and refractory ($\gamma > 0$: the nerve is in refractory mode and does not respond to external stimulation). Excitation happens fast while recovery occurs slowly.

A medium that displays excitability and refractoriness is categorized as an excitable medium. Though the standard Fitzhugh-Nagumo equation is one of the simplest models, it shows complex dynamics that have not been fully investigated. For example, it endorses a stable travelling and pulse solution. However, the pulse can be destabilized by large perturbations. This, therefore drew attention from many researchers. Moreover, the study showed that when $\gamma \in (0, 1)$ ([Kawahara and Tanaka, 1983](#)), the result would be heterozygote inferiority. When $\gamma = -1$, Eq. (4.1) is known as Newell-Whitehead equation and it describes dynamical behaviour near the bifurcation point for the Rayleigh-Benard convection of binary fluid mixtures. It has also been proved that the exact solution of Eq. (4.1) describes the fusion of two travelling fronts of the same sense and converts into a front which connects two stable constant states. [Jackson \(1992\)](#) used Galerkin's approximations to solve Eq. (4.1). [Bell and Deng \(2002\)](#) studied the singular perturbation of N-front travelling waves while [Gao and Wang \(2004\)](#) studied the existence of wavefronts and impulses. [Su \(1994\)](#) investigated the delayed oscillations in nonspatially uniform of Eq. (4.1) while [Krupa et al. \(1997\)](#) studied fast and slow waves of Eq. (4.1). Furthermore, [Schonbek \(1981\)](#) investigated the higher-order derivatives of solutions of Eq. (4.1) whereas, [Chou and Lin \(1996\)](#) studied exotic dynamic behaviour of Eq. (4.1).

Eq. (4.1) has been solved numerically by many methods namely; Adomian Decomposition Method (ADM), Homotopy Pertubation Method (HPM), Variational Iteration Method (VIM), Homotopy Analysis Method (HAM), Differential Transform Method (DTM) and Nonstandard Finite Difference method (NSFD).

We will briefly describe the work performed using these methods in the following paragraph:

ADM has been introduced by [Adomian \(1988\)](#) in early 1980's to show a new way to solve nonlinear functional equations. The method consists of separating the equation under study into linear and nonlinear portions which produce a solution in the form of a sequences. HPM is used to study the accurate asymptotic solutions of nonlinear problems ([Dehghan and Manafian, 2009](#), [Dehghan and Shakeri, 2007](#), [2008c,d](#)). VIM is used to identify the unknown function in parabolic equation ([Dehghan and Shakeri, 2008a,b](#), [Dehghan and Tatari, 2008](#)). DTM is a semi-analytical numerical method that makes use of Taylor series to obtain solutions of differential equations ([Biazar and Mohammadi, 2010](#)).

Our methodology approach is on scheme derived from [Namjoo and Zibaei \(2018\)](#) and nonstandard finite difference scheme ([Mickens, 1989, 2005](#)).

4.2 Organisation of the chapter

The chapter is organised as follows. In section 4.3, we describe the numerical experiment chosen. In section 4.4, we present the construction of numerical scheme from exact solution. We give derivation of the two exact schemes constructed by [Namjoo and Zibaei \(2018\)](#) in section 4.5 and obtain some properties of the scheme. We present some numerical results and tabulate some errors and this is a novelty in our work. In sections 4.6, we describe two nonstandard finite difference methods (NSFD1 and NSFD2) and obtain an improvement for NSFD1 which we call NSFD3 (second novelty in this work) and study some of the properties of the methods. We then present L_1 , L_∞ errors and results on rate of convergence which is third highlight of this work. Section 4.7 highlights the salient features of the chapter.

4.3 Numerical experiment

We solve Eq. (4.1), where $\gamma \in (0, 1)$ and $u(x, t)$ is the unknown function which depends on spatial variable, $x \in [0, b]$ and temporal variable, t . The initial condition is

$$u(x, 0) = \frac{\gamma}{1 + e^{-2A_1x}}, \quad (4.2)$$

and the boundary conditions are given by

$$\begin{aligned} u(0, t) &= \frac{\gamma}{1 + e^{2A_1A_2t}}, \\ u(b, t) &= \frac{\gamma}{1 + e^{-2A_1(b-A_2t)}}, \end{aligned} \quad (4.3)$$

where $A_1 = \frac{\sqrt{2}}{4}\gamma$, $A_2 = \frac{4-2\gamma}{\gamma}A_1$ and $t \in [0, 1]$. The exact solution is given by [Wazwaz \(2009\)](#)

$$u(x, t) = \frac{\gamma}{1 + e^{-2A_1(x-A_2t)}}. \quad (4.4)$$

In [Namjoo and Zibaei \(2018\)](#), they used $\gamma = 0.001$, $b = 1.0$. In this work, we test the performance of the schemes over different values of γ and also over short and long domains at time, $T = 1.0$. We considered short and long domain as some methods might work for short domains and produce less efficient results for longer domains. We also consider a very small value of γ as well as $\gamma = 0.5$. We consider 4 cases:

Case 1 : $\gamma = 0.001$, $b = 1.0$.

Case 2 : $\gamma = 0.001$, $b = 10.0$.

Case 3 : $\gamma = 0.5$, $b = 1.0$.

Case 4 : $\gamma = 0.5$, $b = 10.0$.

4.4 Construction of numerical scheme from exact solution

The equation $u_t + u_x = 0$ and $u_x = b u_{xx}$ have known exact finite difference methods which are

$$\frac{u_m^{n+1} - u_m^n}{k} + \frac{u_m^n - u_{m-1}^n}{h} = 0, \text{ with } k = h \quad (4.5)$$

and

$$\frac{u_m - u_{m-1}}{h} = b \frac{u_{m+1} - u_m + u_{m-1}}{b (e^{h/b} - 1) h}, \quad (4.6)$$

respectively, where h and k represent spatial mesh size and temporal step size respectively. However, there no exact finite difference schemes for most ordinary or partial differential equations including the standard FitzHugh-Nagumo equation and Fisher's equations. Appadu et al. (2016), they solve the equation $u_t + u_x = \alpha u_{xx}$ for $0 < x < 1, t > 0$ with boundary condition $u(0, t) = u(1, t) = 0$ and initial condition $u(x, 0) = 3 \sin(4 \pi x)$. The numerical experiment is from Chawla et al. (2000) and the exact solution is

$$u(x, t) = e^{\left[\frac{1}{2\alpha}(x-\frac{t}{2})\right]} \sum_{j=1}^{\infty} \xi_j e^{-(\alpha_j^2 \pi^2 t)} \sin(j \pi x), \quad (4.7)$$

where

$$\xi_j = \frac{3}{2\alpha} \left[1 + (-1)^{j+1} e^{-\left(\frac{1}{2\alpha}\right)} \right] \left[\frac{1}{\left(\frac{1}{2\alpha}\right)^2 + (j-4)^2 \pi^2} - \frac{1}{\left(\frac{1}{2\alpha}\right)^2 + (j+4)^2 \pi^2} \right].$$

Three numerical methods were used in Appadu et al. (2016) namely; fourth order upwind, NSFD and third order upwind. They considered three different values of α namely; 0.01, 0.1 and 1.0 using $h = 0.1$ at some values of k . Dispersive oscillations were observed with all the three methods when $\alpha = 0.01$. Quite good results were obtained when $\alpha = 0.1$ and $\alpha = 1.0$.

This suggests that one cannot use a given numerical method to solve a certain partial differential equation for any value of the parameters controlling advection and diffusion in this case. It is for this reason that the authors believe that the approach used by Namjoo and Zibaei (2018) to construct schemes from the exact solution should be explored. This approach is fairly new. Zhang et al. (2014) constructed finite difference schemes for Burgers and Burgers-Fisher equations using the exact solution.

4.5 Scheme of Namjoo and Zibaei

We describe how in Namjoo and Zibaei (2018) constructed an explicit and implicit scheme. The analytical solution is

$$u(x, t) = \frac{\gamma}{2} \{1 + \tanh[A_1(x - A_2 t)]\} = \frac{\gamma}{1 + e^{-2A_1(x - A_2 t)}}. \quad (4.8)$$

and boundary and initial conditions can be obtained from (4.8). We use the exact solution from (4.8) in order to obtain approximations for u_x , u_t and u_{xx} . The following approximations are used:

$$\begin{aligned}\partial_x u &= \frac{u(x+h, t) - u(x, t)}{h}, \\ \partial_t u &= \frac{u(x, t+k) - u(x, t)}{k}, \\ \bar{\partial}_x u &= \frac{u(x, t) - u(x-h, t)}{h}, \\ \bar{\partial}_t u &= \frac{u(x, t) - u(x, t-k)}{k}.\end{aligned}\tag{4.9}$$

Using (4.8), we have

$$u(x+h, t) = \frac{\gamma}{1 + e^{-2A_1(x+h-A_2t)}}, \quad u(x, t-k) = \frac{\gamma}{1 + e^{-2A_1(x-A_2t+A_2k)}}.\tag{4.10}$$

If we choose $h = A_2k$, we have $u(x+h, t) = u(x, t-k)$ and $u(x-h, t) = u(x, t+k)$. This gives the following

$$\frac{1}{u(x, t)} - \frac{1}{u(x+h, t)} = \left(\frac{1}{u(x, t)} - \frac{1}{\gamma} \right) (1 - e^{-2A_1h}),\tag{4.11}$$

$$\frac{1}{u(x, t)} - \frac{1}{u(x-h, t)} = \left(\frac{1}{u(x, t)} - \frac{1}{\gamma} \right) (1 - e^{2A_1h}),\tag{4.12}$$

$$\frac{1}{u(x, t)} - \frac{1}{u(x, t+k)} = \left(\frac{1}{u(x, t)} - \frac{1}{\gamma} \right) (1 - e^{2A_1A_2k}),\tag{4.13}$$

$$\frac{1}{u(x, t)} - \frac{1}{u(x, t-k)} = \left(\frac{1}{u(x, t)} - \frac{1}{\gamma} \right) (1 - e^{-2A_1A_2k}).\tag{4.14}$$

We define

$$\begin{aligned}\psi_1 &= \frac{1 - e^{-2A_1h}}{2A_1} \approx h, \quad \psi_2 = \frac{e^{2A_1h} - 1}{2A_1} \approx h \\ \phi_1 &= \frac{1 - e^{-2A_1A_2k}}{2A_1A_2} \approx k, \quad \phi_2 = \frac{e^{2A_1A_2k} - 1}{2A_1A_2} \approx k.\end{aligned}\tag{4.15}$$

The forward difference approximation for u_x is

$$\partial_x u = \frac{u(x+h, t) - u(x, t)}{\psi_1} = \frac{1}{\psi_1} [u(x+h, t) - u(x, t)],\tag{4.16}$$

and using (4.11), we have

$$u(x+h, t) - u(x, t) = \left(\frac{1}{u(x, t)} - \frac{1}{\gamma} \right) (1 - e^{-2A_1h}) u(x, t) u(x+h, t),\tag{4.17}$$

or

$$u(x+h, t) - u(x, t) = \left(\frac{\gamma - u(x, t)}{\gamma u(x, t)} \right) (1 - e^{-2A_1h}) u(x, t) u(x+h, t).\tag{4.18}$$

which can be further simplified as

$$u(x+h, t) - u(x, t) = \left(\frac{\gamma - u(x, t)}{\gamma} \right) (1 - e^{-2A_1h}) u(x+h, t).\tag{4.19}$$

It follows from (4.16) that

$$\partial_x u = \frac{u(x+h, t) - u(x, t)}{\psi_1} = 2A_1 u(x+h, t) \left(1 - \frac{u(x, t)}{\gamma} \right).\tag{4.20}$$

We proceed in the same manner to obtain \bar{u}_x , u_t , \bar{u}_t where \bar{u}_x and \bar{u}_t are backward difference approximations and we have

$$\bar{\partial}_x u = \frac{u(x, t) - u(x - h, t)}{\psi_2} = 2 A_1 u(x - h, t) \left(1 - \frac{u(x, t)}{\gamma} \right), \quad (4.21)$$

$$\partial_t u = \frac{u(x, t + k) - u(x, t)}{\phi_2} = 2 A_1 A_2 u(x, t + k) \left(\frac{u(x, t)}{\gamma} - 1 \right), \quad (4.22)$$

$$\bar{\partial}_t u = \frac{u(x, t) - u(x, t - k)}{\phi_1} = 2 A_1 A_2 u(x, t - k) \left(\frac{u(x, t)}{\gamma} - 1 \right). \quad (4.23)$$

We need to obtain an approximation for u_{xx} . We choose $u_{xx} = \bar{\partial}_x \partial_x u$ and this combination generates an explicit scheme. We have

$$u_{xx} = \bar{\partial}_x \partial_x u = \bar{\partial}_x \left(\frac{u(x + h, t) - u(x, t)}{\psi_1} \right) = \frac{\bar{\partial}_x u(x + h, t) - \bar{\partial}_x u(x, t)}{\psi_1}. \quad (4.24)$$

From Eq. (4.20) and Eq. (4.21), we can easily deduce that

$$u_{xx} = \frac{2 A_1}{\psi_1} u(x, t) \left(1 - \frac{u(x + h, t)}{\gamma} \right) - \frac{2 A_1}{\psi_1} u(x - h, t) \left(1 - \frac{u(x, t)}{\gamma} \right) \quad (4.25)$$

and it follows that

$$u_{xx} = \frac{2 A_1}{\psi_1} (u(x, t) - u(x - h, t)) + \frac{2 A_1}{\gamma \psi_1} u(x, t) (u(x - h, t) - u(x + h, t)). \quad (4.26)$$

We introduce A_2 into Eq. (4.26) by adding and subtracting the expression

$$\frac{A_2}{\psi_1} (u(x, t) - u(x - h, t))$$

so that u_{xx} can be expressed in terms of a time derivative with other expressions. We then have

$$u_{xx} = \frac{2 A_1 + A_2}{\psi_1} (u(x, t) - u(x - h, t)) + \frac{2 A_1}{\gamma \psi_1} u(x, t) (u(x - h, t) - u(x + h, t)) - \frac{A_2}{\psi_1} (u(x, t) - u(x - h, t)). \quad (4.27)$$

Since $h = A_2 k$, we deduce that $\frac{A_2}{\psi_1} = \frac{1}{\phi_1}$. Also $u(x, t + k) = u(x - h, t)$, therefore,

$$\frac{A_2}{\psi_1} (u(x, t) - u(x - h, t)) = \frac{u(x, t) - u(x, t + k)}{\phi_1}. \quad (4.28)$$

This gives

$$u_{xx} = \frac{u(x, t + k) - u(x, t)}{\phi_1} + \frac{2 A_1 + A_2}{\psi_1} (u(x, t) - u(x - h, t)) + \frac{2 A_1}{\gamma \psi_1} u(x, t) (u(x - h, t) - u(x + h, t)), \quad (4.29)$$

which can be rewritten as

$$u_{xx} = \frac{u(x, t + k) - u(x, t)}{\phi_1} + (2 A_1 + A_2) \left(\frac{u(x, t) - u(x - h, t)}{\psi_1} \right) + \frac{2 A_1}{\gamma} u(x, t) \left(\frac{u(x - h, t) - u(x, t)}{\psi_1} + \frac{u(x, t) - u(x + h, t)}{\psi_1} \right). \quad (4.30)$$

From Eq. (4.20) and (4.21) we have

$$u_{xx} = \frac{u(x, t+k) - u(x, t)}{\phi_1} + 2A_1(2A_1 + A_2)u(x, t) \left(1 - \frac{u(x-h, t)}{\gamma}\right) + \frac{2A_1}{\gamma}u(x, t) \left[-2A_1u(x, t) \left(1 - \frac{u(x-h, t)}{\gamma}\right) - 2A_1u(x+h, t) \left(1 - \frac{u(x, t)}{\gamma}\right)\right]. \quad (4.31)$$

We remark that since $A_1 = \frac{\sqrt{2}}{4}\gamma$ and $A_2 = \left(\frac{4-2\gamma}{\gamma}\right)A_1$, we have

$$2A_1 \left(\frac{2A_1}{\gamma}\right) = \frac{4}{\gamma} \left(\frac{2}{16}\gamma^2\right) = \frac{\gamma}{2}, \quad 2A_1(2A_1 + A_2) = \frac{\gamma^2}{2} + \frac{1}{4}\gamma(4-2\gamma) = \gamma. \quad (4.32)$$

Therefore, by using (4.32), (4.31) becomes

$$u_{xx} = \frac{u(x, t+k) - u(x, t)}{\phi_1} + \frac{u^2(x, t)}{2}(u(x+h, t) + u(x-h, t)) - \frac{\gamma}{2}u(x, t)(u(x, t) + u(x+h, t)) + \gamma u(x, t) - u(x, t)u(x-h, t). \quad (4.33)$$

4.5.1 Explicit scheme

We can approximate u_{xx} by a second order central difference approximation using a non-traditional denominator and thus obtain an explicit scheme which discretises Eq. (4.1). Using Eq. (4.33), we have

$$\frac{u_{m+1}^n - 2u_m^n + u_{m-1}^n}{\psi_1\psi_2} = \frac{u_m^{n+1} - u_m^n}{\phi_1} + (u_m^n)^2 \left(\frac{u_{m+1}^n + u_{m-1}^n}{2}\right) - (\gamma u_m^n) \left(\frac{u_m^n + u_{m+1}^n}{2}\right) - u_m^n u_{m-1}^n + \gamma u_m^n, \quad (4.34)$$

Theorem 4.1. *The explicit scheme (4.34) is consistent with the original equation (4.1).*

Proof. By Taylor series expansion we have,

$$\begin{aligned} u_{xx} &= \frac{u(x, t+k) - u(x, t)}{\phi_1} + \frac{u^2(x, t)}{2}(u(x+h, t) + u(x-h, t)) \\ &\quad - \frac{\gamma}{2}u(x, t)(u(x, t) + u(x+h, t)) + \gamma u(x, t) - u(x, t)u(x-h, t) \\ &= \frac{(u + ku_t + \frac{k^2}{2}u_{tt} + \dots) - u}{\phi_1 \approx k} \\ &\quad + \frac{u^2}{2} \left(u + hu_x + \frac{h^2}{2}u_{xx} + u - hu_x + \frac{h^2}{2}u_{xx} + \dots\right) \\ &\quad - \frac{\gamma}{2}u(u + u + hu_x + \frac{h^2}{2}u_{xx} + \dots) + \gamma u - u(u - hu_x + \frac{h^2}{2}u_{xx} + \dots). \end{aligned} \quad (4.35)$$

It follows that

$$\begin{aligned} u_{xx} &= u_t - \frac{k^2}{2}u_{tt} + \dots + \frac{u^2}{2}(2u + h^2u_{xx} + \dots) \\ &\quad - \frac{\gamma}{2}u(2u + hu_x + \frac{h^2}{2}u_{xx} + \dots) + \gamma u - u^2 + huu_x + \frac{uh^2}{2}u_{xx} + \dots \end{aligned} \quad (4.36)$$

Finally we have

$$\begin{aligned} u_{xx} &= u_t + \gamma u - u^2 + u^3 - \gamma u^2 - \frac{k^2}{2}u_{tt} + \frac{h^2u^2}{2}u_{xx} + huu_x + \frac{h^2u}{2}u_{xx} \\ &\quad - \frac{h\gamma u}{2}u_x - \frac{h^2\gamma u}{4}u_{xx} \dots \end{aligned} \quad (4.37)$$

When $k, h \rightarrow 0$, we recover the equation

$$u_{xx} = u_t + \gamma u - u^2 + u^3 - \gamma u^2 = u_t + u(1-u)(\gamma - u). \quad (4.38)$$

□

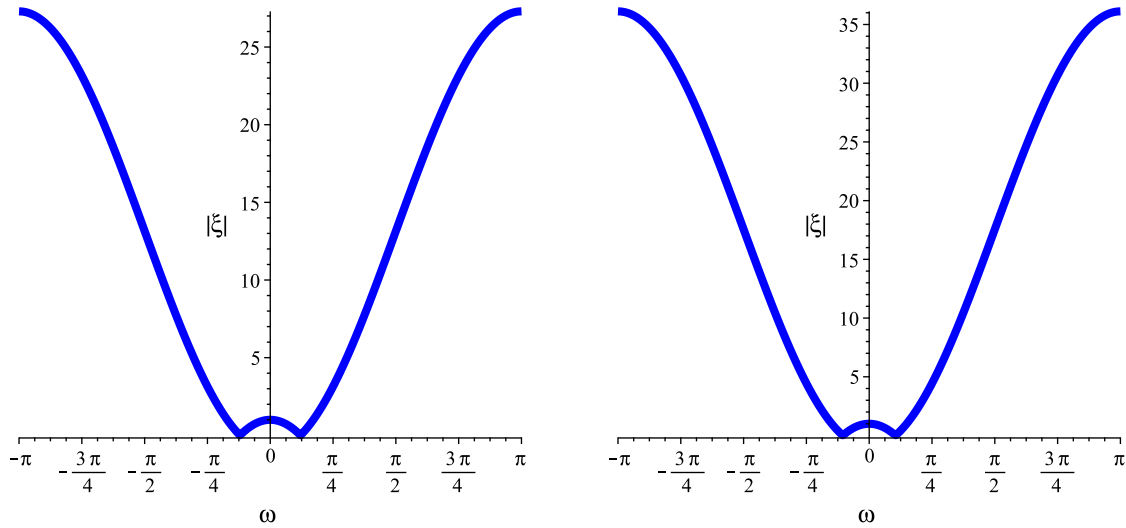
Numerical experiment of explicit scheme

We solve the numerical experiment using $\gamma = 0.001$, $h = 0.1$ for $0 \leq x \leq 1$, and $0 \leq x \leq 10$, for time, $T = 1.0$. Using the functional relationship, $h = A_2 k$ with $\gamma = 0.001$, $h = 0.1$ we obtain $k = 1/14$. We tabulate L_1 and L_∞ errors at some values of k in Tables 4.1 to 4.2 and observe that the method appears to be unstable at $k = 1/14 \approx 0.071$. We next use $\gamma = 0.5$, $h = 0.1$ for $0 \leq x \leq 1$ and $0 \leq x \leq 10$. If we use the functional relationship, $h = A_2 k$ with $\gamma = 0.5$, $h = 0.1$ the value of k must be 0.09428, we use $k = 1/11 \approx 0.0909$. The errors are displayed in Tables 4.3 to 4.4. '-' in Tables 4.1 to 4.4 indicate unbounded values.

Time step (k)	L_1 error	L_∞ error	CPU (s)
0.0005	7.2345×10^{-13}	1.0961×10^{-12}	1.122
0.001	7.1830×10^{-13}	1.0883×10^{-12}	0.811
0.002	7.0800×10^{-13}	1.0727×10^{-12}	0.700
0.004	6.8741×10^{-13}	1.0259×10^{-12}	0.624
0.005	6.7711×10^{-13}	1.0259×10^{-12}	0.662
0.008	—	—	—
0.016	—	—	—
0.032	—	—	—
1/14 \approx 0.071	1.2060×10^2	2.1499×10^2	0.585
0.1	1.3581	1.9441	0.550

Table 4.1: Computation of L_1 and L_∞ errors and CPU time using explicit scheme described by Eq. (4.34) from Namjoo and Zibaei (2018) with $\gamma = 0.001$, $h = 0.1$, $0 \leq x \leq 1$ at time, $T = 1.0$.

First, we fix $h = 0.1$ and $\gamma = 0.001$, $\gamma = 0.5$, and compute k as h/A_2 . A plot of $|\xi|$ against $w \in [-\pi, \pi]$ is then obtained as depicted in Figure 4.1a. We also consider $h = 0.1$ and $\gamma = 0.5$, and obtain plot of $|\xi|$ against $w \in [-\pi, \pi]$ in Figure 4.1b. We observe that explicit scheme is not stable for all values of $w \in [-\pi, \pi]$. Hence the explicit scheme constructed by Namjoo and Zibaei (2018) using the exact solution is not useful scheme due to stability issues.



(a) $h = 0.1, \gamma = 0.001, k = h/A_2$.

(b) $h = 0.1, \gamma = 0.5, k = h/A_2$.

Figure 4.1: Plot of $|\xi|$ against w using explicit scheme described by Eq. (4.34) from Namjoo and Zibaei (2018).

Time step (k)	L_1 error	L_∞ error	CPU (s)
0.0005	7.4612×10^{-11}	8.7850×10^{-12}	3.180
0.001	7.4084×10^{-11}	8.7225×10^{-12}	1.802
0.002	7.3026×10^{-11}	8.5975×10^{-12}	1.273
0.004	7.0911×10^{-11}	8.3474×10^{-12}	0.971
0.005	6.9855×10^{-11}	8.2223×10^{-12}	0.846
0.008	—	—	—
0.016	—	—	—
0.032	—	—	—
1/14 \approx 0.071	1.5906×10^2	1.6740×10^2	0.686
0.1	1.3609	1.9447	0.644

Table 4.2: Computation of L_1 and L_∞ errors and CPU time using explicit scheme described by Eq. (4.34) from Namjoo and Zibaei (2018) with $\gamma = 0.001, h = 0.1, 0 \leq x \leq 10$ at time, $T = 1.0$.

Time step (k)	L_1 error	L_∞ error	CPU (s)
0.0005	6.2098×10^{-5}	9.4197×10^{-5}	1.176
0.001	6.1767×10^{-5}	9.3694×10^{-5}	1.019
0.002	6.1104×10^{-5}	9.2689×10^{-5}	0.925
0.004	5.9779×10^{-5}	9.0680×10^{-5}	0.908
0.005	5.9117×10^{-5}	8.9675×10^{-5}	0.800
0.008	—	—	—
0.016	—	—	—
0.032	—	—	—
1/11\approx0.0909	1.5602×10^{131}	1.1393×10^{133}	0.572
0.1	1.8374×10^{49}	1.0756×10^{50}	0.546

Table 4.3: Computation of L_1 and L_∞ errors and CPU time using explicit scheme described by Eq. (4.34) from [Namjoo and Zibaei \(2018\)](#) with $\gamma = 0.5$, $h = 0.1$, $0 \leq x \leq 1$ at time, $T = 1.0$.

Time step (k)	L_1 error	L_∞ error	CPU (s)
0.0005	6.5901×10^{-3}	1.0134×10^{-3}	3.723
0.001	6.5544×10^{-3}	1.0080×10^{-3}	2.176
0.002	6.4830×10^{-3}	9.9703×10^{-4}	1.661
0.004	6.3403×10^{-3}	9.7515×10^{-4}	1.025
0.005	6.2689×10^{-3}	9.6422×10^{-4}	0.854
0.008	—	—	—
0.016	—	—	—
0.032	—	—	—
1/11\approx0.0909	1.0623×10^{127}	9.4631×10^{127}	0.564
0.1	1.4743×10^{49}	8.3040×10^{49}	0.552

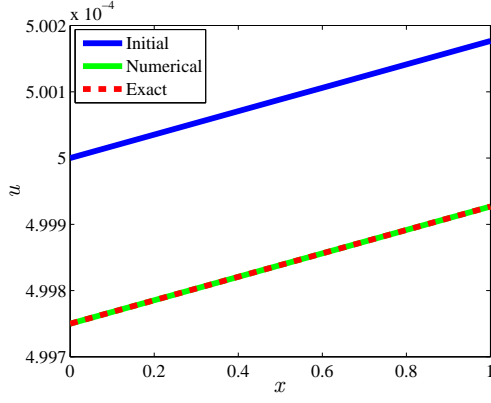
Table 4.4: Computation of L_1 and L_∞ errors and CPU time using explicit scheme described by Eq. (4.34) from [Namjoo and Zibaei \(2018\)](#) with $\gamma = 0.5$, $h = 0.1$, $0 \leq x \leq 10$ at time, $T = 1.0$.

From Tables 4.1 to 4.4, we deduce that functional relationship does not guarantee stability of the scheme. We study the stability analysis of the scheme using Von Neumann stability analysis and method of freezing coefficient ([Durrant, 2010](#)). Using the ansatz, $u_m^n = \xi^n e^{Imw}$, we obtain the amplification factor

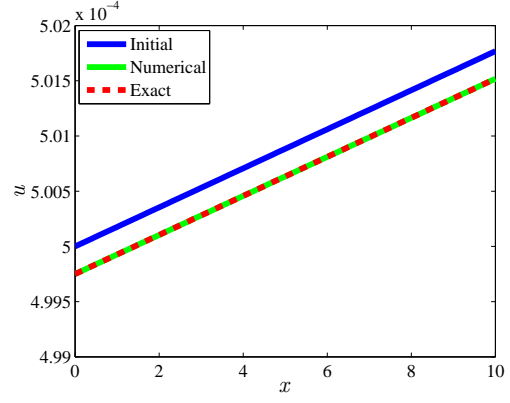
of Eq. (4.34) as

$$\begin{aligned} \xi = \frac{\phi_1}{\psi_1\psi_2}(2 \cos(w) - 2) - \phi_1 u_{max}^2 \cos(w) + \phi_1 \frac{\gamma}{2} u_{max}(1 + \cos(w)) \\ + \phi_1 u_{max} \cos(w) + 1 - \gamma\phi_1 - I\phi_1 u_{max} \left(1 - \frac{\gamma}{2}\right) \sin(w). \end{aligned} \quad (4.39)$$

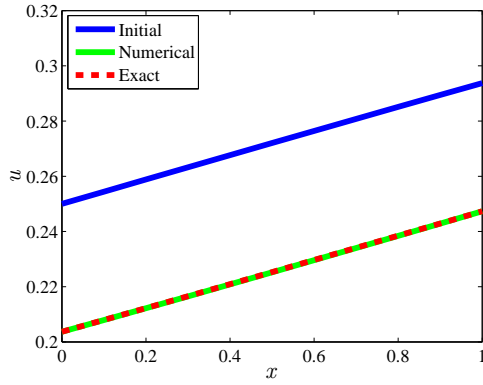
where $\psi_1 = \frac{1-e^{-2A_1 h}}{2A_1}$, $\psi_2 = \frac{e^{2A_1 h}-1}{2A_1}$, $A_1 = \frac{\sqrt{2}}{4}\gamma$. We note that $u_{max} \leq \gamma$ (from some numerical experiments which were carried out). An alternative way to understand why the explicit scheme is unstable for this numerical experiment is explained in the following lines: We consider $h = A_2 k$. Since $A_2 = \left(\frac{4-2\gamma}{\gamma}\right) A_1$ and $A_1 = \frac{\sqrt{2}}{4}\gamma$, this gives $A_2 = \frac{2-\sqrt{2}\gamma}{2}$. Hence $\frac{k}{h} = \frac{1}{A_2} = \frac{2}{2-\sqrt{2}\gamma}$ where $\gamma \in (0, 1)$. This gives $1 < \frac{k}{h} < \frac{2}{2-\sqrt{2}}$ and this can explain the instability of the explicit scheme. It can be shown that the condition for instability for a classical explicit scheme discretising Eq. (4.1) to be $\frac{k}{h^2} < \frac{1}{2}$. We obtain plots of u against x using explicit scheme in Fig.(4.2) using $h = 0.1$, $\gamma = 0.001$, and $h = 0.1$, $\gamma = 0.5$ with $k = 0.005$ (in both cases)



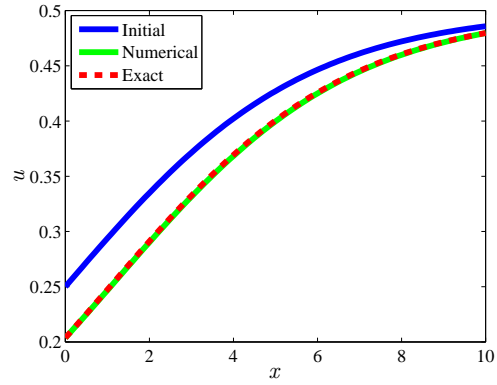
(a) $h = 0.1, \gamma = 0.001, k = 0.0005$.



(b) $h = 0.1, \gamma = 0.001, k = 0.0005$.



(c) $h = 0.1, \gamma = 0.5, k = 0.0005$.



(d) $h = 0.1, \gamma = 0.5, k = 0.0005$.

Figure 4.2: Plot of u against x using explicit scheme described by Eq. (4.34) from Namjoo and Zibaei (2018) at Time, $T = 1.0$ where $x \in [0, 1]$ for 4.2a, 4.2c and $x \in [0, 10]$ for 4.2b and 4.2d.

4.5.2 Implicit scheme

If we choose $u_{xx} = \partial_x \bar{\partial}_x u$, this combination generates an implicit scheme. We have

$$\begin{aligned} \partial_x \bar{\partial}_x u &= \partial_x \left(\frac{u(x, t) - u(x - h, t)}{\psi_2} \right) = \frac{\partial_x u(x, t) - \partial_x u(x - h, t)}{\psi_2}, \\ &= \frac{2A_1}{\psi_2} u(x + h, t) \left(1 - \frac{u(x, t)}{\gamma} \right) - \frac{2A_1}{\psi_2} u(x, t) \left(1 - \frac{u(x - h, t)}{\gamma} \right). \end{aligned} \quad (4.40)$$

It follows

$$\partial_x \bar{\partial}_x u = \frac{2A_1}{\psi_2} u(x + h, t) - \frac{2A_1}{\psi_2} \frac{u(x + h, t)u(x, t)}{\gamma} - \frac{2A_1}{\psi_2} u(x, t) + \frac{2A_1}{\psi_2} \frac{u(x - h, t)u(x, t)}{\gamma}, \quad (4.41)$$

which gives

$$\partial_x \bar{\partial}_x u = \frac{2A_1}{\psi_2} (u(x + h, t) - u(x, t)) + \frac{2A_1}{\gamma \psi_2} u(x, t) (u(x - h, t) - u(x + h, t)). \quad (4.42)$$

We introduce A_2 by adding and subtracting the expression $\frac{A_2}{\psi_2} (u(x+h, t) - u(x, t))$ into (4.42) and we have

$$\begin{aligned} \partial_x \bar{\partial}_x u = \frac{2A_1 + A_2}{\psi_2} (u(x+h, t) - u(x, t)) + \frac{2A_1}{\gamma \psi_2} u(x, t) (u(x-h, t) - u(x+h, t)) \\ - \frac{A_2}{\psi_2} (u(x+h, t) - u(x, t)). \end{aligned} \quad (4.43)$$

Since $h = A_2 k$, it follows that $\frac{A_2}{\psi_2} = \frac{1}{\phi_2}$. Also $u(x+h, t) = u(x, t-k)$. Therefore

$$\frac{A_2}{\psi_2} (u(x+h, t) - u(x, t)) = \frac{u(x, t-k) - u(x, t)}{\phi_2}. \quad (4.44)$$

We thus have

$$\begin{aligned} u_{xx} = \frac{u(x, t) - u(x, t-k)}{\phi_2} + \frac{2A_1 + A_2}{\psi_2} (u(x+h, t) - u(x, t)) \\ + \frac{2A_1}{\gamma} u(x, t) \left(\frac{u(x, t) - u(x+h, t)}{\psi_2} + \frac{u(x-h, t) - u(x, t)}{\psi_2} \right), \end{aligned} \quad (4.45)$$

which can be expressed as

$$\begin{aligned} u_{xx} = \frac{u(x, t) - u(x, t-k)}{\phi_2} + 2A_1(2A_1 + A_2)u(x, t) \left(1 - \frac{u(x+h, t)}{\gamma} \right) \\ + \frac{2A_1}{\gamma} u(x, t) \left[-2A_1 u(x-h, t) \left(1 - \frac{u(x, t)}{\gamma} \right) - 2A_1 u(x, t) \left(1 - \frac{u(x+h, t)}{\gamma} \right) \right]. \end{aligned} \quad (4.46)$$

Further simplification gives

$$\begin{aligned} u_{xx} = \frac{u(x, t) - u(x, t-k)}{\phi_2} + \gamma u(x, t) \left(1 - \frac{u(x+h, t)}{\gamma} \right) \\ - \frac{\gamma}{2} u^2(x, t) \left(1 - \frac{u(x+h, t)}{\gamma} \right) - \frac{\gamma}{2} u(x, t) \left(1 - \frac{u(x, t)}{\gamma} \right) u(x-h, t), \end{aligned} \quad (4.47)$$

and

$$\begin{aligned} u_{xx} = \frac{u(x, t) - u(x, t-k)}{\phi_2} + \gamma u(x, t) - u(x, t)u(x+h, t) \\ - \frac{\gamma}{2} u^2(x, t) + \frac{u^2(x, t)}{2} u(x+h, t) - \frac{\gamma}{2} u(x, t)u(x-h, t) + \frac{u^2(x, t)u(x-h, t)}{2}. \end{aligned} \quad (4.48)$$

It follows

$$\begin{aligned} u_{xx} = \frac{u(x, t) - u(x, t-k)}{\phi_2} + \frac{u^2(x, t)}{2} (u(x+h, t) + u(x-h, t)) \\ - \frac{\gamma}{2} u(x, t) (u(x, t) + u(x-h, t)) - u(x, t)u(x+h, t) + \gamma u(x, t). \end{aligned} \quad (4.49)$$

The implicit scheme is therefore

$$\begin{aligned} \frac{u_{m+1}^n - 2u_m^n + u_{m-1}^n}{\psi_1 \psi_2} = \frac{u_m^n - u_{m-1}^{n-1}}{\phi_2} + (u_m^n)^2 \left(\frac{u_{m+1}^n + u_{m-1}^n}{2} \right) - (\gamma u_m^n) \left(\frac{u_m^n + u_{m-1}^n}{2} \right) \\ - u_m^n u_{m+1}^n + \gamma u_m^n \end{aligned} \quad (4.50)$$

which can be rewritten as

$$\begin{aligned} u_m^{n-1} = u_m^n - \frac{\phi_2}{\psi_1 \psi_2} (u_{m+1}^n - 2u_m^n + u_{m-1}^n) + \frac{\phi_2 (u_m^n)^2}{2} (u_{m+1}^n + u_{m-1}^n) \\ - \phi_2 \gamma \frac{u_m^n}{2} (u_m^n + u_{m-1}^n) - \phi_2 u_m^n u_{m+1}^n + \phi_2 \gamma u_m^n. \end{aligned} \quad (4.51)$$

Theorem 4.2. The implicit scheme (4.51) is consistent with the original equation (4.1).

Proof. The proof is similar as in the case of explicit scheme by using Taylor expansions. □

Numerical experiment of implicit scheme

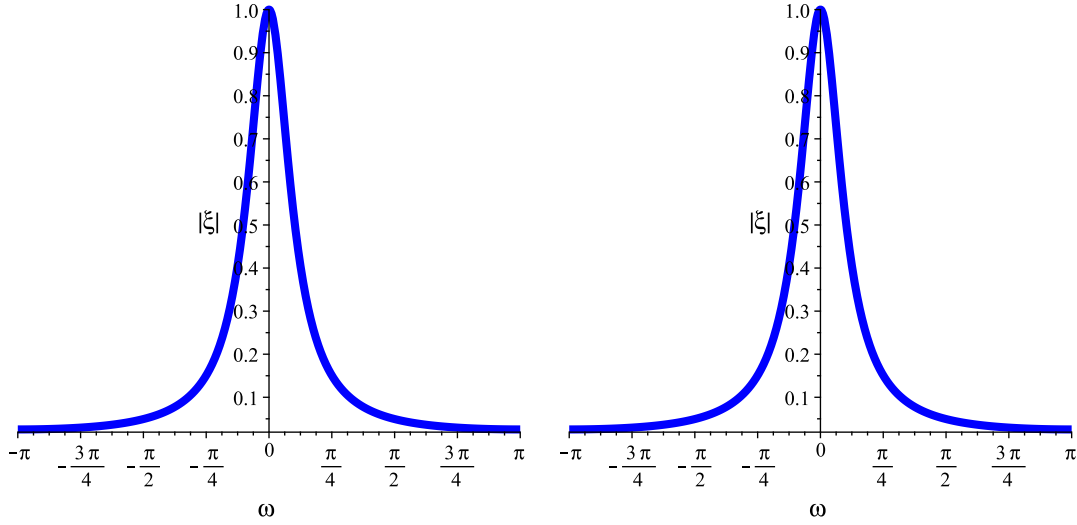
The implicit scheme is given by (4.51) ie

$$u_m^{n-1} = u_m^n - \frac{\phi_2}{\psi_1 \psi_2} (u_{m+1}^n - 2u_m^n + u_{m-1}^n) + \frac{\phi_2 (u_m^n)^2}{2} (u_{m+1}^n + u_{m-1}^n) - \phi_2 \gamma \frac{u_m^n}{2} (u_m^n + u_{m-1}^n) - \phi_2 u_m^n u_{m+1}^n + \phi_2 \gamma u_m^n.$$

The amplification factor of Eq. (4.51) can be obtained from the following

$$\begin{aligned} \xi^{-1} = 1 - \frac{\phi_2}{\psi_1 \psi_2} (2 \cos(w) - 2) + \phi_2 u_{max}^2 \cos(w) + I \phi_2 u_{max} \left(\frac{\gamma}{2} - 1 \right) \sin(w) \\ - \phi_2 u_{max} \left(\frac{\gamma}{2} + 1 \right) \cos(w) - \phi_2 u_{max} \frac{\gamma}{2} + \phi_2 \gamma. \end{aligned} \quad (4.52)$$

Plots of ξ against $w \in [-\pi, \pi]$ for the two cases: $h = 0.1, \gamma = 0.001$ and $h = 0.1, \gamma = 0.5$ are shown in Figures 4.3a and 4.3b and we can deduce the scheme is unconditionally stable in both cases.



(a) $h = 0.1, \gamma = 0.001, k = h/A_2.$

(b) $h = 0.1, \gamma = 0.5, k = h/A_2.$

Figure 4.3: Plot of $|\xi|$ against w using implicit scheme described by Eq. (4.51) from Namjoo and Zibaei (2018).

Time step (k)	L_1 error	L_∞ error
0.0005	7.2041×10^{-11}	8.7556×10^{-12}
0.001	6.2247×10^{-11}	7.5695×10^{-12}
0.002	7.0493×10^{-11}	8.5683×10^{-12}
0.004	6.8431×10^{-10}	8.3186×10^{-12}
0.005	6.7399×10^{-10}	8.1937×10^{-12}
0.008	6.4308×10^{-10}	7.8192×10^{-12}
1/14 \approx 0.071	4.8835×10^{-12}	2.2035×10^{-12}
0.1	2.9959×10^{-11}	3.6599×10^{-12}

Table 4.5: Computation of L_1 and L_∞ errors using implicit scheme described Eq. (4.51) from Namjoo and Zibaei (2018) with $\gamma = 0.001$, $h = 0.1$, $0 \leq x \leq 1$ at time, $T = 1.0$.

Time step (k)	L_1 error	L_∞ error
0.0005	8.1354×10^{-10}	9.1804×10^{-12}
0.001	7.6458×10^{-10}	7.9903×10^{-12}
0.002	8.6291×10^{-10}	8.9924×10^{-12}
0.004	8.3833×10^{-10}	8.7419×10^{-12}
0.005	8.2604×10^{-10}	8.6166×10^{-11}
0.008	7.8916×10^{-10}	8.2408×10^{-12}
1/14 \approx 0.071	1.2821×10^{-11}	2.9990×10^{-13}
0.1	3.4110×10^{-10}	3.6628×10^{-12}

Table 4.6: Computation of L_1 and L_∞ errors using implicit scheme described Eq. (4.51) from Namjoo and Zibaei (2018) with $\gamma = 0.001$, $h = 0.1$, $0 \leq x \leq 10$ at time, $T = 1.0$.

Time step (k)	L_1 error	L_∞ error
0.0005	6.6849×10^{-3}	1.3886×10^{-3}
0.001	8.2833×10^{-3}	1.3837×10^{-3}
0.002	6.6065×10^{-3}	1.3739×10^{-3}
0.004	6.5018×10^{-3}	1.3545×10^{-3}
0.005	6.4495×10^{-3}	1.3447×10^{-3}
0.008	6.2923×10^{-3}	1.3154×10^{-3}
$1/14 \approx 0.071$	4.4010×10^{-3}	7.5572×10^{-4}
$1/11 \approx 0.0909$	4.4861×10^{-4}	9.1301×10^{-4}
0.1	4.5716×10^{-3}	9.9875×10^{-4}

Table 4.7: Computation of L_1 and L_∞ errors using implicit scheme described Eq. (4.51) from [Namjoo and Zibaei \(2018\)](#) with $\gamma = 0.5$, $h = 0.1$, $0 \leq x \leq 1$ at time, $T = 1.0$.

Time step (k)	L_1 error	L_∞ error
0.0005	4.8991×10^{-1}	7.5539×10^{-3}
0.001	4.8961×10^{-1}	7.5500×10^{-3}
0.002	4.8901×10^{-1}	7.5423×10^{-3}
0.004	4.8780×10^{-1}	7.5266×10^{-3}
0.005	4.8719×10^{-1}	7.5188×10^{-3}
0.008	4.8537×10^{-1}	7.4953×10^{-3}
$1/14 \approx 0.071$	4.4764×10^{-1}	6.9953×10^{-3}
$1/11 \approx 0.0909$	4.3641×10^{-1}	6.8410×10^{-3}
0.1	4.3118×10^{-1}	6.7691×10^{-3}

Table 4.8: Computation of L_1 and L_∞ errors using implicit scheme from [Namjoo and Zibaei \(2018\)](#) with $\gamma = 0.5$, $h = 0.1$, $0 \leq x \leq 10$ at time, $T = 1.0$.

Here since we don't have any stability issues with implicit scheme, we choose k , such that $h = A_2 k$.

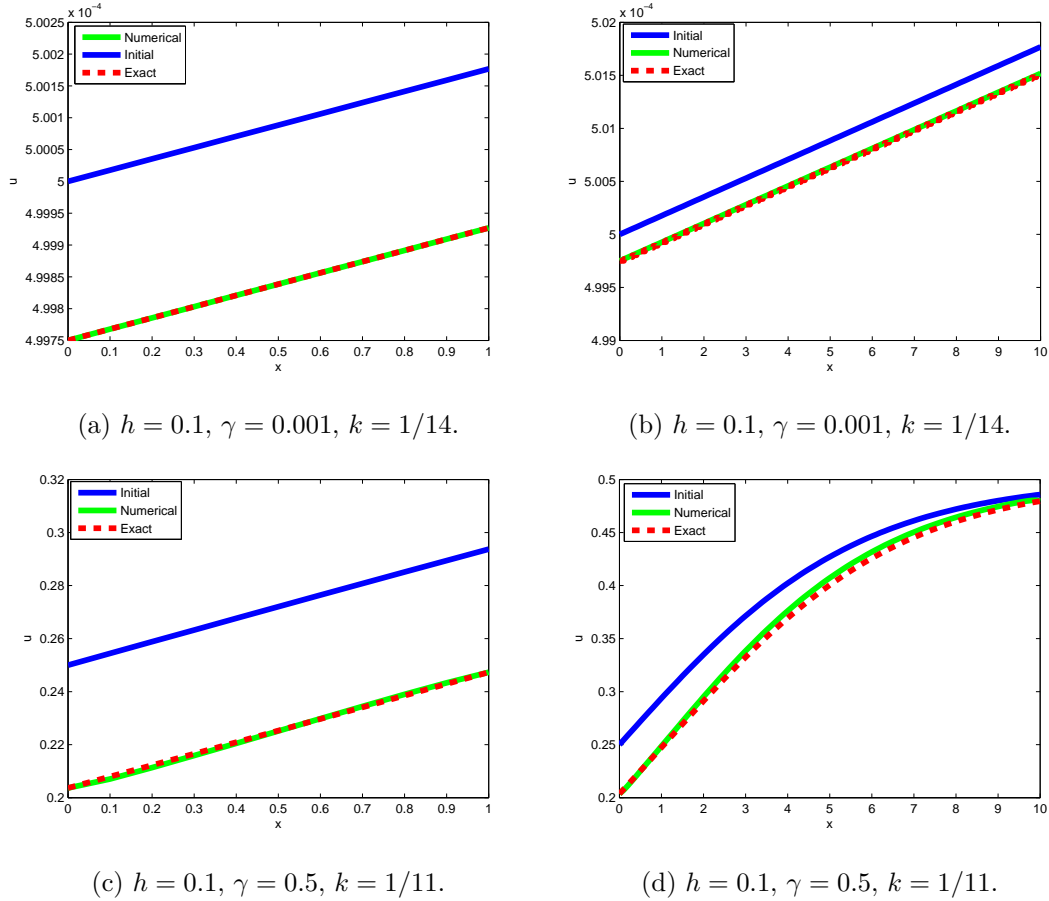


Figure 4.4: Plot of u against x using implicit scheme described by (4.51) from Namjoo and Zibaei (2018) at time, $T = 1.0$ where $x \in [0, 1]$ for 4.4a, 4.4c and $x \in [0, 10]$ for 4.4b and 4.4d.

4.6 Nonstandard Finite Difference Scheme (NSFD)

We present derivation of two versions of Nonstandard Finite Difference Schemes which can be named as NSFD1 and NSFD2 in (Namjoo and Zibaei, 2018). NSFD1 is improved to generate NSFD3 scheme. Please see chapter 2, section 2.1.2 for definitions and properties on NSFD.

4.6.1 NSFD1 scheme

We note that the right hand side of Eq. (4.1) is

$$-u^3 + (1 + \gamma)u^2 - \gamma u.$$

We use the following discrete approximations for the right hand of Eq. (4.1):

$$-\gamma u(x_m, t_n) \approx -\gamma u_m^{n+1}, \quad -(u(x_m, t_n))^3 \approx -\frac{3}{2} (u_{m-1}^n)^2 u_m^{n+1} + \frac{1}{2} (u_{m-1}^n)^3. \quad (4.53)$$

This gives the following scheme

$$\frac{u_m^{n+1} - u_m^n}{\phi_1} - \frac{u_{m+1}^n - 2u_m^n + u_{m-1}^n}{\psi_1\psi_2} = -\frac{3}{2}(u_{m-1}^n)^2 u_m^{n+1} + \frac{1}{2}(u_{m-1}^n)^3 + (1 + \gamma)(u_{m-1}^n)^2 - \gamma u_m^{n+1}, \quad (4.54)$$

where $\psi_1 = \frac{1 - e^{-2A_1 h}}{2A_1}$, $\psi_2 = \frac{e^{2A_1 h} - 1}{2A_1}$ and $\phi_1 = \frac{1 - e^{-2A_1 A_2 k}}{2A_1 A_2}$. A single expression for the scheme is

$$u_m^{n+1} = \frac{(1 - 2R)u_m^n + R(u_{m+1}^n + u_{m-1}^n) + \phi_1 \left((1 + \gamma)(u_{m-1}^n)^2 + \frac{1}{2}(u_{m-1}^n)^3 \right)}{1 + \phi_1 \gamma + \frac{3}{2}\phi_1 (u_{m-1}^n)^2}, \quad (4.55)$$

where $R = \frac{\phi_1}{\psi_1\psi_2}$.

Theorem 4.3. *If $1 - 2R \geq 0$, the numerical solution of Eq. (4.1) satisfies*

$$0 \leq u_m^n \leq 1 \implies 0 \leq u_m^{n+1} \leq 1,$$

and the dynamical consistency holds for all relevant values of n and m .

Remark 4.1. *As stated in the introduction, the concept of nonstandard finite difference required dynamical consistency (positivity, boundedness, preservation of fixed points) which helps to avoid numerical instabilities.*

The fixed points of Eq. (4.1) are $u_1^* = 0$, $u_2^* = 1$ (which are stable) and $u_3^* = \gamma$ which is unstable. Furthermore, [Roeger and Mickens \(2007\)](#) showed preservation of local stabilities of all fixed points.

Proof. For positivity of the scheme given by Eq. (4.55), we have $u_m^{n+1} \geq 0$ if only $1 - 2R \geq 0$, since $u_m^n \geq 0$ by assumption and $1 + \phi_1 \gamma + \frac{3}{2}\phi_1 (u_{m-1}^n)^2 > 0$.

To obtain the condition for positivity of NSFD1, we solve $R = \frac{\phi_1}{\psi_1\psi_2} \leq \frac{1}{2}$ which implies that, by replacing ϕ_1 , ψ_1 , ψ_2 , by their respective expressions, we obtain

$$\left(\frac{1 - e^{-2A_1 A_2 k}}{2A_1 A_2} \right) \left(\frac{2A_1}{1 - e^{-2A_1 h}} \right) \left(\frac{2A_1}{e^{2A_1 h} - 1} \right) \leq \frac{1}{2}, \quad (4.56)$$

which gives

$$k \leq -\frac{1}{2A_1 A_2} \ln \left[1 - \frac{A_2}{4A_1} \frac{(e^{2A_1 h} - 1)^2}{e^{2A_1 h}} \right], \quad (4.57)$$

and finally

$$k \leq -\frac{2}{\gamma(2 - \gamma)} \ln \left[1 - \left(\frac{2 - \gamma}{2\gamma} \right) \frac{(e^{\frac{\sqrt{2}}{2}\gamma h} - 1)^2}{e^{\frac{\sqrt{2}}{2}\gamma h}} \right]. \quad (4.58)$$

We assume that $0 \leq u_m^n \leq \gamma$. If the scheme is bounded, we need to prove that $0 \leq u_m^{n+1} \leq \gamma$ or $u_m^{n+1} - \gamma \leq 0$. Consider

$$\begin{aligned} (u_m^{n+1} - \gamma) \left(1 + \phi_1 \gamma + \frac{3}{2}\phi_1 (u_{m-1}^n)^2 \right) &= (1 - 2R)u_m^n + R(u_{m+1}^n + u_{m-1}^n) \\ &\quad + \phi_1 \left((1 + \gamma)(u_{m-1}^n)^2 + \frac{1}{2}(u_{m-1}^n)^3 \right) \\ &\quad - \gamma - \phi_1 \gamma^2 - \frac{3}{2}\phi_1 (u_{m-1}^n)^2. \end{aligned} \quad (4.59)$$

It follows $(u_{m-1}^n)^3 = u_{m-1}^n (u_{m-1}^n)^2 \leq \gamma (u_{m-1}^n)^2$ since $0 \leq u_m^n \leq \gamma$ for all values for n and m . Therefore,

$$\begin{aligned}
 (u_m^{n+1} - \gamma) \left(1 + \phi_1 \gamma + \frac{3}{2} \phi_1 (u_{m-1}^n)^2 \right) &\leq (1 - 2R)\gamma + 2\gamma R \\
 &+ \phi_1 \gamma^2 + \phi_1 \left(\gamma (u_{m-1}^n)^2 + \frac{\gamma}{2} (u_{m-1}^n)^2 \right) \\
 &- \gamma - \phi_1 \gamma^2 - \frac{3}{2} \phi_1 (u_{m-1}^n)^2 = 0.
 \end{aligned} \tag{4.60}$$

We therefore obtain $u_m^{n+1} - \gamma \leq 0$. Hence NSFD1 satisfies boundedness properties. \square

For $\gamma = 0.001$ and $h = 0.1$, (4.58) gives $k \leq 5.0000 \times 10^{-3}$ while for $\gamma = 0.5$ and $h = 0.1$, we get $k \leq 5.0052 \times 10^{-3}$.

We tabulate L_1 L_∞ errors as well as CPU time and rate of convergence with respect to time (using L_1 error) for the four cases in Tables 4.9 to 4.12. We also obtain plot of u against x at time, $T = 1.0$ in Fig. 4.5.

Time step (k)	L_1 error	L_∞ error	Rate of convergence	CPU (s)
0.005	1.3053×10^{-12}	1.9777×10^{-12}	-	0.561
0.004	1.3362×10^{-12}	2.0246×10^{-12}	-0.1049	0.588
0.002	1.3981×10^{-12}	2.1183×10^{-12}	-0.0653	0.588
0.001	1.4290×10^{-12}	2.1651×10^{-12}	-0.0315	0.688
0.0005	1.4444×10^{-12}	2.1885×10^{-12}	-0.0154	0.745

Table 4.9: Computation of L_1 and L_∞ errors, CPU time and rate of convergence in time using NSFD1 with $\gamma = 0.001$, $h = 0.1$, $0 \leq x \leq 1$ at time, $T = 1.0$.

Time step (k)	L_1 error	L_∞ error	Rate of convergence	CPU (s)
0.005	1.3468×10^{-10}	1.5853×10^{-11}	-	0.772
0.004	1.3786×10^{-10}	1.6228×10^{-11}	-0.1046	0.828
0.002	1.4421×10^{-10}	1.6978×10^{-11}	-0.0649	1.118
0.001	1.4739×10^{-10}	1.7353×10^{-11}	-0.0315	1.561
0.0005	1.4897×10^{-10}	1.7540×10^{-11}	-0.0154	2.991

Table 4.10: Computation of L_1 and L_∞ errors, CPU time and rate of convergence in time using NSFD1 with $\gamma = 0.001$, $h = 0.1$, $0 \leq x \leq 10$ at time, $T = 1.0$.

Time step (k)	L_1 error	L_∞ error	Rate of convergence	CPU (s)
0.005	2.6024×10^{-4}	3.9470×10^{-4}	-	0.565
0.004	2.6311×10^{-4}	3.9905×10^{-4}	-0.0491	0.569
0.002	2.6886×10^{-4}	4.0776×10^{-4}	-0.0312	0.645
0.001	2.7173×10^{-4}	4.1212×10^{-4}	-0.0153	0.685
0.0005	2.7317×10^{-4}	4.1429×10^{-4}	-7.6250×10^{-3}	0.829

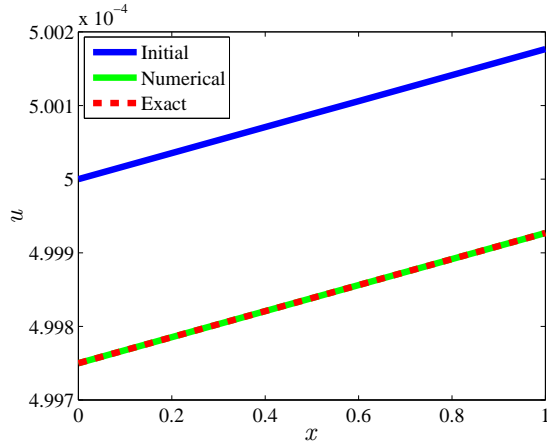
Table 4.11: Computation of L_1 and L_∞ errors CPU time and rate of convergence in time using NSFD1 with $\gamma = 0.5$, $h = 0.1$, $0 \leq x \leq 1$ at time, $T = 1.0$.

Time step (k)	L_1 error	L_∞ error	Rate of convergence	CPU (s)
0.005	2.9989×10^{-2}	4.5242×10^{-3}	-	0.743
0.004	3.0267×10^{-2}	4.5665×10^{-3}	-0.0413	0.749
0.002	3.0825×10^{-2}	4.6515×10^{-3}	-0.0264	1.057
0.001	3.1104×10^{-2}	4.6941×10^{-3}	-0.0129	1.610
0.0005	3.1244×10^{-2}	4.7154×10^{-3}	-6.4790×10^{-3}	2.775

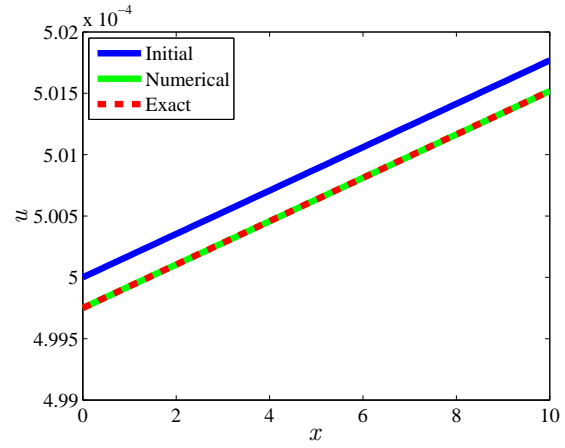
Table 4.12: Computation of L_1 and L_∞ errors, CPU time and rate of convergence using NSFD1 with $\gamma = 0.5$, $h = 0.1$, $0 \leq x \leq 10$ at time, $T = 1.0$.

From Tables 4.9 to 4.12, we deduce that though the L_1 , L_∞ are of the order 10^{-12} , 10^{-10} for cases 1, 2 and of order 10^{-4} , 10^{-2} for cases 3, 4. The rate of convergence with respect to time is negative and this indicates that NSFD1 has convergence issues. This could be due to approximations of $-\gamma u(x_m, t_n)$ by $-\gamma u_m^{n+1}$ and approximation of $-(u(x_m, t_n))^3$ by $-\frac{3}{2} (u_{m-1}^n)^2 u_m^{n+1} + \frac{1}{2} (u_{m-1}^n)^3$ where u_{m-1}^n and u_m^{n+1} are both non-local approximations. $(1 + \gamma)u^2$ can be approximated by $(1 + \gamma)u_{m+1}^n u_{m-1}^n$ or $(1 + \gamma)(u_m^n)^2$. $-(u(x_m, t_n))^3$ can be approximated by $-\frac{3}{2} (u_m^n)^2 u_m^{n+1} + \frac{1}{2} (u_m^n)^3$.

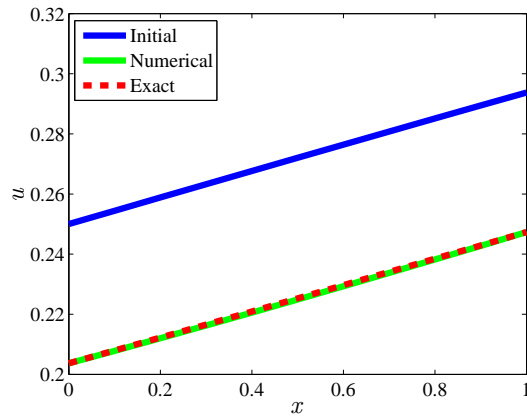
The plot Plot of u against x using NSFD1 is shown in Figure 4.5.



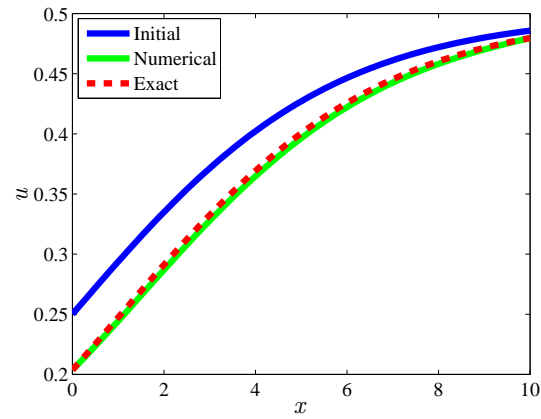
(a) $h = 0.1, \gamma = 0.001, k = 0.0005.$



(b) $h = 0.1, \gamma = 0.001, k = 0.0005.$



(c) $h = 0.1, \gamma = 0.5, k = 0.0005.$



(d) $h = 0.1, \gamma = 0.5, k = 0.0005.$

Figure 4.5: Plot of u against x using NSFD1 scheme at time $T = 1.0$, where $x \in [0, 1]$, for 4.5a, 4.5c and $x \in [0, 10]$ for 4.5b and 4.5d.

4.6.2 NSFD2 scheme

Here we use the following approximations for the right hand of Eq. (4.1):

$$u(x_m, t_n) \approx u_m^{n+1}, \quad (u(x_m, t_n))^2 \approx u_m^{n+1} u_m^n, \quad (4.61)$$

$$(u(x_m, t_n))^3 \approx u_m^{n+1} (u_m^n)^2. \quad (4.62)$$

The NSFD2 scheme when used to discretise Eq. (4.1) is given by

$$\frac{u_m^{n+1} - u_m^n}{\phi_1} - \frac{u_{m+1}^n - 2u_m^n + u_{m-1}^n}{\psi_1 \psi_2} = -u_m^{n+1} (u_m^n)^2 + (1 + \gamma) u_m^{n+1} u_m^n - \gamma u_m^{n+1}. \quad (4.63)$$

or

$$u_m^{n+1} = \frac{(1 - 2R)u_m^n + R(u_{m+1}^n + u_{m-1}^n)}{1 + \phi_1 \gamma - (1 + \gamma)\phi_1 u_m^n + \phi_1 (u_m^n)^2}, \quad \text{where } R = \frac{\phi_1}{\psi_1 \psi_2}. \quad (4.64)$$

Theorem 4.4. *If $1 - 2R \geq 0$ and $1 - \phi_1\gamma^2 \geq 0$, the numerical solution of Eq. (4.1) satisfies*

$$0 \leq u_m^n \leq 1 \implies 0 \leq u_m^{n+1} \leq 1,$$

and the dynamical consistency holds for all relevant values of n and m .

Proof. For positivity of NSFD2, we have $u_m^{n+1} \geq 0$ if only $1 - 2R \geq 0$ and $1 - \phi_1\gamma^2 \geq 0$. The coefficient of u_m^n must be non-negative. We also need to have

$$1 + \phi_1\gamma - (1 + \gamma)\phi_1u_m^n + \phi_1(u_m^n)^2 > 0.$$

We note that $0 \leq u_m^n \leq \gamma$. Hence,

$$\begin{aligned} 1 - [(1 + \gamma)\phi_1u_m^n - \phi_1\gamma] + \phi_1(u_m^n)^2 &\geq 1 + \gamma\phi_1 - \gamma\phi_1 - \gamma^2\phi_1 + \phi_1(u_m^n)^2 \\ &\geq 1 - \phi_1\gamma^2 + \phi_1(u_m^n)^2 \\ &\geq 1 - \phi_1\gamma^2. \end{aligned} \quad (4.65)$$

To obtain the condition for positivity of NSFD2, we solve $R = \frac{\phi_1}{\psi_1\psi_2} \leq \frac{1}{2}$ and $1 - \phi_1\gamma^2 > 0$. Solving $R \leq \frac{1}{2}$ gives

$$k \leq -\frac{2}{\gamma(2-\gamma)} \ln \left[1 - \left(\frac{2-\gamma}{2\gamma} \right) \frac{\left(e^{\frac{\sqrt{2}}{2}\gamma h} - 1 \right)^2}{e^{\frac{\sqrt{2}}{2}\gamma h}} \right]. \quad (4.66)$$

We also need to solve

$$1 - \left(\frac{1 - e^{-2A_1A_2k}}{A_1A_2} \right) \gamma^2 > 0, \quad (4.67)$$

and this gives

$$k \leq -\frac{2}{\gamma(2-\gamma)} \ln \left[1 - \frac{\gamma}{4}(2-\gamma) \right]. \quad (4.68)$$

and finally, we obtain

$$k \leq \begin{cases} -\frac{2}{\gamma(2-\gamma)} \ln \left[1 - \frac{\gamma}{4}(2-\gamma) \right], \\ -\frac{2}{\gamma(2-\gamma)} \ln \left[1 - \left(\frac{2-\gamma}{2\gamma} \right) \frac{\left(e^{\frac{\sqrt{2}}{2}\gamma h} - 1 \right)^2}{e^{\frac{\sqrt{2}}{2}\gamma h}} \right]. \end{cases} \quad (4.69)$$

For boundedness of NSFD2, we assume that $0 \leq u_j^n \leq \gamma$. Consider

$$\begin{aligned} (u_m^{n+1} - \gamma) \left(1 + \phi_1\gamma - (1 + \gamma)\phi_1u_m^n + \phi_1(u_m^n)^2 \right) &= (1 - 2R)u_m^n + R(u_{m+1}^n + u_{m-1}^n) \\ &\quad - \gamma - \gamma^2\phi_1 + \gamma(1 + \gamma)\phi_1u_m^n \\ &\quad - \gamma\phi_1(u_m^n)^2. \end{aligned} \quad (4.70)$$

It follows, since $0 \leq u_m^n \leq \gamma$ for all values for n and m ,

$$\begin{aligned} (u_m^{n+1} - \gamma) \left(1 + \phi_1\gamma - (1 + \gamma)\phi_1u_m^n + \phi_1(u_m^n)^2 \right) &\leq (1 - 2R)\gamma + 2\gamma R \\ &\quad - \gamma - \gamma^2\phi_1 + \gamma(1 + \gamma)\phi_1u_m^n \\ &\quad - \gamma\phi_1(u_m^n)^2. \end{aligned} \quad (4.71)$$

Finally, we have

$$\begin{aligned}
 (u_m^{n+1} - \gamma) \left(1 + \phi_1 \gamma - (1 + \gamma) \phi_1 u_m^n + \phi_1 (u_m^n)^2 \right) &\leq -\phi_1 \gamma \left[(u_m^n)^2 - \gamma u_m^n - u_m^n + \gamma \right] \\
 &= -\phi_1 \gamma (u_m^n - 1)(u_m^n - \gamma).
 \end{aligned} \tag{4.72}$$

Since $0 \leq u_m^n \leq \gamma$ and $\gamma \in (0, 1)$, we have $(u_m^n - 1)(u_m^n - \gamma) \geq 0$ and

$$(u_m^{n+1} - \gamma) \left(1 + \phi_1 \gamma - (1 + \gamma) \phi_1 u_m^n + \phi_1 (u_m^n)^2 \right) \leq 0. \tag{4.73}$$

Therefore we have $0 \leq u_m^{n+1} \leq \gamma$. Hence the boundedness of NSFD2. \square

Solving (4.69) for $\gamma = 0.001$, $h = 0.1$, gives $k \leq 5.0000 \times 10^{-3}$ and $k \leq 5.0012 \times 10^{-1}$. When we solve for $\gamma = 0.5$, $h = 0.1$, we obtain $k \leq 5.0052 \times 10^{-3}$, and $k \leq 5.5370 \times 10^{-1}$.

Hence is NSFD2 scheme is positive definite if

- (i) $k \leq 5.0000 \times 10^{-3}$ when $\gamma = 0.001$,
- (ii) $k \leq 5.0052 \times 10^{-3}$ when $\gamma = 0.5$.

We tabulate L_1 , L_∞ errors, CPU time and rate of convergence in time in Tables 4.13 to 4.16 and obtain plots of u against x in Figure 4.6.

Time step (k)	L_1 error	L_∞ error	Rate of convergence	CPU (s)
0.005	1.0302×10^{-13}	1.5608×10^{-13}	-	0.498
0.004	8.2413×10^{-14}	1.2487×10^{-13}	1.000	0.514
0.002	4.1207×10^{-14}	6.2435×10^{-14}	1.000	0.562
0.001	2.0598×10^{-14}	3.1209×10^{-14}	1.000	0.590
0.0005	1.0303×10^{-14}	1.5611×10^{-14}	0.999	0.685

Table 4.13: Computation of L_1 and L_∞ errors, CPU time and rate of convergence using NSFD2 with $\gamma = 0.001$, $h = 0.1$, $0 \leq x \leq 1$, $T = 1.0$.

Time step (k)	L_1 error	L_∞ error	Rate of convergence	CPU (s)
0.005	1.0609×10^{-11}	1.2486×10^{-12}	-	0.682
0.004	8.4863×10^{-12}	9.9890×10^{-13}	1.000	0.746
0.002	4.2427×10^{-12}	4.9945×10^{-13}	1.000	1.014
0.001	2.1206×10^{-12}	2.4966×10^{-13}	1.000	1.485
0.0005	1.0607×10^{-12}	1.2488×10^{-13}	0.999	2.531

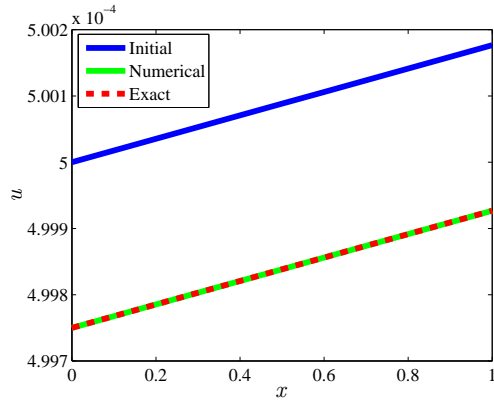
Table 4.14: Computation of L_1 and L_∞ errors, CPU time and rate of convergence using NSFD2 with $\gamma = 0.001$, $h = 0.1$, $0 \leq x \leq 10$, $T = 1.0$.

Time step (k)	L_1 error	L_∞ error	Rate of convergence	CPU (s)
0.005	7.2879×10^{-6}	1.1046×10^{-5}	-	0.611
0.004	5.8241×10^{-6}	8.8276×10^{-6}	1.005	0.668
0.002	2.8964×10^{-6}	4.3902×10^{-6}	1.008	0.678
0.001	1.4325×10^{-6}	2.1715×10^{-6}	1.016	0.724
0.0005	7.0051×10^{-7}	1.0620×10^{-6}	1.032	0.764

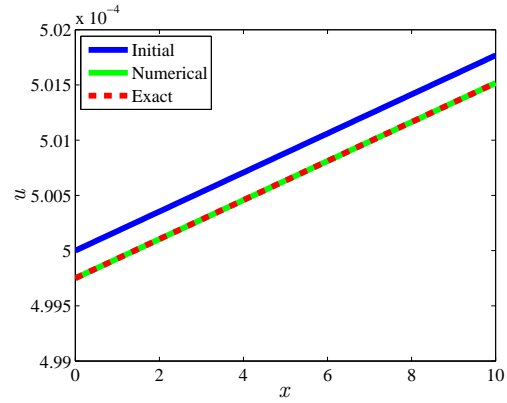
Table 4.15: Computation of L_1 and L_∞ errors, CPU time and rate of convergence using NSFD2 with $\gamma = 0.5$, $h = 0.1$, $0 \leq x \leq 1$, $T = 1.0$.

Time step (k)	L_1 error	L_∞ error	Rate of convergence	CPU (s)
0.005	4.6563×10^{-4}	7.9312×10^{-5}	-	0.696
0.004	3.7403×10^{-4}	6.3679×10^{-5}	0.9817	0.751
0.002	1.9066×10^{-4}	3.2398×10^{-5}	0.9722	1.070
0.001	9.8889×10^{-5}	1.6760×10^{-5}	0.9471	1.372
0.0005	5.2984×10^{-5}	8.9589×10^{-6}	0.9003	2.515

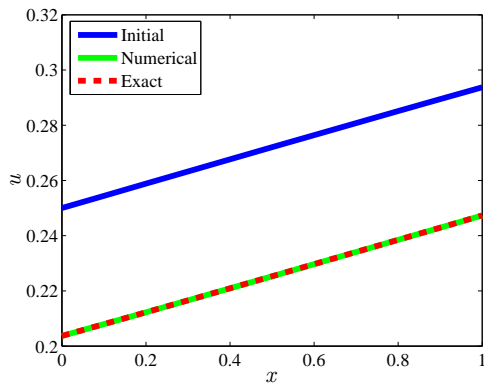
Table 4.16: Computation of L_1 and L_∞ errors, CPU time and rate of convergence using NSFD2 with $\gamma = 0.5$, $h = 0.1$, $0 \leq x \leq 10$, $T = 1.0$.



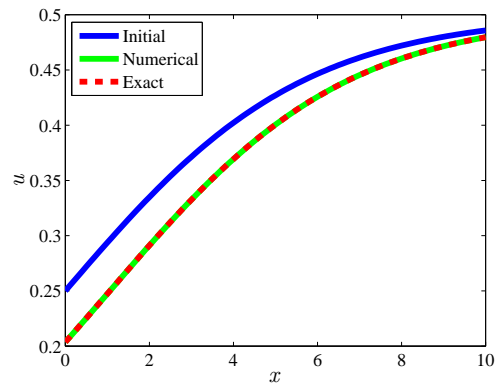
(a) $h = 0.1, \gamma = 0.001, k = 0.0005$.



(b) $h = 0.1, \gamma = 0.001, k = 0.0005$.



(c) $h = 0.1, \gamma = 0.5, k = 0.0005$.



(d) $h = 0.1, \gamma = 0.5, k = 0.0005$.

Figure 4.6: Plot of u against x using NSFD2 scheme at time $T = 1.0$, where $x \in [0, 1]$ for 4.6a, 4.6c and $x \in [0, 10]$ for 4.6b, 4.6d.

4.6.3 NSFD3 scheme

The NSFD1 scheme has convergence issues. We present a slight modification of NSFD1 and we baptise the new scheme as NSFD3. We propose the following

$$\frac{u_m^{n+1} - u_m^n}{\phi_1} - \frac{u_{m+1}^n - 2u_m^n + u_{m-1}^n}{\psi_1\psi_2} = -\frac{3}{2}(u_m^n)^2 u_m^{n+1} + \frac{1}{2}(u_m^n)^3 + (1 + \gamma)(u_m^n)^2 - \gamma u_m^{n+1}, \quad (4.74)$$

where $\psi_1 = \frac{1-e^{-2A_1h}}{2A_1}$, $\psi_2 = \frac{e^{2A_1h}-1}{2A_1}$ and $\phi_1 = \frac{1-e^{-2A_1A_2k}}{2A_1A_2}$. A single expression for the scheme is

$$u_m^{n+1} = \frac{(1 - 2R)u_m^n + R(u_{m+1}^n + u_{m-1}^n) + \phi_1 \left((1 + \gamma)(u_m^n)^2 + \frac{1}{2}(u_m^n)^3 \right)}{1 + \phi_1\gamma + \frac{3}{2}\phi_1(u_m^n)^2}, \quad (4.75)$$

where $R = \frac{\phi_1}{\psi_1\psi_2}$.

Theorem 4.5. *If $1 - 2R \geq 0$, the numerical solution of Eq. (4.1) satisfies*

$$0 \leq u_m^n \leq 1 \implies 0 \leq u_m^{n+1} \leq 1,$$

and the dynamical consistency holds for all relevant values of n and m .

Proof. For positivity, we should have $1 - 2R \geq 0$ and $1 + \phi_1\gamma + \frac{3}{2}\phi_1(u_m^n)^2 > 0$, since $u_m^n \geq 0$.

To obtain the condition for positivity of NSFD3, we solve $R = \frac{\phi_1}{\psi_1\psi_2} \leq \frac{1}{2}$ which is similar condition for positivity of NSFD1. Therefore the condition is

$$k \leq -\frac{2}{\gamma(2-\gamma)} \ln \left[1 - \left(\frac{2-\gamma}{2\gamma} \right) \frac{(e^{\frac{\sqrt{2}}{2}\gamma h} - 1)^2}{e^{\frac{\sqrt{2}}{2}\gamma h}} \right]. \quad (4.76)$$

We assume that $0 \leq u_m^n \leq \gamma$. For the boundedness, we need to prove that $0 \leq u_m^{n+1} \leq \gamma$. We consider

$$\begin{aligned} (u_m^{n+1} - \gamma) \left(1 + \phi_1\gamma + \frac{3}{2}\phi_1(u_m^n)^2 \right) &= (1 - 2R)u_m^n + R(u_{m+1}^n + u_{m-1}^n) \\ &\quad + \phi_1 \left((1 + \gamma)(u_m^n)^2 + \frac{1}{2}(u_m^n)^3 \right) \\ &\quad - \gamma - \phi_1\gamma^2 - \frac{3}{2}\phi_1(u_m^n)^2. \end{aligned} \quad (4.77)$$

Since $0 \leq u_m^n \leq \gamma$ for all values for n and m , we have

$$\begin{aligned} (u_m^{n+1} - \gamma) \left(1 + \phi_1\gamma + \frac{3}{2}\phi_1(u_m^n)^2 \right) &\leq (1 - 2R)\gamma + 2\gamma R \\ &\quad + \phi_1\gamma^2 + \phi_1 \left(\gamma(u_m^n)^2 + \frac{\gamma}{2}(u_m^n)^2 \right) \\ &\quad - \gamma - \phi_1\gamma^2 - \frac{3}{2}\phi_1(u_m^n)^2 = 0. \end{aligned} \quad (4.78)$$

Hence $u_m^{n+1} \leq \gamma$. It follows that NSFD3 satisfies boundedness properties. \square

For $\gamma = 0.001$ and $h = 0.1$, (4.76) gives $k \leq 5.0000 \times 10^{-3}$ while for $\gamma = 0.5$ and $h = 0.1$, we get $k \leq 5.0052 \times 10^{-3}$.

We tabulate L_1 , L_∞ errors as well as CPU time and rate of convergence with respect to time (using L_1 error) for the four cases in Tables 4.17 to 4.20. We also obtain plot of u against x at $T = 1.0$ in Figure 4.7.

Time step (k)	L_1 error	L_∞ error	Rate of convergence	CPU (s)
0.005	1.5460×10^{-13}	2.3424×10^{-13}	-	0.770
0.004	1.2368×10^{-13}	1.8739×10^{-13}	1.000	0.920
0.002	6.1841×10^{-14}	9.3698×10^{-14}	0.999	0.928
0.001	3.0915×10^{-14}	4.6841×10^{-14}	1.000	1.092
0.0005	1.5462×10^{-14}	2.3426×10^{-14}	0.999	1.215

Table 4.17: Computation of L_1 and L_∞ errors, CPU time and rate of convergence in time using NSFD3 with $\gamma = 0.001$, $h = 0.1$, $0 \leq x \leq 1$, $T = 1.0$.

Time step (k)	L_1 error	L_∞ error	Rate of convergence	CPU (s)
0.005	1.5930×10^{-11}	1.8750×10^{-12}	-	0.947
0.004	1.2743×10^{-11}	1.4910×10^{-12}	1.000	1.100
0.002	6.3709×10^{-12}	7.500×10^{-13}	1.000	1.296
0.001	3.1847×10^{-12}	3.7494×10^{-13}	1.000	1.983
0.0005	1.5927×10^{-12}	1.8752×10^{-13}	0.999	2.922

Table 4.18: Computation of L_1 and L_∞ errors, CPU time and rate of convergence in time using NSFD3 with $\gamma = 0.001$, $h = 0.1$, $0 \leq x \leq 10$, $T = 1.0$.

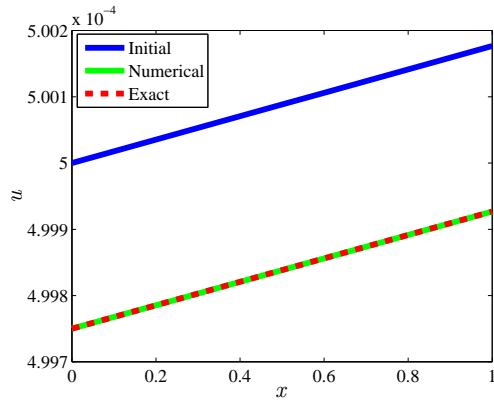
Time step (k)	L_1 error	L_∞ error	Rate of convergence	CPU (s)
0.005	1.4440×10^{-5}	2.1896×10^{-5}	-	0.707
0.004	1.1546×10^{-5}	1.7508×10^{-5}	1.002	0.892
0.002	5.7572×10^{-6}	8.7301×10^{-6}	1.004	0.934
0.001	2.8628×10^{-6}	4.3413×10^{-6}	1.007	1.043
0.0005	1.4157×10^{-6}	2.1469×10^{-6}	1.016	1.093

Table 4.19: Computation of L_1 and L_∞ errors, CPU time and rate of convergence in time using NSFD3 with $\gamma = 0.5$, $h = 0.1$, $0 \leq x \leq 1$, $T = 1.0$.

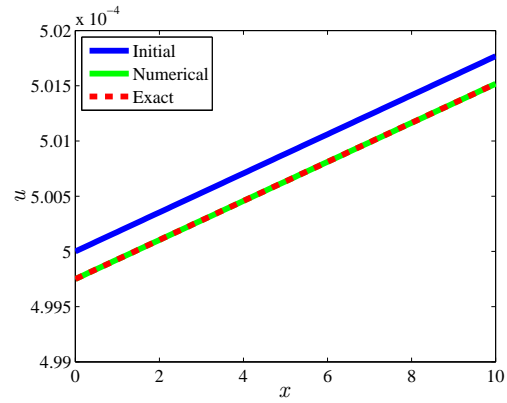
Time step (k)	L_1 error	L_∞ error	Rate of convergence	CPU (s)
0.005	1.2452×10^{-3}	1.9632×10^{-4}	-	0.890
0.004	9.9846×10^{-4}	1.5743×10^{-4}	0.989	0.749
0.002	5.0366×10^{-4}	7.9464×10^{-5}	0.987	1.335
0.001	2.5559×10^{-4}	4.0389×10^{-5}	0.978	1.933
0.0005	1.3138×10^{-4}	2.0838×10^{-5}	0.960	2.775

Table 4.20: Computation of L_1 and L_∞ errors, CPU time and rate of convergence using NSFD3 with $\gamma = 0.5$, $h = 0.1$, $0 \leq x \leq 10$, $T = 1.0$.

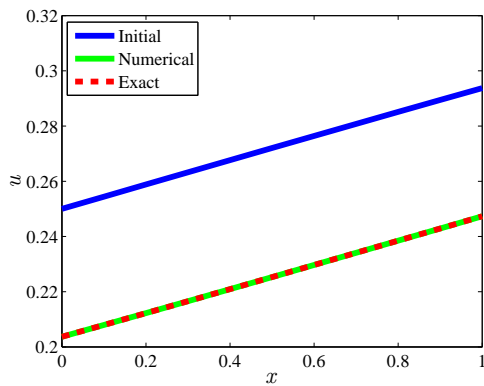
The scheme proposed is quite effective for all the four cases.



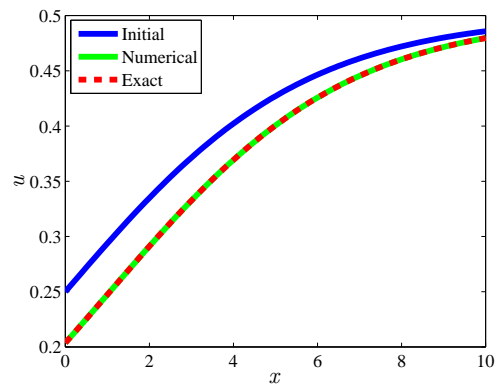
(a) $h = 0.1, \gamma = 0.001, k = 0.0005$.



(b) $h = 0.1, \gamma = 0.001, k = 0.0005$.



(c) $h = 0.1, \gamma = 0.5, k = 0.0005$.



(d) $h = 0.1, \gamma = 0.5, k = 0.0005$.

Figure 4.7: Plot of u against x using NSFD3 scheme at time $T = 1.0$, where $x \in [0, 1]$ for 4.7a, 4.7c and $x \in [0, 10]$ for 4.7b and 4.7d.

4.7 Conclusion

In this chapter, we use five numerical methods namely; two scheme (explicit and implicit) constructed by Namjoo and Zibaei (2018), NSFD1, NSFD2, NSFD3 (which is a modification of NSFD1) in order to solve the FitzHugh-Nagumo equation with specified initial and boundary conditions. Some highlights of this work as compared to the work in Namjoo and Zibaei (2018) are described below.

Firstly we consider another value of γ besides the value 0.001 and we also work with short and long domains. We observe that the results are much better when $\gamma = 0.001$ as compared to $\gamma = 0.5$.

Secondly, we test the two schemes constructed by Namjoo and Zibaei from the exact solution and demonstrate that the explicit scheme has stability issues using numerical experiments and through analysis of the stability. The implicit scheme is quite effective and works when $h = A_2 k$.

Thirdly, NSFD1 has convergence issues due to its rate of convergence result. A modification of NSFD1 is performed to generate NSFD3. NSFD2 and NSFD3 schemes are quite effective methods to solve the FitzHugh-Nagumo equation with reasonable L_1, L_∞ errors and the rate of convergence L in time from

numerical experiment is in agreement with theoretical rate of convergence in time.

The next chapter is to construct numerical methods for a FitzHugh-Nagumo equation of the form

$$u_t - u_{xx} = \beta u(1 - u)(u - \gamma)$$

and use a more challenging initial condition such as $u(x, 0) = \frac{1}{2} - \frac{1}{2} \tanh\left(\frac{\sqrt{\beta}}{2\sqrt{2}}x\right)$. The exact solution is $u(x, t) = \frac{1}{2} - \frac{1}{2} \tanh\left[\frac{\sqrt{\beta}}{2\sqrt{2}}(x - ct)\right]$, where $\beta > 0$, $\gamma \in \mathbb{R}$ and $c = -\sqrt{\frac{\beta}{2}}(2\gamma - 1)$.

Chapter 5

Construction and analysis of some nonstandard finite difference methods for the FitzHugh-Nagumo equation

A short version of this work has been published as [Appadu and Agbavon \(2019\)](#) and presented at ICNAAM 2018. A full version of this work is under review as [Agbavon and Appadu \(2019\)](#).

5.1 Introduction

In this chapter, we consider FitzHugh-Nagumo equation given by

$$u_t - u_{xx} = \beta u(1 - u)(u - \gamma), \quad (5.1)$$

where γ monitors the overall dynamics of the equation and belongs to the interval $(0, 1)$ ([Xu et al., 2014](#)) and is regarded as threshold of Allee effect ([Wang et al., 2011](#)). $u(x, t)$ is the unknown function depending on the temporal variable, t and the spatial variable, $x \in \Omega$ (bounded domain). β is a parameter called intrinsic growth rate [Preston and Wang \(2007\)](#). It is worth to recall that the case where $\beta = 1$ is called classical or standard FitzHugh-Nagumo equation which was our study in previous chapter 4.

Recently, for β depending on time, many authors like [Triki and Wazwaz \(2013\)](#) considered a generalized Fitzhugh-Nagumo equation given by

$$u_t + \alpha(t)u_x - \Gamma(t)u_{xx} + \beta(t)u(1 - u)(\gamma - u) = 0 \quad (5.2)$$

where $\alpha(t)$, $\Gamma(t)$, $\beta(t)$ are arbitrary functions of t , exhibits time-changing coefficients and linear dispersion term. They showed the existence and uniqueness of solitons solutions and used ansatz and tanh method

with specific solitary wave. Jacobi-Gauss-Lobatto collocation method was used by [Bhrawy \(2013\)](#) to solve the generalized Fitzhugh-Nagumo equation. Polynomial differential quadrature method (PDQM) for numerical solutions of the generalized Fitzhugh-Nagumo equation with time-dependent coefficients was also utilized by [Jiwari et al. \(2014\)](#).

5.1.1 Biological description of the parameter γ and β

Allee effect was first introduced by the pioneer W.C. [Allee \(1931\)](#) by demonstrating that goldfish grew faster in water which had previously contained other goldfish than in water which had not. It was named γ , the threshold of Allee effect. Moreover, he carried out an experiment with range of species and concluded that larger groups may spur reproduction, extend survival in adverse conditions and improve a protection ([Allee, 1931, 1938](#)). Despite the fact that the Allee effect is well known, the notion has a range of significations not all of which are allowed by contemporary use. Furthermore, Allee did not give a definition but he plainly considered "certain aspects of survival ([Allee et al., 1949](#))" rather than total fitness and the following definitions follow

- (1) Allee effect is a positive relationship between any component of individual fitness and either numbers or density of conspecifics ([Stephens et al., 1999](#)).
- (2) The Allee effect induces minimum viable population sizes or a threshold value in the critical spatial lengths of the initial distributions below which the populations dies out . It is also the critical value of the spatial length of an initial nucleus (problem of critical aggregation as in [Petrovskii and Shigesada \(2001\)](#)).

Overall, the Allee effect induces a rich variety of spatio-temporal dynamics in the considered epidemiological model. The remark made from the original idea of Allee and its observations is the above definition demands that some measurable component of the fitness of an organism for instance probability of dying or reproducing is significant in a wide population (components of mean fitness meant to provide an overall increase or decrease with increasing abundance will rely on the relative strength of negative density dependence). Moreover, it is worthy to differentiate between component Allee effects which is manifested by a component of fitness and demographic Allee effects which manifest at the level of total fitness ([Stephens et al., 1999](#)). It is shown in [Boukal et al. \(2007\)](#), [Shi and Shivaji \(2006\)](#) that a strong Allee effect assigns to the population that has a negative growth when the size of the population is below certain threshold value while a weak Allee effect means that growth is positive and increasing.

Furthermore, some researchers used logistic growth (in the form of travelling infection waves) and growth with a strong Allee in the modelling of biological or ecological phenomena. Those waves, are waves of extinction, which occur when the disease is introduced in the wake of the invading host population ([Hilker et al., 2007](#)). Moreover, the Allee effect leads to bistability in the local transmission dynamics ([Hilker et al., 2007](#)). In combination with the minimum viable population size, this has serious implications

for eventual control methods, since they do not necessarily depend on reducing the basic reproductive ratio anymore. If the infectiousness of the disease is considerable in comparison with the demographic reproductiveness, the Allee effect becomes less important due to the fact that the population dynamic is dominantly driven by the disease to extinction. Recent results show that the Allee effect produce possible limit cycle oscillations with mass action transmission (Hilker et al., 2007) in the vital dynamics of the model. Furthermore, this vital dynamics are generally governed by a strong Allee effect. This can be caused by difficulties in finding mating partners at small densities, genetic inbreeding, demographic stochasticity or a reduction in cooperative interactions (Courchamp et al., 1999, Dennis, 1989, Stephens et al., 1999). It should be noted, moreover, that the study of Allee dynamics is justified in its own rights, because this is largely lacking in the epidemiological literature (Hilker et al., 2007).

The intrinsic growth rate denoted by β , in the presence of migration, is an accurate measure of how quickly a population would ultimately grow if for instance current age-specific rates of fertility, mortality, and migration were sustained indefinitely in contrast to the actual growth rate of a population, which present equal weight to all migrants despite everything for instance, of their age. For example, migrants are level-headed in by their expected future number of births at the age when they come or go (will not be feigned by migration that happens beyond the end of childbearing (Preston and Wang, 2007)).

Our focus will be on the case $\alpha = 0$, $\Gamma(t) = 1$, β independent of t . Our methodology used on nonstandard finite difference scheme (Mickens, 1989, 2005).

5.2 Organisation of the chapter

The remainder of this chapter is as follows. In section 5.3, we describe the numerical experiment chosen. In section 5.4, we give some information on basic dynamical behaviour of FitzHugh-Nagumo equation. In sections 5.5 to 5.9 we present four versions of nonstandard finite difference schemes and study some of their properties and present some numericals results. In section 5.10 we present error estimate for NSFD3. The study of the relationship between physical behaviour and numerical solution and discussion over the obtained numerical results are done in section 5.11. In section 5.12, some general view over an implicit nonstandard finite difference is given. Section 5.13 highlights the salient features of the paper.

5.3 Numerical experiment

We solve Eq. (5.1) where $u(x, t)$ is the unknown function which depends on the spatial variable, $x \in (-10, 10)$ and temporal variable, t .

The initial condition is $u(x, 0) = \frac{1}{2} - \frac{1}{2} \tanh\left(\frac{\sqrt{\beta}}{2\sqrt{2}}x\right)$ (Kyrychko et al., 2005) and the boundary conditions are

$$u(-10, t) = \frac{1}{2} - \frac{1}{2} \tanh\left[\frac{\sqrt{\beta}}{2\sqrt{2}}(-10 - ct)\right], \quad u(10, t) = \frac{1}{2} - \frac{1}{2} \tanh\left[\frac{\sqrt{\beta}}{2\sqrt{2}}(10 - ct)\right].$$

We note that the initial condition is positive i.e $u(x, 0) \geq 0$.

The exact solution is $u(x, t) = \frac{1}{2} - \frac{1}{2} \tanh \left[\frac{\sqrt{\beta}}{2\sqrt{2}}(x - ct) \right]$, where $\beta > 0$, $\gamma \in (0, 1)$ and $c = -\sqrt{\frac{\beta}{2}}(2\gamma - 1)$. In this work, we consider three cases:

Case 1 : $\beta = 1$, $\gamma = 0.2$.

Case 2 : $0 < \beta < 1$ ($\beta = 0.5$), $\gamma = 0.2$.

Case 3 : $\beta > 1$ ($\beta = 2$), $\gamma = 0.2$.

We test the performance of the schemes over different values of β over the domain, $x \in [-10, 10]$ at time, $T = 0.5$. The spatial step size h is chosen as 0.1. We use some different values for the temporal step size k which must satisfy the condition for positivity.

5.4 Basic dynamical behaviour and a priori bound of Eq. (5.1)

In this section, we present a theorem on the existence and uniqueness of the solution to the dynamical behaviour Eq. (5.1) and a priori bound of the solution. We recall some results from Wang et al. (2011).

Theorem 5.1 (Wang et al. (2011)). *Suppose that $0 < \gamma < 1$ and $\Omega \subset \mathbb{R}^n$ is bounded domain with smooth boundary:*

- (a) *If the initial condition $u_0(x) = u(x, 0)$ is positive ($u_0(x) \geq 0$) then Eq. (5.1) has unique solution $u(x, t)$ such that $u(x, t)$ positive ($u(x, t) \geq 0$) for $t \in (0, \infty)$ and $\bar{\Omega}$;*
- (b) *For any solution $u(x, t)$ of Eq. (5.1), $\limsup_{t \rightarrow \infty} u(x, t) \leq 1$.*

The full proof is in Wang et al. (2011).

5.5 Nonstandard Finite Difference Scheme (NSFD)

We present derivation of five versions of NSFD schemes to discretise

$$u_t - u_{xx} = \beta u(1 - u)(u - \gamma).$$

In all four methods, we use the same discretisation for u_t and u_{xx} . We approximate u_t by $\frac{u_m^{n+1} - u_m^n}{\phi_2(\Delta t)}$ where $\phi_2(\Delta t) = \phi_2(k) = \frac{e^{\beta k} - 1}{\beta}$ and u_{xx} by $\frac{u_{m+1}^n - 2u_m^n + u_{m-1}^n}{\psi_1(\Delta x)\psi_2(\Delta x)}$ where $\psi_1(\Delta x) = \psi_1(h) = \frac{1 - e^{-\beta h}}{\beta}$ and $\psi_2(\Delta x) = \psi_2(h) = \frac{e^{\beta h} - 1}{\beta}$. We expect the theoretical rate of convergence in time to be equal to one.

5.6 NSFD1 Scheme

We note that the right hand side of Eq. (5.1) is $\beta(-u^3 + (1 + \gamma)u^2 - \gamma u)$. We use the following discrete approximations of the right hand side for (5.1) as used by Namjoo and Zibaei (2018):

$$-\beta \gamma u(x_m, t_n) \approx -\beta \gamma u_m^{n+1}, \quad -\beta (u(x_m, t_n))^3 \approx \beta \left(-\frac{3}{2} (u_{m-1}^n)^2 u_m^{n+1} + \frac{1}{2} (u_{m-1}^n)^3 \right), \quad (5.3)$$

$$\beta (1 + \gamma) (u(x_m, t_n))^2 \approx \beta (1 + \gamma) (u_{m-1}^n)^2. \quad (5.4)$$

The following scheme is proposed:

$$\frac{u_m^{n+1} - u_m^n}{\phi_2(k)} - \frac{u_{m+1}^n - 2u_m^n + u_{m-1}^n}{\psi_1(h) \psi_2(h)} = \beta \left(-\frac{3}{2} (u_{m-1}^n)^2 u_m^{n+1} + \frac{1}{2} (u_{m-1}^n)^3 \right) + \beta (1 + \gamma) (u_{m-1}^n)^2 - \beta \gamma u_m^{n+1}. \quad (5.5)$$

A single expression for the scheme is

$$u_m^{n+1} = \frac{(1 - 2R)u_m^n + R(u_{m+1}^n + u_{m-1}^n) + \beta \phi_2(k) \left((1 + \gamma) (u_{m-1}^n)^2 + \frac{1}{2} (u_{m-1}^n)^3 \right)}{1 + \beta \gamma \phi_2(k) + \frac{3}{2} \beta \phi_2(k) (u_{m-1}^n)^2}, \quad (5.6)$$

where $R = \frac{\phi_2(k)}{\psi_1(h) \psi_2(h)}$. As discussed in the introduction, the theory of nonstandard finite difference required dynamical consistency (positivity, boundedness, preservation of fixed points) which help to avoid numerical instabilities.

The fixed points of Eq. (5.1) are $u_1^* = 0$, $u_2^* = 1$ (which are stable) and $u_3^* = \gamma$ which is unstable. Furthermore, Roeger and Mickens (2007) showed preservation of local stabilities of all fixed points.

Theorem 5.2 (Dynamical consistency). If $1 - 2R \geq 0$, the numerical solution of Eq. (5.6) satisfies

$$0 \leq u_m^n \leq 1 \implies 0 \leq u_m^{n+1} \leq 1,$$

and the dynamical consistency (positivity and boundedness) holds for all relevant values of n and m .

Proof. (1) If $1 - 2R \geq 0$, then

$$R = \left(\frac{e^{\beta k} - 1}{\beta} \right) \left(\frac{\beta}{1 - e^{-\beta h}} \right) \left(\frac{\beta}{e^{\beta h} - 1} \right) \leq \frac{1}{2}, \quad (5.7)$$

by replacing $\phi_2(h)$, $\psi_1(h)$, $\psi_2(h)$ by their respective expressions. We have therefore, since $u_m^n \geq 0$ and $1 + \beta \gamma \phi_2(k) + \frac{3}{2} \beta \phi_2(k) (u_{m-1}^n)^2 > 0$, NSFD1 is positive definite under the condition

$$k \leq \frac{1}{\beta} \ln \left[1 + \frac{1}{2\beta} \frac{(e^{\beta h} - 1)^2}{e^{\beta h}} \right]. \quad (5.8)$$

(2) We assume that $0 \leq u_m^n \leq 1$. If the scheme is bounded, we need to prove that $0 \leq u_m^{n+1} \leq 1$.

Consider

$$\begin{aligned} (u_m^{n+1} - 1) \left(1 + \beta \gamma \phi_2(k) + \frac{3}{2} \beta \phi_2(k) (u_{m-1}^n)^2 \right) &= (1 - 2R)u_m^n + R(u_{m+1}^n + u_{m-1}^n) \\ &\quad + \beta \phi_2(k) \left((1 + \gamma) (u_{m-1}^n)^2 + \frac{1}{2} (u_{m-1}^n)^3 \right) \\ &\quad - 1 - \beta \phi_2(k) \gamma - \frac{3}{2} \beta \phi_2(k) (u_{m-1}^n)^2. \end{aligned} \quad (5.9)$$

It follows $(u_{m-1}^n)^3 = u_{m-1}^n (u_{m-1}^n)^2 \leq (u_{m-1}^n)^2$ since $0 \leq u_m^n \leq 1$ for all values of n and m .
Therefore,

$$\begin{aligned}
 (u_m^{n+1} - 1) \left(1 + \beta\gamma\phi_2(k) + \frac{3}{2}\beta\phi_2(k) (u_{m-1}^n)^2 \right) &\leq 1 - 2R + 2R + \beta\gamma\phi_2(k) (u_{m-1}^n)^2 \\
 &\quad + \beta\phi_2(k) \left((u_{m-1}^n)^2 + \frac{1}{2} (u_{m-1}^n)^2 \right) \\
 &\quad - 1 - \beta\gamma\phi_2(k) - \frac{3}{2}\beta\phi_2(k) (u_{m-1}^n)^2 \\
 &= 0.
 \end{aligned} \tag{5.10}$$

Hence $u_m^{n+1} - 1 \leq 0$. Thus, we conclude that NSFD1 scheme is bounded.

□

For positivity and using $h = 0.1$ in (5.8), we obtain

- (a) $k \leq 4.9948 \times 10^{-3}$ for $\beta = 0.5$.
- (b) $k \leq 4.9917 \times 10^{-3}$ for $\beta = 1.0$.
- (c) $k \leq 4.9917 \times 10^{-3}$ for $\beta = 2.0$.

We tabulate L_1 , L_∞ , rate of convergence and CPU time at some different values of k using $\gamma = 0.2$, $h = 0.1$ at time, $T = 0.5$ for three cases namely; $\beta = 0.5, 1.0, 2.0$ using NSFD1 scheme in Tables 5.1, 5.2, 5.3.

Time step (k)	L_1 error	L_∞ error	Rate of convergence	CPU (s)
0.005	1.7339×10^{-2}	2.6693×10^{-3}	-	1.007
0.0025	1.7383×10^{-2}	2.6742×10^{-3}	-3.656×10^{-3}	1.229
0.00125	1.7405×10^{-2}	2.6767×10^{-3}	-1.824×10^{-3}	1.752

Table 5.1: Computation of L_1 , L_∞ errors, rate of convergence and CPU time using NSFD1 for $-10 \leq x \leq 10$, $\gamma = 0.2$, $h = 0.1$, $\beta = 0.5$, $T = 0.5$.

Time step (k)	L_1 error	L_∞ error	Rate of convergence	CPU (s)
0.005	3.4919×10^{-2}	7.4411×10^{-3}	-	1.032
0.0025	3.5051×10^{-2}	7.4613×10^{-3}	-5.443×10^{-3}	1.280
0.00125	3.5117×10^{-2}	7.4715×10^{-3}	-2.713×10^{-3}	1.815

Table 5.2: Computation of L_1 , L_∞ errors, rate of convergence and CPU time using NSFD1 for $-10 \leq x \leq 10$, $\gamma = 0.2$, $h = 0.1$, $\beta = 1$, $T = 0.5$.

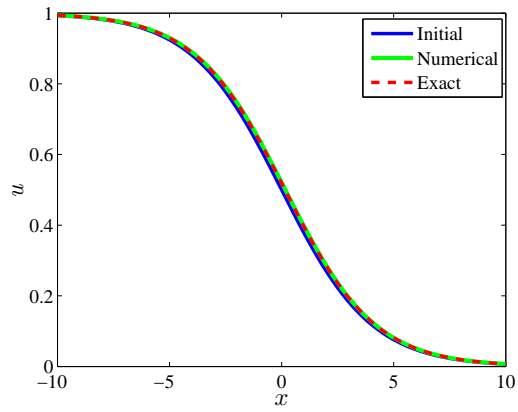
Time step (k)	L_1 error	L_∞ error	Rate of convergence	CPU (s)
0.005	6.9598×10^{-2}	2.0534×10^{-2}	-	0.608
0.0025	6.9987×10^{-2}	2.0625×10^{-2}	-8.041×10^{-3}	0.804
0.00125	7.0182×10^{-2}	2.0671×10^{-2}	-1.205×10^{-2}	1.277

Table 5.3: Computation of L_1 , L_∞ errors, rate of convergence and CPU time using NSFD1 for $-10 \leq x \leq 10$, $\gamma = 0.2$, $h = 0.1$, $\beta = 2$, $T = 0.5$.

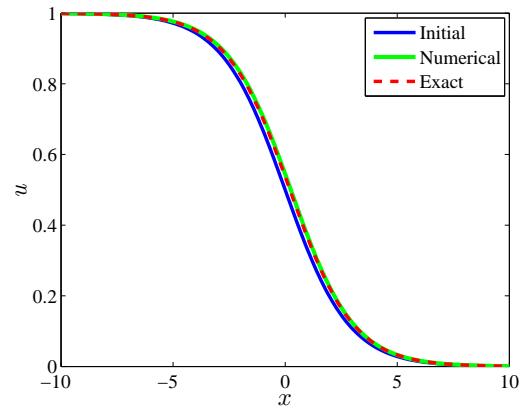
The scheme does not give satisfactory results especially in regards to the rate of convergence. The theoretical rate of convergence with respect time is one.

Plots of u against x for the three cases using NSFD1 scheme are shown in Fig 5.1. Corresponding plot of errors against x are shown in Fig 5.2.

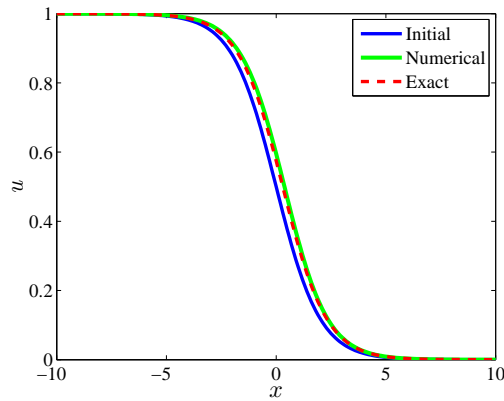
We observe that as we increase the values of β , the profile becomes more stiff and the problem becomes more challenging for the numerical schemes.



(a) $h = 0.1, \beta = 0.5, k = 0.005$.

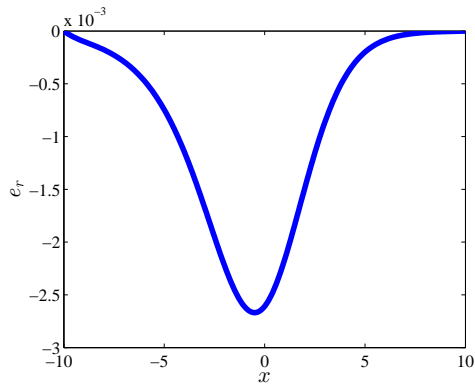


(b) $h = 0.1, \beta = 1, k = 0.005$.

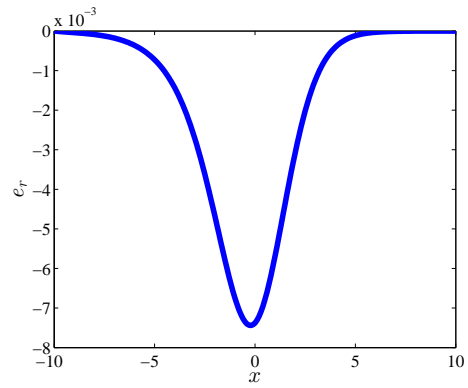


(c) $h = 0.1, \beta = 2, k = 0.005$.

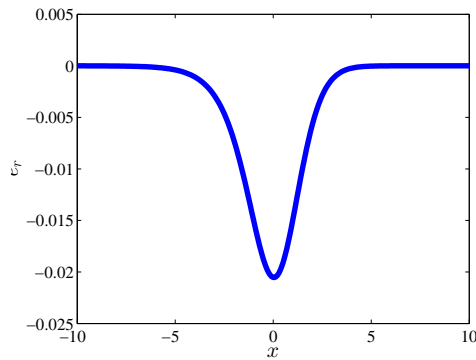
Figure 5.1: Plot of u vs x using NSFD1 scheme at time $T = 0.5$, where $x \in [-10, 10]$ for different values of β namely; 0.5, 1.0, 2.0.



(a) $h = 0.1, \beta = 0.5, k = 0.005$.



(b) $h = 0.1, \beta = 1, k = 0.005$.



(c) $h = 0.1, \beta = 2, k = 0.005$.

Figure 5.2: Plot of error vs x using NSFD1 scheme at time $T = 0.5$, where $x \in [-10, 10]$ for different values of β respectively 0.5, 1.0, 2.0.

We observe that as we increase the values of β , the profile becomes more stiff and the problem becomes more challenging problem for the numerical schemes.

5.7 NSFD2 scheme

In this section we make use of the following approximations from [Namjoo and Zibaei \(2018\)](#) for the right hand of Eq. (5.1):

$$-\beta \gamma u(x_m, t_n) \approx -\beta \gamma u_m^{n+1}, \quad \beta(1 + \gamma)(u(x_m, t_n))^2 \approx \beta(1 + \gamma)u_m^{n+1}u_m^n, \quad (5.11)$$

$$-\beta(u(x_m, t_n))^3 \approx -\beta u_m^{n+1}(u_m^n)^2. \quad (5.12)$$

This gives the following scheme:

$$\frac{u_m^{n+1} - u_m^n}{\phi_2(k)} - \frac{u_m^{n+1} - 2u_m^n + u_m^{n-1}}{\psi_1(h)\psi_2(h)} = \beta \left(-u_m^{n+1}(u_m^n)^2 + (1 + \gamma)u_m^{n+1}u_m^n - \gamma u_m^{n+1} \right), \quad (5.13)$$

which can be rewritten as

$$u_m^{n+1} = \frac{(1 - 2R)u_m^n + R(u_m^{n+1} + u_m^{n-1})}{1 + \beta\phi_2(k)\gamma - \beta(1 + \gamma)\phi_2(k)u_m^n + \beta\phi_2(k)(u_m^n)^2}, \quad \text{where } R = \frac{\phi_2(k)}{\psi_1(h)\psi_2(h)}. \quad (5.14)$$

Theorem 5.3 (Dynamical consistency). If $1 - 2R \geq 0$ and $1 - \beta\phi_2(k) \geq 0$, the numerical solution of Eq. (5.14) satisfies

$$0 \leq u_m^n \leq 1 \implies 0 \leq u_m^{n+1} \leq 1,$$

and the dynamical consistency (positivity and boundedness) holds for all relevant values of n and m .

Proof. (1) If $1 - 2R \geq 0$ and $1 - \beta\phi_2(k) \geq 0$ then NSFD2 is positive definite. Indeed we require $1 + \beta\phi_2(k)\gamma - \beta(1 + \gamma)\phi_2(k)u_m^n + \beta\phi_2(k)(u_m^n)^2 > 0$. and since $0 \leq u_m^n \leq 1$,

$$\begin{aligned} 1 - [\beta(1 + \gamma)\phi_2(k)u_m^n - \beta\phi_2(k)\gamma] + \beta\phi_2(k)(u_m^n)^2 &\geq 1 - \beta\phi_2(k) + \beta\phi_2(k)(u_m^n)^2 \\ &\geq 1 - \beta\phi_2(k). \end{aligned} \quad (5.15)$$

NSFD2 is positive definite under the conditions

$$k \leq \begin{cases} \frac{1}{\beta} \ln(2), \\ \frac{1}{\beta} \ln \left(1 + \frac{1}{2\beta} \frac{(e^{\beta h} - 1)^2}{e^{\beta h}} \right). \end{cases} \quad (5.16)$$

(2) We note that $0 \leq u_m^n \leq 1$. We need to check if NSFD2 is bounded. Consider

$$\begin{aligned} (u_m^{n+1} - 1) \left(1 + \beta\phi_2(k)\gamma - \beta(1 + \gamma)\phi_2(k)u_m^n + \beta\phi_2(k)(u_m^n)^2 \right) &= (1 - 2R)u_m^n \\ + R(u_m^{n+1} + u_m^{n-1}) - 1 - \beta\gamma\phi_2(k) + \beta(1 + \gamma)\phi_2(k)u_m^n - \beta\phi_2(k)(u_m^n)^2. \end{aligned} \quad (5.17)$$

Since $0 \leq u_m^n \leq 1$ for all values for n and m ,

$$\begin{aligned} (u_m^{n+1} - 1) \left(1 + \beta\phi_2(k)\gamma - \beta(1 + \gamma)\phi_2(k)u_m^n + \beta\phi_2(k)(u_m^n)^2 \right) &\leq 1 - 2R + 2R \\ - 1 - \beta\gamma\phi_2(k) + \beta(1 + \gamma)\phi_2(k)u_m^n - \beta\phi_2(k)(u_m^n)^2 &= \\ - \beta\phi_2(k) \left[(u_m^n)^2 - \gamma u_m^n - u_m^n + \gamma \right] &= -\beta\phi_2(k)(u_m^n - 1)(u_m^n - \gamma) \leq 0. \end{aligned} \quad (5.18)$$

Hence $0 \leq u_m^{n+1} \leq 1$ and therefore NSFD2 satisfies the boundedness properties. □

For positivity and using $h = 0.1$, we have from Eq. (5.16)

(a) $k \leq 1.3863$ and $k \leq 4.9948 \times 10^{-3}$ for $\beta = 0.5$.

(b) $k \leq 6.9315 \times 10^{-1}$ and $k \leq 4.9917 \times 10^{-3}$ for $\beta = 1.0$.

(c) $k \leq 3.4657 \times 10^{-1}$ and $k \leq 4.9917 \times 10^{-3}$ for $\beta = 2.0$.

We tabulate L_1 , L_∞ errors, rate of convergence in time and CPU time at some different values of k using $\gamma = 0.2$, $h = 0.1$ at time, $T = 0.5$ for three cases namely; $\beta = 0.5, 1.0, 2.0$, using NSFD2 scheme in Tables 5.4, 5.5 and 5.6.

Time step (k)	L_1 error	L_∞ error	Rate of convergence	CPU (s)
0.005	2.0909×10^{-4}	3.3657×10^{-5}	-	0.502
0.0025	1.0409×10^{-4}	1.8821×10^{-5}	1.006	0.750
0.00125	5.8981×10^{-5}	1.1664×10^{-5}	8.195×10^{-1}	1.107

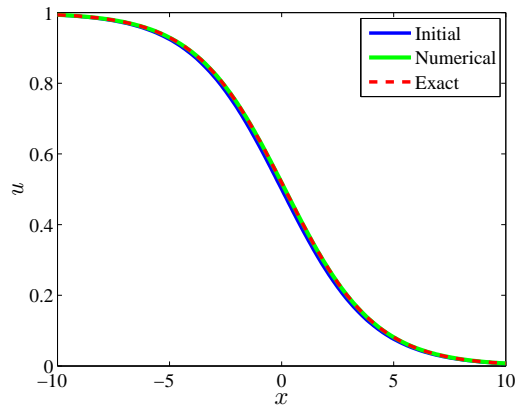
Table 5.4: Computation of L_1 , L_∞ errors, rate of convergence and CPU time using NSFD2 for $-10 \leq x \leq 10$, $\gamma = 0.2$, $h = 0.1$, $\beta = 0.5$, $T = 0.5$.

Time step (k)	L_1 error	L_∞ error	Rate of convergence	CPU (s)
0.005	5.9109×10^{-4}	1.3556×10^{-4}	-	0.939
0.0025	3.1703×10^{-4}	7.8179×10^{-5}	8.987×10^{-1}	1.119
0.00125	2.1886×10^{-4}	5.0919×10^{-5}	5.346×10^{-1}	1.535

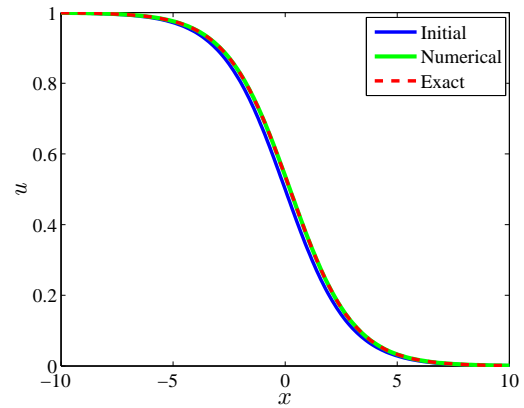
Table 5.5: Computation of L_1 , L_∞ errors, rate of convergence and CPU time using NSFD2 for $-10 \leq x \leq 10$, $\gamma = 0.2$, $h = 0.1$, $\beta = 1$, $T = 0.5$.

Time step (k)	L_1 error	L_∞ error	Rate of convergence	CPU (s)
0.005	1.7319×10^{-3}	5.4629×10^{-4}	-	0.607
0.0025	1.1015×10^{-3}	3.3108×10^{-4}	6.528×10^{-1}	1.293
0.00125	8.8733×10^{-4}	2.3146×10^{-4}	3.119×10^{-1}	1.245

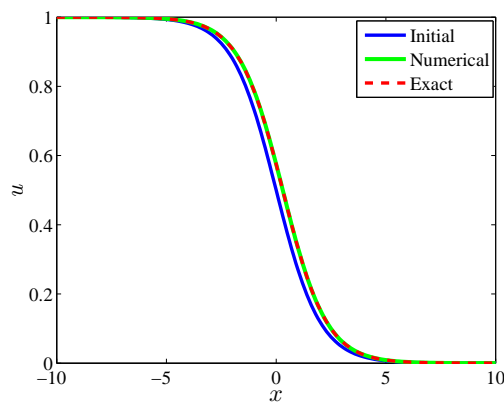
Table 5.6: Computation of L_1 , L_∞ errors, rate of convergence and CPU time using NSFD2 for $-10 \leq x \leq 10$, $\gamma = 0.2$, $h = 0.1$, $\beta = 2.0$, $T = 0.5$.



(a) $h = 0.1, \beta = 0.5, k = 0.005$.



(b) $h = 0.1, \beta = 1, k = 0.005$.

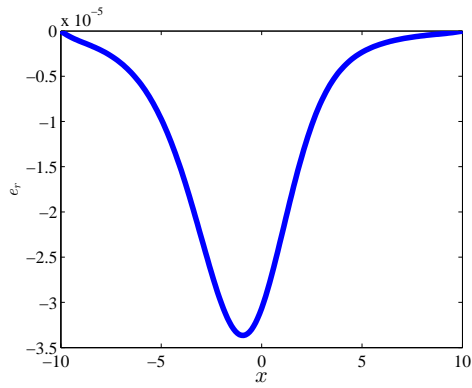


(c) $h = 0.1, \beta = 10, k = 0.005$.

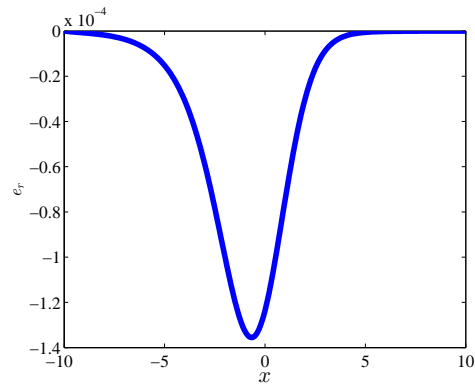
Figure 5.3: Plot of u against x using NSFD2 scheme at time $T = 0.5$, where $x \in [-10, 10]$ for different values of β namely; 0.5, 1.0, 2.0.

The scheme is quite effective especially when $\beta = 0.5, 1.0$. We observe that L_1 error, L_∞ errors are quite small and rate of convergence with respect to time is approximately 1 for the cases $\beta = 0.5, 1.0$ and therefore we deduce that NSFD2 is quite effective for $\beta = 0.5$, and 1.0 with some time steps, k (0.005, 0.0025).

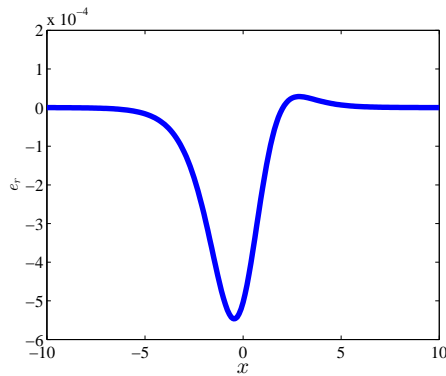
Plots of u against x for the three cases using NSFD2 scheme are shown in Fig 5.3 and 5.4.



(a) $h = 0.1, \beta = 0.5, k = 0.005$.



(b) $h = 0.1, \beta = 1, k = 0.005$.



(c) $h = 0.1, \beta = 2, k = 0.005$.

Figure 5.4: Plot of error against x using NSFD2 scheme at time $T = 0.5$, where $x \in [-10, 10]$ for different values of β respectively 0.5, 1.0, 2.0.

5.8 NSFD3 scheme

We consider the ordinary differential equation

$$\epsilon \frac{du}{dt} = f(u), \quad (5.19)$$

where $f(u) = u(1-u)(u-\gamma)$, and $\epsilon > 0$ is a real parameter, $\gamma \in (0, 1)$. Roeger and Mickens (2007) showed that the following NSFD scheme

$$\epsilon \frac{u^{n+1} - u^n}{\phi_2(\Delta t)} = -(2u^{n+1} - u^n)(u^n)^2 + (1 + \gamma)(u^n)^2 - \gamma u^{n+1}. \quad (5.20)$$

where $\phi_2(\Delta t) = \frac{e^{\frac{\Delta t}{\epsilon}} - 1}{\frac{\Delta t}{\epsilon}}$, preserves positivity and local stabilities of all fixed points. We construct a Nonstandard finite difference scheme using idea from Roeger and Mickens (2007). We propose the following scheme for Eq. (5.1):

$$\frac{u_m^{n+1} - u_m^n}{\phi_2(k)} - \frac{u_{m+1}^n - 2u_m^n + u_{m-1}^n}{\psi_1(h)\psi_2(h)} = \beta \left(-(2u_m^{n+1} - u_m^n)(u_m^n)^2 + (1 + \gamma)(u_m^n)^2 - \gamma u_m^{n+1} \right). \quad (5.21)$$

A single expression for NSFD3 scheme is

$$u_m^{n+1} = \frac{(1 - 2R)u_m^n + R(u_{m+1}^n + u_{m-1}^n) + \beta \phi_2(k) \left((u_m^n)^3 + (1 + \gamma)(u_m^n)^2 \right)}{1 + \beta \phi_2(k) \gamma + 2\beta \phi_2(k) (u_m^n)^2}. \quad (5.22)$$

Theorem 5.4 (Dynamical consistency). If $1 - 2R \geq 0$, the numerical solution of Eq. (5.22) satisfies

$$0 \leq u_m^n \leq 1 \implies 0 \leq u_m^{n+1} \leq 1,$$

and the dynamical consistency (positivity and boundedness) holds for all relevant values of n and m .

Proof. (1) NSFD3 is positive definite if $1 - 2R \geq 0$. The following condition must be satisfied namely,

$$k \leq \frac{1}{\beta} \ln \left(1 + \frac{1}{2\beta} \frac{(e^{\beta h} - 1)^2}{e^{\beta h}} \right). \quad (5.23)$$

(2) We next check if the NSFD3 is bounded:

$$\begin{aligned} (u_m^{n+1} - 1) \left(1 + \beta \phi_2(k) \gamma + 2\beta \phi_2(k) (u_m^n)^2 \right) &= (1 - 2R)u_m^n \\ &+ R(u_{m+1}^n + u_{m-1}^n) + \beta \phi_2(k) \left((u_m^n)^3 + (1 + \gamma)(u_m^n)^2 \right) \\ &- 1 - \beta \gamma \phi_2(k) - 2\beta \phi_2(k) (u_m^n)^2. \end{aligned} \quad (5.24)$$

We note that $0 \leq u_m^n \leq 1$ for all values of n and m . Therefore

$$\begin{aligned} (u_m^{n+1} - 1) \left(1 + \beta \gamma \phi_2(k) + 2\beta \phi_2(k) (u_{m-1}^n)^2 \right) &\leq 1 - 2R + 2R + \beta \phi_2(k) \left(\gamma (u_m^n)^2 + (u_m^n)^2 \right) \\ &+ \beta \phi_2(k) - 1 - \beta \gamma \phi_2(k) - 2\beta \phi_2(k) (u_m^n)^2 = 0. \end{aligned} \quad (5.25)$$

Hence $0 \leq u_m^{n+1} \leq 1$ and therefore NSFD3 satisfies the boundedness properties. \square

We tabulate L_1 and L_∞ errors, rate of convergence in time and CPU time at some different values of k using $\gamma = 0.2$, $h = 0.1$ at time, $T = 0.5$ for three cases namely; $\beta = 0.5, 1.0, 2.0$ using NSFD3 scheme in Tables 5.7, 5.8 and 5.9.

Time step (k)	L_1 error	L_∞ error	Rate of convergence	CPU (s)
0.005	1.3466×10^{-4}	2.0390×10^{-5}	-	0.532
0.0025	6.5704×10^{-5}	8.1762×10^{-6}	1.035	0.862
0.00125	3.2908×10^{-5}	4.6063×10^{-6}	9.975×10^{-1}	1.231

Table 5.7: Computation of L_1 and L_∞ errors, rate of convergence and CPU time using NSFD3 for $-10 \leq x \leq 10$, $\gamma = 0.2$, $h = 0.1$, $\beta = 0.5$, $T = 0.5$.

Time step (k)	L_1 error	L_∞ error	Rate of convergence	CPU (s)
0.005	3.6478×10^{-4}	6.7996×10^{-5}	-	1.063
0.0025	1.8672×10^{-4}	2.4832×10^{-5}	9.661×10^{-1}	1.207
0.00125	1.0268×10^{-4}	2.5881×10^{-5}	8.627×10^{-1}	1.709

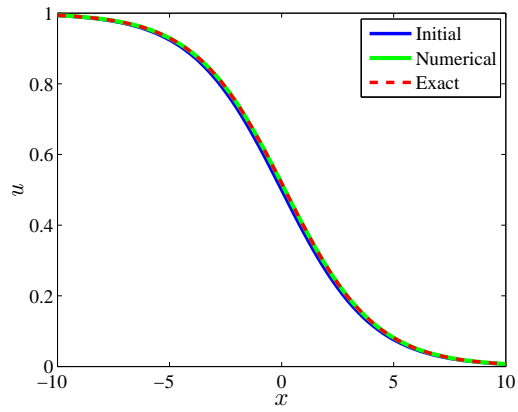
Table 5.8: Computation of L_1 and L_∞ errors, rate of convergence and CPU time using NSFD3 for $-10 \leq x \leq 10$, $\gamma = 0.2$, $h = 0.1$, $\beta = 1$, $T = 0.5$.

Time step (k)	L_1 error	L_∞ error	Rate of convergence	CPU (s)
0.005	1.0211×10^{-3}	1.8991×10^{-4}	-	1.013
0.0025	5.5377×10^{-4}	1.5864×10^{-4}	8.827×10^{-1}	1.443
0.00125	5.4617×10^{-4}	1.6408×10^{-4}	1.993×10^{-2}	2.673

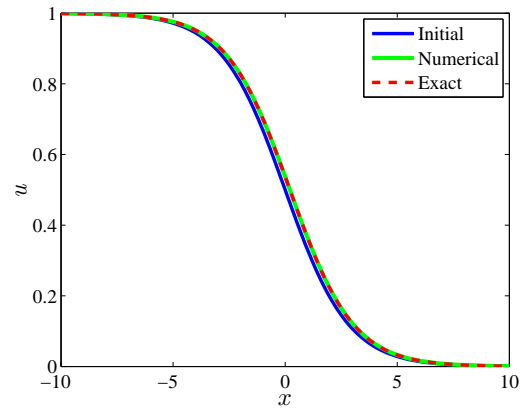
Table 5.9: Computation of L_1 and L_∞ errors, rate of convergence and CPU time using NSFD3 for $-10 \leq x \leq 10$, $\gamma = 0.2$, $h = 0.1$, $\beta = 2$, $T = 0.5$.

The scheme is very effective for all the values $\beta = 0.5, 1.0$ ($\beta \in (0, 1]$). The L_1 and L_∞ errors are quite small and the rate of convergence in time is approximatively one. But when $\beta = 2$, though the L_1 and L_∞ errors are small, the rate of convergence is close to one with some time steps carefully chosen (0.005, 0.0025).

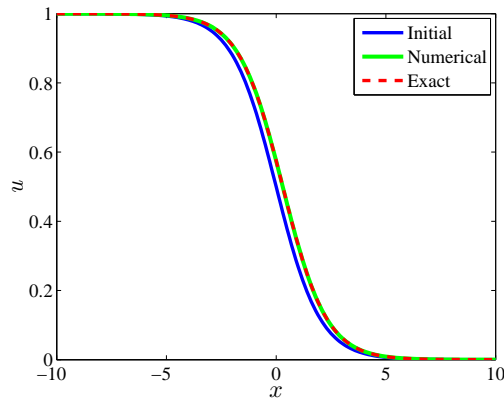
Plots of u against x for the three cases using NSFD3 scheme are shown in Fig 5.5 and corresponding plots of errors against x are displayed in Fig 5.6.



(a) $h = 0.1, \beta = 0.5, k = 0.005$.

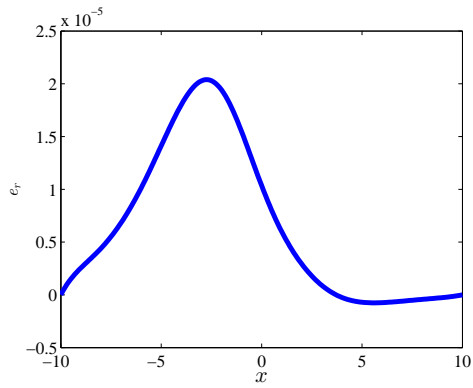


(b) $h = 0.1, \beta = 1, k = 0.005$.

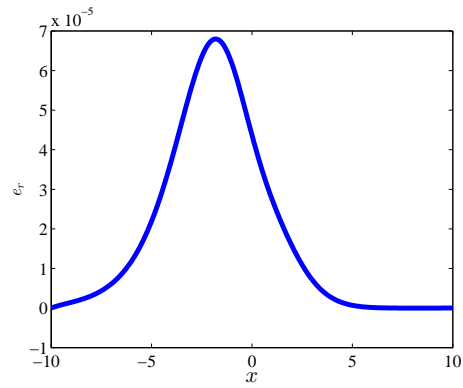


(c) $h = 0.1, \beta = 2, k = 0.005$.

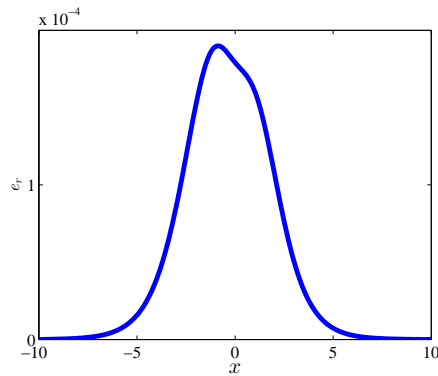
Figure 5.5: Plot of u against x using NSFD3 scheme at time $T = 0.5$, where $x \in [-10, 10]$ for different values of β namely; 0.5, 1.0, 2.0.



(a) $h = 0.1$, $\beta = 0.5$, $k = 0.005$.



(b) $h = 0.1$, $\beta = 1$, $k = 0.005$.



(c) $h = 0.1$, $\beta = 2$, $k = 0.005$.

Figure 5.6: Plot of error against x using NSFD3 scheme at time $T = 0.5$, where $x \in [-10, 10]$ for different values of β respectively 0.5, 1.0, 2.0.

5.9 NSFD4 Scheme

NSFD4 scheme is a modification of NSFD1 scheme. We notice that $-\beta (u(x_m, t_n))^3$ is approximated by $\beta \left(-\frac{3}{2} (u_m^n)^2 u_m^{n+1} + \frac{1}{2} (u_m^n)^3\right)$ instead of $\beta \left(-\frac{3}{2} (u_{m-1}^n)^2 u_m^{n+1} + \frac{1}{2} (u_{m-1}^n)^3\right)$. We use the following approximations:

$$-\beta \gamma u(x_m, t_n) \approx -\beta \gamma u_m^{n+1}, \quad -\beta (u(x_m, t_n))^3 \approx \beta \left(-\frac{3}{2} (u_m^n)^2 u_m^{n+1} + \frac{1}{2} (u_m^n)^3\right), \quad (5.26)$$

$$-\beta (1 + \gamma) (u(x_m, t_n))^2 \approx -\beta (1 + \gamma) (u_m^n)^2. \quad (5.27)$$

Therefore we have,

$$\begin{aligned} \frac{u_m^{n+1} - u_m^n}{\phi_2(k)} - \frac{u_m^{n+1} - 2u_m^n + u_{m-1}^n}{\psi_1(h) \psi_2(h)} &= \beta \left(-\frac{3}{2} (u_m^n)^2 u_m^{n+1} + \frac{1}{2} (u_m^n)^3\right) \\ &+ \beta (1 + \gamma) (u_m^n)^2 - \beta \gamma u_m^{n+1}. \end{aligned} \quad (5.28)$$

Single expression for the scheme is

$$u_m^{n+1} = \frac{(1 - 2R)u_m^n + R(u_{m+1}^n + u_{m-1}^n) + \beta \phi_2(k) \left((1 + \gamma) (u_m^n)^2 + \frac{1}{2} (u_m^n)^3\right)}{1 + \beta \gamma \phi_2(k) + \frac{3}{2} \beta \phi_2(k) (u_m^n)^2}, \quad (5.29)$$

where $R = \frac{\phi_2(k)}{\psi_1(h) \psi_2(h)}$.

Theorem 5.5 (Dynamical consistency). If $1 - 2R \geq 0$, the numerical solution of Eq. (5.29) satisfies

$$0 \leq u_m^n \leq 1 \implies 0 \leq u_m^{n+1} \leq 1,$$

and the dynamical consistency (positivity and boundedness) holds for all relevant values of n and m .

Proof. (1) NSFD4 is positive definite if $1 - 2R \geq 0$. We have $1 + \beta \gamma \phi_2(k) + \frac{3}{2} \beta \phi_2(k) (u_m^n)^2 > 0$ since $u_m^n \geq 0$. It follows

$$k \leq \frac{1}{\beta} \ln \left[1 + \frac{1}{2\beta} \frac{(e^{\beta h} - 1)^2}{e^{\beta h}} \right]. \quad (5.30)$$

(2) By assumption, $0 \leq u_m^n \leq 1$. We have

$$\begin{aligned} (u_m^{n+1} - 1) \left(1 + \beta \gamma \phi_2(k) + \frac{3}{2} \beta \phi_2(k) (u_m^n)^2 \right) &= (1 - 2R)u_m^n + R(u_{m+1}^n + u_{m-1}^n) \\ &+ \beta \phi_2(k) \left((1 + \gamma) (u_m^n)^2 + \frac{1}{2} (u_m^n)^3 \right) \\ &- 1 - \beta \phi_2(k) \gamma - \frac{3}{2} \beta \phi_2(k) (u_m^n)^2. \end{aligned} \quad (5.31)$$

It follows that $(u_m^n)^3 = u_m^n (u_m^n)^2 \leq (u_m^n)^2$ since $0 \leq u_m^n \leq 1$ for all values of n and m . Therefore,

$$\begin{aligned} (u_m^{n+1} - 1) \left(1 + \beta \gamma \phi_2(k) + \frac{3}{2} \beta \phi_2(k) (u_m^n)^2 \right) &\leq 1 - 2R + 2R + \beta \gamma \phi_2(k) (u_m^n)^2 \\ &+ \beta \phi_2(k) \left((u_m^n)^2 + \frac{1}{2} (u_m^n)^2 \right) \\ &- 1 - \beta \gamma \phi_2(k) - \frac{3}{2} \beta \phi_2(k) (u_m^n)^2 \\ &= \beta \gamma \phi_2(k) \left((u_m^n)^2 - 1 \right) \leq 0. \end{aligned} \quad (5.32)$$

Hence $u_m^{n+1} - 1 \leq 0$ and the therefore NSFD4 is bounded. □

For positivity $h = 0.1$ using , we have from Eq. (5.30),

(a) $k \leq 4.9948 \times 10^{-3}$ for $\beta = 0.5$.

(b) $k \leq 4.9917 \times 10^{-3}$ for $\beta = 1.0$.

(c) $k \leq 4.9917 \times 10^{-3}$ for $\beta = 2.0$.

We tabulate L_1, L_∞ errors, rate of convergence and CPU time at some different values of k using $\gamma = 0.2$, $h = 0.1$ at time, $T = 0.5$ for three cases namely; $\beta = 0.5, 1.0, 2.0$, using NSFD4 scheme in Tables 5.10, 5.11 and 5.12.

Time step (k)	L_1 error	L_∞ error	Rate of convergence	CPU (s)
0.005	7.5948×10^{-5}	1.1653×10^{-5}	-	0.987
0.0025	3.5996×10^{-5}	4.2640×10^{-6}	1.077	1.274
0.00125	2.2770×10^{-5}	4.1322×10^{-6}	6.607×10^{-1}	1.659

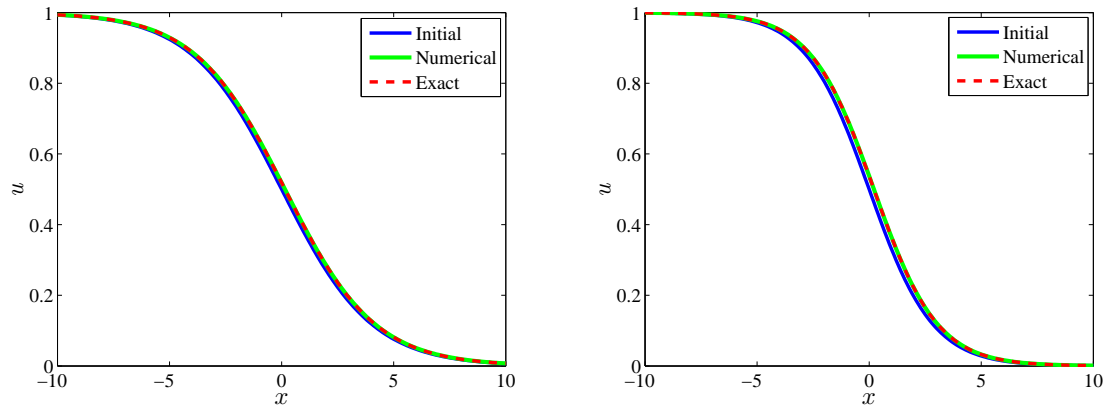
Table 5.10: Computation of L_1, L_∞ errors, rate of convergence and CPU time using NSFD4 for $-10 \leq x \leq 10$, $\gamma = 0.2$, $h = 0.1$, $\beta = 0.5$, $T = 0.5$.

Time step (k)	L_1 error	L_∞ error	Rate of convergence	CPU (s)
0.005	1.9783×10^{-4}	3.4931×10^{-5}	-	0.479
0.0025	1.0298×10^{-4}	2.0513×10^{-5}	9.418×10^{-1}	1.190
0.00125	1.0260×10^{-4}	2.4227×10^{-5}	5.333×10^{-2}	1.652

Table 5.11: Computation of L_1, L_∞ errors, rate of convergence and CPU time using NSFD4 for $-10 \leq x \leq 10$, $\gamma = 0.2$, $h = 0.1$, $\beta = 1$, $T = 0.5$.

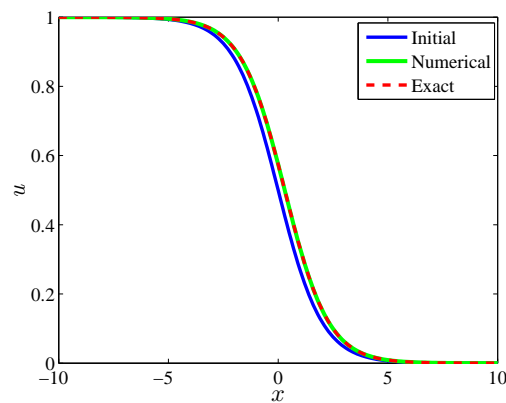
Time step (k)	L_1 error	L_∞ error	Rate of convergence	CPU (s)
0.005	5.7010×10^{-4}	1.1881×10^{-4}	-	0.551
0.0025	4.4661×10^{-4}	1.4439×10^{-4}	3.521×10^{-1}	0.798
0.00125	6.0359×10^{-4}	1.5759×10^{-4}	-4.345×10^{-1}	1.237

Table 5.12: Computation of L_1, L_∞ errors, rate convergence and CPU time using NSFD4 for $-10 \leq x \leq 10$, $\gamma = 0.2$, $h = 0.1$, $\beta = 2$, $T = 0.5$.



(a) $h = 0.1, \beta = 0.5, k = 0.005$.

(b) $h = 0.1, \beta = 1, k = 0.005$.

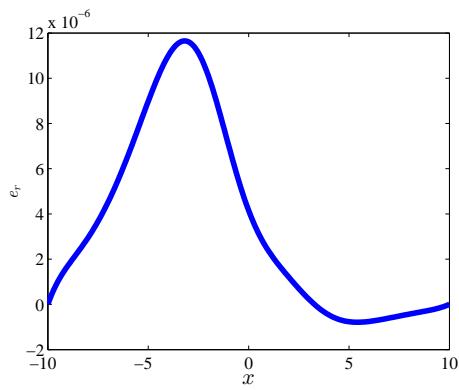


(c) $h = 0.1, \beta = 2, k = 0.005$.

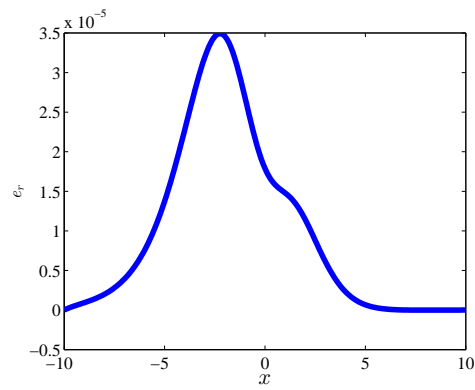
Figure 5.7: Plot of u against x using NSFD4 scheme at time $T = 0.5$, where $x \in [-10, 10]$ for different values of β namely; 0.5, 1.0, 2.0.

The scheme gives good results for $\beta = 0.5, 1.0$ and is an improvement over NSFD1. The scheme is effective for $\beta = 0.5, 1$, provided k is carefully chosen ($k=0.005, 0.0025$). The scheme has convergence rate issue as $\beta = 2.0$.

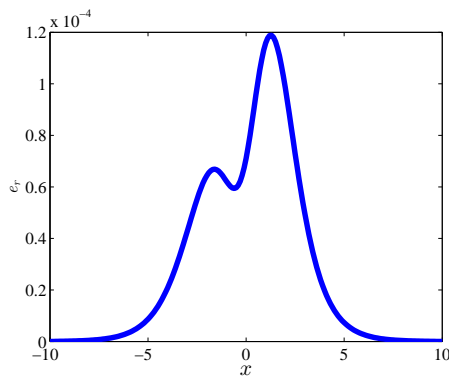
Plots of u against x for the three cases using NSFD4 scheme are shown in Fig 5.7 and plot of errors against x are displayed in Fig 5.8.



(a) $h = 0.1, \beta = 0.5, k = 0.005$.



(b) $h = 0.1, \beta = 1, k = 0.005$.



(c) $h = 0.1, \beta = 2, k = 0.005$.

Figure 5.8: Plot of error against x using NSFD4 scheme at time $T = 0.5$, where $x \in [-10, 10]$ for different values of β respectively 0.5, 1.0, 2.0.

5.10 Errors estimate for NSFD3

In this section, we study the errors estimate for NSFD3. Before any further discussion, we recall some of results from Hoff (1978) and Sanz-Serna and Stuart (1992): We consider the systems of partial differential equations

$$V_t = D(x, t, V)\Delta V + \sum_{j=1}^n M_j(x, t, V) \frac{\partial V}{\partial x^j} + F(x, t, V), \quad (x, t) \in \Omega \times (0, \infty), \quad (5.33)$$

$$V(x, 0) = V_0(x) \quad x \in \Omega, \quad (5.34)$$

$$P(x)[V(x, t) - W(x)] + Q(x) \frac{\partial V}{\partial n} = 0 \quad (x, t) \in \partial\Omega \times (0, \infty) \quad (5.35)$$

Here $\Omega \subset \mathbb{R}^\mu$ is a connected, bounded open set with piecewise smooth boundary and $V(x, t) \in \mathbb{R}^\nu$. Let S be the parallelepiped $S = \prod_{i=1}^\mu [a_i, b_i]$ in V -space. We make the following assumptions:

(a) D , M_j , and P and Q are diagonal matrices.

(b) There is a constant $K_1 > 0$ such that

$$d_i(x, t, V) - \frac{K_1}{2} |m_{ji}(x, t, V)| \geq 0, \quad (x, t, V) \in \bar{\Omega} \times [0, \infty) \times S, \quad \forall i, j.$$

d_i and m_{ji} are bounded and smooth. Furthermore they are i th diagonal entries of D and M respectively.

(c) F is smooth function and verifies $F(x, t, V) \cdot N_s(V) \leq 0$, $\forall (x, t, V) \in \bar{\Omega} \times [0, \infty) \times \partial S$. N is outer normal on S . Also We assume there is constant K_2 such that

$$\left| \frac{\partial F^i}{\partial V^i}(x, t, V) \right| \leq K_2, \quad \forall (x, t, V) \in \bar{\Omega} \times [0, \infty) \times S \text{ and for all } i.$$

(d) $V_0(x)$ and $W(x)$ are in S for relevant x .

(e) $\sup_{i, x, \alpha} |D_x^\alpha V^i(x, t)| < \infty$ for $1 \leq i \leq \mu$, $x \in \Omega$ and $|\alpha| = \sum_{j=1}^\nu |\alpha_j| \leq 4$.

$$\|V\|_p = \sup_{x, \alpha} |D_x^\alpha V^i(x, t)|_\infty. \quad p \text{ nonnegative integer.}$$

We define the finite difference equation

$$\frac{V_m^{n+1} - V_m^n}{k} = \sum_{m=1}^\mu \left\{ \left[D \frac{\Delta_m^2}{(h^m)^2} + M_m \frac{\Delta_m}{(2h^m)} \right] (z_1 V^{n+1} + z_2 V^n) \right\}_m + F, \quad (5.36)$$

where D , M_m and F are evaluated at (x_m, t_n, V_m^n) . Here z_1 and z_2 are nonnegative such that $z_1 + z_2 = 1$.

We also define the error in the numerical method

$$e_m^n = v_m^n - V_m^n \quad (5.37)$$

where v is the exact solution of (5.33)- (5.35) and V is the finite-difference approximation. We state the following theorem from Hoff (1978) and simple case is treated in Sanz-Serna and Stuart (1992) using Dirichlet boundary condition.

Theorem 5.6 (Hoff (1978)). Assume that the solution v of (5.33)- (5.35) is smooth in the sense of assumption (e) and assume that the difference scheme (5.36) is consistent and stable. Then

$$\|e^n\|_\infty \leq \frac{e^{-\sigma t_n}}{l + e^{-(\sigma+p)t_n}} [\|e^0\|_\infty + pl] + \frac{l}{l + e^{-(\sigma+p)t_n}} \text{diam } S, \quad (5.38)$$

where $p = p(t_n)$ is a positive function of t_n which depends upon the parameters appearing in (5.33)- (5.35) and upon $\max_{0 \leq t \leq t_n} \|V(\cdot, t)\|_4$; $l = k + \sum_{m=1}^{\mu} (h^m)^2$; and $\sigma \geq 0$ is arbitrary.

Remark 5.1. Note that the Theorem 5.6 is a general case of the following theorem in which Dirichlet boundary condition is used:

Theorem 5.7 (Sanz-Serna and Stuart (1992)). Under the above assumptions (a) – (e) and under the following condition:

- (1) v approaches an equilibrium and asymptotically stable $t \rightarrow \infty$,
- (2) the grids are refined in such a way that $\frac{k}{h^2} \leq \epsilon \leq \frac{1}{2}$ then there exist constants l_0 and C depending upon only f, v and ϵ , such that for $h < l_0$, the numerical solution V^n exists for all positive integers n and satisfies the error bound.

Then

$$\|e^n\|_2 \leq Cl, \quad l = k + h^2. \quad (5.39)$$

We apply the above theorems to our problem. We take $S = [0, 1]$; $\text{diam}S = 1$; $F = f(u) = \beta u(1 - u)(u - \gamma)$. $D = 1$; $M = 0$; $P(x) = 0$; $Q(x) = 1$. $\nu = 1$; $\mu = 1$. The fixed points of Eq. (5.1) are $u_1^* = 0$, $u_2^* = 1$ and they are asymptotically stable. Also $u_3^* = \gamma$ is fixed point and it is unstable (Roeger and Mickens, 2007). Theorem 5.1 showed that $u_0(x) \in [0, 1]$, $\forall x$ and $u(x, t) \in [0, 1]$, $\forall x, t$. $f(u) = \beta u(1 - u)(u - \gamma)$, is smooth in u . $\partial_s = \{0, 1, \gamma\}$. Hence $0 = f(x, t, 0) \cdot N_s(u) = 0$; $0 = f(x, t, 1) \cdot N_s(u) = 0$; $0 = f(x, t, \gamma) \cdot N_s(u) = 0$. $f_u = \beta\{(1 - u)(u - \gamma) - u(u\gamma) + u(1 - u)\}$. $|f_u|_\infty = \max |f_u| \leq 2\gamma + 1 = K_2$. $u_x = -\frac{\sqrt{\beta}}{4\sqrt{2}} + \frac{\sqrt{\beta}}{4\sqrt{2}} \tanh(\frac{\sqrt{\beta}}{2\sqrt{2}}(x - ct))$. $|u_x| < \infty$ since \tanh is bounded on $[-10, 10]$.

We can conclude since our scheme NSFD3 is dynamical consistent and stable under the condition $k \leq \frac{1}{\beta} \ln \left(1 + \frac{1}{2\beta} \frac{(e^{\beta h} - 1)^2}{e^{\beta h}} \right)$ and $l = \phi_2(k) + \psi_1(h) \psi_2(h)$ and the error bound (error estimate) is

$$\|e^n\|_\infty \leq \frac{e^{-\sigma t_n}}{l + e^{-(\sigma+p)t_n}} [\|e^0\|_\infty + pl] + \frac{l}{l + e^{-(\sigma+p)t_n}},$$

which follows when $t_n \rightarrow \infty$,

$$\|e^n\|_\infty \leq 1.$$

5.11 Relationship between physical behaviour and numerical solution and discussion over the obtained results from NSFD1, NSFD2, NSFD3, NSFD4

The solution $u(x, t)$ is non-negative, bounded and unique

According to Theorem 5.1, the solution $u(x, t)$ is non-negative, bounded and unique for $t \in (0, \infty)$ and $\limsup_{t \rightarrow \infty} u(x, t) \leq 1$. To illustrate Theorem 5.1, we plot the numerical solution against $t \in [0, 20]$ and against $x \in [-10, 10]$ using NSFD3 scheme for instance and the plot is shown in Figure 5.9.

Intrinsic growth rate

We recall as it is in the introduction, the intrinsic growth rate denoted by β in the presence of migration is an accurate measure of how quickly a population would ultimately grow if for instance current age-specific rates of fertility, mortality and migration were sustained indefinitely in contrast to the actual growth rate of the population (Preston and Wang, 2007). In this work, we used three values of β , namely; 0.5, 1.0, 2.0. As we increase β , the profile of the numerical solution at a given time against x becomes stiff as seen from Figures 5.1, 5.3, 5.5 and 5.7.

Remark 5.2. *If β is chosen much larger than the coefficient of diffusion (say $\beta = 10^4$), the profile becomes very stiff and the problem could be classified as singularly perturbed problem. In Agbavon et al. (2019a) (refer to chapter 3), the numerical solution of Fisher's equation with coefficient of diffusion term much smaller than reaction was obtained for the initial condition consisting of an exponential function. NSFD methods were used and range of values of k was quite restricted. To obtain accurate results, very small values of k had to be used. Some modification was made to the NSFD methods.*

Threshold of Allee effect

The threshold of Allee effect is denoted by γ . In this work we use $\gamma = 0.2$ and used four numerical methods. To investigate how γ affects the results, we obtain plots of numerical solution against for different values of γ namely; 0.1, 0.2, 0.3, 0.4, 0.5, 0.6, 0.7, 0.8, 0.9. at time, $T = 0.5$, using NSFD3. The plot is shown in Figure 5.10.

We observe that the numerical solution remains positive and bounded for different values for $\gamma \in (0, 1)$.

Effect of time-step.

For NSFD1, we realise that when the time step becomes smaller, the L_1 and L_∞ errors increase. The rate of convergence becomes so poor and the Computational time (CPU) increases. Normally, when the time step becomes smaller the L_1 and L_∞ errors should decrease if NSFD1 were accurate. That is not

the case. That might be due to the wrong approximation like in [Namjoo and Zibaei \(2018\)](#)

$$-\beta \gamma u(x_m, t_n) \approx -\beta \gamma u_m^{n+1}, \quad -\beta (u(x_m, t_n))^3 \approx \beta \left(-\frac{3}{2} (u_{m-1}^n)^2 u_m^{n+1} + \frac{1}{2} (u_{m-1}^n)^3 \right), \quad (5.40)$$

$$\beta (1 + \gamma) (u(x_m, t_n))^2 \approx \beta (1 + \gamma) (u_{m-1}^n)^2. \quad (5.41)$$

and also the limit 0 of the step size $\psi_1(h)$, $\psi_2(h)$, with which zero-stability is affected and not reached. Another reason might be the inclusion of intrinsic growth rate parameter, β in the problem (5.1). This can cause the instabilities (oscillations, etc). Furthermore, these instabilities might come from the initial condition which is not suitable with the approximation due to the dependence on the initial condition behaviour at infinity and also due to the speed of the wave (the solution of the problem (5.1) is in the form of travelling wave. Hence the need of wave speed). It is known that the initial data in the right queue that defines the wave speed, and it is the right-hand boundary condition that is significant ([Qiu and Sloan, 1998](#)). Furthermore, the speed might not be known in a more difficult problem, and solution in a fixed hint frame with the adequate asymptotic condition at the right queue.

For NSFD2, when the time step becomes smaller, the L_1 and L_∞ errors decrease with reasonable computational time (CPU). This is expected. The rate of convergence are good for small values of β (0.5, 1) with time step not too much smaller ($k = (0.005, 0.0025)$). When the time step becomes smaller, say 0.00125, the rate of convergence becomes not too good (the value of the rate of convergence is far way from the value one). And when β becomes large, this case is solved in [Agbavon et al. \(2019a\)](#) and the profile becomes very stiff (please refer to the remark 5.2).

For NSFD3, when the time step becomes smaller, the L_1 and L_∞ errors decrease with reasonable computational time (CPU) as well. The NSFD3 scheme is effective for all the values $\beta = 0.5, 1.0$ ($\beta \in (0, 1]$). The L_1 and L_∞ errors are good and small. The rate of convergence in time is approximatively one which is expected. But with $\beta = 2$, whereas the L_1 and L_∞ errors are small, the rate of convergence is close to one with some time steps reasonably chosen (0.005, 0.0025).

For NSFD4, when the time step becomes smaller, the L_1 and L_∞ errors decrease with reasonable computational time (CPU) as it is in the case NSFD2, NSFD3. The NSFD4 scheme gives good results for $\beta = 0.5, 1.0$ and is an improvement over NSFD1 like we notice that $-\beta (u(x_m, t_n))^3$ is approximated by $\beta \left(-\frac{3}{2} (u_m^n)^2 u_m^{n+1} + \frac{1}{2} (u_m^n)^3 \right)$ instead of $\beta \left(-\frac{3}{2} (u_{m-1}^n)^2 u_m^{n+1} + \frac{1}{2} (u_{m-1}^n)^3 \right)$. The following approximations are used:

$$-\beta \gamma u(x_m, t_n) \approx -\beta \gamma u_m^{n+1}, \quad -\beta (u(x_m, t_n))^3 \approx \beta \left(-\frac{3}{2} (u_m^n)^2 u_m^{n+1} + \frac{1}{2} (u_m^n)^3 \right),$$

$$-\beta (1 + \gamma) (u(x_m, t_n))^2 \approx -\beta (1 + \gamma) (u_m^n)^2.$$

The scheme is accurate for $\beta = 0.5, 1$, provided that a great care is made in the choice of k ($k = 0.005, 0, 0025$). The scheme has convergence rate issue for $\beta = 2.0$.

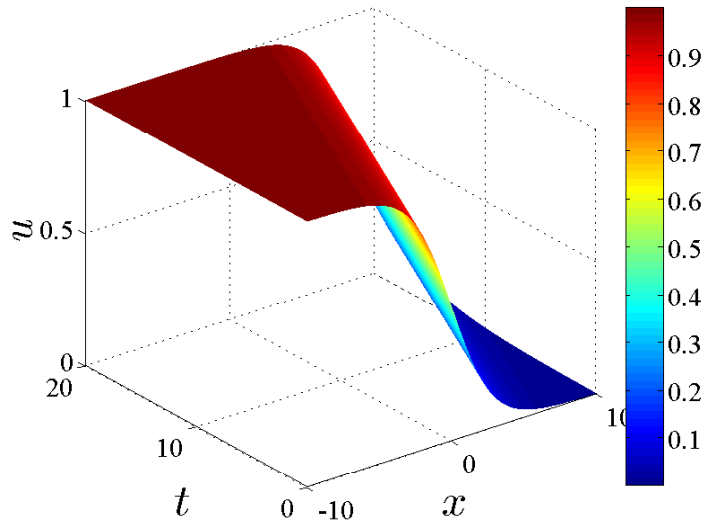


Figure 5.9: Plot of numerical solution, u vs $x \in [-10, 10]$ and vs $t \in [0, 20]$ using NSFD3.

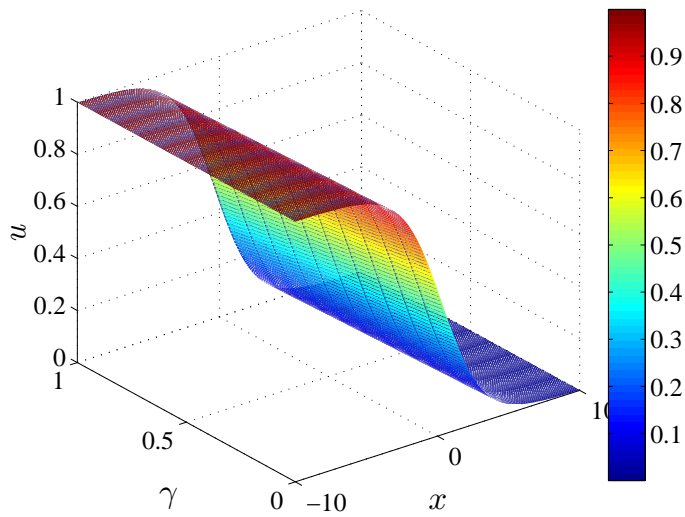


Figure 5.10: Plot of numerical solution, u vs $x \in [-10, 10]$ vs γ using NSFD3 for different values of γ namely; 0.1, 0.2, 0.3, 0.4, 0.5, 0.6, 0.7, 0.8, 0.9.

5.12 Implicit nonstandard finite difference for Fitzhugh-Nagumo equation

All the methods constructed in the previous sections are mostly explicit nonstandard finite difference. In this part of the chapter, we give some general view how the implicit nonstandard finite difference looks like. We propose the following scheme for Eq. (5.1) following [Chen et al. \(2003\)](#):

$$\frac{u_m^{n+1} - u_m^n}{\phi_2(k)} - \frac{u_{m+1}^{n+1} - 2u_m^{n+1} + u_{m-1}^{n+1}}{\psi_1(h)\psi_2(h)} = \beta \left(-(u_m^n)^2 u_m^{n+1} + (1 + \gamma) (u_m^n)^2 - \gamma u_m^{n+1} \right) \quad (5.42)$$

where u_t is approximated by $\frac{u_m^{n+1} - u_m^n}{\phi_2(k)}$ where $\phi_2(k) = \frac{e^{\beta k} - 1}{\beta}$ and u_{xx} is approximated by $\frac{u_{m+1}^{n+1} - 2u_m^{n+1} + u_{m-1}^{n+1}}{\psi_1(h)\psi_2(h)}$ instead of $\frac{u_{m+1}^n - 2u_m^n + u_{m-1}^n}{\psi_1(h)\psi_2(h)}$ like in the case of explicit nonstandard finite difference (NSFD1, NSFD2, NSFD3, NSFD4); where $\psi_1(h) = \frac{1 - e^{-\beta h}}{\beta}$ and $\psi_2(h) = \frac{e^{\beta h} - 1}{\beta}$. The right hand of Eq. (5.1) is

$$\begin{aligned} -\beta \gamma u(x_m, t_n) &\approx -\beta \gamma (u_m^{n+1}), \quad -\beta (u(x_m, t_n))^3 \approx -\beta (u_m^n)^2 u_m^{n+1}, \\ \beta (1 + \gamma) (u(x_m, t_n))^2 &\approx \beta (1 + \gamma) (u_m^n)^2. \end{aligned}$$

It is know from [Chen et al. \(2003\)](#), that for a given an initial value problem

$$u_t = D u_{xx} + \alpha_1 u - \alpha_2 u^3, \quad x \in [0, L], \quad t > 0. \quad (5.43)$$

with an initial and boundary conditions respectively

$$u(x, 0) = \begin{cases} 1, & x \in [0, 1], \\ 0, & x \in [1, 2], \end{cases}, \quad u(0, t) = \begin{cases} 1, & x = 0, \\ 0, & x = 2, \end{cases}$$

and α_1, α_2, D stand for nonnegative real parameters, the implicit nonstandard finite difference which derived from Eq. (5.43) is given by

$$\frac{u_m^{n+1} - u_m^n}{k} - \frac{u_{m+1}^{n+1} - 2u_m^{n+1} + u_{m-1}^{n+1}}{h^2} = \left(-\alpha_2 (u_m^n)^2 u_m^{n+1} + \alpha_1 (2u_m^n - u_m^{n+1}) \right). \quad (5.44)$$

It is proved numerically in [Chen et al. \(2003\)](#) under the conditions $h = 0.05$, $k = 0.001$ and $k = 1$ with $\alpha_1 = \alpha_2 = D = 1$ and $t = 1$ that implicit nonstandard finite difference is more accurate and robust over the explicit nonstandard finite difference schemes for solving nonlinear initial and boundary value problems under the same conditions.

5.13 Conclusion

In this chapter, we construct four nonstandard finite difference schemes namely; NSFD1, NSFD2, NSFD3, NSFD4 to solve FitzHugh-Nagumo equation under three different regimes. The first order time derivative and the second order spatial derivative are approximated in the same manner for all of the methods and it is only the nonlinear polynomial in the partial differential equation which is discretised differently. We derive conditions under which the scheme are positive definite and bounded.

NSFD1 is not effective and gives issues in regard to its rate of convergence. NSFD4 is a major improvement over NSFD1 in terms of L_1 , L_∞ errors and rate of convergence in time. NSFD3 seems the best scheme followed by NSFD4 when we check performance of the methods based on L_1 , L_∞ errors and rate of convergence in time (with respect to L_1 error). We studied error estimate for NSFD3 and found that the estimation cannot go beyond one as we progress in time.

Chapter 6

Conclusion and future work

6.1 Conclusion

In this thesis, finite difference and nonstandard finite difference methods have been used to solve Fisher's and Fitzhugh-Nagumo equations. Some properties and applications of these methods are discussed in chapter 1 and 2.

In chapter 3, we studied the numerical solution of Fisher's equation with coefficient of diffusion term much smaller than coefficient of reaction term. This problem was solved by moving mesh method. We constructed four new schemes based on finite differences and nonstandard finite differences. The four schemes namely; FTCS- ϵ , NSFD- ϵ , FTCS with artificial viscosity, NSFD with artificial viscosity give quite accurate results at larger time-step size and consequently at smaller CPU time compared to moving mesh partial differential equation (MMPDE) and moving mesh differential algebra equation (MMDAE) methods (Qiu and Sloan, 1998). Indeed we have found that L_1 and L_∞ errors computed at optimal time step size and $h = 0.01$ with the four constructed schemes are of order 10^{-4} and 10^{-3} respectively which are better than L_1 and L_∞ errors of the MMPDE and MMDAE methods of order 10^{-3} and 10^{-2} respectively with reasonable computational time. Moreover we obtained a quite good results at larger time-step size. The poor results was obtained in Li et al. (1998) in the case $\rho = 10^4$ when using moving mesh even with small time step size. That let Li et al. (1998) to conclude that moving mesh methods were not recommendable or suitable for computing the travelling wave solution of Fisher's equation over a reasonably large time interval. It is known in Qiu and Sloan (1998) that moving mesh methods give much better results if only the monitor function is carefully chosen to agree the properties of the differential equation and also of the computed solution (even with great care of the monitor function constructed, the computed solution might not be effective if the selected moving mesh method is unsuitable). This is still an open problem. The experiments done in Qiu and Sloan (1998) showed that more investigation on the formulation and analysis of moving mesh methods for reaction diffusion equations is needed (mixture of moving mesh methods and the boundary conditions as in Hagstrom and Keller (1986)). The case we dealt by proposing the four schemes FTCS- ϵ , NSFD- ϵ ,

FTCS with artificial Viscosity, NSFD with artificial viscosity is one way to avoid constructing monitor function. Moreover, the convergence tests of the four proposed methods have been investigated and they are in perfect matching with the analysis.

In chapter 4, we reconsidered the work of [Namjoo and Zibaei \(2018\)](#) and studied the stability analysis since the full investigation about the stability has not been studied (on implicit and explicit methods). The stability analysis is so important in this context (zero-stability in the jargon of [Lambert \(1991\)](#)). We found that the schemes (implicit and explicit) which derived from exact scheme by [Namjoo and Zibaei \(2018\)](#) has stability issue especially, the explicit scheme. We use the amplification factor to study the stability. We found that $|\xi| > 1$ for $w \in [-\pi, \pi]$ while using $k = h/A_2$ and $\gamma = 0.001, 0.5$ (please refer to Figure 4.1). Von Neumann stability analysis is not satisfied (Please refer to Theorem 2.4). The reason of non-stability of explicit might comes from the consideration $k = h/A_2$ made by [Namjoo and Zibaei \(2018\)](#) to construct exact scheme. More investigations need to be done while considering the condition for instance $k > h/A_2$ or $k < h/A_2$ to construct the exact scheme. That might lead to better results. Implicit scheme from [Namjoo and Zibaei \(2018\)](#) has no stability issues (please refer to Figure 4.3). Von Neumann stability analysis is verified.

Furthermore, apart from the stability, we performed also consistency of the discrete scheme with the original differential equation of the discrete method (this one novelty). We described two nonstandard finite difference methods (NSFD1 and NSFD2) from [Namjoo and Zibaei \(2018\)](#). We also obtained an improvement for NSFD1 called NSFD3 (this is the second novelty). We have shown that NSFD1, NSFD2, NSFD3 are dynamical consistency with the original problem 4.1. Although NSFD1 is dynamical consistency, it still has convergence issues. That might be caused by many reasons. One reason is wrong approximation like

$$-\gamma u(x_m, t_n) \approx -\gamma u_m^{n+1}, \quad -(u(x_m, t_n))^3 \approx -\frac{3}{2} (u_{m-1}^n)^2 u_m^{n+1} + \frac{1}{2} (u_{m-1}^n)^3,$$

where u_{m-1}^n and u_m^{n+1} are both non-local approximations. Another reason, might also be the limit 0 of the step size $\psi_1(h), \psi_2(h)$, with which zero-stability is affected and is not attained. That is why NSFD3 scheme is proposed in this work. We realised that the proposed scheme NSFD3 performs better than implicit and explicit methods emerging from the scheme baptised "exact scheme" in term of L_1 and L_∞ errors and rate of convergence with reasonable computational time (CPU).

In chapter 5, we considered more challenging initial and boundary conditions of FitzHugh-Nagumo equations, with some parameter called intrinsic growth rate. We constructed four schemes nonstandard finite difference methods namely; NSFD1, NSFD2, NSFD3, NSFD4. More explanations are done in section 5.11 about why and how NSFD1 is not effective scheme and why and how NSFD3 is better than NSFD1, NSFD2, NSFD4. The latter scheme, NSFD4 is an improvement over NSFD1. The convergence rate and estimate error have been studied. We found that the estimate error of NSFD3 is such that

$$\|e^n\|_\infty \leq \frac{e^{-\sigma t_n}}{l + e^{-(\sigma+p)t_n}} [\|e^0\|_\infty + p l] + \frac{l}{l + e^{-(\sigma+p)t_n}},$$

which follows when $t_n \rightarrow \infty$,

$$\|e^n\|_\infty \leq 1.$$

It is notable that using standard numerical techniques for instance (moving mesh partial differential methods, explicit Euler, Runge-Kutta methods, etc.), to solve initial-value problems often brings numerical instabilities for certain selections of model and discretization parameters (Mickens, 1999, Twizell et al., 1999). Whereas such instabilities (oscillations, chaos, etc.) are generally taken out by using small time steps, the extra computing cost appended with investigating the long-term behaviour of a dynamical system can be considerable. In our chapter 3, 4 and 5, we constructed robust numerical methods (FTCS- ϵ , NSFD- ϵ , FTCS with artificial Viscosity, NSFD with artificial viscosity, NSFD1, NSFD2, NSFD3, NSFD4) that not only apart of small time steps, the extra computing cost, allow large time-steps, but are also pointless of scheme-dependent instabilities for attainable values of the model parameters (apart from NSFD1 in 4 and 5). As a result, we have found that our schemes are more reliable than the standard ones in term of L_1 and L_∞ errors and rate of convergence with sensible computational time (CPU).

6.2 Some limitations of nonstandard finite difference

The results found using NSFD methods to solve Fisher's and Fitzhugh-Nagumo equations showed that the principle of dynamical consistency can be utilised with great effectiveness to place restrictions on NSFD schemes. This signifies that dynamical consistency can be seen as a third fundamental principle, in inclusion to the two stated in the Definition 2.17, for the conceptualisation of a general NSFD methodology for constructing discrete models of partial differential equations. Furthermore another important characteristic which can be incorporated into dynamical consistency for NSFD methods is the transient behaviour of the continuous models NSFD methods approximate. Despite that NSFD schemes are either first or second-order in accuracy, such methods mostly give schemes having the correct transient behaviour (Mickens, 2005). It is worthy to suggested that NSFD schemes can be erected to attain higher-order accuracy (Mickens, 2005). The methodology for doing this is shown in Chen et al. (2003) and in Twizell et al. (1999).

There are two censorious problems that till now have not been acceptably solved using the framework of the NSFD method. These are

- 1) The common difficulty of constructing NSFD schemes for ordinary differential equation that have oscillatory solutions for which the suitable fixed-point is a center. In general, no problems exist for fixed-points that tie in to stable or unstable spirals or nodes (Mickens, 2005).
- 2) The second happens in the discrete modelling of coupled systems of nonlinear reaction-diffusion-advection partial differential equations which involves cross-diffusion terms (Murray, 1989). For instance for these cross-diffusion terms and for two dependent variables u and v , they have the

forms $[f_1(u)v_x]_x$ or $[f_2(v)u_x]_x$ where f_1 and f_2 are positive functions of their respective variables (Mickens, 2005).

Most of numerical methods constructed in this thesis are mostly nonstandard explicit schemes. These methods for nonlinear evolution partial differential equations need functional limitations to hold between the various step-sizes (Hildebrand, 1968). These relations which are more complex for nonlinear evolution partial differential equations usually are found from the study of dynamical consistency (imposing the satisfaction of some physical requirements). This consideration of dynamical consistency helps us to find that the problems we solved in 3, 4, 5 preserve the physical properties (positivity, boundedness, preservation of fixed points). More investigations need to be done while considering implicit nonstandard schemes. Comprehensively, implicit nonstandard schemes demands the use of a tridiagonal solver at every time step (the matrix associated of nonstandard implicit schemes is in diagonally dominant form). The stability of the constructed implicit schemes needs to be investigated using the matrix method (this involves finding the appropriate spectral norms of the associated coefficient matrices at every time step as in Lambert (1991)).

6.3 Future work

Our aim in the future is to extend this work in the following directions:

- 1) to construct nonstandard finite difference methods for 2D and 3D Fisher's and Fitzhugh-Nagumo equations, respectively.
- 2) to construct nonstandard finite difference methods for a general initial and boundary conditions with unknown exact solutions for Fitzhugh-Nagumo equation.
- 3) to study error estimate for the following Fitzhugh-Nagumo parameter-dependent reaction-diffusion systems (Chrysafinos et al., 2013)

$$\begin{cases} u_t - \Delta u + u^3 - u &= -v + f_1 & \text{in } (0, T) \times \Omega \\ u &= 0 & \text{on } (0, T) \times \Gamma \\ u(0, x) &= u_0 & \text{in } \Omega \end{cases} \quad (6.1)$$

$$\begin{cases} v_t - \delta \Delta v &= \epsilon(u - \alpha_1 v) + f_2 & \text{in } (0, T) \times \Omega \\ v &= 0 & \text{on } (0, T) \times \Gamma \\ v(0, x) &= v_0 & \text{in } \Omega \end{cases} \quad (6.2)$$

where Ω stands for a bounded domain in \mathbb{R}^2 , with Lipschitz boundary Γ , u_0 , v_0 and f_1 , f_2 are initial data and forcing terms respectively. The parameters ϵ , δ , α_1 which appear in the problem denote different scales of the physical variables u , v engaged in the model.

3. to investigate some singularly perturbed convective Cahn-Hilliard equations and construct some nonstandard finite difference methods for them.

Bibliography

- Adomian, G. (1988). *Nonlinear stochastic systems theory and applications to physics*, volume 46. Springer Science & Business Media.
- Agbavon, K. M. and Appadu, A. R. (2019). Construction and analysis of some nonstandard finite difference methods for the FitzHugh-Nagumo equation. *Numerical Method for Partial Differential Equation*, Under review.
- Agbavon, K. M., Appadu, A. R., and Khumalo, M. (2019a). On the numerical solution of Fisher's equation with coefficient of diffusion term much smaller than coefficient of reaction term. *Advances in Difference Equations*, 2019(1):146.
- Agbavon, K. M., Appadu, R. A., and Inan, B. (2019b). *Comparative study of some Numerical methods for the standard FitzHugh-Nagumo equation*. Communications in Mathematical Computations and Applications, Springer.
- Allee, W. C. (1931). *Animal Aggregations: A Study in General Sociology*. Chicago: Chicago University. Press. 431 p.
- Allee, W. C. (1938). *The social life of animals*, volume 14729753(645319763). Norton & Company, 1 st edition, New York.
- Allee, W. C., Park, O., Emerson, A. E., Park, T., Schmidt, K. P., et al. (1949). *Principles of animal ecology*. Technical report, Saunders Company Philadelphia, Pennsylvania, USA.
- Ames, W. F. (2014). *Numerical methods for partial differential equations*. Academic Press, 18th edition.
- Anguelov, R., Kama, P., and Lubuma, J. M. S. (2005). On nonstandard finite difference models of reaction–diffusion equations. *Journal of Computational and Applied Mathematics*, 175(1):11–29.

- Anguelov, R. and Lubuma, J. (2001). Contributions to the mathematics of the nonstandard finite difference method and applications. *Numerical Methods for Partial Differential Equations: An International Journal*, 17(5):518–543.
- Appadu, A. R. and Agbavon, K. M. (2019). Comparative study of some numerical methods for FitzHugh-Nagumo equation. In *AIP Conference Proceedings*, volume 2116, page 030036.
- Appadu, A. R., Djoko, J. K., and Gidey, H. (2016). A computational study of three numerical methods for some advection-diffusion problems. *Applied Mathematics and Computation*, 272:629–647.
- Appadu, A. R., Lubuma, J. M. S., and Mphephu, N. (2017). Computational study of three numerical methods for some linear and nonlinear advection-diffusion-reaction problems. *Progress in Computational Fluid Dynamics*, 17(2):114–129.
- Aronson, D. G. and Weinberger, H. F. (1978). Multidimensional nonlinear diffusion arising in population genetics. *Advances in Mathematics*, 30(1):33–76.
- Bell, D. C. and Deng, B. (2002). Singular perturbation of n-front travelling waves in the Fitzhugh–Nagumo equations. *Nonlinear Analysis. Real World Applications*, 3(4):515–541.
- Bell, H. E. (1965). Gershgorin’s theorem and the zeros of polynomials. *The American Mathematical Monthly*, 72(3):292–295.
- Bhrawy, A. H. (2013). A Jacobi–Gauss–Lobatto collocation method for solving generalized Fitzhugh–Nagumo equation with time-dependent coefficients. *Applied Mathematics and Computation*, 222:255–264.
- Biazar, J. and Mohammadi, F. (2010). Application of differential transform method to the generalized Burgers–Huxley equation. *Application and Applied Mathematics*, 5(10):1726–1740.
- Boukal, D. S., Sabelis, M. W., and Berec, L. (2007). How predator functional responses and Allee effects in prey affect the paradox of enrichment and population collapses. *Theoretical Population Biology*, 72(1):136–147.
- Camassa, R., Hyman, J. M., and Luce, B. P. (1998). Nonlinear waves and solitons in physical systems. *Physica D: Nonlinear Phenomena*, 123(1-4):1–20.

- Campbell, J. C. and Shashkov, M. J. (2001). A tensor artificial viscosity using a mimetic finite difference algorithm. *Journal of Computational Physics*, 172(2):739–765.
- Canosa, J. (1973). On a nonlinear diffusion equation describing population growth. *International Business Machines, Journal of Research and Development*, 17(4):307–313.
- Caramana, E. J., Shashkov, M. J., and Whalen, P. P. (1998). Formulations of artificial viscosity for multi-dimensional shock wave computations. *Journal of Computational Physics*, 144(1):70–97.
- Chatelin, F. (1983). *Spectral approximation of linear operators*, volume 65. Society for Industrial and Applied Mathematics (SIAM).
- Chawla, M. M., Al-Zanaidi, M. A., and Al-Aslab, M. G. (2000). Extended one-step time-integration schemes for convection-diffusion equations. *Computers & Mathematics with Applications*, 39(3-4):71–84.
- Chen, B. M. and Kojouharov, H. (1999). Nonstandard numerical methods applied to subsurface biobarrier formation models in porous media. *Bulletin of Mathematical Biology*, 61(4):779–798.
- Chen, Z., Gumel, A. B., and Mickens, R. E. (2003). Nonstandard discretizations of the generalized Nagumo reaction-diffusion equation. *Numerical Methods for Partial Differential Equations: An International Journal*, 19(3):363–379.
- Chen-Charpentier, B. M. and Kojouharov, H. V. (2013). An unconditionally positivity preserving scheme for advection–diffusion reaction equations. *Mathematical and Computer Modelling*, 57(9-10):2177–2185.
- Chou, M. H. and Lin, Y. T. (1996). Exotic dynamic behavior of the forced FitzHugh-Nagumo equations. *Computers & Mathematics with Applications*, 32(10):109–124.
- Chrysafinos, K., Filopoulos, S. P., and Papathanasiou, T. K. (2013). Error estimates for a FitzHugh–Nagumo parameter-dependent reaction-diffusion system. *ESAIM: Mathematical Modelling and Numerical Analysis*, 47(1):281–304.
- Clavero, C., Jorge, J. C., and Lisbona, F. (2003). A uniformly convergent scheme on a nonuniform mesh for convection–diffusion parabolic problems. *Journal of Computational and Applied Mathematics*, 154(2):415–429.

- Colton, D. L., Ewing, R. E., Rundell, W., et al. (1990). *Inverse problems in partial differential equations*, volume 42. Society for Industrial and Applied Mathematics (SIAM).
- Courchamp, F., Clutton-Brock, T., and Grenfell, B. (1999). Inverse density dependence and the Allee effect. *Trends in Ecology & Evolution*, 14(10):405–410.
- Da Silva, E. G. and Zeidan, D. (2017). Numerical simulation of unsteady cavitation in liquid hydrogen flows. *International Journal of Engineering Systems Modelling and Simulation*, 9(1):41.
- Dehghan, M. and Manafian, J. I. (2009). The solution of the variable coefficients fourth-order parabolic partial differential equations by the homotopy perturbation method. *Zeitschrift für Naturforschung A*, 64(7-8):420–430.
- Dehghan, M. and Shakeri, F. (2007). Solution of a partial differential equation subject to temperature overspecification by He’s homotopy perturbation method. *Physica Scripta*, 75(6):778.
- Dehghan, M. and Shakeri, F. (2008a). Application of He’s variational iteration method for solving the Cauchy reaction–diffusion problem. *Journal of computational and Applied Mathematics*, 214(2):435–446.
- Dehghan, M. and Shakeri, F. (2008b). Approximate solution of a differential equation arising in astrophysics using the variational iteration method. *New Astronomy*, 13(1):53–59.
- Dehghan, M. and Shakeri, F. (2008c). Solution of an integro-differential equation arising in oscillating magnetic fields using He’s homotopy perturbation method. *Progress in Electromagnetics Research*, 78:361–376.
- Dehghan, M. and Shakeri, F. (2008d). Use of He’s homotopy perturbation method for solving a partial differential equation arising in modeling of flow in porous media. *Journal of Porous Media*, 11(8).
- Dehghan, M. and Tatari, M. (2008). Identifying an unknown function in a parabolic equation with overspecified data via He’s variational iteration method. *Chaos, Solitons & Fractals*, 36(1):157–166.
- Dennis, B. (1989). Allee effects: population growth, critical density, and the chance of extinction. *Natural Resource Modeling*, 3(4):481–538.

- Doelman, A., Kaper, T. J., and Zegeling, P. A. (1997). Pattern formation in the one-dimensional Gray-Scott model. *Nonlinearity*, 10(2):523.
- Durrant, D. R. (2010). *Numerical methods for fluid dynamics: With applications to geophysics*, volume 32. Springer Science & Business Media.
- Edelstein-Keshet, L. (1988). *Mathematical Models in Biology*, volume 46. Society for Industrial and Applied Mathematics (SIAM), Random House, New York.
- Fisher, R. A. (1937). The wave of advance of advantageous genes. *Annals of eugenics*, 7(4):355–369.
- FitzHugh, R. (1961). Impulses and physiological states in theoretical models of nerve membrane. *Biophysical Journal*, 1(6):445–466.
- Forsythe, G. and Wasow, W. R. (1960). *Finite-Difference Methods for Partial Differential Equations*, *Applied Mathematical Series*. Wiley, New York.
- Frey, P. (2019 (accessed 18 December, 2019)). The finite difference method. Technical report, https://www.ljll.math.upmc.fr/frey/cours/UdC/ma691/ma691_ch6.pdf
- Gao, W. and Wang, J. (2004). Existence of wavefronts and impulses to FitzHugh–Nagumo equations. *Nonlinear Analysis: Theory, Methods & Applications*, 57(5-6):667–676.
- Gazdag, J. and Canosa, J. (1974). Numerical solution of Fisher’s equation. *Journal of Applied Probability*, 11(3):445–457.
- Gear, C. (1971). *Numerical initial value problems in ordinary differential equations*. Prentice Hall PTR, 7 th edition.
- Hagan, P. S. (1982). Traveling wave and multiple traveling wave solutions of parabolic equations. *Society for Industrial and Applied Mathematics/ Journal on Mathematical Analysis*, 13(5):717–738.
- Hagberg, A. and Meron, E. (1994). From labyrinthine patterns to spiral turbulence. *Physical Review Letters*, 72(15):2494.
- Hagstrom, T. and Keller, H. B. (1986). The numerical calculation of traveling wave solutions of nonlinear parabolic equations. *Society for Industrial and Applied Mathematics, Journal on Scientific and Statistical Computing*, 7(3):978–988.

- Hariharan, G., Kannan, K. ., and Sharma, K. R. (2009). Haar wavelet method for solving Fisher's equation. *Applied Mathematics and Computation*, 211(2):284–292.
- Hildebrand, F. B. (1968). *Finite-difference equations and simulations*. Prentice-Hall, second edition.
- Hilker, F. M., Langlais, M., Petrovskii, S. V., and Malchow, H. (2007). A diffusive SI model with Allee effect and application to FIV. *Mathematical Biosciences*, 206(1):61–80.
- Hodgkin, A. L. and Huxley, A. F. (1952). A quantitative description of membrane current and its application to conduction and excitation in nerve. *The Journal of Physiology*, 117(4):500–544.
- Hoff, D. (1978). Stability and convergence of finite difference methods for systems of nonlinear reaction-diffusion equations. *Society for Industrial and Applied Mathematics (SIAM), Journal on Numerical Analysis*, 15(6):1161–1177.
- Houdek, G., Balmforth, N. J., Christensen-Dalsgaard, J., and Gough, D. O. (1999). Amplitudes of stochastically excited oscillations in main-sequence stars. *arXiv preprint astro-ph/9909107*.
- Huang, W., Ren, Y., and Russell, R. D. (1994). Moving mesh partial differential equations (mm-pdes) based on the equidistribution principle. *Society for Industrial and Applied Mathematics (SIAM), Journal on Numerical Analysis*, 31(3):709–730.
- Jackson, D. E. (1992). Error estimates for the semidiscrete galerkin approximations of the FitzHugh-Nagumo equations. *Applied Mathematics and Computation*, 50(1):93–114.
- Jiwari, R., Gupta, R. K., and Kumar, V. (2014). Polynomial differential quadrature method for numerical solutions of the generalized Fitzhugh–Nagumo equation with time-dependent coefficients. *Ain Shams Engineering Journal*, 5(4):1343–1350.
- Johnson, S., Suarez, P., and Biswas, A. (2012). New exact solutions for the sine-Gordon equation in $2+1$ dimensions. *Computational Mathematics and Mathematical Physics*, 52(1):98–104.
- Kawahara, T. and Tanaka, M. (1983). Interactions of traveling fronts: an exact solution of a nonlinear diffusion equation. *Physics Letters A*, 97(8):311–314.
- Keener, J. P. and Sneyd, J. (1998). *Mathematical physiology*, volume 1. Springer.

- Kolmogorov, A. N. (1937). Étude de l'équation de la diffusion avec croissance de la quantité de matière et son application à un problème biologique. *Bulletin of the University of Moskow*, 1:1–25.
- Kreiss, H. (1962). Über die stabilitätsdefinition für differenzgleichungen die partielle differentialgleichungen approximieren. *BIT Numerical Mathematics*, 2(3):153–181.
- Krupa, M., Sandstede, B., and Szmolyan, P. (1997). Fast and slow waves in the FitzHugh–Nagumo equation. *Journal of Differential Equations*, 133(1):49–97.
- Kurapatenko, V. F. (1967). Difference Methods for Solutions of Problems of Mathematical Physics I. *American Mathematical Society, Providence, RI*, 74(17).
- Kyrychko, Y. N., Bartuccelli, M. V., and Blyuss, K. B. (2005). Persistence of travelling wave solutions of a fourth order diffusion system. *Journal of Computational and Applied Mathematics*, 176(2):433–443.
- Lambert, J. D. (1991). *Numerical methods for ordinary differential systems: the initial value problem*. John Wiley & Sons, Inc.
- Landshoff, R. (1955). A numerical method for treating fluid flow in the presence of shocks. Technical report, LOS ALAMOS NATIONAL LAB NM.
- Lax, P. and Nirenberg, L. (1966). On stability for difference schemes; a sharp form of Gårding's inequality. *Communications on Pure and Applied Mathematics*, 19(4):473–492.
- LeVeque, R. J. et al. (2002). *Finite volume methods for hyperbolic problems*, volume 31. Cambridge University Press.
- Li, S., Petzold, L., and Ren, Y. (1998). Stability of moving mesh systems of partial differential equations. *Society for Industrial and Applied Mathematics (SIAM), Journal on Scientific Computing*, 20(2):719–738.
- Liu, G. and Gu, Y. (2005). *An introduction to meshfree methods and their programming*. Springer Science and Business Media, 18th edition.
- Lubuma, J. M.-S. and Patidar, K. C. (2006). Uniformly convergent non-standard finite difference methods for self-adjoint singular perturbation problems. *Journal of Computational and Applied Mathematics*, 191(2):228–238.

- Ma, W. (2005). Integrability, encyclopedia of nonlinear science, a. scott.
- Mickens, R. (1994). *Nonstandard finite difference models of differential equations*. World Scientific.
- Mickens, R. (1999). Nonstandard finite difference schemes for reaction-diffusion equations. *Numerical Methods for Partial Differential Equations: An International Journal*, 15(2):201–214.
- Mickens, R. (2000). *Applications of nonstandard finite difference schemes*. World Scientific.
- Mickens, R. E. (1989). Exact solutions to a finite-difference model of a nonlinear reaction-advection equation: Implications for numerical analysis. *Numerical Methods for Partial Differential Equations*, 5(4):313–325.
- Mickens, R. E. (1997). Relation between the time and space step-sizes in nonstandard finite-difference schemes for the fisher equation. *Numerical Methods for Partial Differential Equations*, 13(1):51–55.
- Mickens, R. E. (2002). Nonstandard finite difference schemes for differential equations. *Journal of Difference Equations and Applications*, 8(9):823–847.
- Mickens, R. E. (2005). Dynamic consistency: a fundamental principle for constructing nonstandard finite difference schemes for differential equations. *Journal of Difference Equations and Applications*, 11(7):645–653.
- Miyata, T. and Sakai, Y. (2012). Vectorized total variation defined by weighted L infinity norm for utilizing inter channel dependency. *19th IEEE International Conference on Image Processing*, pages 3057–3060.
- Mulholland, L. S., Qiu, Y., and Sloan, D. M. (1997). Solution of evolutionary partial differential equations using adaptive finite differences with pseudospectral post-processing. *Journal of Computational Physics*, 131(2):280–298.
- Müller, T. G. and Timmer, J. (2004). Parameter identification techniques for partial differential equations. *International Journal of Bifurcation and Chaos*, 14(06):2053–2060.
- Munyakazi, J. B. and Patidar, K. C. (2013). A fitted numerical method for singularly perturbed parabolic reaction-diffusion problems. *Computational and Applied Mathematics*, 32(3):509–519.

- Murray, J. D. (1989). Biological waves: multi-species reaction diffusion models. In *Mathematical Biology*, pages 311–359. Springer.
- Nagumo, J., Arimoto, S., and Yoshizawa, S. (1962). An active pulse transmission line simulating nerve axon. *Proceedings of the IRE*, 50(10):2061–2070.
- Namjoo, M. and Zibaei, S. (2018). Numerical solutions of FitzHugh–Nagumo equation by exact finite-difference and NSFD schemes. *Computational and Applied Mathematics*, 37(2):1395–1411.
- Noh, W. F. and Protter, M. H. (1963). Difference methods and the equations of hydrodynamics. *Journal of Mathematics and Mechanics*, 12(2):149–191.
- Öziş, T. and Koroğlu, C. (2009). Reply to: “comment on: ‘a novel approach for solving the Fisher equation using exp-function method’ [phys. lett. a 372 (2008) 3836]” [phys. lett. a 373 (2009) 1196]. *Physics Letters A*, 373(12-13):1198–1200.
- Patidar, K. C. (2005). High order fitted operator numerical method for self-adjoint singular perturbation problems. *Applied Mathematics and Computation*, 171(1):547–566.
- Patidar, K. C. (2007). High order parameter uniform numerical method for singular perturbation problems. *Applied Mathematics and Computation*, 188(1):720–733.
- Petrovskii, S. and Shigesada, N. (2001). Some exact solutions of a generalized Fisher’s equation related to the problem of biological invasion. *Mathematical Biosciences*, 172(2):73–94.
- Preston, S. H. and Wang, H. (2007). Intrinsic growth rates and net reproduction rates in the presence of migration. *Population and Development Review*, 33(4):357–666.
- Qiu, Y. and Sloan, D. (1998). Numerical solution of Fisher’s equation using a moving mesh method. *Journal of Computational Physics*, 146(2):726–746.
- Rauch, J. and Smoller, J. A. (1978). Qualitative theory of the FitzHugh–Nagumo equations. *Advances in Mathematics*, 27(1):12–44.
- Recktenwald, G. W. (2004). Finite-difference approximations to the heat equation. *Mechanical Engineering*, 10:1–27.
- Roeger, L. W. and Mickens, R. E. (2007). Exact finite-difference schemes for first order differential equations having three distinct fixed-points. *Journal of Difference Equations and Applications*, 13(12):1179–1185.

- Rüde, U. (1993). *Mathematical and Computational Techniques for Multilevel Adaptive Methods*, volume 13. Society for Industrial and Applied Mathematics (SIAM).
- Ruxun, L., Mengping, Z., Ji, W., and Xiao-Yuan, L. (1999). The designing approach of difference schemes by controlling the remainder-effect. *International Journal for Numerical Methods in Fluids*, 31(2):523–533.
- Sakthivel, R. and Luo, J. (2009). Asymptotic stability of impulsive stochastic partial differential equations with infinite delays. *Journal of Mathematical Analysis and Applications*, 356(1):1–6.
- Sanz-Serna, J. M. and Stuart, A. M. (1992). A note on uniform in time error estimates for approximations to reaction-diffusion equations. *Institute of Mathematics and its Applications (IMA), Journal of Numerical Analysis*, 12(3):457–462.
- Schonbek, M. E. (1981). A priori estimates of higher order derivatives of solutions to the FitzHugh-Nagumo equations. *Journal of Mathematical Analysis and Applications*, 82(2):553–565.
- Shi, J. and Shivaji, R. (2006). Persistence in reaction diffusion models with weak Allee effect. *Journal of Mathematical Biology*, 52(6):807–829.
- Smoller, J. (2012). *Shock waves and reaction—diffusion equations*, volume 258. Springer Science & Business Media.
- Stephens, P. A., Sutherland, W. J., and Freckleton, R. P. (1999). What is the Allee effect? *Oikos*, pages 185–190.
- Strikwerda, J. C. (2004). *Finite difference schemes and partial differential equations*, volume 88. Society for Industrial and Applied Mathematics. Philadelphia. Second edition.
- Stuart, A. and Humphries, A. (1998). *Dynamical systems and numerical analysis*, volume 2. Cambridge University Press.
- Su, J. Z. (1994). On delayed oscillation in nonspatially uniform Fitzhugh-Nagumo equation. *Journal of Differential Equations*, 110(1):38–52.
- Sutton, O. J. (2018). Long time $L^\infty(L^2)$ a posteriori error estimates for fully discrete parabolic problems. *arXiv Preprint arXiv:1803.03207*.

- Taha, T. R. and Ablowitz, M. I. (1984). Analytical and numerical aspects of certain nonlinear evolution equations. iii. numerical, Korteweg-de Vries equation. *Journal of Computational Physics*, 55(2):231–253.
- Toselli, A. and Widlund, O. (2006). *Domain decomposition methods-algorithms and theory*, volume 34. Springer Science and Business Media.
- Triki, H. and Wazwaz, A. (2013). On soliton solutions for the Fitzhugh–Nagumo equation with time-dependent coefficients. *Applied Mathematical Modelling*, 37(6):3821–3828.
- Twizell, E. H., Gumel, A. B., and Cao, Q. (1999). A second-order scheme for the “Brusselator” reaction–diffusion system. *Journal of Mathematical Chemistry*, 26(4):297–316.
- VonNeumann, J. and Richtmyer, R. D. (1950). A method for the numerical calculation of hydrodynamic shocks. *Journal of Applied Physics*, 21(3):232–237.
- Wang, G. W., Xu, T. Z., Johnson, S., and Biswas, A. (2014). Solitons and lie group analysis to an extended quantum Zakharov–Kuznetsov equation. *Astrophysics and Space Science*, 349(1):317–327.
- Wang, J., Shi, J., and Wei, J. (2011). Dynamics and pattern formation in a diffusive predator–prey system with strong Allee effect in prey. *Journal of Differential Equations*, 251(4-5):1276–1304.
- Wazwaz, A. M. (2009). *Partial differential equations and solitary waves theory*. Higher Education Press, Berlin, Springer, 15th edition.
- Wilkins, M. L. (1980). Use of artificial viscosity in multidimensional fluid dynamic calculations. *Journal of Computational Physics*, 36(3):281–303.
- Xu, B., Binczak, S., Jacquir, S., Pont, O., and Yahia, H. (2014). Parameters analysis of Fitzhugh–Nagumo model for a reliable simulation. In *36th Annual International Conference of the IEEE Engineering in Medicine and Biology Society*, pages 4334–4337. IEEE.
- Yatat, V., Couteron, P., and Dumont, Y. (2018). Spatially explicit modelling of tree–grass interactions in fire-prone savannas: A partial differential equations framework. *Ecological Complexity*, 36:290–313.
- Yildirim, A. (2009). Application of He’s homotopy perturbation method for solving the cauchy reaction–diffusion problem. *Computers & Mathematics with Applications*, 57(4):612–618.

- Zabusky, N. J. and Kruskal, M. D. (1965). Interaction of solitons in a collisionless plasma and the recurrence of initial states. *Physical Review Letters*, 15(6):240.
- Zeidan, D. (2016). Assessment of mixture two-phase flow equations for volcanic flows using Godunov-type methods. *Applied Mathematics and Computation*, 272:707–719.
- Zeidan, D., Romenski, E., Slaouti, A., and Toro, E. (2007). Numerical study of wave propagation in compressible two-phase flow. *International Journal for Numerical Methods in Fluids*, 54(4):393–417.
- Zeidan, D., Sekhar, T. R., et al. (2018). On the wave interactions in the drift-flux equations of two-phase flows. *Applied Mathematics and Computation*, 327:117–131.
- Zhang, L., Wang, L., and Ding, X. (2014). Exact finite difference scheme and nonstandard finite difference scheme for Burgers and Burgers-Fisher equations. *Journal of Applied Mathematics*, 2014.
- Zienkiewicz, O., Taylor, R. L., and Nithiarasu, P. and Zhu, J. (1977). *The finite element method*, volume 3. McGraw-hill London.